



**Cape Peninsula
University of Technology**

**The evaluation of an algorithmic model, created for the image
guided radiotherapy treatment couch for integration into
the Pinnacle Treatment Planning System**

by

JACOBUS JOHANNES BOTHA

Thesis submitted in fulfilment of the requirements for the degree

Master of Science: Radiography

in the Faculty of Health and Wellness Sciences

at the Cape Peninsula University of Technology

**Supervisor: Bridget Wyrley-Birch
Clinical supervisor: Hester Burger**

**Bellville
December 2020**

CPUT copyright information

The dissertation/thesis may not be published either in part (in scholarly, scientific or technical journals), or as a whole (as a monograph), unless permission has been obtained from the University

DECLARATION

I, Jacobus Johannes Botha, declare that the contents of this dissertation/thesis represent my own unaided work, and that the dissertation/thesis has not previously been submitted for academic examination towards any qualification. Furthermore, it represents my own opinions and not necessarily those of the Cape Peninsula University of Technology.



5 Decemeber 2020

Signed

Date

ABSTRACT

Introduction. It has been demonstrated that the radiotherapy treatment couch top affects the radiation beams traversing the couch top. These effects include a reduction in the dose at depth, and an increase in the surface dose. This research study involved the investigation of these effects at the study site, and the development and evaluation of an algorithmic couch model for the Varian Exact IGRT (Varian Medical Systems) couch top for incorporation into the Pinnacle³ treatment planning system (Philips Medical Systems). The aim was for the predicted doses at depth on the Pinnacle treatment planning system to be within 3% of the measured doses on the treatment unit.

Materials and methods. The radiological properties of the treatment couch top were measured at the treatment unit with a 20 cm cylindrical phantom for the dose at depth, and a 30 x 30 cm square phantom for the surface doses. The PTW PinPoint and Farmer 0.6 cm³ detectors were used for the dose at depth, and nanoDotTM dosimeters for surface doses. The measurements were done for both 6 MV and 18 MV, as well as for various gantry angles, field sizes and different sections of the couch top. These measured doses at depth were then used to develop the couch model. Additional treatment plans with more complex geometries were used to verify the generalisability of the couch model algorithm. Furthermore, analysis was done to determine how the Pinnacle predicted doses compared with the measured doses if the couch model was ignored by Pinnacle.

Results. The amount of attenuation of the dose by the couch ranged from 1.9% to 4.3% for 6 MV, and from 1.0% to 2.6% for 18 MV. The verification plans resulted in a maximum percentage difference between the Pinnacle predicted doses at depth and the measured doses for these plans of 2.03%. The measured surface doses due to the couch for 6 MV ranged from 86.45% to 98.39%, compared to 36.19% to 47.06% for open beams. For 18 MV it ranged from 60.53% to 83.45%, compared to 23.33% to 36.64% for open beams. All surface doses were reported as percentages of the beam dose at D_{max} . If Pinnacle ignored the couch model, the percentage differences between the predicted doses at depth and the measured doses ranged from 1.85% to 4.14% for 6 MV, and from 0.93% to 2.43% for 18 MV. Pinnacle underestimated the surface doses by almost 50% for 6 MV and more than 50% for 18 MV if the couch model was ignored.

Discussion. It was shown that the beam energy, field size, gantry angle, and couch section all had an impact on the effect of the treatment couch on the dose at depth, as well as the surface dose. It was also shown that if Pinnacle ignored the couch model then Pinnacle overestimated the doses at depth, and underestimated the surface doses, for all beams traversing the couch.

Conclusion. The study concurred that the treatment couch has an effect on the dose at depth and on the surface dose. It was determined that a couch model algorithm was required, and resulted in an improvement of the dose calculation accuracy of the Pinnacle predicted doses at depth to within 2.03% of the measured doses and an improvement in the predicted surface doses to within 10% of the measured surface doses.

ACKNOWLEDGEMENTS

I wish to thank:

- Cape Peninsula University of Technology for accepting me as an MSc student.
- Ms Bridget Wyrley-Birch (Supervisor) for her guidance, patience, time, and her dedication in making this research study possible.
- Ms Hester Burger (Clinical Supervisor) for her guidance, patience, time, dedication, and expertise in the field of radiotherapy.
- The staff of the Medical Physics Department for their support and guidance.
- The staff of the Radiation Oncology Department for their support.
- My parents, Mr SJ Botha and Mrs MM Botha, who sacrificed so much for me over the years. Unfortunately, neither of them has lived to see me complete this.
- My friends who have put up with me having to spend so much time on the studies.
- Landauer® in the USA for supplying the nanoDot dosimeters for this study.
- To the Almighty God for making this possible.

DEDICATION

For my parents, Stefanus Botha and Myra Botha

TABLE OF CONTENTS

| | |
|--|--------------|
| DECLARATION | ii |
| ABSTRACT | iii |
| ACKNOWLEDGEMENTS | v |
| DEDICATION | vi |
| TABLE OF CONTENTS | vii |
| LIST OF FIGURES | xi |
| LIST OF TABLES | xvi |
| GLOSSARY | xviii |
| ACRONYMS AND ABBREVIATIONS | xx |
| CHAPTER ONE: INTRODUCTION | 1 |
| 1.1 Introduction | 1 |
| 1.2 Context of the study | 7 |
| 1.3 Focus of the study..... | 7 |
| 1.4 Scripting background | 8 |
| 1.5 Risk of scripting..... | 9 |
| 1.6 Clarification of the term couch | 9 |
| 1.7 Product names | 10 |
| 1.8 Overview of thesis..... | 10 |
| CHAPTER TWO: LITERATURE REVIEW | 12 |
| 2.1 Introduction | 12 |
| 2.2 Aim of radiotherapy | 13 |
| 2.3 Side-effects of radiotherapy | 14 |
| 2.4 Accuracy of radiotherapy | 14 |
| 2.5 History of couch tops | 16 |
| 2.6 Carbon fibre as a material for treatment couches | 16 |
| 2.7 Problems of carbon fibre | 18 |
| 2.8 Other materials for treatment couches..... | 19 |
| 2.9 Effects of the radiotherapy couch..... | 19 |
| 2.9.1 General effects..... | 19 |
| 2.9.2 Attenuation effects | 20 |
| 2.9.2.1 Type of material | 20 |
| 2.9.2.2 Incident angle..... | 21 |
| 2.9.2.3 Field size | 26 |
| 2.9.2.4 Beam energy | 29 |
| 2.9.2.5 Entry position of beam | 30 |
| 2.9.2.6 A further study of interest | 31 |
| 2.9.3 Surface dose effects | 32 |
| 2.10 Advantages of incorporating the treatment couch into the TPS..... | 41 |
| 2.11 Role of treatment planning..... | 42 |

| | | |
|--|---|-----------|
| 2.12 | Treatment planning systems and the treatment couch | 43 |
| 2.13 | Various approaches to adding the couch effect to TPS | 43 |
| 2.14 | Dose measurements | 50 |
| 2.14.1 | Attenuation measurements | 50 |
| 2.14.2 | Surface dose dosimeters | 52 |
| 2.14.2.1 | Parallel-plate chambers | 52 |
| 2.14.2.2 | Thermoluminescent dosimeters (TLD) | 54 |
| 2.14.2.3 | Radiochromic film..... | 54 |
| 2.14.2.4 | MOSFET | 55 |
| 2.14.3 | Surface dose measurements | 56 |
| 2.14.4 | Build-up region problems | 61 |
| 2.15 | Couch model accuracy..... | 62 |
| 2.16 | Conclusion | 63 |
| CHAPTER THREE: RESEARCH METHODOLOGY | | 64 |
| 3.1 | Introduction | 64 |
| 3.2 | Ethical considerations | 65 |
| 3.3 | Study design | 65 |
| 3.4 | Research question | 66 |
| 3.5 | Aims and objectives of the research | 66 |
| 3.5.1 | Aims | 66 |
| 3.5.2 | Objectives | 67 |
| 3.6 | Equipment..... | 67 |
| 3.7 | Quality assurance | 68 |
| 3.8 | Analysis of the physical treatment couch | 69 |
| 3.8.1 | Physical properties of the couch | 69 |
| 3.8.2 | Radiological properties of the couch | 70 |
| 3.8.2.1 | Attenuation factors | 71 |
| 3.8.2.2 | Evaluating necessity of couch model | 81 |
| 3.9 | Creating the couch model on the Pinnacle TPS | 82 |
| 3.9.1 | Requirements of the Pinnacle TPS couch model/structure..... | 82 |
| 3.9.2 | Scanning the water phantom | 83 |
| 3.9.3 | Setting up plans on the Pinnacle TPS..... | 84 |
| 3.9.4 | Development of the script / algorithm..... | 86 |
| 3.9.4.1 | Removal of the CT Scanner couch | 87 |
| 3.9.4.2 | Couch structures | 89 |
| 3.9.4.3 | Base coordinates | 91 |
| 3.9.4.4 | Translations..... | 93 |
| 3.9.4.5 | Interpolations..... | 93 |
| 3.9.4.6 | Densities and skin thickness of the couch model..... | 99 |
| 3.9.5 | Script process | 102 |
| 3.9.6 | Using the script | 104 |

| | | |
|--|---|------------|
| 3.9.7 | Limitations of the couch modelling method used | 105 |
| 3.10 | Generalisability of the couch model on the Pinnacle TPS | 106 |
| 3.11 | Surface dose..... | 111 |
| 3.12 | Conclusion | 123 |
| CHAPTER FOUR: RESEARCH RESULTS | | 124 |
| 4.1 | Introduction | 124 |
| 4.2 | Actual treatment couch | 124 |
| 4.2.1 | Attenuation effect of the couch..... | 124 |
| 4.2.2 | Mirror angle differences | 135 |
| 4.2.3 | Surface dose effects of the couch..... | 138 |
| 4.3 | Pinnacle predicted doses without a couch structure | 145 |
| 4.3.1 | Calculated attenuation effect without couch..... | 145 |
| 4.3.2 | Calculated surface doses without couch..... | 147 |
| 4.4 | Couch model..... | 149 |
| 4.4.1 | Ease of use | 149 |
| 4.4.2 | Dimensions and shape | 150 |
| 4.4.3 | Attenuation effects of the couch model..... | 153 |
| 4.5 | Generalisability of the couch model | 155 |
| 4.6 | Surface doses of the couch model..... | 162 |
| 4.7 | Conclusion | 168 |
| CHAPTER FIVE: DISCUSSION AND CONCLUSION..... | | 169 |
| 5.1 | Introduction | 169 |
| 5.2 | Actual treatment couch | 169 |
| 5.2.1 | Attenuation effect of the couch..... | 169 |
| 5.2.2 | Mirror angle differences | 171 |
| 5.2.3 | Surface dose effect of the couch..... | 172 |
| 5.3 | Pinnacle predicted doses without a couch structure | 173 |
| 5.3.1 | Calculated attenuation effect without couch..... | 173 |
| 5.3.2 | Calculated surface doses without couch..... | 173 |
| 5.4 | Couch model..... | 174 |
| 5.4.1 | Ease of use | 174 |
| 5.4.2 | Dimensions and shape | 174 |
| 5.4.3 | Attenuation effects of the couch model..... | 175 |
| 5.5 | Generalisability of the couch model | 175 |
| 5.6 | Surface doses of the couch model..... | 175 |
| 5.7 | Conclusion | 176 |
| REFERENCES | | 178 |
| APPENDICES | | 185 |
| APPENDIX A: SASQART LINEAR ACCELERATORS..... | | 185 |
| APPENDIX B: SASQART DOSIMETERS | | 185 |
| APPENDIX C: SASQART TREATMENT PLANNING SYSTEMS | | 185 |

| | |
|---|-----|
| APPENDIX D: VARIAN EXACT IGRT COUCH SPECIFICATIONS | 185 |
| APPENDIX E: DOSIMETERS | 185 |
| Appendix E1: PinPoint Chambers | 185 |
| Appendix E2: Farmer Chambers | 185 |
| Appendix E3: nanoDot Dosimeters..... | 186 |
| APPENDIX F: PINNACLE SCRIPT FILES | 186 |
| Appendix F1: Couch_Varian_IGRT_v_3_8.Script | 186 |
| Appendix F2: SliceCaptureZ.Script..... | 186 |
| APPENDIX G: PYTHON SCRIPT FILE | 186 |
| APPENDIX H: COUCH BASE COORDINATES | 186 |
| APPENDIX I: COUCH SKIN THICKNESSES..... | 186 |
| APPENDIX J: ETHICS APPROVALS | 187 |
| Appendix J1: Ethics Approval (Cape Peninsula University of Technology)..... | 187 |
| Appendix J2: Ethics Approval (Research Committee, Groote Schuur Hospital)..... | 190 |
| Appendix J3: Data Collection Permission Approval (Radiation Oncology Department, Groote Schuur Hospital) | 193 |
| APPENDIX K: NOTCHES ON COUCH | 194 |

LIST OF FIGURES

| | |
|---|----|
| Figure 1.1: A 3D graphics model of a high energy x-ray treatment unit called a linear accelerator..... | 2 |
| Figure 1.2: The 3D graphics model of a linear accelerator as seen from the patient's feet looking towards the gantry..... | 3 |
| Figure 3.1: The main dimensions of the Varian IGRT couch..... | 69 |
| Figure 3.2: The cross-sections of the Varian IGRT couch..... | 69 |
| Figure 3.3: Indicating the five (5) main sections of the Varian IGRT couch..... | 70 |
| Figure 3.4: The 20 cm cylindrical phantom with the PinPoint chamber | 72 |
| Figure 3.5: Part of the IGRT couch showing some of the indexing notches..... | 73 |
| Figure 3.6: The position of the phantom for the attenuation measurements for the thin section of the couch..... | 74 |
| Figure 3.7: The position of the phantom for the attenuation measurements for the sloping of the couch | 74 |
| Figure 3.8: The position for the phantom for the attenuation measurements for the thick section of the couch..... | 74 |
| Figure 3.9: Position of the phantom so that the active part of the PinPoint is at the isocentre | 75 |
| Figure 3.10: The gantry angles used for the open (unattenuated) beam measurements..... | 76 |
| Figure 3.11: Showing how the gantry angles 100° to 180° only cover one side of the couch | 77 |
| Figure 3.12: Gantry angles 100° to 260° in 20° increments | 78 |
| Figure 3.13: The height of the couch caused the steep angles (100° and 260°) to miss the couch | 78 |
| Figure 3.14: The anterior half of these beams missed the couch and the centres fell exactly on the sloping edge of the couch..... | 79 |
| Figure 3.15: The final angles used for the measurements of the attenuation of the radiation beams by the couch..... | 79 |
| Figure 3.16: The cradles are wide enough apart to not be in the beams | 80 |
| Figure 3.17: With gantry angles 130° and 230° the anterior part of the beams travel through a shorter thickness of couch than the posterior part..... | 81 |
| Figure 3.18: The field of view (FOV) of the scans | 84 |
| Figure 3.19: The couch of the Toshiba Aquilion LB wide bore CT Scanner on the CT image | 88 |
| Figure 3.20: The couch removal plane on the Pinnacle treatment planning system | 89 |
| Figure 3.21: Showing how the CT scanner couch is not covered by the treatment couch structure..... | 89 |
| Figure 3.22: The couch space structure shown as a colourwash..... | 90 |
| Figure 3.23: The external couch structure (a) shown in relation to the couch space structure (b) | 90 |
| Figure 3.24: The internal couch structure (c) shown in relation to the external couch structure (a) and the couch space structure (b)..... | 91 |

| | |
|---|-----|
| Figure 3.25: The cross-section levels of the couch for which the base contours were created | 92 |
| Figure 3.26: Superimposed scatter plots of the coordinates of the three sets of base contours of the couch | 92 |
| Figure 3.27: The couch structure added on the CT slice after the ROI files imported | 93 |
| Figure 3.28: The two regions of the couch where interpolations were required to create the external shape of the couch, the superior region (a) and the sloping section (b) | 94 |
| Figure 3.29: Showing how the base contours of the front end of the couch and the thin section of the couch only change in the X-direction | 94 |
| Figure 3.30: The logic behind Interpolation A for the superior part of the couch | 95 |
| Figure 3.31: Showing how the base contours of the thin section of the couch and the thick section of the couch only change in the Y-direction | 96 |
| Figure 3.32: Linear interpolation for the sloping section | 97 |
| Figure 3.33: The logic for Interpolation C for creating the coordinates for the internal couch contours | 99 |
| Figure 3.34: The initial couch skin (indicated here by the arrow) could only have a single density | 100 |
| Figure 3.35: The new anterior-posterior contour for the external couch structure | 100 |
| Figure 3.36: The new lateral contour for the external couch structure | 100 |
| Figure 3.37: The new anterior-posterior contour and lateral contours combined for the external couch structure | 101 |
| Figure 3.38: The inner couch structure overlying the new external couch structures | 101 |
| Figure 3.39: Showing how the CT Scan images are compared with the position of the couch to see which CT slices fall outside the couch | 102 |
| Figure 3.40: The information that the end-user can specify for the relative position of the couch inside the Pinnacle treatment plan | 105 |
| Figure 3.41: Schematic representation of the front view of the square phantom | 106 |
| Figure 3.42: The square phantom showing the positions of the detector | 107 |
| Figure 3.43: Schematic representation of the square phantom showing the dose reading position for the reference doses and the attenuated dose | 109 |
| Figure 3.44: Schematic representation of the square phantom showing the dose reading position for the reference doses and the attenuated dose | 110 |
| Figure 3.45: Schematic representation of the square phantom showing the dose reading positions for the reference doses of the attenuated dose | 110 |
| Figure 3.46: Examples of the nanoDot™ dosimeters in their plastic pouch | 112 |
| Figure 3.47: The beam arrangements used for the surface dose measurements (the 10 x 10 and 20 x 20 beams are shown superimposed) | 114 |
| Figure 3.48: Beam entry points marked on phantom to facilitate nanoDot positioning | 117 |
| Figure 3.49: The square enabled quick positioning of the nanoDot dosimeters | 118 |
| Figure 3.50: The extra measurements were taken with the chamber in the top chamber position | 118 |
| Figure 3.51: Percentage depth dose data on Pinnacle for 6 MV for 10 x 10 and 20 x 20 .. | 120 |
| Figure 3.52: Percentage depth dose data on Pinnacle for 18 MV for 10 x 10 and 20 x 20 | 121 |
| Figure 3.53: The calculation dose points used for the 6 MV beams | 121 |

| | |
|--|-----|
| Figure 3.54: The calculation dose points used for the 18 MV beams..... | 122 |
| Figure 4.1: The effect of the gantry angle on the attenuation by the treatment couch for the 6 MV energy and all three sections of the treatment couch..... | 126 |
| Figure 4.2: The effect of the gantry angle on the attenuation by the treatment couch for 18 MV energy and all three sections of the treatment couch..... | 126 |
| Figure 4.3: Demonstrating the reduced attenuation of the medium couch section at 130° and 230°, as compared to the thin couch section, for the 10 x 10 cm | 127 |
| Figure 4.4: The effect of the field size on the attenuation by the treatment couch of 6 MV energy and the thin section of the treatment couch..... | 128 |
| Figure 4.5: The effect of the field size on the attenuation by the treatment couch for 6 MV energy and the medium section of the treatment couch..... | 128 |
| Figure 4.6: The effect of the field size on the attenuation by the treatment couch for 6 MV energy and the thick section of the treatment couch | 129 |
| Figure 4.7: The effect of the field size on the attenuation by the treatment couch for 18 MV energy and the thin section of the treatment couch..... | 129 |
| Figure 4.8: The effect of the field size on the attenuation by the treatment couch for 18 MV energy and the medium section of the treatment couch..... | 130 |
| Figure 4.9: The effect of the field size on the attenuation by the treatment couch for 18 MV energy and the thick section of the treatment couch | 130 |
| Figure 4.10: The effect of the beam energy on the attenuation by the treatment couch for 10 x 10 cm field size and the thin section of the treatment couch | 132 |
| Figure 4.11: The effect of the beam energy on the attenuation by the treatment couch for 10 x 10 cm field size and the medium section of the treatment couch | 132 |
| Figure 4.12: The effect of the beam energy on the attenuation by the treatment couch for 10 x 10 cm field size and the thick section of the treatment couch..... | 133 |
| Figure 4.13: Chart showing maximum differences in measurements between 120° and 240° angle..... | 136 |
| Figure 4.14: Chart showing minimum differences in measurements between 120° and 240° angle..... | 136 |
| Figure 4.15: Chart showing that the 120° and 240° differences are consistent for all three sections of the couch for 6 MV, 10 x 10 cm field size..... | 137 |
| Figure 4.16: Chart showing that the 120° and 240° differences are consistent for all three sections of the couch for 18 MV, 10 x 10 cm field size..... | 137 |
| Figure 4.17: Comparing the influence of field size on the measured surface doses for the 6 MV and 18 MV..... | 138 |
| Figure 4.18: Comparing the influence of field size and the treatment couch on the measured surface doses for 6 MV..... | 139 |
| Figure 4.19: Comparing the influence of field size and the treatment couch on the measured surface doses for 18 MV..... | 140 |
| Figure 4.20: Comparing the influence of incident angle on the measured surface doses for 6 MV for the three couch sections | 141 |
| Figure 4.21: Comparing the influence of incident angle on the measured surface doses for 18 MV for the three couch sections | 141 |
| Figure 4.22: Demonstrating the open beam surface dose differences between the measured doses and the doses calculated by Pinnacle for 6 MV | 142 |

| | |
|--|-----|
| Figure 4.23: Demonstrating the open beam surface dose differences between the measured doses and the doses calculated by Pinnacle for 18 MV | 143 |
| Figure 4.24: Demonstrating the percentage differences between the Pinnacle predicted surface doses and the nanoDot surface doses for the open beams | 143 |
| Figure 4.25: The percentage depth dose curves obtained using the CC13 chamber, PFD dosimeter, Markus chamber, TLD chips and the Monte Carlo simulation, for the 6 MV photon beam with a 10 × 10 cm field | 144 |
| Figure 4.26: Overestimation by the Pinnacle treatment planning system for 6 MV, 10 x 10 cm for the three couch sections..... | 146 |
| Figure 4.27: Overestimation by the Pinnacle treatment planning system for 18 MV, 10 x 10 cm for the three couch sections..... | 146 |
| Figure 4.28: Demonstrating the degree of underestimation of the surface dose by Pinnacle treatment planning system for 6 MV if the treatment couch is ignored..... | 148 |
| Figure 4.29: Demonstrating the degree of underestimation of the surface dose by Pinnacle treatment planning system for 18 MV if the treatment couch is ignored..... | 149 |
| Figure 4.30: Comparing the shapes of the superior sections of the real Varian IGRT couch (on the left) and the scripted couch model in the Pinnacle treatment planning system (on the right)..... | 150 |
| Figure 4.31: The couch model structures on the CT scan of the Varian IGRT couch at a level superior to H4 notch on superior end of couch..... | 150 |
| Figure 4.32: The couch model structures on the CT scan of the Varian IGRT couch on the level of the H4 notch | 151 |
| Figure 4.33: The couch model structures on the CT scan of the Varian IGRT couch at a level between the H3 and H4 notches | 151 |
| Figure 4.34: The couch model structures on the CT scan of the Varian IGRT couch on the level of the H3 notch | 151 |
| Figure 4.35: The couch model structures on the CT scan of the Varian IGRT couch on the level of the H2 notch | 151 |
| Figure 4.36: The couch model structures on the CT scan of the Varian IGRT couch on the level of the H1 notch | 152 |
| Figure 4.37: The couch model structures on the CT scan of the Varian IGRT couch on the level of the 0 notch..... | 152 |
| Figure 4.38: The couch model structures on the CT scan of the Varian IGRT couch on the level of the F1 notch | 152 |
| Figure 4.39: The couch model structures on the CT scan of the Varian IGRT couch between the F1 and F2 notches..... | 152 |
| Figure 4.40: Comparison of the measured attenuated doses, and the Pinnacle predicted doses (with and without the couch) for 6 MV beams traversing the couch..... | 155 |
| Figure 4.41: Comparison of the measured attenuated doses, and the Pinnacle predicted doses (with and without the couch) for 18 MV beams traversing the couch when the couch model incorporated | 155 |
| Figure 4.42: Schematic representation of the square phantom showing the dose reading position for the reference doses and the attenuated doses..... | 156 |
| Figure 4.43: Schematic representation of the square phantom showing the dose reading position for the reference doses and the attenuated doses..... | 158 |
| Figure 4.44: Schematic representation of the square phantom showing the dose reading position for the reference doses and the attenuated doses..... | 159 |

| | |
|---|-----|
| Figure 4.45: Comparison of the percentage differences between the Pinnacle calculated doses and measured doses for the 6 MV verification plans for the different chamber position analyses..... | 161 |
| Figure 4.46: Comparison of the percentage differences between the Pinnacle calculated doses and measured doses for the 18 MV verification plans for the different chamber position analyses..... | 161 |
| Figure 4.47: Comparing the percentage differences between the Pinnacle predicted surface doses and the nanoDot surface doses, with, and without the couch model for 6 MV through the thin section of the couch | 165 |
| Figure 4.48: Comparing the percentage differences between the Pinnacle predicted surface doses and the nanoDot surface doses, with, and without the couch model for 6 MV through the medium section of the couch | 165 |
| Figure 4.49: Comparing the percentage differences between the Pinnacle predicted surface doses and the nanoDot surface doses, with, and without the couch model for 6 MV through the thick section of the couch | 166 |
| Figure 4.50: Comparing the percentage differences between the Pinnacle predicted surface doses and the nanoDot surface doses, with, and without the couch model for 18 MV through the thin section of the couch | 166 |
| Figure 4.51: Comparing the percentage differences between the Pinnacle predicted surface doses and the nanoDot surface doses, with, and without the couch model for 18 MV through the medium section of the couch | 167 |
| Figure 4.52: Comparing the percentage differences between the Pinnacle predicted surface doses and the nanoDot surface doses, with, and without the couch model for 18 MV through the thick section of the couch | 167 |
| | |
| Figure 5.1: Cross-section of thick section of treatment couch showing the paths the centres of the beams at 220° and 230° will travel through skin of couch | 171 |
| Figure 5.2: Cross-section of thick section of treatment couch showing the paths the centres of the beams at 120° might travel through skin of the couch..... | 171 |

LIST OF TABLES

| | |
|---|-----|
| Table 2.1: Comparison of the beam attenuation as a result of the different couch tops and inserts | 17 |
| Table 2.2: Comparison of the surface doses as a result of the couch tops and inserts | 18 |
| Table 2.3: 18 MV photon beam attenuation by the ICT couch | 28 |
| | |
| Table 3.1: The densities used for the various couch structures | 104 |
| Table 3.2: Summary of the attenuated beams in the six plans used for checking the generalisability of the couch model..... | 108 |
| Table 3.3: The three surface dose plans for each energy | 113 |
| Table 3.4: The fields for 6 MV that were actually measured using the nanoDots. The same field arrangements were also measured for 18 MV | 115 |
| | |
| Table 4.1: Summary of attenuation by the treatment couch for the gantry angles (Figure 3.15) and the different sections of the couch..... | 125 |
| Table 4.2: Summary of the influence of field size on the attenuation by the treatment couch for 6 MV | 131 |
| Table 4.3: Summary of the influence of field size on the attenuation by the treatment couch for 18 MV | 131 |
| Table 4.4: Summary of the influence of beam energy on the attenuation by the treatment couch | 134 |
| Table 4.5: Summary of the attenuation produced by the IGRT treatment couch for 6 MV (the highest values are highlighted) | 135 |
| Table 4.6: Summary of the attenuation produced by the IGRT treatment couch for 18 MV (the highest values are highlighted)..... | 135 |
| Table 4.7: The Pinnacle percentage depth dose data for the surface region | 144 |
| Table 4.8: Summary of the overestimation of the dose by Pinnacle if treatment couch is ignored for the 6 MV energy | 147 |
| Table 4.9: Summary of the overestimation of the dose by Pinnacle if treatment couch is ignored for the 18 MV energy | 147 |
| Table 4.10: The percentage difference between the Pinnacle calculated doses and required doses for 6 MV..... | 154 |
| Table 4.11: The percentage difference between the Pinnacle calculated doses and required doses for 18 MV..... | 154 |
| Table 4.12: Percentage differences between Pinnacle calculated doses and measured dose for the verification plans for the 6 MV beams (measured at chamber position 1, and using reference doses at chamber position 1) | 157 |
| Table 4.13: Percentage differences between Pinnacle calculated doses and measured dose for the verification plans for the 18 MV beams (measured at chamber position 1, and using reference doses at chamber position 1) | 157 |
| Table 4.14: Percentage differences between Pinnacle calculated doses and measured dose for the verification plans for the 6 MV beams (measured at chamber position 2, and using reference doses at chamber position 2) | 158 |

| | |
|---|-----|
| Table 4.15: Percentage differences between Pinnacle calculated doses and measured dose for the verification plans for the 18 MV beams (measured at chamber position 2, and using reference doses at chamber position 2) | 159 |
| Table 4.16: Percentage differences between Pinnacle calculated doses and measured dose for the verification plans for the 6 MV beams (attenuation dose readings at chamber position 2, reference doses readings at chamber position 1)..... | 160 |
| Table 4.17: Percentage differences between Pinnacle calculated doses and measured dose for the verification plans for the 18 MV beams (attenuation dose readings at chamber position 2, reference doses readings at chamber position 1) | 160 |
| Table 4.18: Summary of the measured surface doses and the Pinnacle predicted surface doses for the beams traversing the treatment couch for 6 MV | 163 |
| Table 4.19: Summary of the measured surface doses and the Pinnacle predicted surface doses for the beams traversing the treatment couch for 18 MV | 164 |

GLOSSARY

| | |
|---------------------|---|
| CT scanner | Computerised Tomography (CT) Scanner. An imaging device used to acquire scans of a patient in 3D. |
| D_{max} | When a radiation beam interacts with tissue, the maximum dose does not fall on the outer surface. The radiation needs to travel a certain depth through the tissue before we see the maximum amount of radiation (maximum dose or D_{max}). This region is called the build-up region and is responsible for the skin-sparing effect. The dose at D_{max} is defined as 100% and then after this point the radiation dose decreases as the depth increases, the energy being absorbed within the tissue. |
| Electrometer | Device used to measure charge. These electrometers have specially designed circuits to be able to measure the tiny ionisation currents or charges which are generated when ionisation chambers are exposed to ionising radiation. (Khan, 2011). |
| EPID | Electronic portal imaging device. This is a device fitted to many modern linear accelerators and is used to verify patient setup during radiotherapy treatments. |
| Field of view (FOV) | This is the maximum diameter of the area of the scanned object that is represented in the reconstructed image. On the treatment planning system only pixels which fall within the field of view will be included in the volume used for the calculation of the radiation dose. |
| Gantry | This is a moving head of a linear accelerator and can rotate through 360° . This allows the radiation to be given from all angles without the patient having to change position. |
| Gray | This is a measure of absorbed radiation dose. The abbreviation of gray is Gy. One gray is defined as: $D = \frac{de}{dm}$ <p>Where D is the absorbed dose, de is the mean energy imparted by the ionising radiation to matter of mass dm.</p> <p>1 gray = 1 joule per kilogram (1 Gy = 1 J.kg⁻¹).</p> |
| IGRT | Image guided radiotherapy In image guided radiotherapy (IGRT) imaging techniques are used to ensure that the patient is in the correct position for the radiotherapy treatment. The imaging is done with the patient setup on the treatment couch before the treatment starts. |
| IMRT | Intensity-modulated radiation therapy (IMRT) is an advanced radiotherapy technique for the treatment of tumours. In IMRT the radiation beams are manipulated to conform to the shape of a tumour. |

| | |
|----------------------------|--|
| Ionisation chamber | An electrical device which detects various types of ionising radiation. |
| Ionising radiation | This is radiation which has enough energy to be able to remove bound electrons from the orbit of an atom. This results in the atom changing from its normal neutral state to an ionised (or charged) state. |
| Isocentre | The isocentre is the point in space about which the gantry, collimator and couch of the linear accelerator rotate. There are two isocentres which should ideally be the same point in space. <ul style="list-style-type: none"> • Mechanical isocentre: The point in space about which the gantry, collimator and couch rotate. • Radiation isocentre: The point where the radiation beams intersect if the above parts are rotated. |
| Linear Accelerator (Linac) | This is a megavoltage radiotherapy treatment unit which generates high-energy x-rays or electrons. It is the most commonly used treatment device in modern external beam radiotherapy and is used to treat all parts of the body. |
| Phantom | The phantom is a device which is tissue equivalent and is used to simulate the in vivo effect of radiation on the patient. |
| Radiolucency | Characteristic of a material which allows x-rays to pass through it more freely. |
| Radiotherapy | This is a treatment modality used in the treatment of cancer. It uses ionising radiation to treat the cancer cells. |
| RapidArc™ | RapidArc™ is a trademarked VMAT treatment technique produced by Varian Medical Systems. |
| SAD | Source to Axis Distance. Here the centre of the target volume is positioned at the isocentre of the treatment unit. |
| Skin sparing | The maximum dose for megavoltage photon beams (for example the beams from linear accelerators) will occur at a certain depth below the skin/surface and not on the surface itself. This is the sparing effect and is an important feature in megavoltage photon beams in that it reduces the dose to the skin and thus ensures that the skin is not necessarily a dose limiting structure. (Podgorsak, 2005). |
| SSD | Source to Surface Distance. The SSD is the distance from the source of the radiation to the surface of the patient or phantom. |
| TPS | Treatment planning system. |
| VMAT | Volumetric Modulated Arc Therapy (VMAT) is the newer version of IMRT. In VMAT the treatment is delivered while the gantry is rotating around the patient. During the rotation the radiation beam is continuously reshaped and the intensity of the radiation beam changed. This makes the treatment more accurate in that the radiation is delivered only to the intended target. |

ACRONYMS AND ABBREVIATIONS

The more commonly used acronyms and abbreviations are listed below.

| | |
|---------|---|
| AAPM | American Association of Physicists in Medicine |
| CC | Collapsed cone |
| EBRT | External beam radiotherapy |
| ECT | Exact couch top |
| EPID | Electronic portal imaging device |
| FOV | Field of view |
| HPCSA | Health Professions Council of South Africa |
| IARC | International Agency for Research on Cancer |
| ICRU | International Commission on Radiation Units |
| ICT | Imaging Couch Top |
| IGRT | Image guided radiotherapy |
| IMRT | Intensity-modulated radiation therapy |
| MOSFET | Metal oxide semiconductor field-effect transistor |
| MRI | Magnetic resonance imaging |
| OAR | Organs at risk |
| OLS | Optically stimulated luminescence |
| PDI | Portal dose image |
| PETG | Polyethylene terephthalate glycol |
| PMMA | Polymethylmethacrylate |
| PTV | Planning target volume |
| QA | Quality assurance |
| REC | Research Ethics Committee |
| RF | Radiofrequency |
| ROI | Region of interest |
| RTT | Radiation therapy technologist |
| SABS | South African Bureau of Standards |
| SASQART | South African Standards for Quality Assurance in Radiotherapy |
| TLD | Thermoluminescent dosimeter |
| TPS | Treatment planning system |
| VMAT | Volumetric modulated arc therapy |
| WET | Water equivalent thickness |
| WHO | World Health Organization |

CHAPTER ONE: INTRODUCTION

1.1 Introduction

Cancer remains a major health threat globally. The International Agency for Research on Cancer (IARC) reported that there were 14.1 million new cancer patients and 8.2 million deaths attributable to cancer in 2012 (Abshire & Lang, 2018), and according to the World Health Organisation (2017) three years later in 2015 there were about 8.8 million deaths attributable to cancer worldwide. In 2018 there were an estimated 18.1 million new cancer cases and 9.6 million cancer deaths (Bray et al., 2018).

In 2015 the WHO estimated that cancer is the first or second leading cause of death in people up to the age of 70 years in 91 of 172 countries, and in a further 22 countries it ranks third or fourth (Bray et al., 2018).

All of this highlights the need for a proper cancer treatment that is safe and effective (Abshire & Lang, 2018).

One of the common modalities used for the treatment of cancer is radiotherapy. It is estimated that radiotherapy will form part of the treatment regime of 52% of all cancer patients in England at some stage in their lives (Evans & Staffurth, 2017). This conforms well with what Delaney et al. (2005) found in their Australian study where they found that the percentage of all cancer patients who would benefit from radiotherapy at some point in their treatment is 52.3%. In the United States the number of patients who will be prescribed to receive radiotherapy at some point is estimated at 60% (Abshire & Lang, 2018). The aim of the radiotherapy can either be to cure the patient (radical treatment) or to alleviate and control symptoms (palliative treatment) (Evans & Staffurth, 2017, Hussain & Muhammad, 2017). Radiotherapy formed part of the treatment in 40% of all patients who were cured of their cancer (Evans & Staffurth, 2017).

Radiotherapy uses ionising radiation. It is called ionising radiation because the radiation has a high enough energy to be able to liberate electrons from atoms and molecules, thus creating ions (Hawley, 2013, American Cancer Society, 2016). In the treatment of cancer the types of ionising radiation which are used predominantly are x-rays, gamma rays and electrons (Kirthi Koushik et al., 2013).

Radiotherapy can be delivered from outside the body (external beam radiotherapy – EBRT), or from within the body. The latter includes injected radioisotopes, as well as brachytherapy where radioisotopes are implanted within the target area in the patient's body (Evans & Staffurth, 2017, Hussain & Muhammad, 2017).

For this study the researcher looked only at external beam radiotherapy. The radiation is delivered by high energy x-ray treatment units and the radiation is aimed at the affected (target) area of the patient from outside the body of the patient (Figure 1.1). The treatment units have a gantry which is able to rotate about a fixed point in space (called an isocentre) around the patient in order to be able to treat from any angle in three dimensions (Figure 1.2).

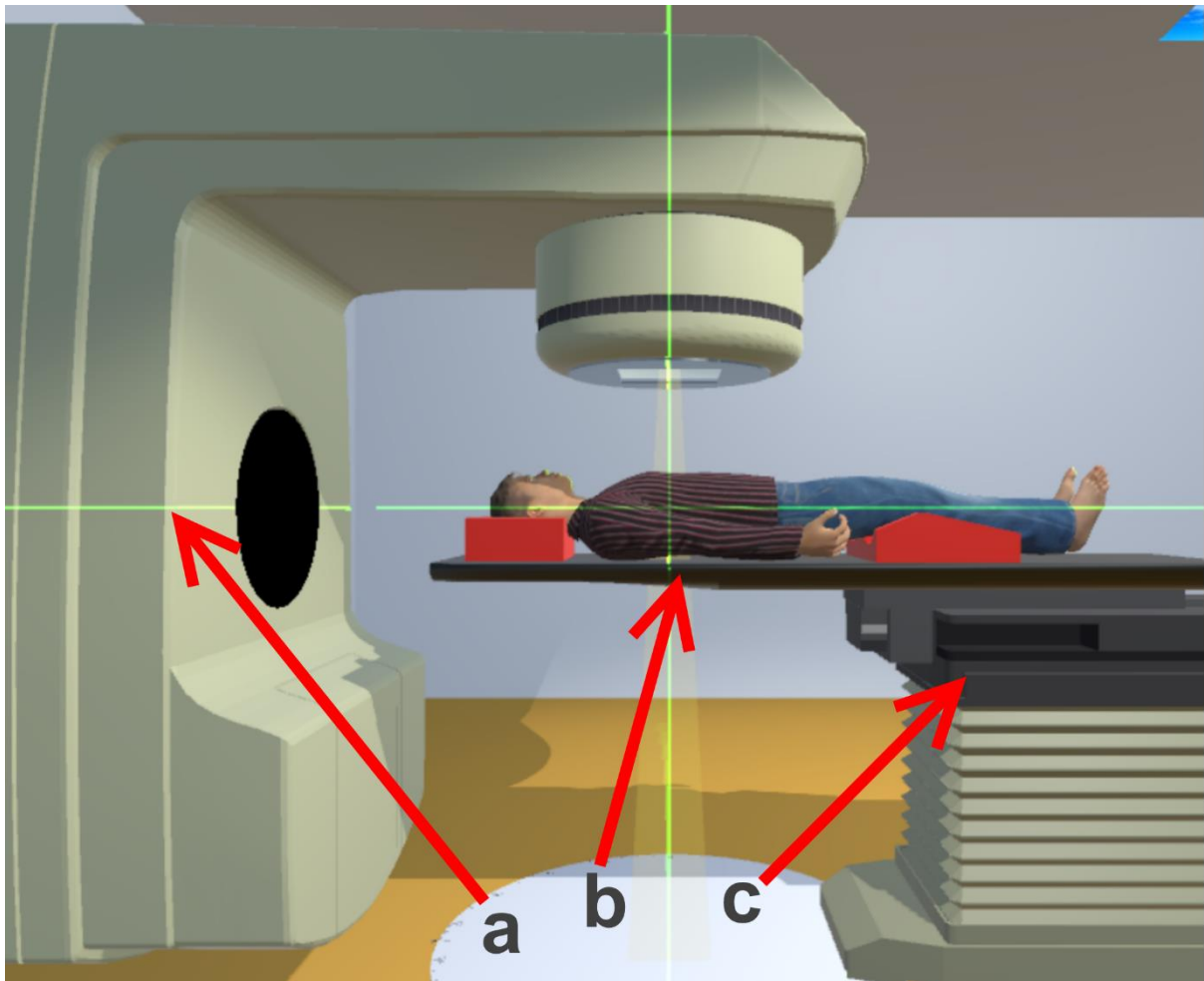


Figure 1.1: A 3D graphics model of a high energy x-ray treatment unit called a linear accelerator

a) This is the gantry which can rotate around the patient. b) The treatment couch top that supports the patient. c) The couch support structures which allow the couch to move vertically, laterally, longitudinally, as well as rotate.

(Radiotherapy Simulation software (Botha, 2019))

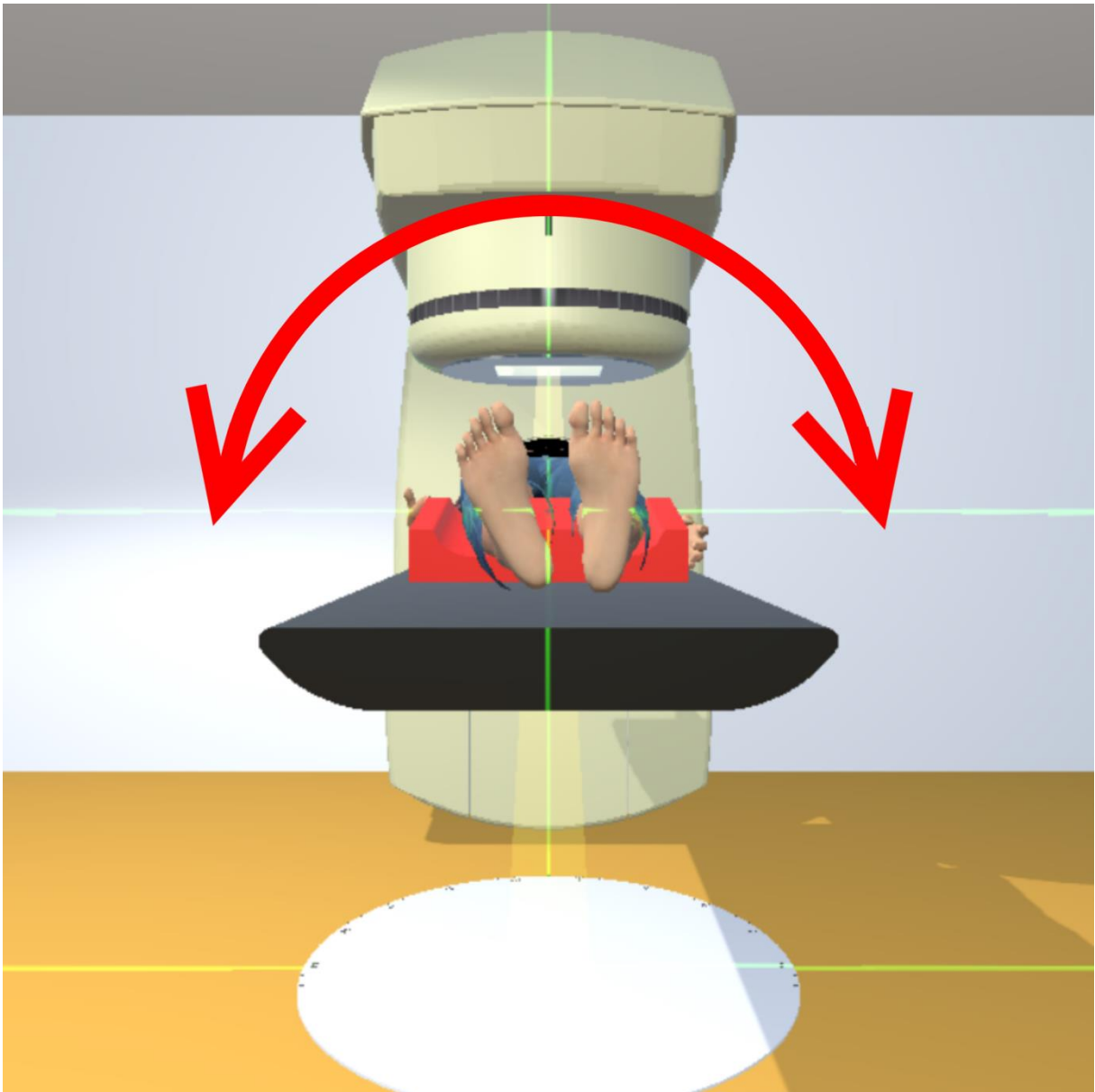


Figure 1.2: The 3D graphics model of a linear accelerator as seen from the patient's feet looking towards the gantry

The arrows indicate the rotation of the gantry around the patient. To simplify the image, the couch support structures have been removed.

(Radiotherapy Simulation software (Botha, 2019))

The ionising radiation is effective in treating cancer because the radiation damages the malignant cells. Unfortunately, the normal cells of the patient are also affected because, in order for the radiation to reach the target (cancerous) area it needs to pass through normal tissue. In order to reduce the radiation dose to the normal tissues of the patient and to increase the dose to the target area, more than one beam of radiation is usually administered from multiple angles (Barrett et al., 2009). The angles from which the radiation beams will be administered to the patient are determined by the location and size of the target area, and also by the location and sensitivity of the organs at risk (OAR) within the patient. Organs at risk are

those critical organs or tissues whose sensitivity to radiation, and their position relative to the treatment area, can affect the way the treatment is planned; for example, in terms of the placement of radiation beams and the exact radiation dose that can be delivered to the target area (Barrett et al., 2009). This factor, as well as the fact that multiple beams are required in modern radiotherapy, means that it is not always possible to avoid treating through other materials, for example the treatment couch, when treating patients (Munjaj et al., 2006).

According to Mills (2012) the radiotherapy process is composed of three major sections. These sections are: acquisition; analysis; and delivery. Acquisition involves determining what needs to be treated and a large part of this is imaging; for example, using a CT scanner. Analysis includes the treatment planning phase where the best way to treat the patient is determined. Finally, there is the delivery of the treatment to the patient.

Thus, a usual sequence of events for a cancer patient who requires radiotherapy is as follows. The patient undergoes a CT scan in order to acquire images of the area of the body where the treatment needs to be delivered. These images will then be imported into a Treatment Planning System (TPS), where the radiation oncologist will delineate the exact target area to be covered by the radiotherapy. The designated staff (radiation therapy technologist (RTT), medical dosimetrist or medical physicist) then use this information to plan the radiotherapy treatment on the treatment planning system. Once the plan is approved by the radiation oncologist and verified by medical physics, the treatment plan is transferred to the appropriate treatment unit. At the treatment unit, the parameters from the treatment plan are used to position the patient as appropriate, and to then deliver the radiotherapy treatment as per the required protocol.

Inaccuracies in the radiation treatment of cancer patients may lead to adverse effects such as poor local tumour control or increased normal tissue side-effects (Buzdar et al., 2013). In each of the different events in the management and treatment of a cancer patient, possible errors and uncertainties play a role in the accuracy of the treatment ultimately delivered to the patient. These errors need to be removed, or at least minimised, where possible (Buzdar et al., 2013). Therefore, it is very important that the treatment is accurately and appropriately planned on a TPS. Once the treatment plan is approved according to the designated quality assurance and treatment protocols, it is then also just as important that the planned treatment is accurately delivered on the treatment unit. According to Gopan et al. (2016) the treatment planning process is the source of most of the errors occurring in radiation oncology. The aim of this study was to improve the accuracy of one aspect in the treatment planning phase.

Radiotherapy requires high levels of dosimetric and geometric accuracy, and in order to calculate and predict the radiation doses for the treatment plans correctly, the treatment

planning systems need to mimic the real world as closely as possible. When ionising radiation passes through any matter, some of the radiation is absorbed by that matter and thus the amount of radiation that travels further will be reduced. For this reason, all matter that the radiation passes through (including the treatment couch) needs to be taken into account for the dosimetry calculation when the treatment is planned. The algorithms of certain treatment planning systems only account for the radiation interactions and attenuation in the patient, and do not account for the additional effects of the treatment couch. This may affect the accuracy of the calculated doses of the treatment plan. This research is aimed at developing a computer-based algorithm which will accurately model the Varian IGRT treatment couch for the Philips Pinnacle™ treatment planning system, and ultimately increase the accuracy of the predicted dose in order to treat the patient optimally.

Modern treatment couches are made from carbon fibre and some filler material to add some strength. Manufacturers are using carbon fibre because it has specific characteristics making it ideal for the use in radiotherapy, namely that carbon fibre allows high transmission of the radiation beam; it has high specific strength; is lightweight; and it has good physical resistance (Sedaghatian et al., 2017). Furthermore, carbon fibre results in a couch with a high degree of radiolucency and therefore less attenuation of the radiation beam (Spezi et al., 2008, Gerig et al., 2010). However, couch attenuation is still an issue, and this is especially true for the oblique gantry angles where the radiation beam will have a longer distance to travel through the couch. McCormack et al. (2005) have shown that the attenuation of the radiation beam by carbon fibre increases as the incident angle of the radiation beam increases.

As was mentioned earlier, the radiation beam needs to traverse normal tissue in order to reach the cancerous target area and thus all normal tissue structures surrounding the target area will receive radiation dose. Thus cancer patients who are treated with radiotherapy often experience a number of possible side-effects, including various skin reactions (Kirthi Koushik et al., 2013). Glover and Harmer (2014) stated that about 85% of patients receiving radiotherapy will get some or other skin reaction. These side-effects may be early-stage or late stage and are dose-dependent. Some of the early-stage skin reactions include erythema and desquamation (Glover & Harmer, 2014, Morgan, 2014, Seite et al., 2017). Occasionally, late effects such as telangiectasia, pigmentation, cutaneous atrophy, dermal sclerosis and keratoses may occur (Seite et al., 2017).

Apart from the attenuation of the radiation, the carbon fibre also has effects on the skin dose received by the patient and thus the skin sparing (De Ost et al., 1997, Gerig et al., 2010). This absorption of the dose by the carbon fibre couch can result in skin toxicity due to the increased radiation dose to the upper layers of the skin (Sedaghatian et al., 2017).

Similarly, ignoring the attenuation effect of the treatment couch can result in overestimation of the radiation dose at the planning target volume (PTV) area. For some situations this error can be even as high as 16% (Myint et al., 2006), depending on the type of couch and its construction. This will lead to an under-treatment to the designated planning target volume.

At the study site the treatment units have two different radiation energies. These energies are 6 MV and 18 MV. The 18 MV beam has a higher energy than the 6 MV beam and will be attenuated less than the 6 MV beam, but the amount of attenuation is still measurable.

On the Pinnacle treatment planning system the planning software calculates the radiation dose that the target area will receive by using the density of each pixel of the CT Scan images. Unfortunately, when the patient is scanned, the patient is supported by a CT Scanner couch and not the treatment couch. This means the CT Scanner couch will appear on the CT images as pixels and, if left as is, the computer will be using the density of the CT Scanner couch in the calculation. Therefore, when these CT images are used in the treatment planning system, the CT Scanner couch needs to be “removed” and replaced with the actual treatment couch of the treatment unit on which the treatment is planned for (Van Prooijen et al., 2010). This is especially important if part of the radiation dose needs to be delivered through this treatment couch so that the attenuation of the radiation through the treatment couch can be incorporated in the final predicted doses.

Many treatment planning systems do not account for the treatment couch and do not provide built-in couch models and thus various departments attempt different ways of adding the treatment couch to the treatment plans (Hu et al., 2011).

The radiation oncology department (at the study site) has a Varian IGRT Treatment couch on all three of the Linear Accelerators. The IGRT couch does not have a uniform shape and thickness when viewed from end to end. (See Figure 3.1).

Literature searches have indicated that no algorithm models currently exist that model the entire length, width and thickness of the Varian IGRT couch in terms of shape, density and radiological attenuation properties.

Modern radiotherapy requires expensive, high-technology equipment, as well as very expensive infrastructure. It also requires a large staff complement (Delaney et al., 2005). The complex equipment necessitates highly trained staff and very involved quality assurance programmes and procedures to maintain the safety and accuracy required in radiotherapy

(Nystrom & Thwaites, 2008). This cost and effort will be nullified, to a degree, if the effect of the treatment couch is not taken into consideration.

1.2 Context of the study

Radiotherapy treatment planning systems allow radiation beams to be accurately delivered to patients by simulating dose delivery according to validated dose calculation algorithms, which are based on CT-derived patient imaging. If these algorithms do not account accurately for the effect of the treatment couch, or do not take the couch into account at all, the predicted dosimetry within the patient may be incorrectly represented on the treatment planning system. Subsequently, these incorrect doses are transferred to the treatment units and delivered to the patients. Currently, relatively crude approximations are used to account for the attenuation by the couch at the study site. In addition, the irregular shape and construction of the Varian IGRT couch means that the influence of the couch may vary depending on the exact position and angle of the beam relative to the couch. The treatment planning systems at the study site do not accurately model the entire length, width and thickness of the Varian IGRT couch in terms of shape, density and radiological attenuation properties. At the time this study was conducted correction factors were used to adjust the predicted doses by the Pinnacle treatment planning system in order to try to minimise the error in the doses used for the treatment of the patients on the treatment units. There is a correction factor for each of the three sections of the couch (thin, medium/sloping, thick) and the users need to decide on which section of the couch the affected area of the patient is situated, and then use the relevant correction factor. Unfortunately, since a single correction factor is used for each section of the couch, the correction factors cannot easily account for different incident angles of the radiation beams on the treatment couch. In addition, a single correction factor can also not accurately account for situations where the field spills over into another section of the couch; for example, if part of the field is within the thin section of the couch and part of the field is within the sloping section of the couch.

1.3 Focus of the study

The main focus of this study was to determine if an algorithmic model of the Varian IGRT couch within the Pinnacle treatment planning system would improve the accuracy of the dose calculations for beams traversing the treatment couch.

At the study site there are two treatment planning systems, Pinnacle (Philips Medical Systems) and Eclipse (Varian Medical Systems). Neither of these two systems has built-in, incorporated ways to take the full treatment couch into account for the calculations of the treatment doses for the radiation treatment of the cancer patients. The Eclipse treatment planning system has

three discrete couch structures for the three sections of the couch (thin, medium, and thick), but it does not model the full Varian IGRT couch top as a single structure. This study focused on the Pinnacle treatment planning system because the Pinnacle provides scripting functionality for clinical applications. This means that with the scripting the clinical treatment plans in Pinnacle can be affected and changed. The Eclipse treatment planning system also provides scripting functionality, but the version currently at the study site does not allow scripting of any of the clinical aspects of treatment plans.

Only the Varian IGRT couch was used in the study. All three of the linear accelerator treatment units at the study site are equipped with the Varian IGRT couch and it is the only couch in use at the study site. The full name of the Varian IGRT couch is the Varian Exact® IGRT couch. In this thesis, when the name IGRT couch, or Varian IGRT couch is used, it refers to the Varian Exact® IGRT couch.

Only external beam radiotherapy was considered for the study, due to the fact that in brachytherapy the radiation does not pass through a couch first before entering the patient.

The focus was also only on static radiotherapy beams and not arc or rotation therapy. With static beams the gantry is rotated to a specific angle (as was planned on the treatment planning system) and then while the gantry is stationary at that angle the full amount of radiation is delivered for that beam.

Lastly, the study focused on both radiation energies available at the study site, namely 6 MV and 18 MV energies (BJR Sup-25 TPR_{20,10} 10 x 10 cm values of 0.677 and 0.775, respectively) (Mani et al., 2017).

This study involved the development of the scripts and algorithm to create the Varian IGRT treatment couch in the Pinnacle treatment planning system for the treatment planning of each radiotherapy patient, as well as the evaluation of the couch model.

1.4 Scripting background

Philips Medical Systems provided the scripting functionality within the Pinnacle treatment planning system, but they do not provide support. This is due to the fact that the end-user can create scripts that can change parameters in the clinical treatment plan, even changes that can adversely affect the outcome of the treatment delivery. The responsibility for this lies solely with the end-user and not with Philips Medical Systems. As Philips Medical Systems do not provide support for scripting, they also do not supply any user manuals on scripting and how to do it. The knowledge that the researcher gained in scripting was due to the Pinnacle users'

community. The researcher found an example script (Riis, 2007) for creating a script in Pinnacle. This was a very basic couch and the process ultimately used by the researcher for this study was completely different, but the example script was very useful in showing how to start doing scripting in Pinnacle. The researcher also found a booklet (Geoghegan, 2007) which was compiled by Sean Geoghegan, a Medical Physicist at Royal Perth Hospital. This booklet contained some of the scripting syntax and the classes and functions used in Pinnacle scripting.

1.5 Risk of scripting

Since the scripting on the Pinnacle treatment planning system allows the treatment plans to be altered for the clinical treatments of the patients, there is an inherent risk in using scripting. If care is not taken critical parameters (e.g. beam energies, beam angles, doses, monitor units) in the treatment plans may be inadvertently altered, resulting in serious injury or even death to the patients if there is incorrect treatment that could result in under- or over-dosage. As mentioned in the previous section, Philips Medical Systems has provided the scripting functionality in the Pinnacle treatment planning system, but they do not provide support or documentation for the scripting. It is for the end-user to use at his/her own risk.

Therefore, it is of the utmost importance that any script which is created for clinical use be tested and verified carefully before being released for clinical use. Subsequently, it is then also very important for the end-users to ensure that the correct script is being used when running the scripts, and to validate the plan before using it on the treatment unit for the treatment of the patient (Philips Medical Systems, 2013a). A good method for verification of the treatment plans is the use of pre-treatment physics plan review (Gopan et al., 2016).

1.6 Clarification of the term couch

The modern radiotherapy treatment couch generally consists of multiple parts and sections. First, there is the actual surface that the patient is positioned on, which is usually referred to as the couch top. The couch top is mounted on a couch support structure. The couch support structures include a number of different sections and electric motors which allow the couch and couch top to be moved accurately in the vertical, longitudinal and lateral directions in order to allow three-dimensional positioning of the patient for the treatment. Finally, there is the base plate which is mounted in the floor of the treatment room. The base plate provides stability to the treatment couch, as well as allowing the couch to be rotated about the isocentre. The couch support structures are mounted on the base plate.

When treating patients on the treatment unit, every part of the treatment unit, including the gantry and couch, needs to be taken into account in order to avoid collisions or injury to staff and patients when moving the individual components into the appropriate positions. However, it is generally only the couch top which needs to be considered in terms of attenuation of the radiation beam and thus possible effects on the target dose and skin dose for the patient's treatment. In this thesis, when the radiation effects of the couch are referred to it means the effect of the couch top itself.

1.7 Product names

This paragraph clarifies some of the trade names used in the thesis.

The treatment planning system used is the Philips Pinnacle³ treatment planning system by Philips Medical Systems. Pinnacle³ is a trademark of Philips Medical Systems. Whenever the terms "Pinnacle treatment planning system" or "Pinnacle" are used in the thesis they refer to the Pinnacle³ treatment planning system by Philips Medical Systems.

The treatment couch top used for the research was the Varian Exact IGRT Couch by Varian Medical Systems. Whenever the term "Varian IGRT couch" is used in the thesis it refers to the Varian Exact IGRT Couch by Varian Medical Systems.

The treatment unit used was the Varian Clinac 2300 C/D linear accelerator by Varian Medical Systems. Whenever the term "treatment unit" is used in the thesis it refers to the Varian Clinac 2300 C/D linear accelerator by Varian Medical Systems.

Varian, Varian Medical Systems, Clinac, and Exact are registered trademarks.

The CT Scanner used was the Toshiba Aquilion LB wide bore CT Scanner. Whenever the term "CT Scanner" is used in the thesis it refers to the Toshiba Aquilion LB wide bore CT Scanner.

Possible exceptions to the use of these terms are in Chapter 2 in the Literature Review where the different authors might have referred to them differently in their articles or where a generic term like "CT Scanner" might refer to a different manufacturer's product.

1.8 Overview of thesis

Most of the images in this thesis were produced from a software program that the researcher himself is creating as part of a teaching, training, and simulation tool for radiotherapy and will be cited as follows: (Botha, 2019).

A brief outline of the chapters of the thesis follows.

Chapter 2 – Literature Review

This chapter is an overview of research and appropriate literature in order to show the focus and placement of this research study. General aspects of radiotherapy are discussed before looking specifically at the radiotherapy treatment couch and its effects on the outcome of the radiotherapy treatment. It should be noted that some articles/sources are more than 10 years old because not many studies have been done so far on this particular treatment planning software. Furthermore, there is a limited number of studies which have used the same treatment couch, as well as the same treatment planning system as were used in this research study.

Chapter 3 – Research and Methodology

This chapter details how this research was approached, and looks at a step-by-step description of all the aspects that went into doing the study and designing the couch model. Finally, it describes how the couch model was verified.

Chapter 4 – Research Results

This chapter presents all the results obtained during the study.

Chapter 5 – Discussion and Conclusion

Finally, we look at what this study accomplished in terms of the initial aims for the study, and whether the study has highlighted any future studies that might be embarked on as a result of this study.

CHAPTER TWO: LITERATURE REVIEW

2.1 Introduction

Since the discovery of x-rays in 1895 by Wilhelm Conrad Roentgen, and then of radium by Marie Curie in 1898, radiation has become an important tool in the treatment of cancer. Radiotherapy was first practised in the early part of the twentieth century using radium and very low energy x-ray machines. In fact, only a year after x-rays were discovered it was used as treatment modality for a breast cancer patient. This was done by Emil Herman Grubbe, even though the physical properties and biological effects of x-rays were not yet fully understood (Gianfaldoni et al., 2017). Since then radiotherapy has been constantly evolving with the utilisation of advancing technology and the benefits afforded by contemporary materials. Hussain and Muhammad (2017) pointed out that modern radiotherapy depends heavily on the ongoing advance of technology.

This research involved modelling of the Varian IGRT treatment couch on the Pinnacle treatment planning system.

A number of studies have been done looking at the effect of treatment couches, especially carbon fibre, on the radiation beam. The majority of these studies looked at treatment couches other than the Varian IGRT couch. These studies have been included in this literature review to demonstrate that the carbon fibre itself affects the radiation beam. So far in literature, no studies were found that dealt with modelling of the Varian IGRT treatment couch on the Pinnacle treatment planning system. Only a few studies were found that determined the attenuation caused by the Varian IGRT treatment couch.

A review of the literature found on this subject is presented in this chapter to provide the focus for the placement and role of this study.

Many studies included in this literature review also looked at the effect of immobilisation devices and couch rails on the beam attenuation. The researcher has not focussed on the effect of these couch rails in doing the literature review, because the Varian IGRT couch itself does not have any couch rails.

Some of the studies are more than 10 years old, but unfortunately there is only a limited number of studies found in the literature so far.

In this chapter the author briefly looks at the role of radiotherapy generally, but focuses specifically on the effects of the treatment couch on the treatment plan and consequent dosimetry.

2.2 Aim of radiotherapy

The obvious overriding purpose of radiotherapy is to treat cancer patients using radiation, and it is noted that radiation is potentially a dangerous modality and should not be applied without some care and thought to specific protocols. Radiotherapy involves a knowledge of multiple processes including radiation safety (Owadally & Staffurth, 2015, Evans & Staffurth, 2017).

Radiation is an important modality in the treatment and potential cure of cancer patients (Kirthi Koushik et al., 2013). It is the definitive treatment of choice for many cancers, but also plays an important role when patients may not be eligible or suitable for other modalities, such as surgery and/or chemotherapy (Evans & Staffurth, 2017). Even if cure is not an option (e.g. when dealing with advanced cancers), radiotherapy often still plays a vital role in minimising symptoms, such as pain, or obstructions (American Cancer Society, 2016).

A primary aim of radiotherapy is to administer a high enough radiation dose to the tumour target region in order to 'kill' the tumour (Hayashi et al., 2009). At the same time it is essential to aim for a favourable therapeutic ratio; give as much radiation dose as possible to the tumour area, while trying to keep the radiation dose to the surrounding, normal tissue as low as possible and within normal tissue dose tolerance (Cherry & Duxbury, 2009, Kirthi Koushik et al., 2013, Zeman et al., 2013, Hussain & Muhammad, 2017). This is achieved by planning the delivery in such a way that the treatment beams cover the target area, while trying to avoid the normal tissue and critical structures in order to minimise the radiation dose to these areas (Buzdar et al., 2013). Rather than having a single radiation beam aimed at the target area, it is advantageous to have multiple gantry angles for multiple beams (Sheykhoo et al., 2017). Therefore, multiple radiation beams are employed to facilitate a uniform dose around the target volume, while minimising the dose in the surrounding normal tissues (Podgorsak, 2005). Achieving the primary aim of radiotherapy is complicated by a multiplicity of factors, which include: voluntary and involuntary movement of the patient; setup variations; and attenuation of the beam by setup and positioning devices, for example, the treatment couch (Yu et al., 2017). The use of digital advanced technology can make the accurate treatment of the patient more readily achievable (Abshire & Lang, 2018).

However, technology is not all that is important. Knowledge, expertise and proper examination and diagnosis of the patient, as well as the skill and experience of the operatives at all stages in the process, still play a major role in radiotherapy. Radiotherapy can only produce good and

ethical results if it is remembered that the patient's clinical context is still the most important factor in determining the optimal treatment. For example, it will not be appropriate (or perhaps even ethical) putting a patient through a prolonged, radical radiotherapy regime if the patient has metastatic disease, or has some other severe, life-threatening medical condition (Barrett et al., 2009).

2.3 Side-effects of radiotherapy

In most cases the tumour area that is being treated by radiotherapy is surrounded by normal tissue and/or critical structures. This is one of the reasons for the side-effects of radiotherapy. These side-effects determine the radiation dose that can be administered to the patients. The type of side-effects will be determined by a number of factors, including the total dose, dose per fraction, the type of tissue, and the volume of the treated area (Kirthi Koushik et al., 2013).

In external beam radiotherapy part of the skin is always in the path of the radiation beam, and it follows that a common side effect of radiotherapy is acute skin reaction (Bolderston et al., 2006, Harris et al., 2012, Leventhal & Young, 2017). Up to 95% of all patients who receive radiation therapy may experience radiation-induced skin injury (Leventhal & Young, 2017) and in some cases this could lead to a situation where the full planned radiation dose cannot be delivered to the patient (Harris et al., 2012). These skin reactions can range from erythema and dry desquamation, up to moist desquamation and even ulceration in very severe cases (Bolderston et al., 2006). Further chronic skin effects as a result of radiation therapy can include skin atrophy, telangiectasis and fibrosis (Leventhal & Young, 2017).

Various factors can influence the risk of radiotherapy-induced skin reactions. Some of these factors are intrinsic to the patient, for example, age of the patient, diabetes, obesity (Collins, 2018), malnutrition, smoking, excessive skin folds, underlying vascular or connective tissue disease, and genetic factors, for example inherited DNA repair deficiencies (Leventhal & Young, 2017). As can be expected, other factors are radiotherapy specific and these include the location of the treatment area, high doses to large treatment fields (Collins, 2018), the energy of the radiation beams, the total radiation dose, the fractionation schedule, and combination of the radiation therapy with chemotherapy (Leventhal & Young, 2017). In addition to these factors, skin infections or the use of chemical substances (for example deodorants and perfumes) can also increase the radiation reaction experienced by the patient (Collins, 2018).

2.4 Accuracy of radiotherapy

There is risk for errors in any system, but if we understand what the risks are, protocols and procedures can be formulated so that any potential errors can be avoided, or at least caught

before they cause damage. The actions of individual people can result in errors, but the working environment and procedures put in place by the organisation can help to focus these actions. Any change in the work practice procedures could involve an additional risk for error, unless care is taken and the matching procedures updated to reflect the change (The Royal College of Radiologists et al., 2008). It is vitally important, therefore, to have a robust dosimetric quality assurance programme in place for all aspects of radiotherapy in order to ensure that the patients' treatments are completed correctly and safely (Vieira et al., 2003).

It is the responsibility of the multidisciplinary radiotherapy department to ensure that the delicate balance between treating the disease competently with its accompanying side-effects is not marred by errors or untoward incidents during any of the multiple processes that form part of the radiotherapy journey of the patient (The Royal College of Radiologists et al., 2008).

Accuracy in radiotherapy is of critical importance because we are dealing with people's health and lives. On a basic level, if the target area was not correctly determined, or if the dose is not delivered correctly to this target area, it may adversely impact on the efficacy of the treatment on the tumour, or increase normal tissue or critical structure complications (Buzdar et al., 2013).

Every step in the radiotherapy process, whether it be treatment planning, the actual treatment, or the dosimetry thereof, carries risk. This is because an error in any of these steps can have serious implications for the patient's treatment efficacy or safety. That is why the industry is always striving for technological advancements in radiotherapy which will allow more accurate and effective treatments for the patients. However, with this technology there is also additional susceptibility for error, not only because of the added complexities of these technologies and the introduction of more automated radiotherapy techniques, but also human error. The complexities of modern radiotherapy techniques require robust and comprehensive quality assurance programmes to ensure that any potential error in the correct treatment of the patient is detected before it occurs, and eliminated (Malicki, 2012).

Venselaar et al. (2001) stated that in order to deliver successful radiotherapy treatment to a cancer patient it is vital to reduce errors and uncertainties during the dose calculation phase, but the dose calculation is just one step amongst many in the whole radiotherapy process. Venselaar et al. (2001) stated that for a successful delivery of radiotherapy an overall accuracy of $\pm 3.5\%$ is required when considering the dose delivered to the ICRU specification point. This leaves a very small margin for error in the dose calculation phase. Ahnesjo and Aspradakis (1999) determined that for future development the goal for accuracy in radiotherapy can be 2% for the dose calculation phase, and an overall accuracy of 3%.

2.5 History of couch tops

Practitioners in the field of radiotherapy have always been looking at improving radiotherapy couches. An example of this is reported in a 1961 article in the British Medical Journal which described how a new radiotherapy couch was designed and built because the standard couch did not meet all the needs of the radiotherapy department at St. Thomas Hospital in London (Wiernik, 1961). The new features required were that the couch top be adjustable in various directions horizontally, as well as vertically; and the ability to move the whole couch in any direction. Nowadays these are the standard features that are found in modern radiotherapy couch units.

Linac treatment couches originally featured a tennis-racket portion in order to reduce the amount of beam attenuation and skin dose at the radiation beam entrance/exit caused from the denser material of the couch (Sheykhoo et al., 2017). The disadvantage of the tennis-racket, however, was its lack of rigidity, and over time this resulted in loss of elasticity and a subsequent increase in the 'sag' of the patient, which resulted in set-up inaccuracies (Opoku et al., 2012). Thus manufacturers started looking at other materials for couch tops, such as carbon fibre (Opoku et al., 2012, Sheykhoo et al., 2017).

De Mooy (1991) was one of the first authors to describe carbon fibre as a material for use in the manufacture of radiotherapy devices. He describes how they started to explore and manufacture various patient support structures from carbon fibre inhouse in the Radiotherapy Department at The Netherlands Cancer Institute.

The characteristics which are required for couch material for use in radiotherapy are high permeability, rigidity to prevent sagging and to properly support the patient, and it must not increase the surface dose to the patient (Tamura et al., 2018).

Apart from the couch needing to be made from a material which is suitable for the megavoltage treatment doses, many departments are moving towards advanced techniques such as intensity-modulated radiation therapy (IMRT) and image guided radiotherapy (IGRT) where the location of the target volume needs to be verified for each treatment on the treatment unit. This means that the couch material must be suitable for patient dose-delivery, as well as on-line imaging (Njeh et al., 2012).

2.6 Carbon fibre as a material for treatment couches

Carbon fibre is a material well suited to be used in the construction of radiotherapy treatment couches. Carbon fibre has a high specific strength as well as a high modulus of elasticity (De

Ost et al., 1997). Because of its strength, carbon fibre reduces sagging of the treatment couch under the weight of the patient (McCormack et al., 2005) and does not require strengthening steel frames (Pope et al., 2007). In addition, carbon fibre is lightweight and it has good radiolucent or radio-transparent properties (De Ost et al., 1997, Myint et al., 2006, Pope et al., 2007, Mihaylov et al., 2009, Sedaghatian et al., 2017) due to its low density. Initially, the high cost of carbon fibre was a disadvantage for general use in radiotherapy, however once sporting equipment companies started using it for the manufacture of sports equipment, the cost decreased and this made it a more viable material for many applications (De Mooy, 1991).

Meara and Langmack (1998) have shown that carbon fibre has lower percentage build-up values than other materials (for example polymethylmethacrylate (PMMA) and polyethylene terephthalate glycol (PETG) copolyester) traditionally used in radiotherapy. They used three different carbon fibre sandwich construction samples for their study and found that the percentage build-up values for the carbon fibre samples varied between 36% and 59% (using 5 MV, 6 MV and 8 MV energy beams), compared to between 62% and 97% for the other materials.

Seppala and Kulmala (2011) investigated the increased beam attenuation and surface dose produced by eight different couch tops, including the Varian IGRT couch. Their study also highlighted the favourable characteristics of carbon fibre for treatment couches, including its high specific strength and high beam transmission (radiolucency). Table 2.1 and Table 2.2 demonstrate the attenuation and surface dose effects of the different couches used in the study. The maximum attenuation produced by the Varian IGRT couch for 6 MV was 4.7% and the surface dose for 6 MV was 90.8% and 94.0% of the dose at D_{max} for 10 x 10 and 20 x 20, respectively.

Table 2.1: Comparison of the beam attenuation as a result of the different couch tops and inserts

(Seppala & Kulmala, 2011:4)

| | 6 MV | | | 15 MV | | |
|--------------------------|---------|------|----------------------|---------|------|----------------------|
| | GA 180° | Max. | Average (100° -180°) | GA 180° | Max. | Average (100° -180°) |
| BrainLAB | 3.6 | 8.7 | 5.0 | 2.4 | 5.9 | 3.3 |
| Qfix kVue Standard | 2.1 | 5.2 | 2.9 | 1.4 | 3.3 | 1.9 |
| MEDTEC | 1.9 | 7.1 | 2.9 | 1.5 | 5.0 | 2.1 |
| Varian Exact IGRT | 1.9 | 4.7 | 2.4 | 1.3 | 3.1 | 1.6 |
| DIGNITY AirPlate | 1.9 | 3.6 | 2.3 | 1.2 | 2.4 | 1.5 |
| Universal Sandwich Panel | 1.5 | 7.3 | 2.8 | 1.0 | 5.0 | 2.0 |
| Qfix kVue DoseMax | 1.3 | 8.1 | 2.2 | 1.0 | 5.4 | 1.4 |
| Varian Grid Insert | 0.3 | 10.8 | 1.3 | 0.2 | 7.4 | 0.9 |

Table 2.2: Comparison of the surface doses as a result of the couch tops and inserts

(Seppala & Kulmala, 2011)

| | 6 MV | | 15 MV | |
|--------------------------|-----------------------|-----------------------|-----------------------|-----------------------|
| | 10×10 cm ² | 20×20 cm ² | 10×10 cm ² | 20×20 cm ² |
| Measured Surface Dose | 44.3 | 53.4 | 27.6 | 39.1 |
| Corrected Surface Dose | 35.2 | 44.3 | 21.0 | 32.6 |
| Dose at Dmax | 100.0 | 100.0 | 100.0 | 100.0 |
| BrainLAB | 98.6 | 99.4 | 84.5 | 89.9 |
| Varian Exact IGRT | 90.8 | 94.0 | 69.6 | 77.7 |
| Universal Sandwich Panel | 90.2 | 93.2 | 69.2 | 76.9 |
| MEDTEC | 90.1 | 93.4 | 69.1 | 77.3 |
| Qfix kVue Standard | 88.5 | 92.1 | 66.9 | 75.2 |
| DIGNITY AirPlate | 86.0 | 89.8 | 66.0 | 74.3 |
| Qfix kVue DoseMax | 75.1 | 80.9 | 52.8 | 63.0 |
| Varian Grid Insert | 61.2 | 69.0 | 41.0 | 51.7 |

2.7 Problems of carbon fibre

As seen in Section 2.6, carbon fibre has many properties which make it very suitable for use in the manufacture of devices in radiotherapy, and thus it is important to consider the carbon fibre couch influence on the radiation beam, especially for larger incident beam angles (McCormack et al., 2005, Poppe et al., 2007). The attenuation of the dose at the isocentre by the couch top should not be ignored, and it should be taken into account and corrected for in the dose calculations of treatment planning (Meydanci & Kemikler, 2008). Mihaylov et al. (2008) pointed out that it is very important to not ignore these effects for the sake of correct calculation of the dose and for patient quality assurance. According to Chyou and Lorenz (2017) ignoring the attenuation effect of the treatment couch can result in significant dosimetry errors.

Furthermore, Langmack (2012) pointed out that carbon fibre has several other practical disadvantages. First, specialised equipment and skill are required to manufacture devices from carbon fibre and this makes the devices expensive. Second, carbon fibre is also not ideal material for use as a couch top or immobilisation device in magnetic resonance imaging (MRI) scanners as it is a conductive material. Thus, when carbon fibre is used in an MRI scanner, eddy currents can be produced, and this can result in the carbon fibre heating up and causing radiofrequency (RF) shadowing artefacts in MRI imaging (Langmack, 2012, Opoku et al., 2012). In their study to assess RF heating and MR image quality effects Jafar et al. (2016) noted the RF shadowing effect of the carbon fibre flatbed insert when used in MRI imaging for radiotherapy planning.

Carbon fibre itself is also expensive and thus is not always a feasible option for a department, especially in developing countries where budgets may be limited (Opoku et al., 2012).

2.8 Other materials for treatment couches

According to Langmack (2012) new composite materials are being developed which have similar strength and radiolucency properties to carbon fibre. Many of these composites can be crafted in a standard well-equipped workshop. This tends to make them more cost effective than carbon fibre. They are also not conductive and therefore can be used as MRI imaging accessories. An example of this type of composite is a composite consisting of fibre glass and polypropylene.

Opoku et al. (2012) demonstrated in their study of couch top transmission factors that even in this technological age, a 'low-tech' material such as wood is still an option for radiotherapy treatment couch tops, as it is light and rigid. They noted, however, that with cobalt-60 wood does not have the properties of radiolucency, and that further analysis of the surface doses was needed for the wooden couch top.

Tamura et al. (2018) describe a couch top, called the HM couch, consisting of two thin layers of glass fibre 'sandwiching' a layer of polycarbonate foam. The polycarbonate is very light and has a high weight resistance. It is also strong, rigid and solid. Tamura et al. (2018) have shown in their study that this couch resulted in a lower skin toxicity than a carbon fibre couch. The HM couch succeeded in reducing the surface doses by 7.9% for 6 MV photons and by 9.9% for 10 MV photon compared to the carbon fibre.

2.9 Effects of the radiotherapy couch

2.9.1 General effects

Treating a patient through the treatment couch has certain effects to the treatment plan, namely: an increase in the skin/surface dose; and, a reduction in the dose which reaches the target area (McCormack et al., 2005, Sedaghatian et al., 2017).

Vanetti et al. (2009) noted that there can be significant errors in the dose which can have a clinical significance if the treatment couch is omitted from the dose calculations, particularly in the case of lower beam energies and for rotation therapies, such as IMRT and Varian RapidArc™. Their study used the Varian IGRT couch model provided on the Eclipse treatment planning system.

The next sections look in more detail at the attenuation of the beam and surface dose effects that result from the radiation beam in contact with the couch top.

2.9.2 Attenuation effects

Many studies have investigated the attenuation effect of treatment couches and the various factors that influence the degree of attenuation produced by the treatment couch, or the inserts, when placed in the path of the beam. These factors include: the type of material that the couch or inserts are made from; the gantry angle (or more correctly the incident angle of the beam relative to the orientation of the couch or insert); the field size of the beam; and, the energy of the radiation. The effects of these factors have been demonstrated by various researchers.

2.9.2.1 Type of material

One of the earlier studies which investigated the attenuation effect of carbon fibre on high energy photon beams was by De Ost et al. (1997) who used various types of carbon fibre inserts, as well as inserts made from Plexiglass (PMMA) and wooden hardboard. These inserts were all positioned as for patients' treatment. They found two effects of these inserts on the radiation beams: an increase in the surface dose; and attenuation of the radiation beam.

In terms of the transmission of radiation through the inserts, De Ost et al. (1997) found that all the materials tested allowed between 95% and 100% transmission of the radiation. The carbon fibre performed better, allowing between 99% and 100% transmission. The study concluded that even though carbon fibre is translucent, the effect carbon fibre has on the beam must still be considered when in clinical use. This is also because of its effect on surface dose and thus on the skin-sparing effect for the patient's treatment plan. It must be noted that this study investigated the older technology carbon fibre inserts.

A further study by Meara and Langmack (1998) also investigated the feasibility of using carbon fibre for radiotherapy. They looked at three different samples of carbon fibre in the form of sandwich panels, as well as polymethylmethacrylate (PMMA) and PETG copolyester. The study found that the carbon fibre samples all had better transmission than the other materials tested. For all the carbon fibre samples the percentage transmission was better than 99%, compared to about 95% and 98% for the other materials.

Seppala and Kulmala (2011) investigated the increased beam attenuation and surface dose by different treatment couches. They looked at eight different couch tops, including the Varian IGRT couch. Their study also highlighted the favourable characteristics of carbon fibre for treatment couches, including its high specific strength and high beam transmission (radiolucency). The study looked at two beam energies, 6 MV and 15 MV, using a Varian 2100 C/D linear accelerator. The measurements were all done in a cylindrical Plexiglass (PMMA) phantom. The field size for all the measurements was 10 cm x 10 cm. For the beam attenuation measurements they used multiple gantry angles from 90° to 180° in 5° increments.

Seppala and Kulmala (2011) found that the type of couch (possibly due to manufacturing processes and different material compositions), beam energy and gantry angle all played roles in the beam attenuation by the couch. For the 6 MV beam the maximum attenuation ranged from 3.6% to 10.8% with the Varian IGRT couch producing 4.7% attenuation. For the 15 MV beam the maximum attenuation was between 2.4% and 7.4%. Here the Varian IGRT couch resulted in an attenuation of 3.1%.

In conclusion, Seppala and Kulmala (2011) suggested that the beam attenuation and influence on surface dose by the couch needs to be mathematically modelled to ensure dose accuracy to the patients and to quantify the skin doses.

2.9.2.2 Incident angle

McCormack et al. (2005) specifically studied the effect of the gantry angle on the amount of attenuation caused by the carbon fibre couch inserts. The treatment couch used for the study was a C-arm type consisting of a thin Melinex ® polyester film sheet (approximately 0.35 mm thick) and a removable Sinmed Posisert insert panel. The panel construction consisted of two layers of 0.5 mm carbon fibre on either side of a high impact polystyrene foam. The dimensions of the panel were 805 mm long, 500 mm wide and 27 mm in thickness.

All the measurements were done using the Electra SLi linear accelerator using the 6 MV photon energy and a field size of 10 x 5 cm². For the measurements they used a digital electrometer (SN4, PTW Freiburg), a 0.125 cm³ thimble ionisation chamber (TM31002-1089, PTW Freiburg) and a 15 cm diameter solid water phantom (WT1). They placed the chamber in the centre of the water phantom, and the phantom was positioned so that the chamber was at the isocentre with a SAD of 100 cm. The measurements were done at eight different gantry angles starting at 180° (the beam at normal incidence to the carbon fibre insert) and then rotating the gantry towards the horizontal in 10° increments. This means that the angle of incidence ranged from 0° to 70°. The measurements were done with the beam passing through the carbon fibre insert and then again with the carbon fibre insert removed. Here the phantom was repositioned so that the chamber was again at the isocentre.

McCormack et al. (2005) found that there was a significant increase in the attenuation of the beam with increasing angle of incidence. The attenuation ranged from 2.2% for the 0° incidence to 8.7% for the 70° incidence. They also pointed out that each department should assess the influence of all ancillary therapy equipment for themselves and not rely on the findings of other departments as the structure of the carbon fibre and couch might not be perfectly uniform throughout.

Even though McCormack et al. (2005) used a different couch than the one that was used by the researcher in this study, it illustrates the importance of taking the gantry angle into account when the beam passes through the treatment couch.

Munjal et al. (2006) performed a study to investigate the impact of beam attenuation by a carbon fibre couch and other immobilisation devices on the planning and treatment in IMRT. They noted that although many treatment planning systems have the capability to calculate direct beam incident attenuation factors, most treatment planning systems do not account for the attenuation for oblique incident angles.

Munjal et al. (2006) used the 6 MV photon beam on a Siemens PRIMUS KXE2 linear accelerator and a MED-TEC (USA) carbon fibre treatment couch. The couch had a tennis racket covered with a Mylar sheet and was equipped with side rails. The dose measurements were performed using a CAPINTEC-CII Wellhofer electrometer and an IC-15 ion chamber. To evaluate the attenuation by the couch alone Munjal et al. (2006) fitted the detector with a build-up cap and positioned the detector on a stand in air so that the detector was at the isocentre. The doses were measured at multiple gantry angles from 0° to 360° in 10° increments.

Munjal et al. (2006) found that the attenuation by the carbon fibre couch was significant. The maximum attenuation they measured was 2.96% at the oblique angle of 120° (incident angle of 60°). At 180° (normal incident angle of 0°) the attenuation was 1.22%. This study further showed that attenuation is dependent on the incident angle of the beam to the couch.

Poppe et al. (2007) also investigated the changes in the surface dose and attenuation of radiation due to carbon fibre couches. One of the advantages they emphasised for the use of carbon fibre for couch tops, is that carbon fibre is strong and does not require strengthening steel frames. This, together with the relatively radiolucent property of carbon fibre, makes these couches less of a limiting factor for the gantry angle of the treatment unit. However, it is noted that it is still important to consider the couch influence on the radiation beam, particularly for the larger incident beam angles. This study was done for two gantry angles (150° and 180°), and two photon energies, 6 MV and 10 MV. The carbon fibre couch they used in the study was a RM2/4 tabletop. In addition to the carbon fibre couch, they also had a carbon fibre accessory board in place that was used for the treatments.

Poppe et al. (2007) found that the carbon fibre (just the carbon fibre couch) had transmissions of between 96% and 98% for the 6 MV beams, and between 97% and 98% for the 10 MV beams, respectively. For both energies the transmission was less for the oblique angle of

150%. Poppe et al. (2007) concluded that the effect of carbon fibre couches on the radiation beam must be carefully considered.

Meydanci and Kemikler (2008) also investigated the attenuation of the beam and a change in the surface dose caused by the carbon fibre couch. They included smaller field sizes in their study and depth doses and surface doses were measured for 2 x 2 cm, 3 x 3 cm, 4 x 4 cm, 5 x 5 cm, 10 x 10 cm, 25 x 25 cm, and 40 x 40 cm at a 0° gantry angle with a Markus parallel-plate chamber (23343; PTW). The measurements were all performed using the Oncor Impression IMRT+ linear accelerator (Siemens) utilising both the 6 MV and 18 MV photon energies. The carbon fibre couch top was from Reuther Medizin Technik (Mülheim-Kärlich, Germany). The couch top had a hollow construction and the carbon fibre outer wall thickness was between 0.6 and 0.8 mm. The dimensions of the couch top were 50 x 230 x 12 cm and the density was 1.8 g.cm⁻³.

For the attenuation measurements for oblique fields, Meydanci and Kemikler (2008) used a 25 cm diameter cylindrical polystyrene phantom with a 0.125 cm³ semi-flexible ionisation chamber (TM31010-0789; PTW, Freiburg, Germany) and digital electrometer (Unidos; PTW, Freiburg, Germany). The chamber was positioned in the centre on the phantom and the phantom position on the couch top with the chamber at the isocentre at 100 SAD. Only a 10 x 10 cm field was used for these oblique field attenuation measurements. The measurements were done with the gantry angle ranging from 0° to 180°.

Meydanci and Kemikler (2008) found that the attenuation caused by the carbon fibre couch top increased as the incident angle increased for both photon energies. For 180° (0° incident angle) the attenuation was 3% and 2% for 6 MV and 18 MV, respectively. The maximum attenuation was found to be at 120° (60° incident angle) and was 5.6% and 4% for 6 MV and 18 MV, respectively. Meydanci and Kemikler (2008) concluded that the attenuation of the dose at the isocentre by the couch top should not be ignored but should be taken into account and corrected.

In Japan, Hayashi et al. (2010) also investigated the effect of carbon fibre couch tops on photon beams. In this study Hayashi et al. (2010) did a series of four phantom measurements. For all the series they used the following detectors: a Ramtec 1000plus digital electrometer (TOYO-Medic Co. Ltd., Tokyo, Japan); and a 0.125 cm³ thimble ionisation chamber (PTW, Freiburg, Germany). In one of the series they looked specifically at the effect of the angle on the attenuation by the treatment couch. They used two treatment couches, their old couch, the Exact Couch Top (ECT: Varian Medical Systems, Palo Alto, CA, USA) and their current couch, the Imaging Couch Top (ICT). The ICT is 5 cm thick and is constructed from solid carbon fibre

without any mesh areas. In this measurement series Hayashi et al. (2010) compared the beam attenuation by the couches at different gantry angles. They used a 16 cm diameter spherical water-equivalent phantom (ST-1100: Elimpex-Medizintechnik, Moedling, Austria). The chamber was placed in the centre of the phantom and the phantom positioned so that the chamber was at the isocentre. The phantom was placed on both types of couches, and also placed in such a way that the beam did not pass through any other material before it entered the phantom. The gantry angles used were from 0° to 330° in 30° increments. The field sizes ranged from 4.2 x 4.2 cm to 10 x 10 cm.

Hayashi et al.'s (2010) results showed that the gantry angle is a factor in the amount of beam attenuation. For both couches significant attenuation was measured for gantry angles between 120° and 240°. Attenuation was the highest for both couches at the oblique angles of 120° and 240°.

Further research investigated the dose impact on IMRT and volumetric modulated arc therapy (VMAT) due to attenuation of the beam by the treatment couch, and a study by Li et al. (2011) measured the attenuation of two Varian couches, the standard Varian Exact couch with sliding support rails and the Varian Exact IGRT couch. The review of this study focuses on Li et al.'s (2011) results for the IGRT couch as that is the type of couch which has been used by the researcher at the study site where the research for this thesis was performed.

Li et al. (2011) pointed out that posterior oblique beams are used routinely in IMRT and VMAT, and that attenuation of the beam by the couch is significant when these beams pass through the couch. The measurements were done for both 6 MV and 18 MV photon beams on two Varian Clinac 21EX linear accelerators. One of the linear accelerators had the standard couch fitted and the other one the IGRT couch. The IGRT couch is manufactured from carbon fibre and the thickness of the couch varies from superior to inferior. A CIVCO (Kalona, IA) cylindrical acrylic MTQA 1500 phantom and a Farmer ion chamber (PTW, Freiburg, Germany) were used for the measurements. The Farmer chamber was inserted in the centre of the phantom and the phantom then positioned so that the Farmer chamber was at the isocentre of the linear accelerator. The chamber was used to measure the relative dose. To determine a reference dose (where no attenuation occurred) they measured doses at 0°, 90° and 270° gantry angles and used the mean of these doses. At these angles the beams did not pass through the couches. Next, measurements were taken for gantry angles from 180° to 270° and from 90° to 270° in 2° steps. All these measurements were taken for both photon energies, both couches and for different field sizes. The field sizes used were 3 x 3 cm, 5 x 5 cm and 10 x 10 cm. The measurements were taken on both the couches at two levels along the longitudinal axis, at the levels where an adult patient's head and pelvis would be positioned.

Li et al. (2011) found that for the IGRT couch the amount of attenuation by the couch was not so strongly dependent on the angle of the beam as for the standard couch with the support rails, but that the gantry angle still affected the amount of attenuation.

Seppala and Kulmala (2011) investigated the increased beam attenuation and surface dose of eight different couch tops, including the Varian IGRT couch. The study used two beam energies, 6 MV and 15 MV, of a Varian 2100 C/D linear accelerator. The measurements were all completed using a cylindrical Plexiglass (PMMA) phantom. The field size for all the measurements was 10 cm x 10 cm. For the beam attenuation measurements multiple gantry angles from 90° to 180° in 5° increments were used.

Seppala and Kulmala (2011) found that the type of couch, beam energy and gantry angle all played roles in the beam attenuation by the couch and that the amount of attenuation increased as the incident angle increased. For the 6 MV beam the maximum attenuation ranged from 3.6% to 10.8% with the Varian IGRT couch producing 4.7% attenuation. For the 15 MV beam the maximum attenuation was between 2.4% and 7.4%. Here the Varian IGRT couch resulted in an attenuation of 3.1%.

In their study to develop a couch model for their planning system, Van Prooijen et al. (2010) also found that the incident angle played a role in the amount of attenuation caused by the couch. They further found that the steeper the incident angle, the higher the degree of attenuation by the couch. From their data it looks like the attenuation increased from about 3.5% to almost 6% as the gantry angle increased from 217° to 222°. There were higher attenuation values as well, almost 18% at 237°, but the couch has movable rails and these high attenuation values could be due to the denser couch rails.

Njeh et al. (2009) investigated the attenuation effect of the BrainLAB carbon fibre imaging couch (Feldkirchen, Germany) for various beam angles on the Novalis Tx™ treatment unit. They used a 0.65 cm³ Farmer-type Exradin model A12 ionization chamber, (Standard Imaging, Middleton, WI, USA), a Max 4000 electrometer (Standard Imaging, Middleton, WI, USA), a delrin (1.42 g/cm³) cylindrical build-up cap (1.4 cm thick) for the 6 MV, and a brass (8.455 g/cm³) cylindrical build-up cap (0.8 cm thick) for the 18 MV measurements. The gantry angles used for the measurements were 180° (0° incident angle on the couch) and counter-clockwise in 10° increments to 90° for both a 5 x 5 cm field size and a 10 x 10 cm field size. The results concurred with other studies that the degree of attenuation by the treatment couch is dependent on the gantry angle. For 6 MV the highest attenuation measured was 10% at gantry

angle of 120° (for the 5 x 5 cm field size). For 18 MV the highest was 3.7% at 110° (also for the 5 x 5 cm fields size).

2.9.2.3 Field size

Myint et al. (2006) studied the treatment dose error due to beam attenuation by a carbon fibre couch top. They measured the attenuation of the photon beams travelling obliquely through the carbon fibre support rails of a treatment couch. The study included both 6 MV and 18 MV photon energies on a Siemens Mevatron linear accelerator at the Ottawa Hospital Regional Cancer Centre. The treatment couch used in this study was a Medtec indexed patient positioning system (IPPS™). The treatment couch consisted of carbon fibre rails and grid panels. This was another study which has shown that both field size and beam energy have an effect on the attenuation of the beam by a treatment couch. Here both the in-air and in-phantom measurements showed similar tendencies. The largest attenuation of 16.2% was found for the smaller field size of 5 x 5 cm and the lower energy of 6 MV.

Measurements were done both in air and within a phantom. The in-air and in-phantom measurements were taken at various positions along the longitudinal axis of the couch, covering the solid region of the couch, as well as the strut region. For the in-air measurements they used an RK Chamber (model 8305) and Keithley Therapy Dosimeter (model 35040). Here a 0.4 cm thick brass build-up cap was used for the 6 MV photon beam, and a 0.8 cm thick brass build-up cap for 18 MV photon beam. A 20 x 20 x 20 cm³ acrylic block phantom was used for the in-phantom measurements. Here a NE 2571 ion chamber and NE 2570 electrometer were used with the chamber positioned at the centre of the phantom. The measurements were done both for the beam passing through the couch rails, as well as not passing through the couch rails. For both beam energies field sizes of 5 x 5 cm and 10 x 10 cm were used. All the measurements were done with a gantry angle of 225°. Myint et al. (2006) chose this angle because it is commonly used in radiotherapy and it maximised the amount of carbon fibre in the path of the beam.

Hayashi et al. (2010) investigated the attenuation through two couch tops, the Exact Couch Top (ECT: Varian Medical Systems, Palo Alto, CA, USA) and the Imaging Couch Top (ICT). The study used the following equipment: a Ramtec 1000plus digital electrometer (TOYO-Medic Co. Ltd., Tokyo, Japan) and a 0.125 cm³ thimble ionisation chamber (PTW, Freiburg, Germany); and a water-equivalent phantom (Tough Water phantom, Kyoto Kagaku Co. Ltd., Kyoto, Japan) with the chamber inserted 10 cm from the base of the phantom. The phantom was irradiated from the posterior using a 6 MV photon beam through the ECT (both through the mesh part and the solid part) and through the ICT, and without any couch material in the

beam. A SAD of 100 cm was used with the following field sizes: 4.2 x 4.2 cm, 6 x 6 cm, 8 x 8 cm and 10 x 10 cm.

Their results showed that there was a reduction in the dose by the carbon fibre and that this was dependent on the field size with the attenuation larger for the smaller field sizes. For the ECT this attenuation ranged from 5.61% and 0.41% (through the solid and through the mesh parts respectively) for the 4.2 x 4.2 cm field size; and 4.90% and 0.22% (through the solid and through the mesh parts, respectively) for the 10 x 10 cm field size. For the ICT the attenuation ranged from 5.07% for the 4.2 x 4.2 cm size to 4.31% for the 10 x 10 cm size.

Although Hayashi et al. (2010) investigated different couches to that used in this research study, their study shows that carbon fibre couch tops in general can have a significant effect on the attenuation of the beam and that the gantry angle and field size play a significant role in the amount of beam attenuation.

Sheykhoo et al. (2017) investigated the Monte Carlo simulations of the effects of the treatment couch. This study seems to involve only Monte Carlo simulations, but it has been included in this literature review for completeness. The study first verified that there was satisfactory agreement between the Monte Carlo calculations and measured data for various situations. In the study the 6 MV photon beam of the Siemens Primus Plus linear accelerator, and the 550 TXT couch with TT-D carbon fiber table top (Siemens MedicalSolution, Erlangen, Germany) were simulated for three field sizes (5 x 5 cm, 10 x 10 cm, and 20 x 20 cm). Here it was also shown that the degree of attenuation due to the treatment couch increases as field size decreases.

Tugrul (2018) investigated the attenuation effect of the CIVCO carbon fibre couch and field size on the dose and they looked at 3 x 3 cm, 5 x 5 cm, 10 x 10 cm and 15 x 15 cm field sizes. The measurements were done with a 30 x 30 cm solid water phantom (PTW-RW3) and 0.6 cm³ PTW Farmer ion chamber for 6 MV and 15 MV photon beams. Tugrul's (2018) results were in agreement with the other studies discussed, where the study also found that the attenuation of the radiation beam by the couch decreases as the field size increases. For the 180° gantry angle the dose absorption ratios of the carbon fibre couch for 6 MV were 1.52%, 0.69%, 0.33% and 0.25% for the 3 x 3 cm, 5 x 5 cm, 10 x 10 cm and 15 x 15 cm field sizes, respectively, and for the 15 MV beam they were 0.95%, 0.27%, 0.20% and 0.05%

As discussed previously, Njeh et al. (2009) investigated the attenuation effect of the BrainLAB carbon fibre imaging couch (Feldkirchen, Germany) for two different field sizes (a 5 x 5 cm field size and a 10 x 10 cm field size) for various beam angles on the Novalis Tx™ treatment unit.

The results concurred with other studies that the degree of attenuation by the treatment couch is dependent on the field size. For both photon energies and most of the gantry angles the attenuation effect by the couch decreases as the field size increases. For 6 MV the 5 x 5 cm and 10 x 10 cm field sizes showed attenuation values of 4.9% and 3.4%, respectively. The pattern is less noticeable for the 18 MV energy, and in fact for 18 MV for the more oblique angles of 130° and steeper, it seemed as if there is an increase in the attenuation effect by the couch as field size increases (Table 2.3).

Table 2.3: 18 MV photon beam attenuation by the ICT couch
(Njeh et al., 2009:22)

| <i>Angle</i> | <i>Couch</i> | |
|--------------|-----------------|-------------------|
| | <i>5 × 5 cm</i> | <i>10 × 10 cm</i> |
| 100 | -0.5 | -1.3 |
| 110 | 3.7 | 3.5 |
| 120 | 3.6 | 3.4 |
| 130 | 2.1 | 2.1 |
| 140 | 1.3 | 1.4 |
| 150 | 0.9 | 1 |
| 160 | 0.7 | 0.9 |
| 170 | 0.6 | 0.8 |
| 180 | 0.6 | 0.7 |

Studies by Gerig et al. (2010) and Li et al. (2011) also demonstrated that the degree of radiation attenuation by the treatment couch is dependent on the field size and that the attenuation decreases as the energy and field size increases.

Li et al. (2011) investigated the attenuation by two Varian couches, the standard Varian Exact couch with sliding support rails and the Varian Exact IGRT couch. The measurements were done for both 6 MV and 18 MV photon beams on two Varian Clinac 21EX linear accelerators, one unit with the standard couch fitted and the other one, the IGRT couch.

The results of this study by Li et al. (2011) showed that for the 6 MV photon energy the dose differences due to the IGRT couch was between 3.8% and 4.8% for the 5 x 5 cm field size, and between 2.9% and 4.1% for the 10 x 10 cm field size. For a 5 x 5 cm field size and 6 MV

beam the maximum dose error at the level of the patient's head was 3.9%, and at the level of the pelvis it was 4.8%. For a 5 x 5 cm field size and 18 MV beam the maximum dose error at the level of the patient's head was 2.2% and at the level of the pelvis it was 3.2%.

2.9.2.4 Beam energy

Myint et al. (2006) investigated the beam attenuation of their treatment couch with both 6 MV and 18 MV photon energies on a Siemens Mevatron linear accelerator at the Ottawa Hospital Regional Cancer Centre. The treatment couch used in this study was a Medtec indexed patient positioning system (IPPS™) which consisted of carbon fibre rails and grid panels.

Myint et al.'s (2006) results showed that the beam energy affects the amount of beam attenuation caused by the treatment couch. Here both the in-air and in-phantom measurements showed similar tendencies. The largest attenuation of 16.2% was found for the smaller field size of 5 x 5 cm and the lower energy of 6 MV.

Poppe et al. (2007) when investigating the effect of the beam angle on changes in the attenuation of radiation due to carbon fibre couches used two gantry angles (150° and 180°), and two photon energies, 6 MV and 10 MV. They also confirmed that the amount of beam attenuation by the couch decreases as beam energy increases. Their results showed that the carbon fibre couch has transmissions of between 96% and 98% for the 6 MV beams and between 97% and 98% for the 10 MV beams, respectively.

Gerig et al. (2010) also investigated the influence of the beam energy on the attenuation effect by the treatment couch. The study used two types of carbon-fibre treatment couches, a CIVCO couch and a Medical Intelligence couch. These were placed in the radiation beam between the beam source and a phantom in which the dose was measured. The beam attenuation was measured at multiple gantry angles and for three photon energies 6 MV, 10 MV and 18 MV, on two treatment units.

Gerig et al. (2010) also found that the radiation attenuation due to the treatment couches decreased as the beam energy increases. For the CIVCO couch the maximum attenuation for the 6 MV energy was approximately 6.6%, and for the 18 MV energy it was approximately 4.4%. These were for a 10 x 10 cm field size on the Siemens linear accelerator.

Li et al. (2011) also demonstrated that the beam energy impacts the amount of attenuation of the beam by the treatment couch. They looked at the attenuation by two Varian couches, the standard Varian Exact couch with sliding support rails and the Varian Exact IGRT couch. Li et al. (2011) showed that for the 5 x 5 cm field size the dose differences due to the IGRT couch

were between 3.9% and 4.8% for the 6 MV photon energy, and between 2.2% and 3.2% for the 18 MV photon energy. For the standard couch (also for the 5 x 5 cm field size) the dose differences were between 5.0% and 13.3% for the 6 MV photon energy and between 3.6% and 8.3% for the 18 MV photon energy.

Seppala and Kulmala (2011) investigated the beam attenuation by the couch, and amongst other factors they looked at the influence of the beam energy. The study looked at eight different couch tops (including the Varian IGRT couch), two beam energies, 6 MV and 15 MV, using a Varian 2100 C/D linear accelerator.

Like the previous studies outlined, Seppala and Kulmala (2011) also found that the beam energy affected the amount of beam attenuation by the couch in that the amount of attenuation decreased with increasing beam energy. For the 6 MV beam the maximum attenuation ranged from 3.6% to 10.8% with the Varian IGRT couch producing 4.7% attenuation. For the 15 MV beam the maximum attenuation was between 2.4% and 7.4%. Here the Varian IGRT couch resulted in an attenuation of 3.1%. Kunz et al. (2010) in measuring the Varian IGRT couch concurred that the higher the beam energy the lower the attenuation.

Van Prooijen et al. (2010) studied two different couches. The Sinmed Mastercouch on the Elekta Synergy (Elekta, United Kingdom) linear accelerator and the Exact Couch system on the Varian Clinac (Varian Medical Systems, U.S.A.) linear accelerator. They found that for both couches (and for all the parts of the couches) the amount of attenuation decreases as the radiation energy increased.

Tugrul (2018) also looked at the attenuation effect of the CIVCO carbon fibre couch of the beam energy on the dose. Two photon beam energies, 6 MV and 15 MV, for 3 x 3 cm, 5 x 5 cm, 10 x 10 cm and 15 x 15 cm field sizes were measured using a 30 x 30 cm solid water phantom (PTW-RW3) and 0.6 cm³ PTW Farmer ion chamber. For beam energy their results were also in agreement with other studies in that the degree of attenuation of the radiation beam by the couch decreases as the beam energy increases. Tugrul's (2018) results were all for the 180° gantry angle where it was found that the dose absorption ratios of the carbon fibre couch for the 3 x 3 cm field size were 1.52% and 0.95% for 6 MV and 18 MV, respectively; for 5 x 5 cm they were 0.69% and 0.27%; for 10 x 10 cm they were 0.33% and 0.20%; and, for 15 x 15 cm they were 0.25% and 0.05%.

2.9.2.5 Entry position of beam

The effect of the entry position of the beam on the couch has been demonstrated by a number of researchers, including McCormack et al. (2005) who are often cited when looking at the

effect of the gantry angle. As a result of the changes in gantry angle the incident beam will enter different parts of the couch for each beam. Each beam then traverses different parts and thicknesses of the couch and this affects the degree of attenuation.

Kunz et al. (2010) measured the attenuation by the Varian IGRT couch at various positions on the couch and found that the thick part of the couch produces a higher attenuation than the thin section of the couch.

Li et al. (2011) studied different parts of the couch in terms of the attenuation experienced by two Varian couches, namely: the standard Varian Exact couch with sliding support rails, and the Varian Exact IGRT couch.

They took measurements for gantry angles from 180° to 270° and from 90° to 270° in 2° steps. All these measurements were taken for both 6 MV and 18 MV photon energies, both couches and for different field sizes. The field sizes used were 3 x 3 cm, 5 x 5 cm and 10 x 10 cm. The measurements were taken on both the couches at two levels along the longitudinal axis, at the levels where an adult patient's head and pelvis would lie.

Li et al. (2011) showed that for the 6 MV photon energy the dose differences due to the IGRT couch were between 3.8% and 4.8% for the 5 x 5 cm field size, and between 2.9% and 4.1% for the 10 x 10 cm field size. For a 5 x 5 cm field size and 6 MV beam the maximum dose error at the level of the patient's head was 3.9%, and at the level of the pelvis it was 4.8%. For a 5 x 5 cm field size and 18 MV beam the maximum dose error at the level of the patient's head was 2.2%, and at the level of the pelvis it was 3.2%. The higher dose error at the level of the pelvis could be because the couch is thicker at that level and therefore more attenuation is caused at that level.

2.9.2.6 A further study of interest

Opoku et al. (2012) investigated the effect of the couch on the dose at various treatment depths. Their study was done on a Cobalt-60 treatment unit and a wooden couch, but it is included in this review to demonstrate that regardless of the material used for the construction of the treatment couch the couch effect must be considered. Opoku et al. (2012) investigated the attenuation of the wooden couch as a function of the treatment depth for isocentric setups. The measurements were done for a 10 x 10 cm field size on the Cobalt-60 treatment unit. They used a Farmer-type 0.125 cc volume flexi cylindrical ionization chamber type, a PTW UNIDOS 10002 electrometer, a 40 cm x 40 cm x 2 cm wood sample (same material as the couch top) and a 30 cm x 30 cm Perspex phantom with slabs of 1 cm and 0.5 cm thicknesses (PTW type 2687 Perspex phantom). The incident angle of the beams to the phantom was 0°. The

ionisation chamber was placed in a 2 cm thick slab which fits the chamber. To ensure the required backscatter and electronic equilibrium the ionisation chamber was always 15 cm above the bottom of the phantom. Phantom slabs could then be placed on top of the chamber in order to vary the treatment distance from 1.5 cm to 13.5 cm in increments of 2 cm.

Opoku et al. (2012) found that the transmission factor for the couch decreased with increasing treatment depth. There was a 3.45% decrease in the transmission factor from 1.5 cm depth to 13.5 cm depth and the transmission factors were 0.960 and 0.928, respectively. They concluded that a single transmission factor to manually correct for the effect of the treatment couch may not be valid for all treatment depths and the variation of the transmission factor with depth should be included in the planning process.

2.9.3 Surface dose effects

The surface dose is defined as the dose which is deposited at the boundary between the air and the phantom (Devic et al., 2006), or the air and the patient's skin (Apipunyasopon et al., 2013).

Podgorsak (2005) explains that the maximum dose for megavoltage photon beams (for example the beams from linear accelerators) will occur at a certain depth below the skin/surface and not on the surface itself. The fact that the maximum dose falls below the surface and not on the surface is called the skin-sparing effect and is an important feature in megavoltage photon beams in that it reduces the dose to the skin and thus ensures that the skin is not necessarily a dose limiting structure. The surface dose is determined by the beam energy, as well as the field size. The higher the beam energy, the lower the surface dose will be. Furthermore, as the field size increases the surface dose will also increase for a given beam energy.

A report of task group No. 176 of the American Association of Physicists in Medicine (AAPM), refers to the skin dose as the ratio of the absorbed dose at 0.1 mm depth to the maximum absorbed dose along the central axis of the beam. The 0.1 mm is a good approximation for the depth of the basal cell layer of the skin (Olch et al., 2014).

As mentioned, the surface dose and the dose in the build-up region increases with field size. This is caused by an increase in the number of scattered electrons in the air and collimator system (Gursoy et al., 2018).

In general, the surface dose will be affected by electron contamination from the head of the linear accelerator, the incident angle of the radiation, beam modifiers, air gap, as well as the treatment technique (Eyadeh et al., 2017).

The degree of skin sparing is affected by contaminating electrons and many factors may determine the amount of electron contamination. The electron contamination can be increased when the source to skin distance is reduced, or if the field size is increased. The contamination can also increase when external materials are added into the beam and placed close to the patient (Carl & Vestergaard, 2000).

Skin sparing is jeopardised when radiation passes through devices which are next to the patient's skin, for example the treatment couch. This is especially a problem when dealing with specific techniques, such as: single fractions; hypofractionations; and overlapping stereotactic fields. If the treatment couch is ignored in the treatment planning system algorithms it can lead to a significant increase to the dose in the build-up region which the clinician might not be aware of. This increase in the dose in the build-up region is especially prevalent at the shallower depths (Chan et al., 2012).

Hoppe et al. (2008) studied acute skin toxicities experienced after stereotactic body radiation therapy for Stage I non-small-cell lung cancer. They found that a number of patients developed skin toxicities, these occurring specifically when treating lesions which were close to the skin of the posterior chest wall and when using fewer treatment fields. They surmised that this skin toxicity could be from a reduction in the skin sparing due to the beam having to pass through the couch and other immobilisation devices.

According to Tamura et al. (2018) various studies have shown that the radiation effects of using both a carbon fibre couch and immobilisation devices can result in at least grade 2 skin toxicity for stereotactic body radiation treatment. In their more recent study they wanted to establish if a polycarbonate couch would result in a lower skin dose than a carbon fibre couch. They compared a novel rigid couch (HM couch) and a carbon couch (iBeam Couchtop STANDARD, BrainLab, Heimstetten, Germany). They also had three low-density Styrofoam boards (1.5 cm, 3.0 cm and 5 cm thick) and compared the measurements for the carbon fibre couch, with the individual Styrofoam boards placed on the couch and without the styrofoam boards. The surface doses were measured on a TrueBeam (Varian Medical Systems, Palo Alto CA, USA) linear accelerator for both 6 MV and 10 MV photon beams using a solid water phantom (Gammex RMI, Miccleton WI, USA), and a Markus plane-parallel ionisation chamber (PTW, Freiburg, Germany). For all the beams the field size was 10 x 10 cm and the source to surface distance (SSD) was 100 cm.

Tamura et al. (2018) found that when comparing the two couch tops and the styrofoam board the surface dose for just the carbon fibre couch was highest. When using the carbon fibre couch with the 5.0 cm styrofoam board, or the HM couch, the surface dose was reduced by 7-9%.

Tamura et al. (2018) concluded that to reduce the skin dose on an existing carbon fibre couch a low-density material of at least 5 cm can be placed on the couch. However, this would introduce extra thickness in the couch-patient combination and could therefore increase the risk of collisions. Here it was noted that the HM couch was a good alternative because potentially it could reduce the skin dose to the same degree, but with reduced chance of collisions.

Mellenberg (1995) studied the effect devices had on the surface and build-up region doses if the devices were in the radiation beam. This study found that any material placed in the beam pathway to the patient would increase the surface and build-up region doses. This increase in surface dose could then potentially result in the skin also becoming a dose limiting organ. The increase in the surface and build-up region doses is primarily dependent on the thickness and density of the material.

Apart from an attenuation effect, De Ost et al. (1997) found that inserts in the path of the beam also caused an increase in the surface dose. All the inserts increased the surface dose as compared to a beam which did not pass through an insert (an open beam). Carbon fibre increased the surface dose less than Plexiglass and wood, but it was still significantly more than with the open beam. They also found that the increase in surface dose for all the inserts decreased as the photon energy increased. This included the high photon energy of 23 MV where the carbon fibre inserts increased the surface doses to between 29% and 34% (up from 21% for the open beam). As mentioned in section 2.9.6, De Ost et al. (1997) concluded that despite its favourable properties for use in radiotherapy, the effect that carbon fibre has on the skin-sparing effect must still be considered when used for the treatment of patients.

Meara and Langmack (1998) pointed out if the skin-sparing effect is reduced significantly by the beam passing through devices it could lead to severe skin effects, including erythema, moist desquamation and even permanent hair loss.

Devic et al. (2006) warned that it is important to know the dose in the build-up region. Even though there is a skin-sparing effect, the skin might become a dose limiting structure if high doses need to be delivered to tumours located at deeper locations.

Butson et al. (2002) investigated the variations in skin dose caused by linear accelerator couch material. For this study Butson et al. (2002) used a 6 MV photon beam on the Varian 2100C linear accelerator and they tested two types of treatment couch inserts, a Varian carbon fibre couch insert and a Varian tennis string couch insert. The construction of the inserts was as follows: the carbon fibre insert had a square ribbing construction of 2 mm wide and 3 mm thick. The size of the grid openings was 1.8 cm². To increase the patient's comfort a 0.62 mm thick Mylar sheet was placed over the ribbing. The tennis string insert was constructed from a square woven pattern of tennis string material. The cylindrical tennis string had a diameter of 1 mm. The square pattern was 1.4 cm in size and here a 0.4 mm thick Mylar sheet was placed over the ribbing.

For the study, Gafchromic MD-55-2 radiochromic film was used and the appropriate care and precautions were taken as per the AAPM TG-55 recommendations. The film was placed on the treatment couch inserts as well as in solid water at a depth of 1 mm. A further 15 cm of solid water was also placed on top of the film to provide material for backscatter. The measurements were done with the beam passing through the couch insert and the beam perpendicular to the insert. Various field sizes were used from 10 x 10 cm² all the way up to 40 x 40 cm² at 100 cm SSD. Measurements were also done for beams not passing through the couch inserts.

Butson et al. (2002) found that both types of couch inserts increased the skin dose. The Mylar itself added to the increase in skin dose when the beam passed through the couch. Looking at the dose to the basal layer of the skin, the peak dose (as a percentage of D_{max}) for the carbon fibre / Mylar couch ranged from 67% for a 10 x 10 cm² field size to 74% for the 40 x 40 cm² field size. For the tennis string / Mylar couch the peak dose ranged from 43% for a 10 x 10 cm² field size to 55% for the 40 x 40 cm² field size. However, because of the grid like construction of both of these couch inserts, the peak dose was not the same over the whole field size. The average doses (also as a percentage of D_{max}) for the carbon fibre / Mylar couch ranged from 48% for a 10 x 10 cm² field size to 61% for the 40 x 40 cm² field size; and, for the tennis string / Mylar couch it ranged from 35% for a 10 x 10 cm² field size to 46.5% for the 40 x 40 cm² field size. For the open fields (beam not passing through the couch) the peak doses ranged from 16% for a 10 x 10 cm² field size to 42% for the 40 x 40 cm² field size.

This study showed that the carbon fibre couch resulted in a higher increase in the skin dose than the tennis string couch. The increase in skin dose due to the Mylar sheet was significantly affected by the thickness of the Mylar sheet. This study by Butson et al. (2002) has shown that

when an object is placed in the beam and next to patients when treating, the effect of that object on the skin dose should be considered.

Butson et al. (2007) conducted a further study to look at the variation in skin dose due to the angle of beam incidence in grid carbon fibre couch tops. The authors defined the skin dose as a dose measured at an effective depth of 0.15 mm. They also noted that this was the effective point of measurement for the EBT Gafchromic film. For this study, they used a 6 MV photon beam on the Varian 2100C linear accelerator at a fixed SSD of 100 cm. The couch was the Varian grid carbon fibre Exact couch top insert. The insert had a carbon fibre square grid with dimension of 17 mm². The grid ribbing was 1.8 mm wide and 3 mm thick. A Mylar sheet (0.62 mm thick) was placed over the ribbing for patient comfort.

In this study an Attix parallel plate ionisation chamber was used for the point dose measurements and half a layer of the EBT Gafchromic film was placed over the active volume of the Attix chamber. This was to simulate the same effective depth of measurements as with the EBT Gafchromic film. The EBT Gafchromic film was used for the profile and two-dimensional map measurements. The measurements were done with the detectors positioned on a 30 x 30 x 30 cm³ solid water slab phantom and the grid couch top positioned over the detectors. The field sizes used ranged from 5 x 5 cm² to 40 x 40 cm² and the beam incident angle ranged from 0° to 60° in increments of 15°. All the results were stated as a percentage of the maximum dose at D_{max} .

Butson et al. (2007) showed a large variation in the skin dose depending on whether the beam passed through the ribbing of the grid or through the Mylar sheet only. This resulted in a wave-like dose profile and was seen for all the field sizes. It was noted that random patient positioning might result in an averaging out of these skin dose waves over the course of treatment. For the 10 x 10 cm field size at 0° incident angle the peak skin dose measured was 55% and the minimum (trough) dose 27%. For other incident angles for the 10 x 10 cm size, the minimum and maximum skin doses were 35% and 60% at 30°; 42% and 65% at 45°; and 52% and 70% at 60° incident angle. As the field size increased the skin dose through the grid also increased, for example the minimum and maximum doses for the 40 x 40 cm² field size for the 0° incident angle was 58% and 81%, respectively.

Butson et al. (2007) have shown that as with the increase of field size and incident angle, the skin dose also increased. The average skin doses ranged from 30% at 0° to 57% at 60° for the 5 x 5 cm² field size, and to 64% at 0° to 89% at 60° for the 40 x 40 cm² field size.

Meydanci and Kemikler (2008) investigated the attenuation of the beam and also the change in the surface dose caused by the carbon fibre couch. Smaller field sizes were included in the study. The measurements were all done on the Oncor Impression IMRT+ linear accelerator (Siemens) utilising both the 6 MV and 18 MV photon energies. The carbon fibre couch top was from Reuther Medizin Technik (Mülheim-Kärlich, Germany). The couch top had a hollow construction with the carbon fibre outer wall thickness between 0.6 and 0.8 mm. The dimensions of the couch top were 50 x 230 x 12 cm and the density was 1.8 g.cm⁻³.

For the surface dose measurements, Meydanci and Kemikler (2008) used a RW3 solid water phantom (PTW, Freiburg, Germany) with a Markus parallel-plate chamber (23343; PTW, Freiburg, Germany) and the Unidos electrometer. The field sizes used were 2 x 2 cm, 3 x 3 cm, 4 x 4 cm, 5 x 5 cm, 10 x 10 cm, 25 x 25 cm, and 40 x 40 cm. The measurements were all done at SSD of 100 cm. The phantom was positioned on the couch top and measurements were done at a gantry angle of 0° to exclude the effect of the couch and again at 180° to include the effect of the couch.

Meydanci and Kemikler (2008) found that for both beam energies the surface dose increased with field size, with a bigger increase seen for the smaller field sizes. The increase for 6 MV energy was from 10% to 42% as the field size increased from 5 x 5 cm to 40 x 40 cm. The increase for 18 MV was from 6% to 40% for the same increase in field size. It was noted that when the beam passed through the carbon fibre couch top the surface dose in the build-up region increased; and that the relative surface dose was less for small fields than for larger fields. For the field sizes less than 5 x 5 cm, the couch top increased the surface dose from 7.5% to 63% for 6MV, and from 4% to 43% for 18 MV. Thus, the surface dose with the carbon fibre couch top increased nearly sevenfold for the 5 x 5 cm field and was much greater for fields smaller than 5 x 5 cm. This increase is nearly five times that for the couch top for the 10 x 10 cm field size and almost twice as large as for the 40 x 40 cm field size.

Meydanci and Kemikler (2008) concluded that there is a clinically significant increase in the surface dose by a carbon fibre couch top and a decrease in the skin-sparing effect.

Gerig et al. (2010) also investigated the influence of the treatment couch on the surface dose. The study used two types of carbon-fibre treatment couches, a CIVCO couch and a Medical Intelligence couch. These were placed in the radiation beam between the beam source and a phantom in which the beam attenuation and dose build-up was measured. Gerig et al. (2010) showed that there was an increase in the skin dose when the beam first passed through a treatment couch. For 6 MV photons an increase in the skin dose from about 17% to 80% was seen.

Seppala and Kulmala (2011) investigated the increased beam attenuation and surface dose in eight different couch tops, including the Varian IGRT couch. The study looked at two beam energies, 6 MV and 15 MV, using a Varian 2100 C/D linear accelerator. The measurements were all done in a cylindrical Plexiglass (PMMA) phantom. The field size for all the measurements was 10 cm x 10 cm. For the surface dose measurements, a water-equivalent phantom, a single gantry angle of 180° and field sizes of 10 cm x 10 cm and 20 cm x 20 cm were used.

Seppala and Kulmala (2011) showed a wide range of results for the surface dose amongst the different couches for the two energies and the two field sizes. However, all the couches showed increased surface dose. The measured surface dose for the open beam (thus without the beam travelling through the couch) for the 6 MV beam was 44.3% and 53.4% for the 10 cm x 10 cm and 20 cm x 20 cm sizes, respectively. At the same beam energy, the Varian IGRT couch resulted in a surface dose of 90.8% for the 10 cm x 10 cm size and a surface dose of 94.0% for the 20 cm x 20 cm size. For the 15 MV beam, the measured surface dose for the open beam for the 10 cm x 10 cm and 20 cm x 20 cm sizes were 27.6% and 39.1%, respectively. At this beam energy the Varian IGRT couch resulted in a surface dose of 69.6% for the 10 cm x 10 cm size and a surface dose of 77.7% for the 20 cm x 20 cm size.

Gursoy et al. (2018) demonstrated that the carbon fibre couch top used in their study resulted in a significant increase in the surface dose, as well as a drastic decrease in the skin-sparing effect. They found that when the beam travelled through the treatment couch, the surface dose was almost seven times higher for a 10 x 10 cm field size as compared to the open beam, and almost four times higher for a 20 x 20 cm field size. Furthermore, the couch top almost doubled the skin dose at a 1 mm depth for both the 6 MV and 18 MV photon energies. For example, they found that for the 10 x 10 cm field size and the 6 MV beam the skin dose percentage without the couch in the beam was 40.31%, and with the couch it was 88.86%.

Court et al. (2010) voiced concern that many studies focused on the attenuation of carbon fibre couches and not so much on their effect on skin sparing. They investigated the effect of three carbon fibre couches on skin sparing. The three couches were the IGRT insert for Exact couch (Varian), IGRT couch (Varian), Robotic Couch (BrainLAB) with the regular tennis-racket insert (Varian) on each couch, and these measurements were compared with no couch in the beam. The study used a 10 x 10 cm field size on each of 6 MV and 10 MV photon energies and the TPR was measured in the build-up region using a thin-window parallel plate ion chamber (Capintec PS-033) in solid water. They found that carbon fibre couches can significantly reduce the skin sparing, and in severe cases even remove skin sparing.

Court et al. (2010) argue that the loss of skin sparing might not be so significant in multifield techniques, but that it can be of clinical significance in high fraction anterior-posterior parallel opposed fields or single fields treating posteriorly through the couch. For these two techniques the skin doses may increase to 90%, or more, of the prescribed dose, depending on which couch is used in a clinic

Mihaylov et al. (2011) investigated how the carbon fibre couch impacts on the skin dose for volumetric modulated arc therapy. They used a carbon fibre couch by BrainLab (BrainLab, Heimstetten, Germany) and the couch model was added to the Pinnacle (Philips Radiation Oncology Systems, Fitchburg, WI) treatment planning system by autocontouring. The study was a retrospective study of five prostate plans and five lung plans. The reason for using these sites was because it was thought the effect of the couch would be significant since there are large areas of contact between the posterior skin of the patient and the couch for these sites. For each patient they created two VMAT treatment plans. For the first plan only a single partial arc using 6 MV photon beam was used. For the second plan the partial arc from the first plan was divided into two or three separate segments. The anterior segments were planned for 6 MV and the posterior segments with 18 MV. For each of the two plans for a patient the prescribed dose and dose limits for the critical structures were identical and both plans were normalised such that 95% of the PTV received the same prescribed dose, this being 76 Gy and 62 Gy for the prostate and lung plans, respectively.

Mihaylov et al. (2011) found that the skin dose for the single energy (6 MV) plans was higher than that for the mixed energy plans where the 18 MV beams were passing through the couch, but it was found that for both plans larger skin doses could result. In some of the 6 MV cases they observed skin doses as high as about 80% of the prescribed dose. For the mixed beam plans the skin dose could be as high as 68% of the prescribed dose.

Rijken et al. (2018) also found that immobilisation devices and carbon fibre couch tops can increase the skin dose from megavoltage photon beams, particularly for VMAT treatments. They mention one study where an increase in skin dose due to the couch was as high as 81% of the prescribed dose.

For their study on Monte Carlo simulations of the effects of the treatment couch, Sheykhoo et al. (2017) concentrated more on the skin dose effect. They first verified that there was satisfactory agreement between the Monte Carlo calculations and measured data for various situations. In the study the 6 MV photon beam of the Siemens Primus Plus linear accelerator,

and the 550 TXT couch with TT-D carbon fiber table top (Siemens MedicalSolution, Erlangen, Germany) were simulated for three field sizes (5 x 5 cm, 10 x 10 cm, and 20 x 20 cm).

Sheykhoo et al. (2017) found that when the beam traversed the carbon fibre couch, the build-up curve is shifted towards the surface of the phantom. The skin toxicity due to the beam traversing the couch was found to be higher for smaller field sizes. There was a sevenfold increase in the skin dose for the 5 x 5 cm field size, compared with a fivefold increase for the 10 x 10 cm field size and a threefold increase for the 20 x 20 cm field size. Looking at the actual percentages, the carbon fibre increases the skin dose from 13.68% to 91.68% for the 5 x 5 cm, from 18.92% to 97.35% for the 10 x 10 cm, and from 28.76% to 99.53% for the 20 x 20 cm field sizes. Sheykhoo et al. (2017) concluded that even though the effect of the treatment couch on beam attenuation and skin dose could very well have an impact on the accuracy of the dose calculations, it is largely ignored in some commercial treatment planning systems.

As part of their study Tugrul (2018) looked at the effect of the CIVCO carbon fibre couch on the surface and build-up region doses and they looked at 6 MV and 15 MV photon energies. The measurements were done with a parallel plate ion chamber. The measurements were only done for a 10 x 10 cm field size for gantry angles 0° (without the couch) and 180° (with the couch) and the measurements started at the surface with 1 mm depth intervals. Tugrul (2018) also found that the carbon fibre has a bolus effect in that it causes an increase in the surface and build-up region doses. There is also a shift of the maximum depth doses towards the surface. For 6 MV the couch effect increased the surface dose from 14% to 70%, and for 15 MV it increased from 11.34% to 53.03%. For 6 MV at 5 mm depth the couch effect increased the dose from 82.2% to 94.9%, and at 10 mm from 96.6% to 99.4%. For 15 MV at 5 mm depth the couch effect increased the dose from 59.9% to 78.4%, and for 10 mm from 80.6% to 90.3%. This study has also shown that treating through a carbon fibre couch results in an increase in surface dose and a decrease in skin sparing.

Poppe et al. (2007) and Njeh et al. (2012) also found that the presence of the couch resulted in significant increases in the surface dose. Poppe et al. (2007) determined that for the 6 MV beam the surface dose increased by a factor of 1.79 and they mentioned that the effect of carbon fibre couches on the radiation beam must be carefully considered. Njeh et al. (2012) stated that this increase in skin dose due to the couch was dependent on dose prescription, the amount of the beam which actually passes through the couch and the incident angle of the beam to the couch.

There seems to be a consensus that the treatment couch results in an increase in the surface dose and decrease in the skin sparing. The surface dose is dependent on the beam energy

and the field size, as well as the type of material that the beam passes through. The surface dose decreases with increasing beam energy, and increases with increasing field size.

2.10 Advantages of incorporating the treatment couch into the TPS

Apart from trying to correct the possible dose errors as seen in section 2.9, there is also a case of needing to visualise the couch within the treatment planning system. According to Meyer et al. (2001), in IMRT none of the beams in a treatment plan should pass through the treatment couch. In IMRT many more beams are often required compared to conventional techniques. The more beams added to a treatment plan, the higher the likelihood that some of the beams will intersect the treatment couch. It is important therefore to be able to visualise the treatment couch on the screen when positioning the treatment beams. If the couch model is not added to the planning system, valuable time might be required to go and check the plan's feasibility prior to the patient arriving for treatment, or even when the patient is on treatment. This is time that the modern busy radiotherapy department can ill afford. Meyer et al. (2001) investigated three different couches in their study and found that for two of the couches standard IMRT plans would be affected by the couch, for the first couch 63% of the plans had some beams intersecting with the couch, and for couch two it was 34%.

When the full treatment couch is modelled in the treatment planning system it allows the dosimetrist to visualise the couch and avoid using radiation beams which would pass through the treatment couch, if possible. This could save time as it would eliminate having to do mock setups of a plan. Otherwise, failing that, it allows the planning system to calculate the effects of the couch as part of the dose prediction (Van Prooijen et al., 2010).

Incorporating the treatment couch into the treatment planning system could also help to improve uncertainties and inaccuracies in the dose as a result of the treatment couch (Cherry & Duxbury, 2009), while Chan et al. (2012) feel that it is crucial for the treatment planning system to be able to include the beam attenuation and bolus effect of the treatment couch into the calculation, especially for image guided radiation therapy.

Myint et al. (2006) also stated that neglecting the attenuation by a carbon fibre treatment couch can result in significant errors when treating radiotherapy patients and if the couch can be included in the dose calculation by the treatment planning system, this error can be significantly reduced. In their study investigating the effect of the treatment planning system they found that the treatment couch introduced an error of up to 7.4% when looking at the dose measured on the treatment unit (with the treatment couch) and the dose calculated on the Theraplan (without the couch). When they introduced the treatment couch into the calculations they found that the

Theraplan treatment planning system overcompensated for the treatment couch, but the total error was reduced to less than 1.4%.

There is a distinct advantage in having the treatment planning system account for the effects of the couch. Some of the newer treatment planning systems do allow the couch to be modelled in the planning system and this allows for a much better agreement between the predicted doses by the planning system and the measured doses, as was demonstrated by recent studies (Li et al., 2011).

The advantage for skin dose accuracy is stressed by Chan et al. (2012) and it is especially important for single fraction or hypofractionated treatments to have an accurate calculation of the skin doses. Chan et al. (2012) noted that the best solution would be if the treatment planning system could accurately calculate skin doses by incorporating the effects of the treatment couch within the planning system.

2.11 Role of treatment planning

Radiotherapy treatment planning is a vital part in the radiotherapy process and it is very important to ensure that it is done correctly (Fraass et al., 1998).

Broadly, the treatment planning phase is where an optimal, individualised treatment plan is created for each patient. This involves determining the arrangement and number of radiation beams required for the patient in order to deliver the required radiation dose to the target area, while minimising the dose to surrounding normal tissue structures, particularly critical structures (Evans & Staffurth, 2017). Treatment planning as a whole, however, involves further processes. It includes patient positioning and immobilisation, localisation of the tumour, creation of the treatment design (plan), dose calculation, and then plan verification (Fraass et al., 1998).

A definition of the treatment planning process is “the process used to determine the number, orientation, type, and characteristics of the radiation beams (or brachytherapy sources) used to deliver a large dose of radiation to a patient in order to control or cure a cancerous tumor or other problem” (Fraass et al., 1998).

Treatment planning has changed a great deal since the early days. The primary aim of treatment planning is to create a blueprint which will convert the therapeutic wishes of the oncologist into an accurate treatment for the patient (Cherry & Duxbury, 2009). In other words, the treatment planning phase involves determining the exact region that needs to be treated (target volume), the normal structures which might impact on the delivery of the treatment, as

well as the positioning and shaping of an adequate number of treatment beams (Zeman et al., 2013).

The planning process is a complex process and therefore it involves many uncertainties. Each of these uncertainties should be evaluated to determine its influence on the final treatment plan which will be used to deliver the treatment to the patient (Fraass et al., 1998). Gopan et al. (2016) also mention that the treatment planning phase is a major source of potential errors. Therefore, everything completed in the planning phase needs to be carefully scrutinised by medical physics, and also by other staff members involved in the journey of the patient through radiotherapy.

2.12 Treatment planning systems and the treatment couch

According to Van Prooijen et al. (2010) the role that the treatment couch plays in the accuracy of the treatment plan is actually rarely considered during the planning process.

Chan et al. (2012) also mention this fact and note that many treatment plans do not include the treatment couch in the dose calculation. This still seems to be the case even though many studies have shown that the treatment couch has a significant effect on the skin dose. This omission of the couch effect leads to underestimations in the treatment planning system's calculations of the skin dose.

The Eclipse treatment planning system (Varian Medical System) does have the Varian IGRT couch as a structure. The Eclipse has three separate structures for the IGRT couch to accommodate the three thicknesses of the couch: a thin structure (5 cm in anterior-posterior direction); medium (6.25 cm in anterior-posterior direction); and thick (7.5 cm in anterior-posterior direction). The disadvantage of this is that only one of the structures can be used at a time and the user has to select one of these thicknesses. In the researcher's experience if a patient then, for example, has a long field which spans different thicknesses of the couch the model does not account accurately for that.

2.13 Various approaches to adding the couch effect to TPS

Some researchers have investigated the incorporation of the treatment couches into various treatment planning systems, or dose adjustments for the effect of the treatment couch.

Probably the most effective method or workflow for incorporating the effect of the treatment couch in the treatment planning system would be to use identical couches on the CT Scanner and on the treatment units (Zhang et al., 2017). This way the CT scans will include the

information of the identical couch on which the patient will be positioned when the treatment is delivered. However, this is seldom possible due to compatibility of the couches and different vendors.

A common approach for trying to correct the discrepancy, due to the effect of the treatment couch, between the actual dose and the dose predicted by treatment planning systems, is the use of correction factors. A number of studies investigated this approach.

One such study was done by Hayashi et al. (2010) where they constructed a correction equation to correct the isocentre dose for their stereotactic radiotherapy treatments because their treatment planning system could not correct for the beam attenuation.

As part of their study looking at the effect of the gantry angle on the amount of attenuation due to the treatment couch, McCormack et al. (2005) also investigated constructing correction factors to compensate for the couch attenuation. They concluded that it is possible to acquire correction factors based on central axis attenuation to be used for individual cases to account for beam attenuation. However, care should be taken when using these correction factors because they may result in a further increase in skin dose, as well as an increase in the dose delivered. They suggested that because the attenuation of the beam at oblique angles can be so high, the effect of the carbon fibre on the beam should ideally be incorporated into the dose calculations.

Munjal et al. (2006) stated that although many treatment planning systems have capability to handle direct beam incident attenuation factors, most treatment planning systems do not account for the attenuation of oblique incident angles. Munjal et al. (2006) were unable to adjust their treatment planning system to account for the beam attenuation because the CT couch and treatment couch were not made of the same materials. Therefore, they also resorted to using manual couch attenuation correction factors.

Chyou and Lorenz (2017) noted that the simplest method to account for the attenuation effect of the couch is by using correction factors. This can be a single factor, or a table of 'look-up' values of the couch transmission factors. These transmission factors are the ratios of the dose measurement values of the beam passing through the couch and for an open beam. If using a table of values, these transmission factors should be measured for each energy and multiple gantry angles. After the treatment plan has been calculated by the treatment planning system, the monitor units could be manually adjusted by using the correction factors from the 'look-up' table. However, this approach is not perfect. Manual calculations are prone to human error, especially where there may be multiple 'look-up' tables for different couches, or if interpolation

is required. Manual factors are also not suitable for rotation therapy techniques where the path of the radiation through the treatment couch is continuously changing.

To create a more accurate dose correction method, Chyou and Lorenz (2017) created a couch model which consisted of contours of the treatment couch created within the treatment planning system. This was then saved as a DICOM RT structure set. When a patient plan is done this DICOM RT structure set can then be imported into the patient CT data set. When this approach is used the density of the couch structures need to be determined so that the effects of the couch can be accurately calculated by the treatment planning system. These densities can be determined directly from the CT scan of the treatment couch using CT numbers, but a more accurate method is to do couch attenuation measurements and to manually adjust the couch structure densities until the dose calculations by the treatment planning system match the actual measured doses.

Hayashi et al. (2010) tried to develop a method for correction of the beam attenuation by using derived equations. They did measurements specifically to be used for possible correction equations for the attenuation. They used their current couch, the Imaging Couch Top (ICT, BrainLAB). The chamber was placed at the isocentre in the centre of the spherical water-equivalent phantom with the phantom positioned on the ICT. The phantom was irradiated from all directions in 10° increments using a field size of 10 x 10 cm. All these measurements were to be used for the construction of the equations to be used to correct for the beam attenuation for clinical use. The equations were then to be used for adjusting the isocentre dose in the treatment planning system. According to Hayashi et al. (2010) the equations worked well at a depth of around 10 cm. A point to note here is that in this study the aim was to incorporate the correction method for the beam attenuation within the treatment planning system itself and not to do an external correction equation.

Seppala and Kulmala (2011) suggested that the beam attenuation and influence on surface dose by the couch needed to be mathematically modelled to ensure dose accuracy to the patients and to quantify the skin doses.

A study looking at incorporating the Varian Exact couch (Varian Medical System) in the Eclipse treatment planning system (Varian Medical System) was done by Wagner and Vorwerk (2011). According to these authors, in the Eclipse treatment planning system couches from the same vendor can easily be inserted into each CT scan set. In the study, Wagner and Vorwerk (2011) attempted to determine the correct parameter values for the Hounsfield units for each part of the couch. This was done by determining the actual attenuation of the treatment couch on the treatment unit and then comparing these attenuations with the attenuation of the dose as

calculated by the Eclipse treatment planning system. The Hounsfield unit values for the different sections of the couch model were then adjusted until the two sets of attenuations (one set from the treatment unit couch and the other from the treatment planning systems) matched. Wagner and Vorwerk (2011) used the 6 MV and 20 MV energy beams on the Varian Clinac 2300 C/D linear accelerator. The field size was 10 x 10 cm and multiple gantry angles from 0° to 360° in 5° increments were used in the study. The measurements were done using a Farmer chamber (PTW, Freiburg, Germany) inserted into a PMMA cylindrical phantom.

Wagner and Vorwerk (2011) determined that in Eclipse, the Varian Exact couch could be modelled sufficiently, but the Hounsfield unit values had to be manually adjusted for each patient. For this researcher it was not very clear how Wagner and Vorwerk (2011) proceeded in incorporating the Varian Exact couch into the Eclipse treatment planning system.

Another study investigating the incorporation of a couch model into their treatment planning system was done by Hu et al. (2011). They reported that even though the attenuation of the beam by treatment couches is a real issue, most commercial treatment planning systems do not take this into account adequately. Because of this lack of an accurate couch model in many of the planning systems, it is not always possible for the staff to know if any oblique beams will pass through any part of the couch until the patient is set up on the treatment unit for treatment. This is because the planning staff do not have a couch model on the planning system which they can visualise. For this reason Hu et al. (2011) said that a couch model should be incorporated into the treatment planning system so that the checking and calculation of attenuation can be done whilst planning, and time can be saved on the treatment unit.

Hu et al. (2011) used a standard treatment couch, Siemens ZXT system, with a PMMA couch top, and the planning system was a Pinnacle 8.0 TPS (Philips Medical Systems, Fitchburg, WI). To model the couch on the treatment planning system they used model-based segmentation, which is an automatic organ delineation tool on the treatment planning system. First, the couch was scanned using a Philips Big Bore Brilliance CT and the CT images imported into Pinnacle. The outlines of the couch were then contoured manually and checked using the user manuals from the vendor. After this a surface mesh was generated using the model-based segmentation. These meshes, together with density information of the couch were stored as a model.

To test the accuracy of the model Hu et al. (2011) performed measurements and calculations for ten different setups on different parts of the couch to give them a comparison between calculated and measured values. For dose verification a 2D array of ion chambers, MatriXX (IBA Dosimetry GmbH, Germany) was used. The measurements for the attenuation by the

couch were done for three oblique gantry angles of 180°, 220° and 235°. For the measurements without the attenuation, gantry angles of 0°, 40° and 55° were used. The measurements were all done using a 10 x 10 cm field size and the 6 MV photon energy.

Hu et al. (2011) found that the presence of a couch model in the treatment planning system is useful in helping to determine, during the planning process, if any of the beams intersect with the treatment couch. If intersections exist, beams can be repositioned and recalculated, if required, before the patient starts treatment on the treatment unit. They did find that to be completely accurate, a method must exist to be able to index the patient's position accurately on the treatment couch to ensure the position is exactly the same every day. A limitation on treatment planning systems is the field of view because the dose calculation only takes into consideration those structures which are within the field of view. This means that if part of the couch model for a particular patient is outside the field of view, any attenuation due to that part of the couch will not be calculated. However, Hu et al. (2011) noted that in Pinnacle the visualisation of the model-based segmentation is not limited by the field of view, and even if parts of the couch are outside the field of view, the couch model can still be used to check any possible intersections of the beam and couch.

Van Prooijen et al. (2010) investigated incorporating the treatment couch contours directly into the treatment planning system. They developed this process within the department and they called it "fusing couch top CT information with the patient CT dataset" (Van Prooijen et al., 2010:129). They created contour data sets of the treatment couches by performing a CT scan of the treatment couches, and then by use of engineering drawings and the physical measurements of the couches to create accurate contours of the parts of the couches. This created a secondary image set. When a patient plan was to be planned the regions of interest from the relevant couch secondary image set were transferred to the primary image set of the patient. For this they used the Syntegra fusion tool which is part of the Pinnacle treatment planning system. To allow the treatment planning system to incorporate the couch contours in the dose calculations, Van Prooijen et al. (2010) then assigned densities to the couch structures. These densities were determined by measurements.

Van Prooijen et al. (2010) found that this method was a viable solution for them. It allowed them to evaluate a treatment plan accurately in terms of the clinical effects of the treatment couch. The process did not add significantly to the overall time required for a treatment plan and it could be automated to a large degree.

Mihaylov et al. (2008) investigated the incorporation of their couch into their treatment planning system. Their approach was the closest to the method used in this thesis research and also utilised Pinnacle scripting. They used a BrainLab ExacTrac couch (BrainLab, Heimstetten,

Germany) and the Pinnacle treatment planning system (Philips Medical Systems). Their approach was to contour the couch on the CT slices and override the densities of the CT couch. Arbitrary densities were then assigned to the couch structures. To verify the couch model treatment plans were created for beams with incident angles to the couch of 0°, 30°, 50°, 75°, 83° for field sizes from 5 x 5 cm to 25 x 25 cm in 5 cm increments. Measurements were then performed on the Varian Clinac 21EX (Varian Medical Systems, Palo Alto, CA) for both 6 and 18 MV energies. Mihaylov et al. (2008) found that with their method the Pinnacle treatment planning system was able to model the couch attenuation properties to within 2%. It is not clear how the script handled the contouring part of the couch model. It also does not appear as if their model has functionality for specifying a lateral offset, for cases where the patient might need to be positioned laterally on the couch.

Chan et al. (2012) also added the couch into their treatment planning system by creating contours after doing a CT scan of the couch. They used a cone-beam CT. Attenuation measurements of the couch at the treatment unit were done and these values used to determine an electron density to assign to the couch structure in the treatment planning system. The contours were then added into a plan whenever there were any radiation beams traversing the couch. They do not describe the method of achieving these steps, but they do stress that it is important to index the position of the patient relative to the couch carefully because of the changing thickness of the couch in the longitudinal direction.

Rijken et al. (2018) investigated using a simple method for the treatment planning system to include the skin dose effects of VMAT treatments for patients in contact with immobilisation devices including the treatment couch. They used a CIRS 002LFC thorax phantom (Computerized Imaging Reference Systems, Inc., Norfolk, VA, USA) which was scanned on a CT scanner and the images then imported into the Pinnacle³ 9.10 (Koninklijke Philips N.V., Amsterdam, the Netherlands) treatment planning system, and a 4 x 4 cm² 360° arc was planned and then delivered to the phantom. They then separated the dose calculation into eight grid regions (which represented the full axial area of the phantom) and each region was assigned a correction factor. These correction factors were determined by measurement using GarchromicTM EBT3 film (Ashland Specialty Ingredients, Bridgewater, NJ, USA) positioned on a phantom so that each piece of film coincided with one of the eight grid regions. This allowed them to be able to correct the skin dose calculations by scaling the skin doses in the individual grid regions. This method was then tested with two test treatments of a humanoid phantom using a hypofractionated stereotactic body radiotherapy technique. The surface dose results were verified with dosimetric film.

Rijken et al. (2018) found that with this technique they had managed to improve the skin dose predictions by 76% and ultimately brought the accuracy of the predicted values by the treatment planning system to within 3% of the measured values.

Savini et al. (2016) investigated adding the couch to the treatment planning system as a geometric model. The couch was the Varian Exact IGRT couch (Varian Medical Systems, Palo Alto, CA) and the planning system was the RayStation (RaySearch Laboratories AB, Stockholm, Sweden). They measured the attenuation produced by the couch in a cylindrical PMMA phantom with a Farmer ionization chamber (FC-65G, IBA Dosimetry, Germany) at its centre on a Trilogy linear accelerator (Varian Medical Systems, Palo Alto, CA) 6 MV photon beam. The field size was 10 x 10 cm. The phantom was irradiated at a gantry angle of 0° and also for each gantry angle between 110° and 250° in 5° increments. The attenuation measurements were all relative measurements and the open beam measurement at 0° was used as the reference. These measurements were completed for each of the three sections of the couch, thin, medium, and thick. Three geometric couch models (one of each section of the couch) were created within the treatment planning system. Each geometric model consisted of a constant 4 mm thick skin surrounding an inner homogeneous structure. A CT scan of the IGRT couch (couch CT) was used for comparison. The densities of the geometric models were determined so that a good agreement between the measured and the calculated attenuations could be obtained.

The results of the study by Savini et al. (2016) showed that adding geometric models of the couch in the planning system is a viable option. They used two approaches, adding a couch CT in the plan and using the geometric model in the plan. Both methods produced results within 1% of the measured values. However, the geometric model approach turned out to be a more flexible solution since the densities could be modified to obtain a better agreement with measured values. In several situations the geometric model couch also performed better than the couch CT.

Njeh et al. (2012) modelled the BrainLAB imaging couch top in the Pinnacle treatment planning system. This was done by using a CT scan of the couch and importing that into the Pinnacle treatment planning system. The couch on the the CT images was then contoured, using a Pinnacle add-on called the model based segmentation module. The contoured couch model was then added to the organ model library from where it can be added to treatment plans. A solid water phantom consisting of three slabs of 30 x 30 cm was used for dose verification. A CT scan was done of the phantom and this was imported into Pinnacle. Plans were created in Pinnacle, the couch model added and then calculated. Densities for the couch model were determined. Njeh et al. (2012) also wanted to test the effect on the skin dose, and a 2 mm thick

region of interest was added around the phantom to represent the skin. The phantom was then setup on the Novalis Tx™ treatment unit. Dose was delivered for a 10 x 10 cm field size and for gantry angles from 180° and in 10° increments to horizontal. Njeh et al. (2012) determined that the carbon fibre couch was modeled successfully in the Pinnacle treatment planning system. They also recommended that the couch should be included in the treatment planning system so that its effects can be incorporated into plans by the treatment planning system.

The next study did not involve any correction of the effect of the treatment couch on the radiation, but the study is included in this literature review for completeness. Bandi et al. (2011) were investigating an automated method to remove the CT scanner couch from the CT images. This was done because the CT scanner couch was considered to be a useless artefact on the images which was not contributing worthwhile information. In fact, Bandi et al. (2011) claimed that the CT Scanner couch could in some cases even hide anatomical information. One of the problems they encountered was that the patient is in direct contact with the couch. Therefore, simple threshold techniques cannot easily distinguish between couch and patient. Another problem is that there is couch sag due to the patient's weight and thus the movement of the couch along the axial slices may not be even. They began with the assumption that the couch shape was similar over all the slices. Their algorithm determined the couch structure on each slice and created a mathematical mask which would then remove the CT Scanner couch from the CT images. It is not clear how this was done, but it seems as if the mask overwrites the individual pixels on the CT images. The validation for this process was done by radiologists. According to Bandi et al. (2011) the process removed 95% of the CT Scanner couches successfully from the CT images and in the rest of the cases the couch was only partially removed.

2.14 Dose measurements

2.14.1 Attenuation measurements

The attenuation measurements are generally straightforward measurements, and this is described in some detail in section 2.9.2. These measurements are also usually relative measurements as shown by Chyou and Lorenz (2017) where they determined the attenuation of the couch by taking dose measurements with the couch in the path of the beam, and without the couch in the path of the beam, and taking the ratio of these readings.

A different approach to determining the attenuation effect of the treatment couch was done by Vieira et al. (2003). In their study they looked at measurements of photon beam attenuation by a treatment couch by means of an electronic portal imaging device (EPID). Their initial aim was the establishment of a dosimetric quality assurance program in their clinical department. A part of establishing the program was using the EPID to verify that the planned fields from the

treatment planning system were correctly reproduced by the treatment unit. The EPID images taken during the patients' treatments were also used to verify and correct the patient setup, as well as to verify the internal patient anatomy.

During the process of designing the quality assurance program Vieira et al. (2003) noticed that the EPID images taken during treatment demonstrated significant attenuation of the beam by the carbon fibre components of the treatment couch and immobilisation devices. This created a problem because it impeded accurate dosimetric verification of the treatment beams. Posterior beams passing through the treatment couch is also very common in IMRT techniques and the beam attenuation could result in lower doses being delivered to the patients. As a result of this finding Vieira et al. (2003) decided to further investigate the matter with a study measuring the attenuation using the EPID, and additional EPID measurements were done in the absence of patients.

Vieira et al. (2003) used a Clinac 2300 C/D linear accelerator (Varian Oncology Systems, USA) with an Exact treatment couch (Varian Oncology Systems, USA). The Exact couch has two translatable rails and a couch insert. The standard insert for the Exact couch has a grid pattern. The rails and insert are made from carbon fibre. A solid insert can also be used to reduce sagging. The solid insert (MED-TEC, Orange City, USA) was constructed from two layers of carbon fibre with a foam material in the middle. The EPID used was a fluoroscopic Theraview NT EPID (Cablon Medical, Leusden, The Netherlands). Each EPID image acquired for the study was converted to portal dose images (PDI) by applying corrections such that the PDIs were proportional to dose. They included 17 patients in this study and all patients were treated with 6 MV photon beams with EPID images taken for each fraction. For each image the EPID was at a source-to-detector distance of 170 cm. To investigate the variations in the dosimetric measurements due to beam attenuation, EPID images were also taken for the beams passing through the couch in the absence of patients both with and without the couch and immobilisation devices. These images were taken at 170 cm source-to-detector distance and with the same parameters as for treatment. From all these images 2D transmission images were derived.

Vieira et al. (2003) also performed measurements using an ionisation chamber to verify the EPID measurements. They positioned a NE 2571 ionisation chamber in a 30 x 30 x 10 cm² polystyrene phantom at a depth of 1 cm. This was positioned in such a way that the chamber was also at a distance of 170 cm from the focus. Thus, attenuation of the 6 MV beam by the immobilisation devices and the couch inserts was measured using both the EPID and ionisation chamber.

The results of the attenuation due to the couch showed the EPID with an attenuation of 3.2% by the solid couch insert; while in comparison the ionisation chamber showed an attenuation of 3.0%. Therefore Vieira et al. (2003) noted the usefulness of the EPID to assess beam attenuation. An added benefit of using the EPID to measure the attenuation is that it is measured in 2D and not just at a single point as with the ionisation chamber; and furthermore, the EPID image can easily be evaluated for any beam orientation.

Vieira et al. (2003) concluded that there is definitely a need to account for the treatment couch and immobilisation devices during treatment planning, but they also acknowledge that including the couch in the planning system is not straightforward. EPID images can be used to look at the attenuation of the beam by the treatment couch and immobilisation devices in 2D.

2.14.2 Surface dose dosimeters

There are various dosimeters available with which to measure surface dose and each has their own advantages and disadvantages. A brief overview of the following dosimeters is made: parallel-plate chambers, thermoluminescent dosimeters, radiochromic film; and MOSFET semi-conductors. In the next section, a brief overview of certain research studies using some of these dosimeters for surface dose measurement will be outlined.

2.14.2.1 Parallel-plate chambers

Two types of parallel-plate chambers, extrapolation and plane-parallel, could be used for surface dose measurements and both have consequent advantages and disadvantages.

Extrapolation Chambers

This type of parallel-plate ionisation chamber has a small, variable, sensitive volume. The upper electrode is composed of a thin carbon coated foil and the collecting electrode is a disk-shaped region within a guard ring. The beam enters through the upper electrode and the bottom electrode is connected to the electrometer. It is mentioned above that the extrapolation chamber has a variable volume. The volume can be adjusted by changing the spacing between the electrodes through micrometer screws. This makes the dosimeter very accurate. The surface dose can be determined by measuring the ionisation per unit volume as a function of the spacing between the two electrodes (Khan, 2011).

The advantages and disadvantages of extrapolation chambers

The advantages of extrapolation chambers can be listed as follows:

- The extrapolation chamber has a good response in regions without electronic equilibrium (Apipunyasopon et al., 2013);

- These chambers are useful for surface dose measurements of orthovoltage and megavoltage x-rays and for the dosimetry of β rays and low energy x-rays (Podgorsak, 2005). This is the most accurate dosimeter for the measurement of surface and build-up region doses for megavoltage photon beams (Akbas et al., 2016);
- Extrapolation chambers do not suffer as much as other ion chambers from perturbations (Tugrul, 2018).

The disadvantages of extrapolation chambers as a surface dosimeter can be listed as follows:

- They are not commonly found in most departments and there they are not widely used;
- They are not that suitable for a busy clinic because the measuring process is time-consuming (Apipunyasopon et al., 2013);
- They are more cumbersome to use than plane-parallel chambers (Khan, 2011).

Plane-Parallel Chambers

In contrast to the extrapolation chambers the plane-parallel chambers have a fixed spacing between the electrodes. Apart from that they are very similar to the extrapolation chambers. Some examples of this type of dosimeter are PTW Markus, Memorial, Capintec, and Pitman (Khan, 2011). These chambers are used for measurements of lower energy electron energies (less than 10 MeV), as well as for measurements of doses at the surface and in the build-up region (Podgorsak, 2005).

The advantages and disadvantages of plane-parallel chambers

An advantage of the use of plane-parallel chambers is that they have hardly any attenuation at the wall of the chamber because of a very thin wall/window. These chambers are good alternative dosimeters to the extrapolation chambers because they have thin entrance windows (Akbas et al., 2016). They can thus also be used to measure the dose at various depths in the build-up region by placing layers of phantom material on top of it. Excluding the extrapolation chambers, these chambers are the dosimeters of choice to measure the surface dose of a phantom, or the dose in high dose gradient regions (Khan, 2011).

A possible disadvantage of plane-parallel chamber is that there is a problem with some of these chambers in that they have an insufficient guard width and they then require substantial fluence perturbation corrections (Podgorsak, 2005). They overrespond in the build-up region because of the internal dimensions. This can be corrected for by using Gerbi's overresponse correction factors for the specific chamber (Akbas et al., 2016). Another disadvantage of these chambers is that they can only be used for measurements in phantoms. This is due to their size and physical geometry (Akbas et al., 2016).

2.14.2.2 Thermoluminescent dosimeters (TLD)

The most common type consists of lithium fluoride with a trace amount of magnesium. Their use is quite flexible because they are manufactured in a multitude of shapes and sizes to be useable in many situations (Khan, 2011).

Advantages and disadvantages of TLDs

Advantages of TLDs are that they can be reused provided they are annealed correctly and recalibrated. In general they are considered to be tissue equivalent and for use in megavoltage beams they are not dependent on the energy of the beam. TLD readings persist very well with less than a 5% fade of the data over 12 weeks. TLDs can be used to measure dose from 10^{-2} Gy up to 10^3 Gy. TLD can be used to measure dose in the build-up regions (Khan, 2011). TLDs are able to measure doses with an accuracy of 2% (Kinhikar et al., 2009), although Khan (2011) suggests an accuracy of about 3%.

Thermoluminescent dosimeters are commonly used for in vivo dosimetry, but they have a number of disadvantages. When the measurement information is read on the TLDs the information is deleted and therefore they are not suitable if the dose information must be permanently stored. They require annealing, and reading the measurements is time-consuming. A further disadvantage is that the TLD chips provide uncertainties in the skin dose estimation. This is due to a limitation in the finite size of the chips (Kinhikar et al., 2009).

2.14.2.3 Radiochromic film

The most common radiochromic films used in dose measuring are GafChromic EBT film and Double-layer GafChromic MD-55-2 film.

Radiochromic film is a colourless film and when it is exposed to radiation it develops a blue colour. A dye on the film becomes polymerised when radiation passes through it. This polymer then equates to the amount of radiation exposure by using a densitometer to determine the amount of light which is transmitted through the polymer (Podgorsak, 2005).

Advantages and disadvantages of radiochromic film

The use of radiochromic film has been found to have a number of advantages. Radiochromic films are very suitable for measurements of dose in high dose gradient regions in radiotherapy because they have a high spatial resolution, they are not very dependent on energy and they are almost tissue equivalent (Fiandra et al., 2006). According to Fiandra et al. (2006) the cost of these films is also affordable for a department. Radiochromic film is suitable for doses from 10^{-2} Gy up to 10^6 Gy, they are not sensitive to visible light, and they do not require any

processing (physical, chemical, or thermal) (Khan, 2011). This is because they are self-developing and thus do not require any developer, fixer, darkroom equipment, or even film cassettes (Podgorsak, 2005). They can also be scanned with multiple devices, including commercially available laser scanners and charge-coupled device microdensitometer cameras (Khan, 2011).

Two possible disadvantages are that these films need to be calibrated before use, and they are sensitive to ultraviolet light and temperature (Khan, 2011). Furthermore, the readings from the EBT film are dependent on the densitometer used (Fiandra et al., 2006).

2.14.2.4 MOSFET

This is a type of semiconductor; and MOSFET stands for metal oxide semiconductor field-effect transistor. They are miniature silicon transistors. When MOSFET is exposed to ionising radiation a charge is generated which causes a change in the threshold voltage. The dose can be measured during, or post-irradiation (Podgorsak, 2005).

Advantages and disadvantages of MOSFET

The dose measurement information is available immediately after exposure. The amount of radiation that is absorbed is determined by a shift in the threshold voltage before and after exposure. Other advantages include good sensitivity, reproducibility and stability with not much temperature effect (Kinhikar et al., 2009), their small size, reusability, can do multiple point dose measurements, and they can store a dose history (Akbas et al., 2016).

Kinhikar et al. (2009) also found that the measurements by the MOSFET are quite independent of field size, and there is also negligible angular dependence for 360°. They also found in terms of the reproducibility that the inter-fraction deviations ranged from 1% to 1.4%.

A single MOSFET can be used over a large energy range, in fact, it can be used over the full range of photon and electron energies. There is no energy correction needed for megavoltage energies. There are also no dose rate corrections needed (Podgorsak, 2005).

In terms of disadvantages, MOSFETs are a little bit dependent on temperature, but this has been rectified by special double detector systems. MOSFETs are also sensitive to any changes in the bias voltage. The readings do not persist perfectly and the readings need to be taken within a specified time after they were irradiated. Lastly, MOSFETs have a limited life span. (Podgorsak, 2005).

2.14.3 Surface dose measurements

In this section we look at the experiences of other researchers in the measurements of the surface doses. The reason that surface doses in radiotherapy are so important is that if the dose to the skin becomes too high the skin becomes a dose limiting structure. This can lead to acute skin reactions or delayed skin reactions, and can affect the overall radiation treatment. The surface dose is affected by field size, source to skin distance (SSD), beam angle, beam energy, and beam modifiers (for example blocks and multileaf collimators) (Akbas et al., 2016).

Already in 1998, Butson et al. (1998) looked at radiochromic film for the measurement of surface doses, specifically at off-axis and peripheral skin doses. The reason they looked at radiochromic film was because it can give a data set which includes the full surface dose profile. This makes it very suitable for measuring off-axis and peripheral skin doses and it can be used in both phantoms and in vivo. For their study they used the following: 6 MV, 10 MV and 18 MV photon energies on two Varian 2100C linear accelerators and Gafchromic MD55-2 film. The film was positioned perpendicular to the beam on the surface of a solid water phantom and they did a double-exposure on the film. This was to correct for non-uniformity. After exposure the film was analysed with a 670 nm red GaAlAs ultrabright LED on a converted Scanditronix RFA300 densitometer. Butson et al. (1998) found that the effective measurement depth with the film for megavoltage photon energies was 0.17 ± 0.03 mm water equivalent. They also found that skin dose increased with field size and this was true for all points inside and outside the field. They concluded that GafChromic film is a very suitable dosimeter for skin dose measurements, especially in regions where high dose gradients are found. Any errors encountered with the MD55-2 radiochromic film could be attributed mainly to non-uniform film thickness and optical defects as a result of marks on the film, for example scratches and fingerprints.

Chung et al. (2005) looked at the accuracy of two treatment planning systems in calculating the dose at the surface and build-up regions by comparing them with the measurement obtained by using radiochromic film. One of the treatment planning systems was the Pinnacle treatment planning system. They specifically looked at MLC-based IMRT treatment for head and neck cancer. For the setup they used two semicylindrical solid water slabs. Gafchromic film (Nuclear Associates, Division of Victoreen, Inc., Carle Place, NY; GafChromic™ dosimetry medium) was inserted in the middle of the two slabs. They then created two identical targets in the planning systems, a shallow target at 0.5 cm down from the top surface of the phantom and a deep target at 6 cm down from the top surface. Different gantry angles were used for each target. For the shallow target these were 20°, 90°, 165°, 240° and 310°, and for the deep target 0°, 70°, 145°, 220° and 290°. MLC plans were created and then the planned fields were

measured on the Varian 6 MV 2100C linear accelerator (Varian Medical Systems, Inc., Palo Alto, CA).

Chung et al. (2005) found that both treatment planning systems were reasonably accurate in predicting the doses except at very shallow depths (from the surface down to 0.2 cm). Both treatment planning systems overestimated the surface dose for both target cases. The overestimation ranged between 7.4 % and 18.5 % with respect to the prescribed dose. A source of uncertainty is the potential nonuniformity of the radiochromic film, especially where the film is cut. Where the film gets damaged the film automatically starts to develop and this results in additional nonuniformity where the damage occurred. For this study the measurements from those areas of the film were ignored.

Gursoy et al. (2018) found that any Marcus chamber is good enough to produce reliable measurements of percentage depth dose at depths beyond the build-up region, but the accuracy of any measurements within the build-up region is very much dependent on which detector is used.

Akbas et al. (2016) looked at measurements of surface and build-up region doses, and they compared the Markus parallel-plate ionisation chamber, GafChromic EBT3 film and the MOSFET detector. For their measurements they looked at 6 MV and 15 MV photon beams, for 5 x 5 cm, 10 x 10 cm and 20 x 20 cm field sizes at gantry angles of 0°, 30°, 60°, 80°. Akbas et al. (2016) contended that the most accurate way to measure surface and build-up region doses is with extrapolation chambers. Unfortunately not all departments have access to these.

Regardless of which dosimeter is used the build-up thickness of that dosimeter must be taken into account in order for the dose measurement to be accurate. According to Akbas et al. (2016) the water equivalent thickness (WET) is used to characterise the penetration range of the ion beam. WET is the equivalent thickness of liquid which will stop the ion beam the same as a certain thickness of the given material. A problem with different dosimeters is that they are all made from different materials, each with its own effective measurement depth. Therefore the WET of each dosimeter must be considered.

Akbas et al. (2016) found that the surface dose is dependent on the field size, incident angle and the particular dosimeter used. The surface dose increases with field size and surface dose increases as the incident angle increases. This was true for all dosimeters. A problem with different dosimeters is that each dosimeter has a specific measurement depth and this results in the measurements varying amongst the different dosimeters. If care is not taken this can lead to errors in terms of the surface and build-up region doses.

In comparing the three dosimeters Akbas et al. (2016) concluded that the MOSFET measured the highest for the surface and build-up region doses. The MOSFET however gave lower readings for the first 5 mm, provided that the WET values of the dosimeters and the same water equivalent depths are used. At these depths the EBT3 film had readings closer to those of the Markus chamber. The readings for the MOSFET were the highest for oblique angles. At lower beam energies the difference in the readings amongst the dosimeters was the greatest when looking at the surface doses at a depth of 0.07 mm.

Some of the advantages and disadvantages that Akbas et al. (2016) highlighted were as follows: The MOSFET is more suited for in vivo usage because of its physical properties. It is easy to use and the results are available immediately. The EBT3 film has good dosimetric properties, but the disadvantages are that it is not ideal for in vivo usage. In addition, the EBT3 film also requires a waiting period and a calibration curve.

Chan et al. (2012) looked at using radiochromic EBT2 films in their study where they wanted to verify the skin dose which resulted from the bolus effect of an Alpha-cradle and the Varian Exact IGRT® couch. They used the EBT2 film because using TLD, diode, MOSFET dosimeters only provides discrete measurement points on the skin surface. They managed to verify the predicted skin doses from the treatment planning system using the EBT2 film.

An extensive study was done by Devic et al. (2006) where they tried to determine a correction procedure for accurate skin doses measurements at a reference depth of 70 μ using radiochromic film. The radiochromic films used were the GafChromic® dosimetry films (HS, XR-T and EBT). These films have effective measurement points at depths just beyond 70 μ . This depth was used because that is the depth recommended by the ICRP and the International Commission on Radiation Units (ICRU) for practical dose assessments and that depth is more or less the boundary between the epidermis and dermis layers of the skin. The reason the radiochromic films were used was because of their high spatial resolution and low spectral sensitivity and this is ideal for measuring dose distributions in high dose gradient regions. In addition to the films, they also used the Attix parallel-plate ionisation chamber, a homemade extrapolation chamber, and TLDs. The measurements were done with 6 MV photon beams on the Varian 2300 CD linear accelerator (Varian, Palo Alto, CA). The dosimeters were positioned at a SSD of 100 cm on the surface of a phantom constructed from solid water slabs.

According to the measurements Devic et al. (2006) found that for a 10 x 10 cm 6 MV photon beam the PDD increases from 14% to 40% in the first millimetre of the build-up region. Any dosimeter which needs to be used for surface dose measurements must be correctly

calibrated. In addition to that, corrections must also be applied. The corrections used for the three GafChromic® films were 15% for both EBT and HS, and 16% for XR-T for a depth of 70 μ . The measurements agreed very well with Monte Carlo simulations, except at very shallow depths. The results have also shown that if one ignores the skin dose correction factors when using single film measurements, the skin doses would be overestimated by 5%, 6%, and 7% for the EBT, HS, and XR-T, respectively.

Devic et al. (2006) concluded that it is not just enough to know the effective measurement point of the dosimeter used, but that the overall PDD curve behaviour within the first millimeter of the skin must also be known.

Eyadeh et al. (2017) investigated the use of poly(vinyl alcohol) cryogel dosimeters for the measurement of skin dose. They acknowledged that radiochromic film has advantages for measuring the surface dose in two dimensions. However, a disadvantage of film is that it is not always easy to form to complex contours of the human body and a more flexible dosimeter is then required. This is where gel dosimeters might come in very useful. Cryogels (a type of gel dosimeter) are flexible and can thus be used on complex skin contours. Apart from that poly(vinyl alcohol) cryogels (PVA-C) based dosimeters might possibly also be used at the same time as a dosimetric bolus for an accurate estimation of skin surface dose. The advantages of PVA-C is its flexibility and stability, and it can be loaded with radiosensitive material, for example ferrous benzoic xylene orange (FBX), which can then be used to determine dose in two and three dimensions. That means that these cryogels have two useful functions. They can be used as a build-up material, as well as an in vivo dosimeter.

For the study Eyadeh et al. (2017) used translucent FBX-PVA-C as radiochromic bolus, as well as EBT-2 GafChromic film. The film was placed under the radiochromic bolus and irradiated with gantry angles from 0° to 90° and this was used to determine a relationship between the skin surface dose and the dose measured with the bolus. The film was used as their gold standard for determining the skin dose. The average ratio of bolus-film dose over the range 0° - 90° was used as a single correction factor to convert the dose measured in the bolus to a dose at the skin surface.

Eyadeh et al. (2017) found that FBX-PVA-C radiochromic bolus may be an accurate dosimeter to use for the estimation of skin surface doses with only a single correction factor for in vivo dosimetry where the skin dose is important.

Kinhikar et al. (2009) investigated using MOSFET and TLD for skin dose measurements in tomotherapy for head and neck patients. They wanted to determine the skin dose inside the

mask and compare those doses with what the treatment planning system predicts. Two patients were used in the study and the plans were calculated on the tomotherapy treatment planning system (TomoPlan, V2.2). The MOSFET and TLD measured the skin dose for the first patient at 90% and 92% of the prescribed dose, respectively. The variation in the skin dose between the MOSFET and TLD was 2.2%. For the second patient the measurements were 88% for MOSFET and 86% for TLD. Here the variation was 2.3%. In contrast, for both patients the treatment planning system predicted the skin dose to be 100%. Here the treatment planning system overestimated the skin dose by 10-12%.

According to Kinshikar et al. (2009) MOSFET is a suitable and accurate dosimeter for skin dose measurements in high dose gradient regions.

Apipunyasophon et al. (2013) did measurements of surface dose and dose in build-up region for the 6 MV photon energy, using various dosimeters, and compared it with the EGS4nrc Monte Carlo simulation package. The Monte Carlo simulated data were used as the gold standard. All measurements were done on the Varian Clinac 23EX linear accelerator for the 5 x 5, 10 x 10, 15 x 15 and 20 x 20 cm field sizes. The percentage depth doses were measured from the surface all the way to a depth of 30 cm in 2 mm increments. These measurements were made in a Blue water phantom (Wellhofer Scanditronix, Germany). The detectors used for these measurements were a compact cylindrical ionisation chamber of type CC13 (Wellhofer Scanditronix, Germany) and a silicon p-type photon semiconductor dosimeter of type PFD (Wellhofer Scanditronix, Germany). They also measured the central axis depth dose in a 30 x 30 x 20 cm³ solid water equivalent phantom slabs (RMI, Model-457) at depths of 0, 0.2, 0.3, 0.5, 1, 1.2, 1.5, 2.0 and 3.0 cm. Here they used the parallel-plate ionisation chamber (Markus 23392, PTW-Freiburg) and the TLD (HARSHAW Chemical Co, Solon, OH).

Apipunyasophon et al. (2013) found that at depths beyond the maximum dose there was good agreement between the Monte Carlo simulated data and the measured data for all the dosimeters, but not in the build-up region. All the dosimeters overestimated the dose near the surface, but for all of the dosimeters the surface dose was shown to increase with increasing field size.

Foo and Stensmyr (2013) investigated the accuracy of the dose calculations by the Eclipse™ (Varian Medical Systems, Palo Alto, CA, USA) treatment planning system (TPS) when using virtual couch top models. They assessed the Flat panel and Unipanel couch tops for the Varian Exact Couch. They wanted to assess the effect in the presence of air gaps between the couch and the patient and they also did not just want to look at this in terms of a single point, but for a range of depths. Three sets of CT scans were done for each couch for a setup with no air

gap, with a 5 cm air gap, and a 10 cm air gap. In Eclipse the virtual couch models were superimposed on the CT scanner couch. For each couch top a plan with a single beam at 0° incident angle to the couch was used with a 10 x 10 cm and 15 x 30 cm field size for the Flat panel couch and Unipanel couch, respectively. Afterwards the plans were delivered using the 6 MV photon energy on the Varian Clinac 6EX (Varian Medical Systems, Palo Alto, CA, USA) linear accelerator. The dosimeters used were the CC04 (Scanditronix–Wellhofer, Germany) cylindrical ion chamber and a Roos-type PPC40 (Scanditronix–Wellhofer, Germany) plane-parallel chamber.

Foo and Stensmyr (2013) found that a point dose measurement at a single depth may not be a good reflection of what is happening at the other depths. This study has also demonstrated that the build-up region is difficult to do a dose assessment on. The largest discrepancy in the doses measured and predicted by the planning system was in the build-up region, and this was more pronounced in the depths up to 0.5 cm because of the high dose gradient here.

2.14.4 Build-up region problems

There are two aspects which make accurate assessment of doses in the surface and build-up regions problematic. These are inaccuracies in the actual measurements of these doses and then also the inaccuracies of the treatment planning systems in these regions.

Chung et al. (2005) assert that the dose in the surface and build-up regions remains difficult to ascertain. One of the reasons is because of electron contamination from the linear accelerator head. Another factor is also the potential inaccuracies of the dosimeters for measuring the dose in these regions.

A main complication with accurate measurements of dose within the build-up region is that contaminated electrons within the beam and secondary electrons from the irradiated medium may result in perturbations within the build-up region. There is a high dose gradient in this region because these electrons drop off rapidly as depth increases because of large numbers of interactions with the atoms of the medium (Apipunyasopon et al., 2013).

Gursoy et al. (2018) report that it is very difficult to measure and evaluate surface doses, and Sheykhoo et al. (2017) agree and say that there are significant uncertainties in the high dose gradient regions.

Akbas et al. (2016) point out that even though it is important to understand what the surface dose is doing, it is notoriously difficult to accurately measure it at those shallow depths. One

reason is that the measurements vary for each measurement tool because of their individual physical properties.

According to Cherry and Duxbury (2009) there are limitations in how accurate computer planning algorithms can model high-dose gradient regions. These regions include tissues near the skin surface.

This is acknowledged by Eyadeh et al. (2017) who also say that most treatment planning systems are not accurate in predicting the dose in the build-up region. They go further by saying that modern treatment planning systems can only predict the skin dose to within 25% and for most of them it is accomplished by extrapolation of measured data. Monte Carlo simulation is accurate in predicting build-up region doses, but not all clinics have access to this. To overcome the limitations of the treatment planning systems it is preferable to verify the doses in these problematic areas by in vivo measurements.

Kinhikar et al. (2009) say that some treatment planning systems can overestimate the surface dose by up to 18.5%.

Rijken et al. (2018) also state that commercial treatment planning systems cannot accurately predict surface doses produced by megavoltage photon beams.

Bedford et al. (2003) describe the commissioning of the Pinnacle³ treatment planning system for four Elekta linear accelerators. Their measurements of the beam data were quite substantial, and they also fitted a Monte Carlo model of the accelerator head to the measured data, and they then extracted the parameters for the beam model for Pinnacle³. They also compared their results with a second treatment planning system. However, even with all this they found that in the build-up region the accuracy of the Pinnacle treatment planning system was slightly lacking. Bedford et al. (2003) say that to be able to accomplish a more accurate prediction of doses in the build-up region the maximum depth for the electron contamination must be set so high that it does not make sense, even compared with the Monte Carlo simulations, as well as other measurements. They concluded that the Pinnacle parameters probably have additional effects, apart from the electron contamination.

2.15 Couch model accuracy

The final treatment plan for a patient must always be checked to confirm that the doses predicted by the treatment planning system are correct (Childs & Bidmead, 2012).

Whenever a department utilises a couch model that was created by another department the model and its densities must be checked to ensure that it provides the correct results on the treatment planning system (Chyou & Lorenz, 2017).

2.16 Conclusion

The research studies and literature which have been reviewed in this chapter have demonstrated that even though carbon fibre is a good material to use for radiotherapy couch tops, it definitely has an effect on radiation beams which traverse the carbon fibre. It has two important effects which cannot be ignored. First, it reduces the dose at depth, due to attenuation of the beam, and second, it increases the surface dose to the patient when it is placed between the patient and the radiation beam. Furthermore, there are various factors which affect the degree of these effects. The amount of attenuation produced by the couch top and the increase in the surface dose (as a result of the couch top) are both dependent on the beam energy, field size, incident angle, as well as the part of the couch that the beams traverse. All of this highlighted that there was a need to analyse the impact of the treatment couch at the study site and attempt to improve the accuracy of the predicted doses by the Pinnacle treatment planning system.

CHAPTER THREE: RESEARCH METHODOLOGY

3.1 Introduction

All the measurements for this study were done using phantoms and dose calculations used the dose to water concept. Water is considered to be soft tissue equivalent due to its similar effective atomic number, mass attenuation and absorption coefficients (Aslam et al., 2016), which means that it has absorbing and scattering characteristics that match closely those of soft tissue and muscle. The dose measurements in this study were done in water only to avoid any uncertainty and complexities that may arise as a result of the dose algorithm and their inherent inaccuracies in multiple tissue density. In this research study the collapsed cone (CC) convolution calculation algorithm was used on Pinnacle TPS. Chopra et al. (2018) mention that the accuracy of dose calculations varies very much from one treatment planning system to another when they have to contend with tissue inhomogeneities. In contrast, they found that the different treatment planning systems investigated had very good agreement in the calculation accuracies for various field sizes and depths when a homogeneous phantom was used.

It was also for this reason that the couch model created in this study was not tested using clinical tissue data.

The study involved five distinct but connected processes.

1. Initial attenuation measurements: The actual couch was measured to determine the attenuation effect by the Varian IGRT couch at the study site. For these plans standard geometries were used. All the fields were open, square fields.
2. Determining overestimation of dose by Pinnacle if the couch was not considered in the calculation: Those beam configurations used for the initial attenuation measurements were created in Pinnacle and calculated without any couch model in Pinnacle to determine by how much Pinnacle overestimates the doses for beams which traverse the real couch at the treatment unit. This was to determine if the amount of dose overestimation warrants the creation of a couch model.
3. Couch model creation: Here the script and computer programs were created.
4. Verification plans: Once the couch model was created verification plans were created to investigate the generalisability of the couch model. The initial attenuation measurements were done with standard geometries and the verification plans used complex, non-standard geometries.
5. Surface dose effects of the couch: The surface dose effect of the treatment couch was not used in the development of the couch model, but the surface dose effects needed

to be investigated to determine if the couch model succeeded in improving the accuracy of the surface dose predictions by the Pinnacle treatment planning system.

For all the attenuation measurements the researcher investigated the attenuation at depth. Measurements were made at the centre of the 20 cm cylindrical phantom, hence for all angles considered, the depth of measurement was 10 cm. For the square phantom the depth varied with angle, with all depths being at more than 5 cm, to exclude shallow depths where electron contamination or dose build up effects would add uncertainty.

3.2 Ethical considerations

The study was a pure phantom-based study involving mathematical computer modelling and dosimetry. The study did not involve any actual patient data or human participants and did not affect the direct management of any current patients.

Data were collected after normal working hours and it did not interfere with the clinical programme or service delivery at the study site. There was a sufficient number of Pinnacle treatment planning system workstations at the study site for the researcher to use during work hours, but the majority of the time spent on the Pinnacle was after normal working hours.

The only risk was occupational risk to the researcher. Here the normal risk of working with ionising radiation applied. The researcher is a registered radiation worker with the Health Professions Council of South Africa (HPCSA) and the South African Bureau of Standards (SABS) and was wearing a thermoluminescent dosimeter (TLD) personal radiation monitor at all times. The researcher followed the standard radiation protection principles while working with the ionising radiation.

Ethics approval process for the research study was obtained and granted by:

- Research Ethics Committee (REC) of the Faculty of Health and Wellness Sciences, Cape Peninsula University of Technology: REC Approval Reference No.: **CPUT/HW-REC 2018/H7** 13 March 2020 – see Appendix J1;
- Research committee, Groote Schuur Hospital 17th March 2020 – see Appendix J2.

Permission for the collection of data for research purposes in the department of radiotherapy at the study site was given by Head of the Division – see Appendix J3.

3.3 Study design

This was a quantitative, experimental study where the outcome was to improve the predicted doses as calculated by the Pinnacle treatment planning system. The study used continuous,

numerical data types which requires descriptive statistics. For each situation that was investigated the setups and measurements were repeated three times to help reduce random errors. The mean and standard deviation were calculated for each set of repeated measurements, and the mean values were used in the analyses. All the analyses were done using Microsoft Excel.

3.4 Research question

Can the accuracy of the dose calculation on the Pinnacle treatment planning system be improved for beams that are directed through the treatment couch by introducing an algorithm that models the effect of the couch?

Hypothesis 1: The use of an algorithm that incorporates the dimensions and properties of the treatment couch will improve the accuracy of dose determination at depth, compared to no couch structure included during the planning process.

Hypothesis 2: The angle of beam delivery through the couch affects the dose correction required at depth.

Hypothesis 3: The energy of the beam affects the dose correction required at depth.

Hypothesis 4: The use of an algorithm that incorporates the dimensions and properties of the treatment couch will improve the accuracy of the predicted skin dose in the presence of a treatment couch.

3.5 Aims and objectives of the research

3.5.1 Aims

The primary aim of this study is to increase the accuracy of the treatment of the cancer patients by increasing the accuracy of the predicted dose calculated by the treatment planning system for radiation beams which pass through the treatment couch. The aim is for the predicted doses on the Pinnacle treatment planning system to be within 3% of the measured doses on the treatment unit.

Ahnesjo and Aspradakis (1999) determined an overall accuracy in radiotherapy of 5% and an accuracy for the treatment planning system of 3%. Ahnesjo and Aspradakis (1999) indicated that for future development this can probably be reduced to an overall accuracy of 3%, and an accuracy of 2% for the treatment planning system. For this research study it was decided to aim for a 3% overall accuracy on the treatment planning system, including all contributors.

It was not part of the scope of this study to determine the individual impact of the contribution from the studied effects on the total TPS uncertainty.

3.5.2 Objectives

1. Develop an algorithm for incorporating the Varian IGRT Treatment Couch into the Pinnacle treatment planning system. The resultant couch model needs to be accurate in terms of:
 - a. The external shape and dimensions. (These are important because distance measurements taken on the plan need to be accurate);
 - b. The radiological properties. (This is important because the attenuation of the radiation dose, as predicted by the treatment planning system, needs to be consistent with the actual attenuation occurring on the treatment unit).
2. Evaluate the reliability and accuracy of the algorithm and resultant couch model on the calculated plans for radiotherapy. This will be validated by creating test plans on the Pinnacle treatment planning system and then measuring the doses on a phantom on the treatment unit to confirm the generalisability of the couch model.
3. Develop a robust way of including the couch model in the Pinnacle treatment planning system.
4. Develop a rigorous method of indexing the patient to the treatment couch so that the patient position on the treatment couch for treatment is aligned with the same geometry as was used when the patient was planned on the treatment planning system.
5. The algorithm needs to be user-friendly, fast and reliable.
6. Have a single algorithm which will create the full couch.

3.6 Equipment

- Varian Exact IGRT couch.
- Pinnacle Treatment Planning System (Version 9.8).
- Varian Clinac 2300 C/D linear accelerator – Both the 6 MV and 18 MV energy photon beams were used.
- Toshiba Aquilion LB wide bore CT Scanner.
- Phantoms
 - 20 cm Cylindrical water phantom (for the attenuation measurements of the radiation beam)
 - 30 x 30 cm Perspex square phantom (for the testing of the generalisability of the couch model and for the surface/skin dose measurements).
- Detectors

- PTW PinPoint detector - Type 31016 (for the attenuation measurements of the radiation beam).
- PTW Farmer 0.6 cm³ detector – Type 30013 (for the treatment plans to verify the generalisability of the couch model).
- Landauer® nanoDot™ Dosimeters (for the surface dose measurements).
- PTW Unidos electrometer.
- Python programming language
 - Python is a high-level programming language for general-purpose programming.
 - Python is already incorporated in the Unix Operating System on which the Pinnacle treatment planning system runs.

3.7 Quality assurance

The equipment items used in the study are all subject to QA as specified in South African Standards for Quality Assurance in Radiotherapy (SASQART).

For this study the following QA measures were important on the linear accelerator (See attached Appendix A):

- Output constancy for photons – This is a relative dosimetry quality assurance check and is done on a daily basis (Appendix A, Page 1, Designator DL4);
- Reference dosimetry – This is absolute dosimetry quality assurance check done annually and it is performed according to the IAEA TRS-398 protocol (Appendix A, Page 2, Designator AL6).

At the study site, linear accelerators are calibrated such that 1 gray (Gy) per 100 monitor units (MU) is delivered to D_{max} by a 10 cm x 10 cm field size at 100 cm SSD.

For this study relative dosimetry was used in the determination of the attenuation properties of the treatment couch, as well as for the measurements to verify the accuracy and generalisability of the developed couch model.

The detectors are subject to regular calibrations at a standard calibration laboratory. This is done every two years as set out in the SASQART document for Major Dosimetry. See attached Appendix B.

The QA for the Pinnacle treatment planning system is specified in the SASQART document for Treatment Planning Systems. See attached Appendix C.

For this study an important QA check of the treatment planning system was for the CT geometry/density. The Pinnacle treatment planning system uses physical densities and not electron density. The script which was developed to create and incorporate the treatment couch model in the planning system also uses physical densities.

3.8 Analysis of the physical treatment couch

3.8.1 Physical properties of the couch

The Varian IGRT treatment couch has a length of 200 cm and a width of 53 cm (Figure 3.1). The water equivalence of the couch is 5.2 mm in the thin section of the couch and 8.4 mm in the thick section. This information is from the specification pamphlet from the suppliers (Appendix D). The dimensions were also verified by measurements with a tape measure at the study site. A further observation is that the couch is non-regular in shape in all directions. Figure 3.1 (a) illustrates the curves at the superior and inferior ends of the couch. Figure 3.2 illustrates the cross-section of the couch.



Figure 3.1: The main dimensions of the Varian IGRT couch

Image (a) on top is a view from above (from anterior), and image (b) is a view from the lateral side (Radiotherapy Simulation software (Botha, 2019))



Figure 3.2: The cross-sections of the Varian IGRT couch

Image (a) on top is a cross-section through the thin section of the couch, and image (b) is a cross-section through the thick section of the couch (Radiotherapy Simulation software (Botha, 2019))

For this study the couch was subdivided into five distinct sections (Figure 3.3). These sections have the following dimensions:

Section A: This is the superior end of the couch. It has a length (superior to inferior) of 14 cm and a thickness (anterior to posterior) of 5 cm.

Section B: This is the thin section of the couch. It has a length of 26 cm, a thickness of 5 cm and a uniform cross-section over the full length of this section.

Section C: This is the sloping section between the thin and thick sections. It has a length of 36 cm and the thickness starts at 5 cm at its superior end and increases linearly to 7.5 cm at its inferior end.

Section D: This is the thick section. It has a length of 124 cm, a thickness of 7.5 cm and a uniform cross-section over the full length of this section.

Section E: This is a detachable section on the inferior end of the couch. It has a length of 15 cm and a thickness of 7.5 cm. This section was ignored for this study because the couch cannot be positioned in such a way that radiation through this section will interact with the patient for treatments.



Figure 3.3: Indicating the five (5) main sections of the Varian IGRT couch

Image (a) on top is a view from above (from anterior),
and image (b) is a view from the lateral side

A – The superior section of the couch; B – Thin section of the couch
C – Sloping section of the couch; D – Thick section of the couch
E – Detachable inferior section of the couch
(Radiotherapy Simulation software (Botha, 2019))

Previously, a CT Scan of the Varian IGRT treatment couch was performed in order to verify that the couch model produced by the algorithm was accurate in terms of the shape and dimensions.

3.8.2 Radiological properties of the couch

The radiological properties of the couch were determined by measuring the actual effect of the treatment couch on the radiation at the treatment unit.

3.8.2.1 Attenuation factors

The initial dose measurements were done to determine the actual attenuation of the radiation dose by the Varian IGRT couch at the study site. Here relative dosimeter measurements were done for the open beam (no couch in the radiation beam) and the attenuated/closed beam (with the couch in the radiation beam) in order to determine the attenuation properties of the couch. It was decided that absolute dosimetry was not required because the measurements for the open beam and attenuated beams for a particular set of variables were done together. Therefore, the measurements in the set were all done in the same environmental/ambient temperature and pressure conditions. This meant that no temperature and pressure corrections were required.

All measurements were done using the 20 cm cylindrical water phantom and the study focused on dose to water, as was mentioned in section 3.1.

All the measurements were done on the Varian Clinac 2300 C/D linear accelerator using both the 6 MV and 18 MV radiation energies. Both energies were used because literature has shown that the radiation energy plays a significant role in the effect of the couch on the radiation (De Ost et al., 1997, Poppe et al., 2007, Gerig et al., 2010, Seppala & Kulmala, 2011).

The 20 cm cylindrical phantom was used together with a PTW PinPoint detector and the PTW Unidos dosimeter to measure the dose (Figure 3.4). It was decided to use the PTW PinPoint detector because it was designed for the measurement of relative beam profiles for megavoltage radiation treatment units and it is rated for field sizes of 2 x 2 cm all the way up to 30 x 30 cm (Appendix E1: PinPoint Chambers). All the measurements were done on the electrometer in picocoulombs (pC). It was not necessary to convert these readings to gray because they were treated as relative measurements.

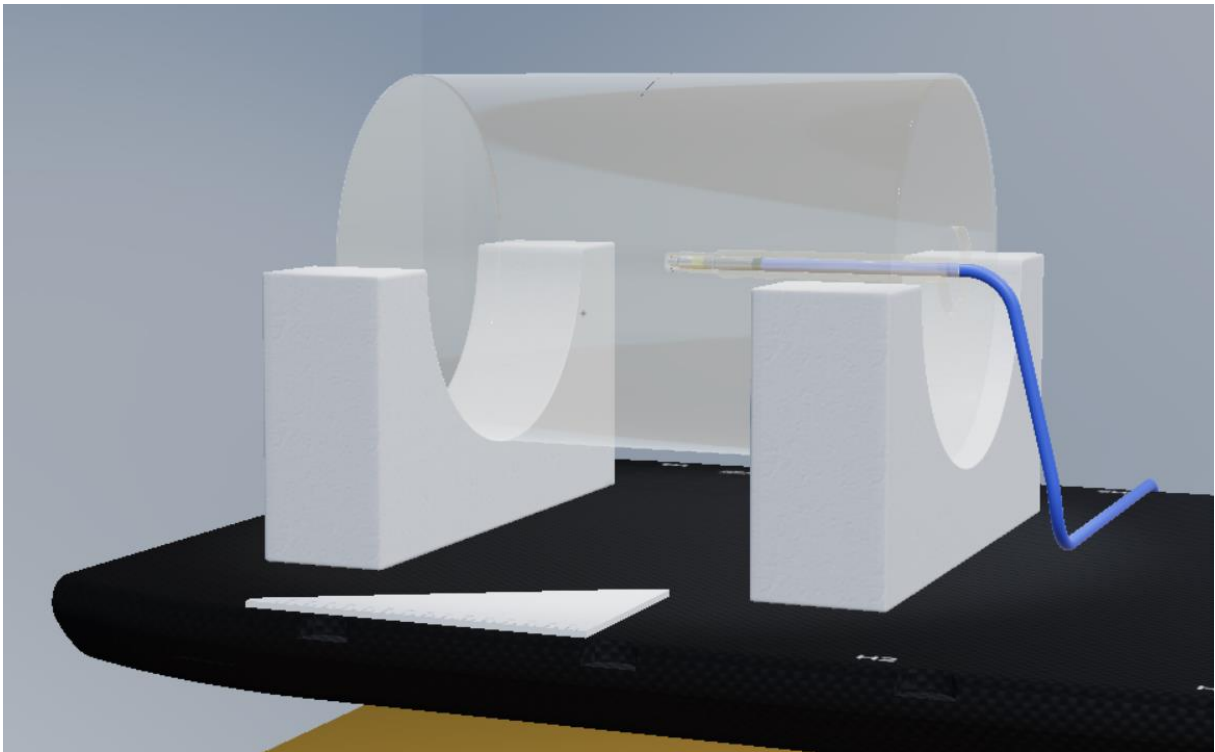


Figure 3.4: The 20 cm cylindrical phantom with the PinPoint chamber
(Radiotherapy Simulation software (Botha, 2019))

The phantom was positioned on the treatment couch and the detector placed in the central cavity of the phantom. The cylindrical shape of the phantom ensured that there would always be equal thicknesses of phantom between the detector and the radiation source, regardless of the gantry angle. This meant that any variation in the radiation dose at the detector is due to the angle of incidence of the radiation beams on the attenuating couch and not due to any variations in the thickness of the phantom. The phantom was set up in such a way that the detector was situated at the isocentre (100 SAD). The phantom was positioned at three positions on the treatment couch along the midline in order to measure attenuation values which represented the various sections of the couch. The indexing notches on the couch were used to be able to reproduce the setup (Figure 3.5). The three positions were as follows:

- On the thin section of the couch: 6 cm superior to the superior edge of the H3 notch (Figure 3.6);
- In the sloping section of the couch: On the superior edge of the H1 notch (Figure 3.7);
- On the thick section of the couch: Bottom edge of the F1 notch (Figure 3.8).

The measurements were done for these different sections of the couch because the distance that the radiation travels through material affects the amount of attenuation which the material produces.



Figure 3.5: Part of the IGRT couch showing some of the indexing notches
(Radiotherapy Simulation software (Botha, 2019))

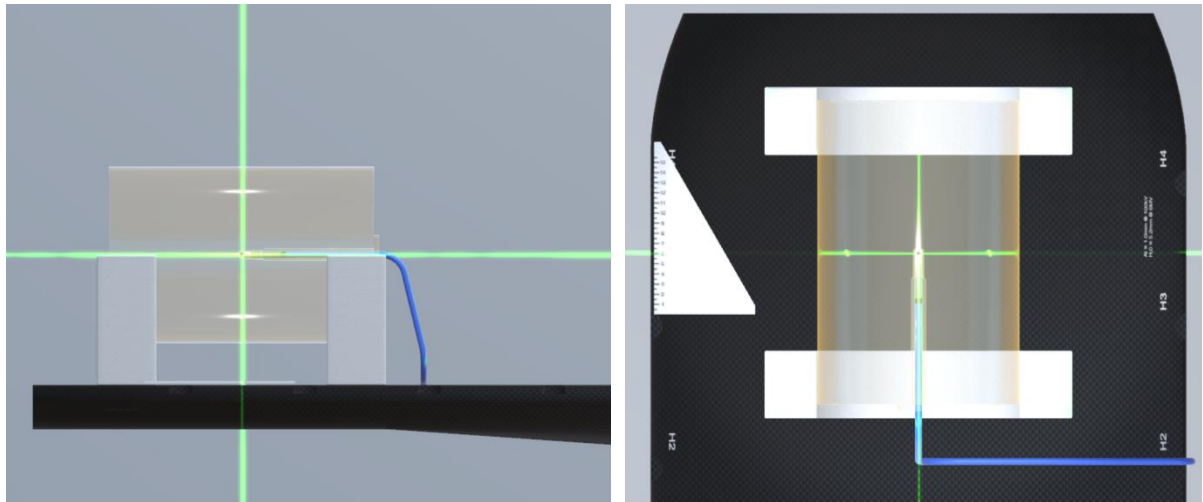


Figure 3.6: The position of the phantom for the attenuation measurements for the thin section of the couch
 (Radiotherapy Simulation software (Botha, 2019))

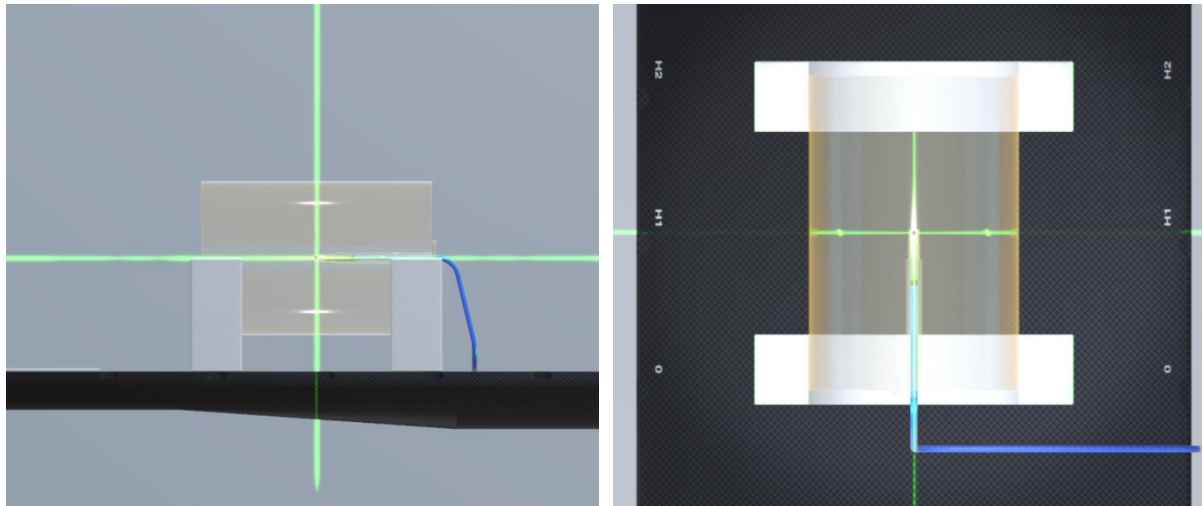


Figure 3.7: The position of the phantom for the attenuation measurements for the sloping of the couch
 (Radiotherapy Simulation software (Botha, 2019))

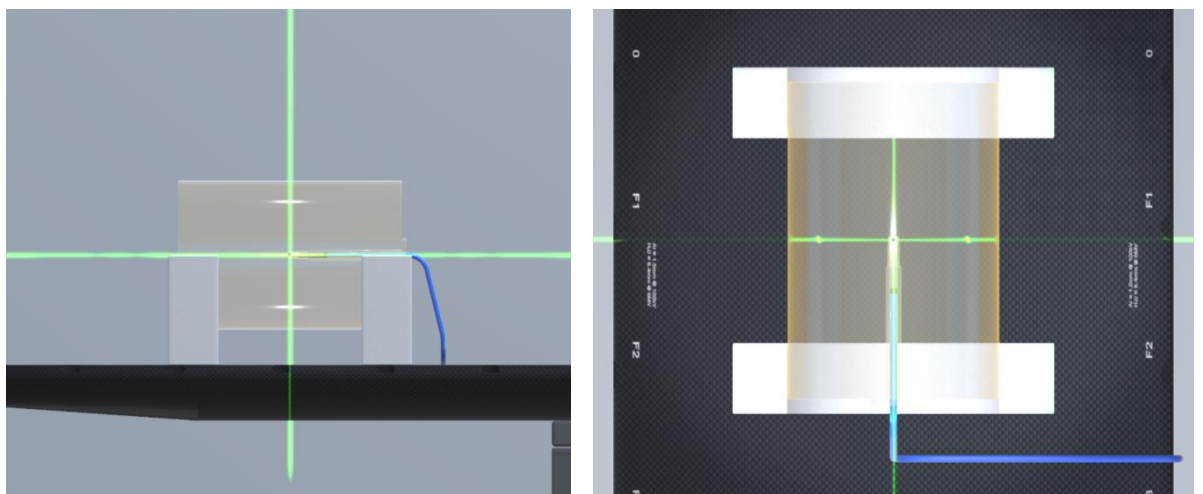


Figure 3.8: The position for the phantom for the attenuation measurements for the thick section of the couch
 (Radiotherapy Simulation software (Botha, 2019))

For each of these positions the lateral, vertical lasers were used to position the couch accurately at the desired longitudinal level. The couch was also centred laterally to the zero position. The phantom was then positioned so that the active part of the detector was at the isocentre at 100 SAD (Figure 3.9). On the first setups for each of the three couch positions the vertical couch positions were recorded. On subsequent setups, after the phantom was positioned, the current couch vertical positions were checked against the recorded values. These recorded vertical positions turned out to hold for all the subsequent measurements. The vertical heights of the couch for the three positions at which the measurements were done were as follows:

- -14.9 cm for the thin section of the couch;
- -14.8 cm for the middle of the sloping section;
- -14.7 cm for the thick section.

These heights showed that the couch slopes up slightly towards the superior end of the couch. This is in line with what was expected because the couch is calibrated to slope up when there is no weight on the couch so that when a patient is positioned on the couch the weight of the patient will bring the couch towards a level position.

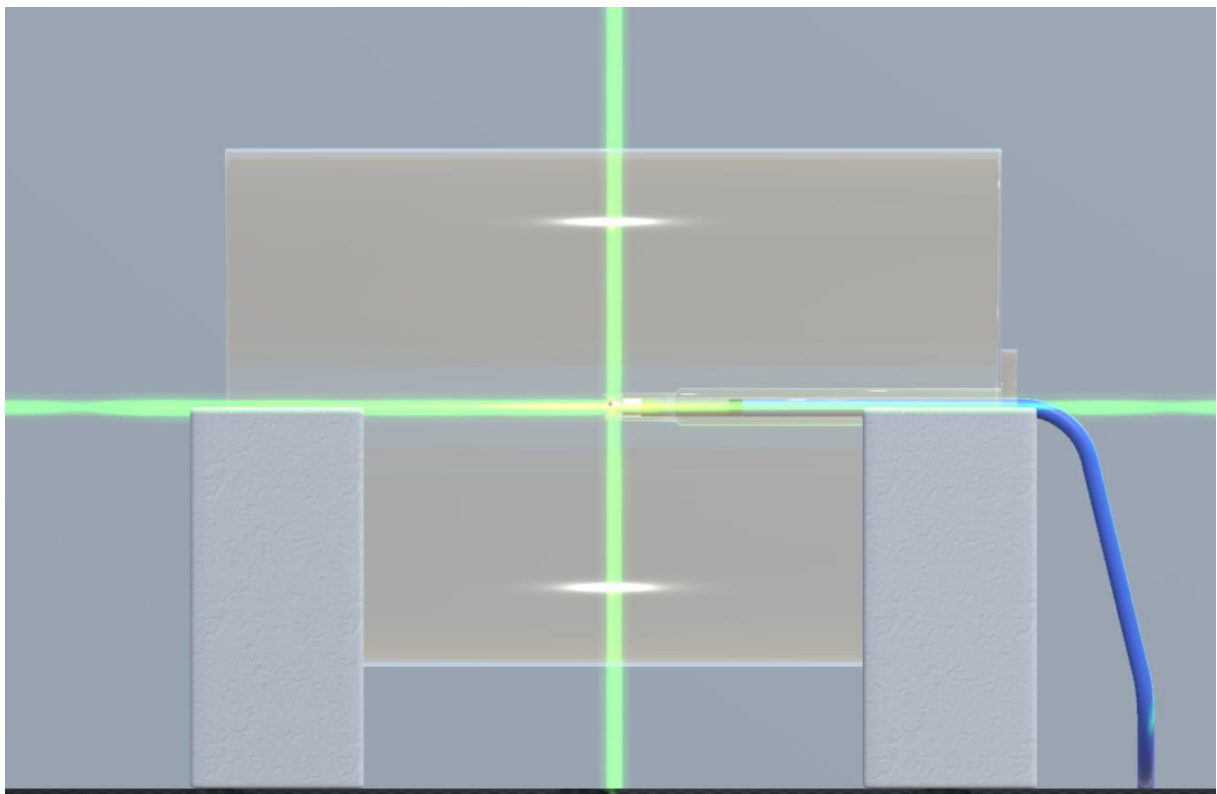


Figure 3.9: Position of the phantom so that the active part of the PinPoint is at the isocentre
(as indicated by the lasers)
(Radiotherapy Simulation software (Botha, 2019))

For the open beam the gantry angles used were 0° , 90° and 270° (Figure 3.10). Since only air affects the open beam no additional angles were required. The 0° , 90° and 270° angles were chosen because they would give a good indication of the accuracy of the phantom setup. The doses from the 0° , 90° and 270° angles should be the same; therefore, if the 0° dose varied it could indicate that the vertical distance to the detector was not correct, and if the 90° and 270° doses varied it would indicate that the lateral position of the phantom was not correct. All the attenuation measurements were relative measurements and the mean of the 0° , 90° and 270° doses was used as the reference for the relative attenuation.

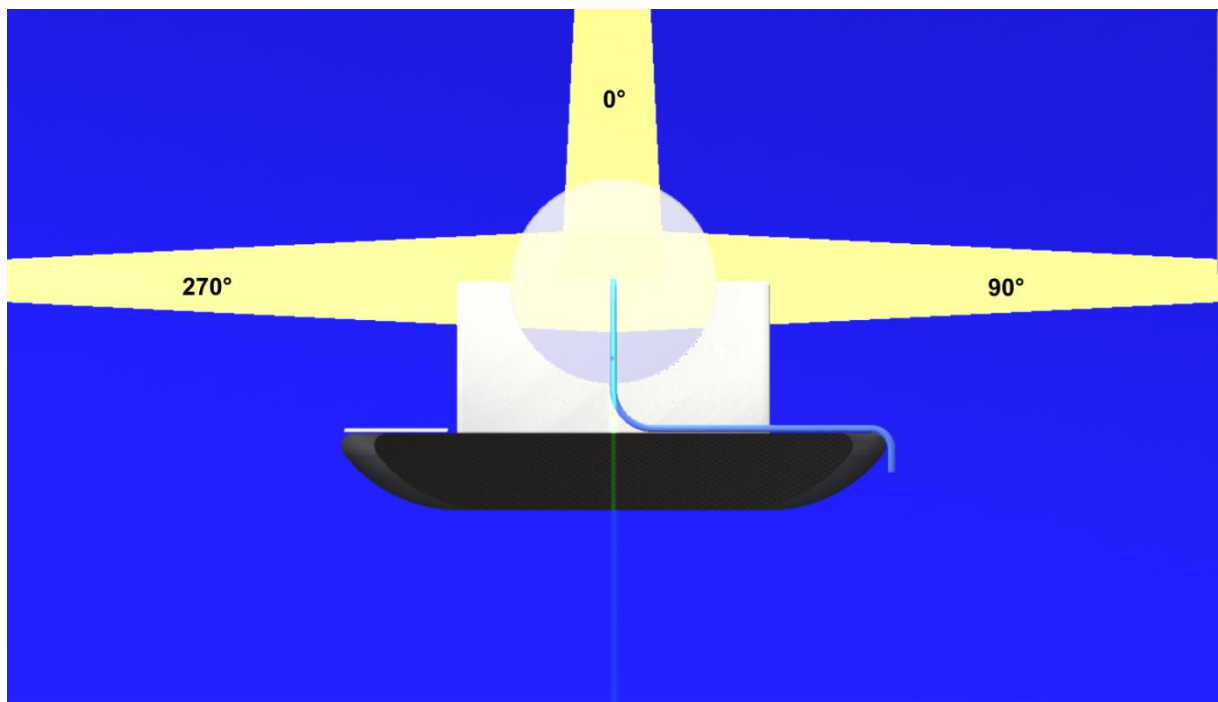


Figure 3.10: The gantry angles used for the open (unattenuated) beam measurements
(This is viewed from the inferior of the couch towards the gantry)
(Radiotherapy Simulation software (Botha, 2019))

For the attenuated beams the initial plan was to look at gantry angles of 100° to 180° in 10° increments. This would only have covered one half of the couch (Figure 3.11). It was decided to rather cover both sides of the couch by using gantry angles from 100° to 260° in 20° increments (Figure 3.12). After the first set of measurements for the thin section of the couch was done, it became clear that the chosen gantry angles had to be adjusted. The cylindrical phantom rests on each end on a support cradle made from polystyrene (Figure 3.4). This resulted in the steeper angles, 100° and 260° , missing the couch completely (Figure 3.13).

Thus, it was decided to omit angles 100° and 260° , but to add 130° and 230° angles around the lateral edges of the couch to give more dose measurement values where the couch shape

changes (Figure 3.17). Furthermore, it was observed that with 120° and 240° angles the anterior half of the beam was in air and the centre of the beam was falling on the sloping edge of the couch (Figure 3.14). These were noted so that the dose values measured at these angles could be carefully evaluated on the treatment planning system. The final gantry angles which were used for the attenuated beams were as follows (Figure 3.15): 120°, 130°, 140°, 160°, 180°, 200°, 220°, 230°, and 240°.

For the beams from 140° to 220° it was decided that 20° increments were sufficient because these beams entered on the uniform flat bottom part of the couch top and there was limited variation in the shape of the couch.

It was important to measure the attenuation at multiple angles because literature has shown that the gantry angle (and thus the beam incident angle on the couch) affects the impact of the couch on the radiation beam (McCormack et al., 2005, Poppe et al., 2007, Seppala & Kulmala, 2011).

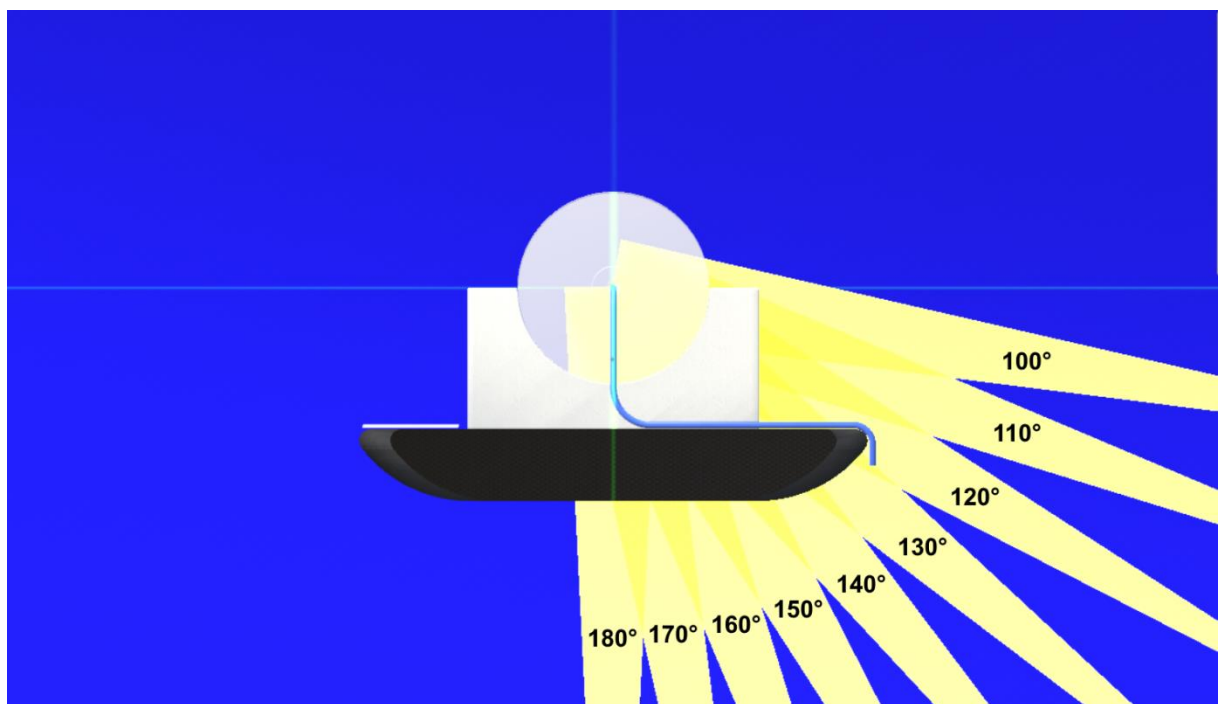


Figure 3.11: Showing how the gantry angles 100° to 180° only cover one side of the couch
(This is viewed from the inferior of the couch towards the gantry)
(Radiotherapy Simulation software (Botha, 2019))

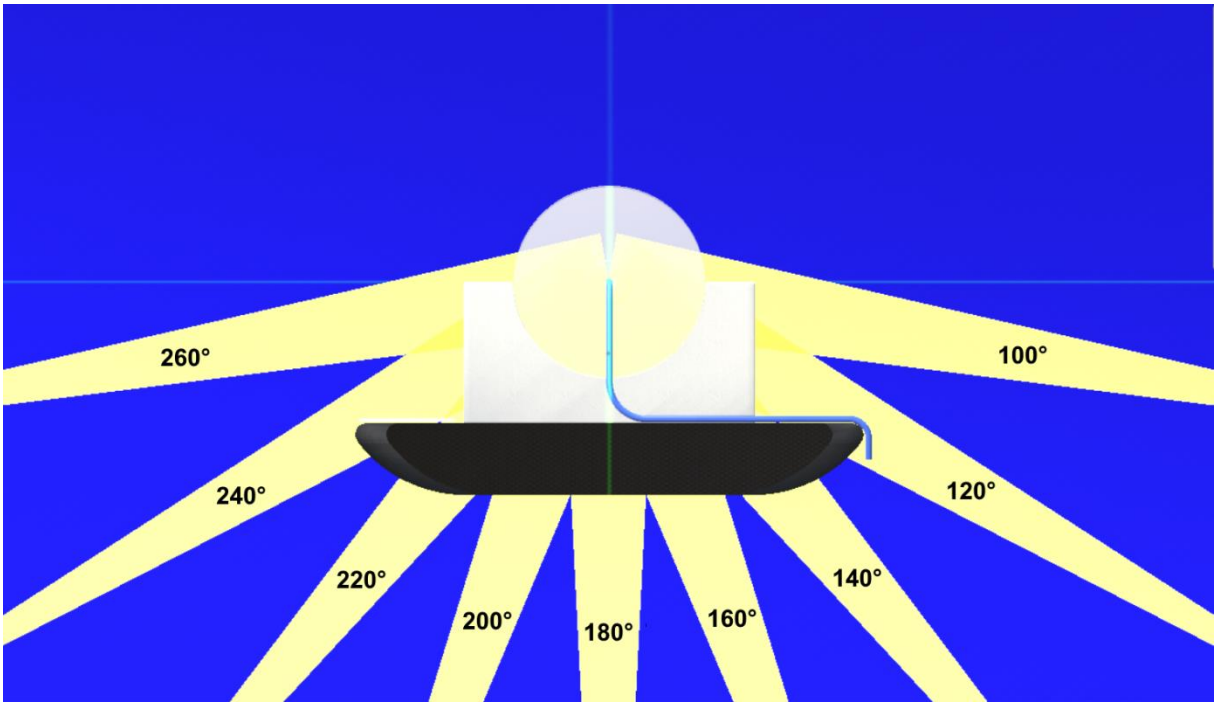


Figure 3.12: Gantry angles 100° to 260° in 20° increments
 (This is viewed from the inferior of the couch towards the gantry)
 (Radiotherapy Simulation software (Botha, 2019))

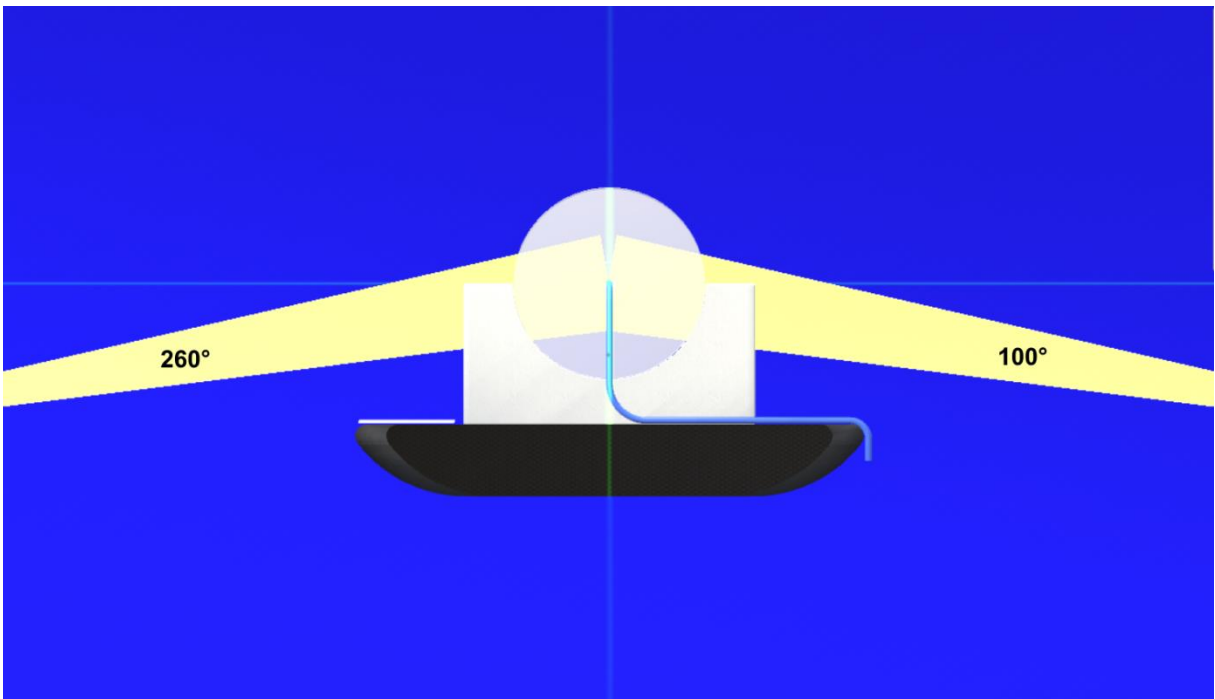


Figure 3.13: The height of the couch caused the steep angles (100° and 260°) to miss the couch
 (This is viewed from the inferior of the couch towards the gantry)
 (Radiotherapy Simulation software (Botha, 2019))

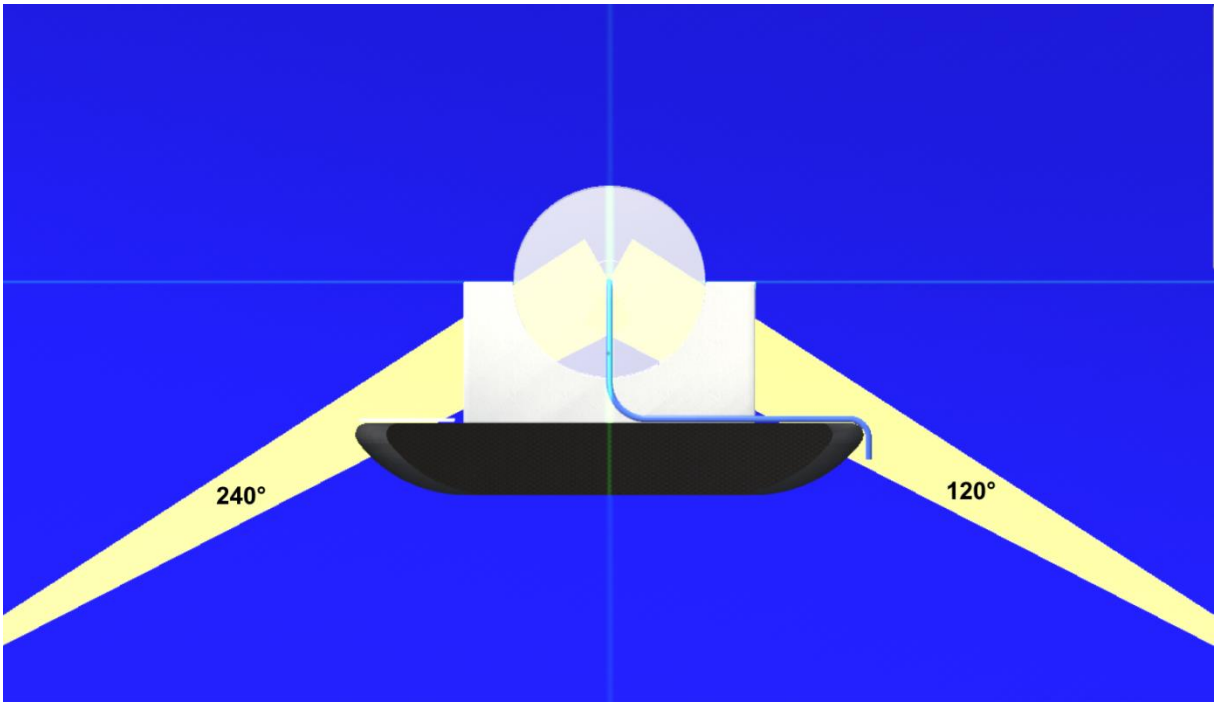


Figure 3.14: The anterior half of these beams missed the couch and the centres fell exactly on the sloping edge of the couch
 (This is viewed from the inferior of the couch towards the gantry)
 (Radiotherapy Simulation software (Botha, 2019))

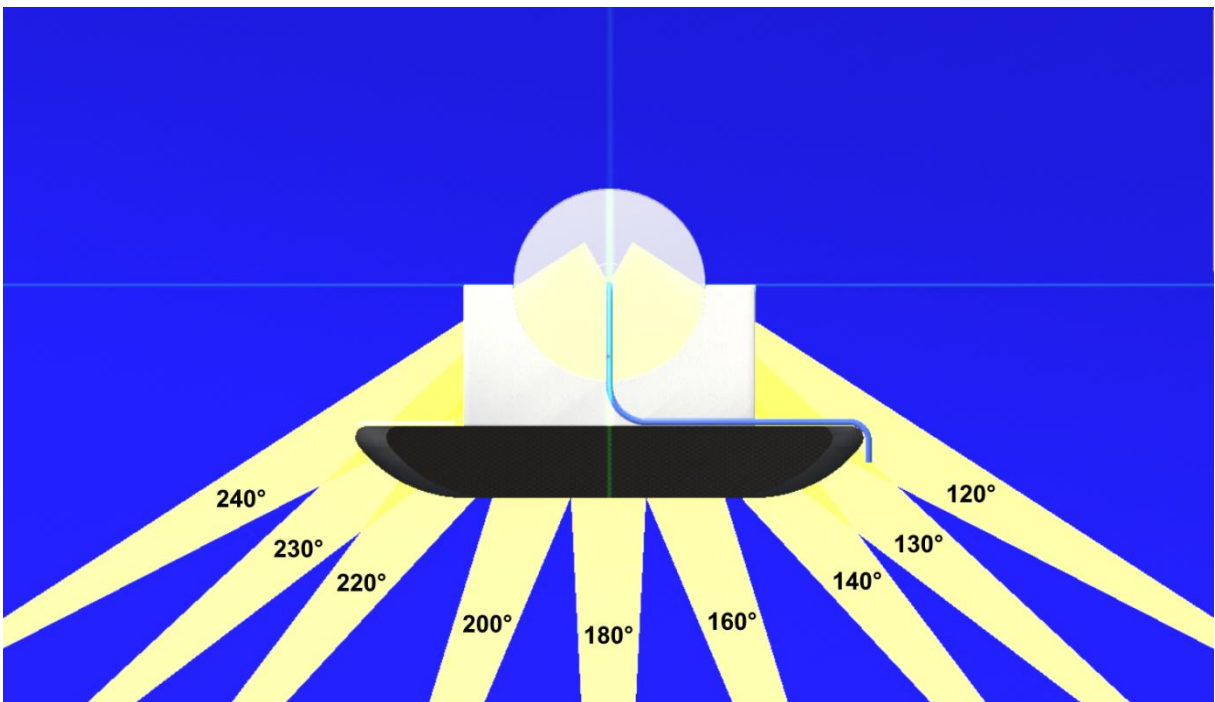


Figure 3.15: The final angles used for the measurements of the attenuation of the radiation beams by the couch
 (This is viewed from the inferior of the couch towards the gantry)
 (Radiotherapy Simulation software (Botha, 2019))

The support cradles of the phantom are thin enough and the phantom long enough to ensure that none of the beams (even for the 15 x 15 cm field sizes) passed through the cradles and therefore any attenuation of the beams by the cradles did not have to be considered (Figure 3.16).

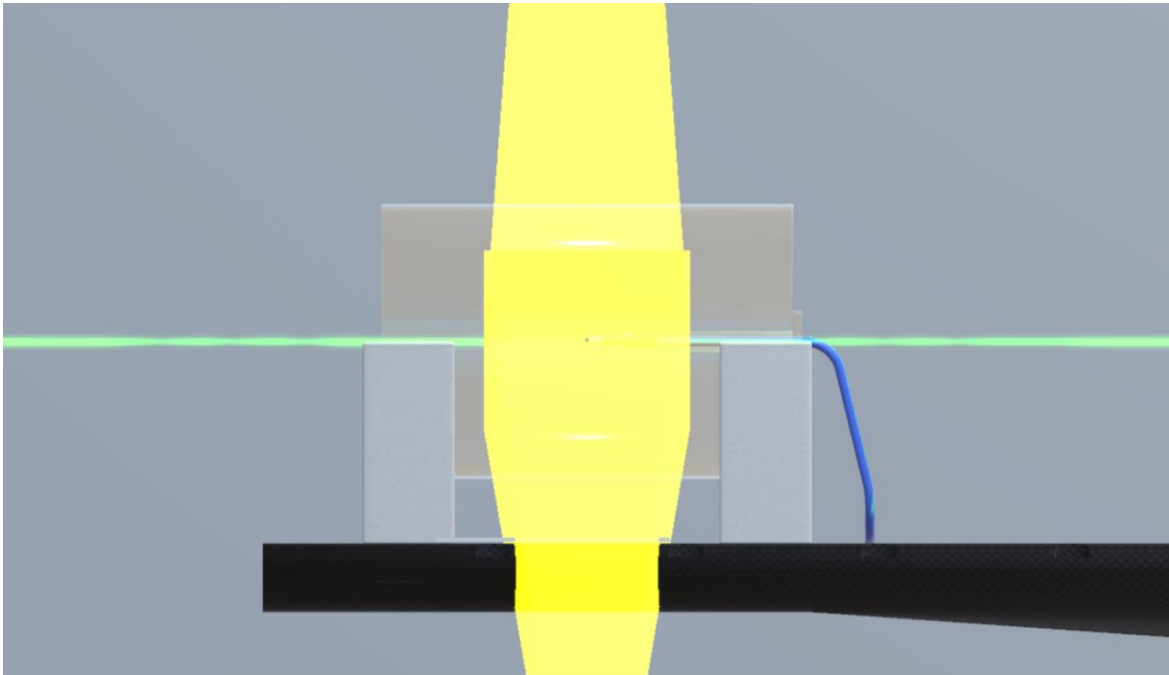


Figure 3.16: The cradles are wide enough apart to not be in the beams
(Here it is demonstrated with the 15x15 cm field size)
(Radiotherapy Simulation software (Botha, 2019))

At each gantry angle, the dose was measured for 5 x 5 cm, 10 x 10 cm, and 15 x 15 cm field sizes for both 6 MV and 18 MV radiation energies. All the measurements were done three times and each time it was a completely new, independent setup. The reason the study looked at different field sizes as well, is that the field size also plays a role in determining the effect of the couch on the radiation beam (Gerig et al., 2010, Seppala & Kulmala, 2011).

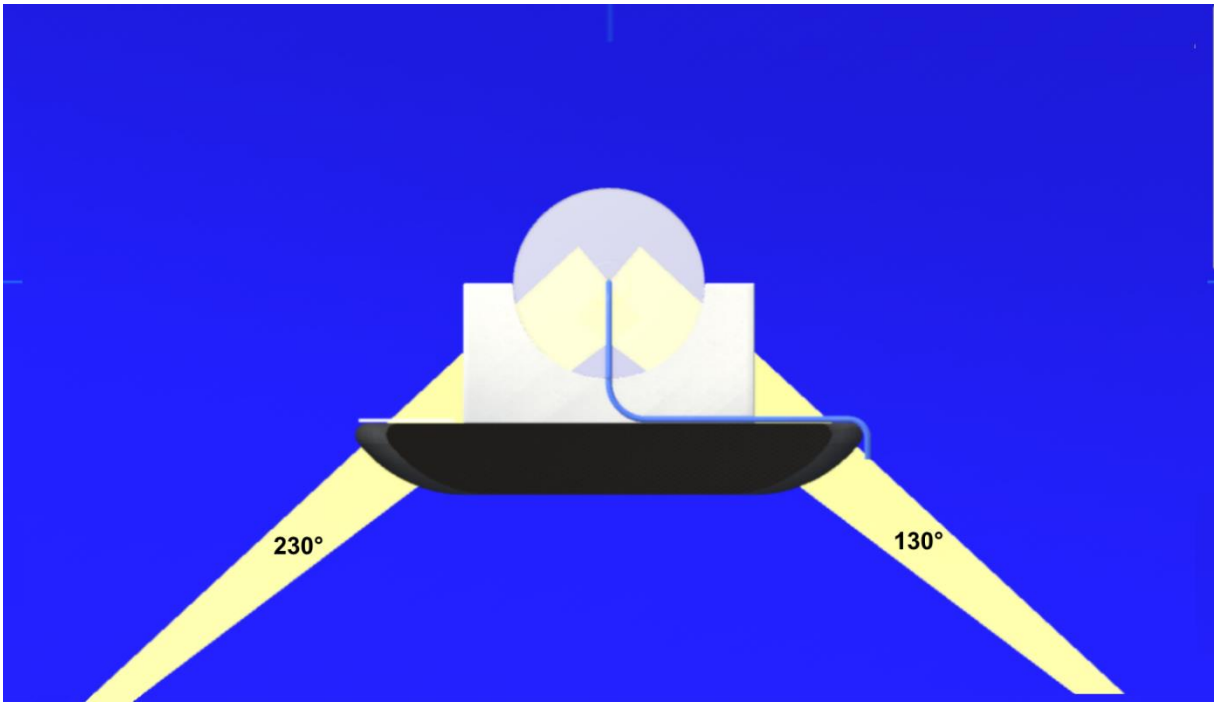


Figure 3.17: With gantry angles 130° and 230° the anterior part of the beams travel through a shorter thickness of couch than the posterior part
 (This is viewed from the inferior of the couch towards the gantry)
 (Radiotherapy Simulation software (Botha, 2019))

Attenuation correction factors were calculated as follows using the normalised doses (similar to the formula used by Hayashi et al. (2010)):

$$\text{Attenuation correction factor} = \frac{\text{Open beam dose}}{\text{Attenuated beam dose}}$$

For all the graphs showing the results the attenuation correction factors have been used.

The attenuation percentage was calculated as follows:

$$\text{Attenuation} = \frac{\text{Open beam measurement} - \text{Closed beam measurement}}{\text{Open beam measurement}} \times 100$$

The attenuation percentage was used in the results in the tables providing summaries of the attenuation produced by the treatment couch.

3.8.2.2 Evaluating necessity of couch model

The doses which have been measured on the treatment unit with the actual Varian IGRT couch were then compared with the doses that the Pinnacle treatment planning system calculated if it did not take the treatment couch into account. This was to see if the Pinnacle treatment planning system overestimated the doses for beams which traverse the treatment couch, and

if so, by how much. This would give an indication if it was necessary to incorporate a couch model in the Pinnacle treatment planning system to improve accuracy of the predicted doses. For this analysis Pinnacle plans were created which duplicated the parameters used when the initial attenuation measurements were done. For the initial attenuation measurements there were eighteen different treatment plans, involving two energies, three field sizes, and three sections of the couch. However, here the couch was ignored in the plans and it was not necessary to consider the different couch sections so only six plans were required. The six plans only needed to look at two energies and three field sizes. The calculated dose for each field in Pinnacle for a particular energy and field size combination (with the couch ignored) were compared with the measured doses for corresponding energy and field size combinations for the three couch sections. This gave an indication of how much Pinnacle overestimated the doses for each couch section. Here again the gantry angles of 120° and 240° were excluded.

The measured doses and the Pinnacle doses were normalised to their respective open (unattenuated) field doses. The overestimations (as a percentage) by Pinnacle were calculated as follows:

$$\text{Overestimation} = \frac{\text{Pinnacle dose} - \text{Measured dose}}{\text{Measured dose}} \times 100$$

3.9 Creating the couch model on the Pinnacle TPS

3.9.1 Requirements of the Pinnacle TPS couch model/structure

The external size and shape of the couch structure in the treatment planning system needed to be identical to the real treatment couch. It was equally important that the couch structure be created exactly in the correct position within the treatment plan relative to the patient's position; for example, if the patient will be positioned for treatment with the top of the head 10 cm inferior to the top of the couch and the patient 5 cm to the left of the couch midline, then the couch structure must be created on the treatment plan to match that position. This was important for a number of reasons. The main reason was to ensure that the actual situation was simulated accurately within the treatment planning system. Any measurements which were taken from the treatment plan (for example SSD measurements) would then exactly reflect the real situation at the treatment unit when the patient was being treated. It would also ensure that any beams interacting with the couch will interact with the couch identically in both the treatment planning system, as well as on the treatment unit, in terms of the incident angle and section of the couch. Furthermore, if the shape, dimensions and position of the couch in the treatment planning system are created accurately, it will help as a visual check for the planning

staff to help them avoid selecting beam parameters which might result in collisions on the treatment unit itself.

Apart from these visible characteristics of the couch, the virtual couch structure in the treatment planning system also needed to mimic the radiological properties of the real treatment couch. This meant that the beams interacting with the couch in the treatment planning system needed to be affected to the same degree as the corresponding beams on the treatment unit.

As mentioned above, it was important to recreate the external properties (dimensions and shape) of the couch accurately. However, it was not so important to be able to recreate the inner construction of the couch accurately. The aim here was to recreate the radiological effect of the real couch and not necessarily the exact detail of the inner construction and densities of the real couch. The real IGRT treatment couch has an outer skin and an inner core of lower density than that of the skin. The plan was to still create a couch structure which has an outer skin and inner core, but that the thicknesses of these regions, as well as their densities, be determined and set so that the overall radiological effect of the couch structure created in the Pinnacle treatment planning system mimics that of the real couch.

3.9.2 Scanning the water phantom

A CT scan was acquired of the 20 cm cylindrical phantom. The full length of the phantom was scanned with a slice thickness of 2 mm. The phantom scan set was imported into the Pinnacle treatment planning system. It was considered important to ensure that the CT scan is done with a large enough field of view (FOV) in order for the full width of the couch structure to completely fit within the field of view. Any structures/contours situated outside this field of view would not be included in the calculation of the doses by the Pinnacle treatment planning system. At the study site the wide bore CT Scanner was used for the scanning of the phantom, but the default field of view is not automatically set to be large enough to fit the couch structure. The CT scans had to be repeated for the phantom, because the initial scan set had a field of view size of 40 x 40 cm² and the couch is 53 cm wide. For the second scan set the field of view was set to “Extra large” (Figure 3.18).

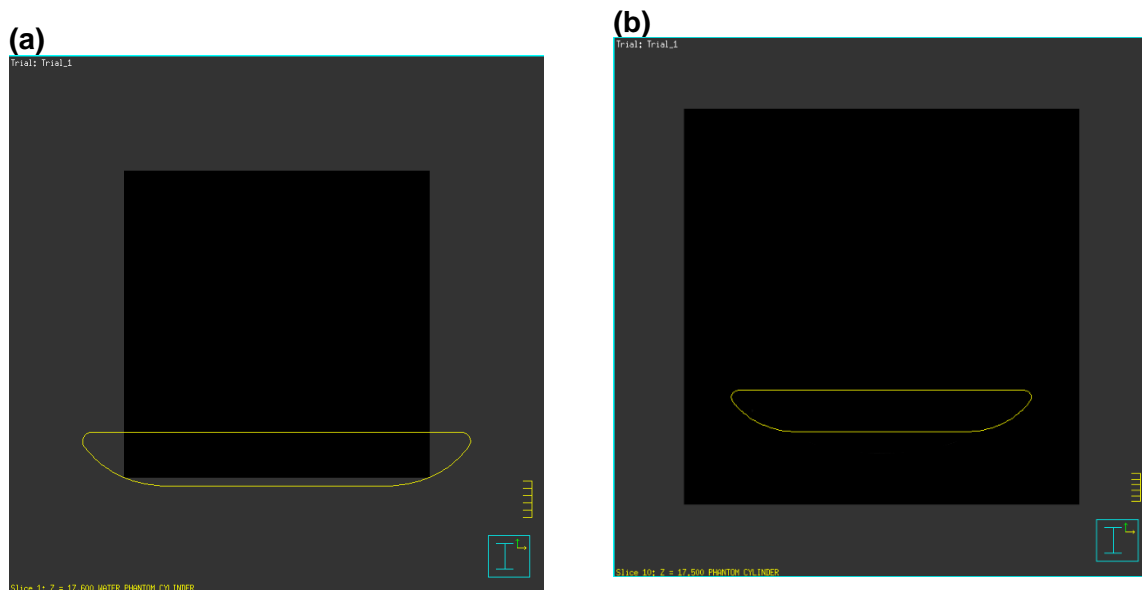


Figure 3.18: The field of view (FOV) of the scans

The black square represents the FOV. (a) The default FOV on the CT Scanner at the study site is not large enough for the full width of the couch structure.

(b) The Extra Large FOV setting is large enough for the couch structure.
(Pinnacle treatment planning system screen shot by the researcher)

3.9.3 Setting up plans on the Pinnacle TPS

The phantom was contoured on the Pinnacle treatment planning system. The CT origin was then set to coincide with the position of the active part of the PinPoint chamber within the phantom. A separate plan was created for each set of parameters (beam energy, field size, and section of the couch), resulting in eighteen separate plans (two beam energies, three field sizes, and three different couch sections). Each plan had twelve beams with the following gantry angles:

0°, 90°, 270°, 120°, 130°, 140°, 160°, 180°, 200°, 220°, 230°, and 240°.

These plans were then used to determine the required densities and skin thickness for the couch model created by the scripts. In section 3.9.4 the development of the script is described in more detail.

The Pinnacle treatment planning system uses a convolution superposition algorithm which calculates the dose distributions from precalculated kernels using collapsed cone calculation methods. Because of this the algorithm can calculate modifications of the dose distributions due to placement of any beam modifiers in the beam, the surface of the patient, as well as tissue heterogeneities (Philips Medical Systems, 2013b).

The Pinnacle treatment planning system does not see a body structure like some other treatment planning systems. Pinnacle requires density in order to be able to calculate dose (Philips Medical Systems, 2013a). This is why it is important to make sure that the dose grid is set correctly to include what needs to be calculated. For this study the Pinnacle dose grid was specified such that it was large enough in the x- and y-coordinates to ensure that the dose grid covers the full phantom and the space where the couch structure will be created, as well as large enough in the z-coordinates to account for the largest field size used in the study. The dose grid resolution was initially set to $0.3 \times 0.3 \times 0.3 \text{ cm}^3$. This meant that no section of the couch could be thinner than 0.3 cm to allow detection of the correct density value. It was essential to confirm that the calculation model used in testing would allow detection of all elements of the couch, with the correct density for each element. After trial plans were used as a pilot, the dose grid resolution was changed to $0.2 \times 0.2 \times 0.3 \text{ cm}^3$ to allow enough flexibility in the skin thicknesses in order to attempt a couch skin thickness which would produce the desired radiological result. This was to 'fine-tune' and thus specify accurately the parameters of the couch model. The resolution in the z-direction was left at 0.3 cm as it is not in the direction of the beam path, and to facilitate calculation speed. This would also not affect the accuracy of the dose convolution calculation substantively as the density of the couch is uniform and the shape changes slowly in the z-direction. After experimentation with the values of the parameters in the trial plans, the final skin thicknesses which were determined and used for the couch model ranged between 0.4 and 0.6 cm.

As was mentioned in section 3.9.1, it was not so important to be able to recreate the inner construction of the couch accurately, but rather to be able to reproduce the radiological effect of the treatment couch. The model was modified to produce a compromise between the actual scanned shell thickness and density, and the required model thickness and density to ensure accurate detection on the grid. More important than this, however, was that the model produced radiological characteristics which had the similar predicted attenuations in the Pinnacle TPS as the measured attenuations produced by the real treatment couch.

Because the Pinnacle TPS calculates any densities that it encounters within the dose grid, it provides a parameter, called "Outside-patient air threshold". This is a value that Pinnacle uses to differentiate between the patient and the surrounding air, and is used to determine the initial starting point of calculation. At the study site the value used for the Outside-patient air threshold is 0.6 g/cm^3 . Pinnacle starts its dose calculations as soon as it encounters densities above 0.6 g/cm^3 and once the dose calculation has started Pinnacle then considers all densities in the calculations (including densities below 0.6 g/cm^3).

Following this, the monitor units for each beam were specified on the plan and the calculated dose recorded. For each beam, 100 monitor units were specified, as was used when the doses were measured on the treatment unit. All the calculations were done using the collapsed cone (CC) convolution calculation algorithm.

After evaluation of the chosen beam angles it was found that there was a marked difference in the measured values between the 120° and 240° angles. Investigation of the geometry revealed these angles resulted in a partial miss of the couch structure (Figure 3.14) and the decision was taken to exclude them from the study.

The vertical distance between the centre of the chamber and the top of the couch when the measurements were done on the treatment unit was 14.7 cm. This meant that in Pinnacle TPS the top of the created couch structure also needed to be 14.7 cm posterior to the centre of the chamber. The laser reference position was set to intersect the centre of the chamber on the CT scan and the Y-coordinate (anterior-posterior) of the laser reference position was -0.1 cm. This meant that the top of the couch on Pinnacle needed to be at -14.8 cm (-0.1 cm -14.7 cm) and for all the initial plans used to model the couch structure the couch removal Y coordinate was then set to -14.8 cm. The script uses this coordinate to position the top of the couch structure.

3.9.4 Development of the script / algorithm

It is noted that the script performs multiple functions, namely:

1. It collects all the required information from the patient's treatment plan on the Pinnacle treatment planning system;
2. It simulates the removal of the CT Scanner couch from the CT scan images;
3. It calculates the coordinates for each point that makes up the couch structure for each slice that requires a couch structure and writes this information to text files;
4. Finally, the script imports these text files into the treatment plan as ROI (region of interest) structures.

The script consists of two separate, main script files/programs. The first script program is a built-in part of the Pinnacle treatment planning system scripting utility and this part of the script collects all the required parameters and values from the particular Pinnacle patient plan as well as from user input (see Appendix F for this part of the script). The second script program is a Python program. Python is a high-level programming language. The reason Python was used is that it was already available on the Unix server of the Pinnacle treatment planning system and the syntax is similar to the C++ and C# programming languages that the researcher was already familiar with. The Python program also provided more power and flexibility than the

built-in Pinnacle scripting utility alone, and the Python program was used to perform the complex calculations and loops required for the couch structure. The Python program is responsible for the actual calculations of the coordinates for the couch structure, as well as the creation of the couch ROI text files. After the Python program has completed, the first script program then imports these couch ROI structures into the particular patient's plan. Appendix G contains the full Python program.

3.9.4.1 Removal of the CT Scanner couch

When the patient has a CT scan, the patient is positioned on a CT Scanner couch and as a result this couch is then incorporated into the CT images as pixels (Figure 3.19). This CT Scanner couch is different from the treatment couch, both in size and construction. The CT Scanner couch must be "removed" from the CT images in the treatment planning system such that the CT Scanner couch is not taken into account when the dose is calculated for the patient's treatment. This is important because in the treatment planning system it is required to mimic what will happen when the patient is undergoing treatment, and the patient will not be positioned on the CT Scanner couch for treatment, but on the treatment couch.

The CT Scanner couch is part of the pixels which make up the CT images and to physically remove the couch pixels from the CT images is outside the scope of this study. For this study the method used to remove the CT Scanner couch was to instruct the Pinnacle treatment planning system to ignore the densities of the CT Scanner couch. The Pinnacle treatment planning system provides some functionality to remove the effect of the CT Scanner couch. This functionality is in the form of a couch removal plane. This is a plane in the XZ-dimension and the user can specify the Y-coordinate of this plane in the 2D window (Figure 3.20). The user then usually positions this couch removal plane at the top (anterior) surface of the CT Scanner couch. Everything below (posteriorly) to this couch removal plane is then ignored by Pinnacle so that it is not taken into account for SSD measurements or dose calculations.

For this study, the CT Scanner couch was to be replaced by a couch model which represents the Varian IGRT treatment couch; thus the treatment couch model needed to be positioned at the same anterior-posterior position as the CT Scanner couch, as that was the height at which the patient was positioned. The script uses the couch removal plane to determine the level in the Y-direction where the new couch structure must be positioned. However, if the couch removal line is left at the position as described above after the new couch model was added, it will also cause the new couch structure to be obscured from Pinnacle. For Pinnacle to recognise the new couch structure, the couch removal line needs to be positioned below the new couch structure after the couch structure was created in the plan. This causes another potential problem. If the CT Scanner couch is wider than the new couch structure (or if the new

couch needs to be positioned to the left or right of midline due to a lateral offset) then a situation could arise where the CT Scanner couch can still affect the Pinnacle dose calculations. This is shown in Figure 3.21.

This problem was solved by creating a separate structure and placing it over the CT Scanner couch with the anterior of the structure at the anterior of the CT Scanner couch, and the width of this structure spans the full width of the field of view in the treatment planning system. The thickness of this structure (in the Y-direction) was made to be the same as that of the IGRT treatment couch at its thickest section which is 7.5 cm. A density of zero is assigned to this new contour and this density overrides the densities of the CT Scanner couch. This contour is called the couch space and will be described in more detail in the next section. The couch removal plane is then positioned at the bottom (posterior) of the couch space structure.

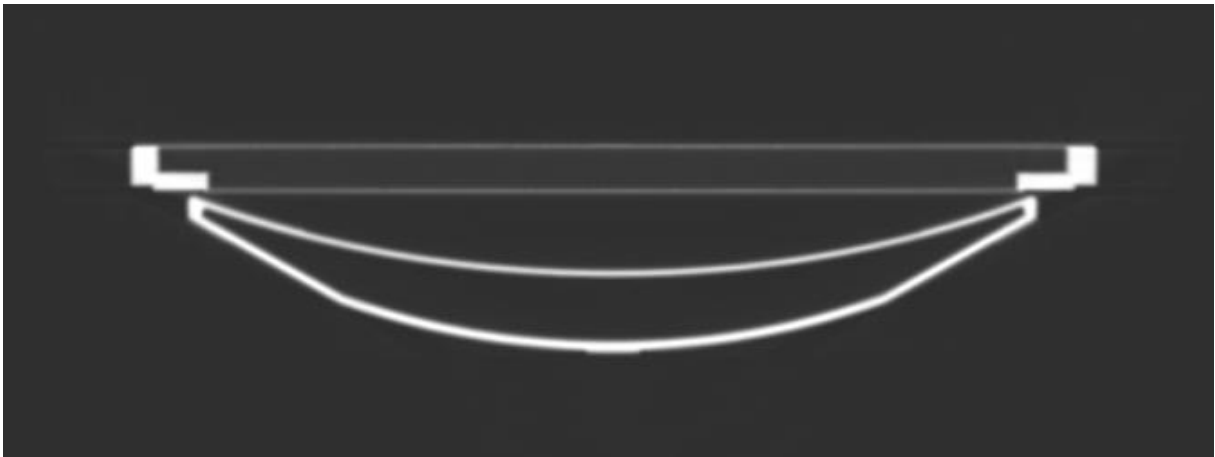


Figure 3.19: The couch of the Toshiba Aquilion LB wide bore CT Scanner on the CT image
(Pinnacle treatment planning system screen shot by the researcher)

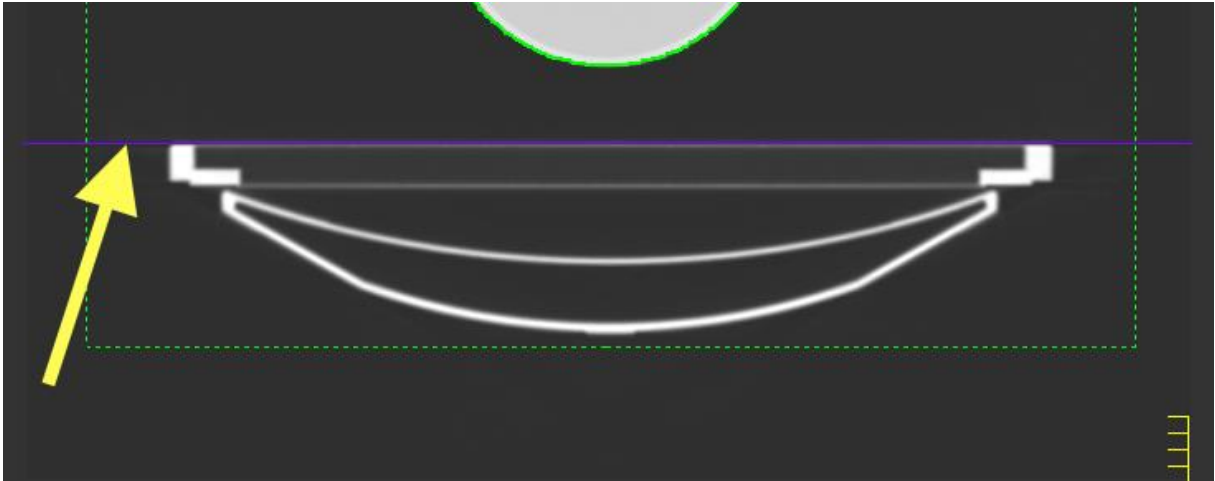


Figure 3.20: The couch removal plane on the Pinnacle treatment planning system

Everything below this plane is ignored by Pinnacle. The couch removal plane is indicated by the arrow.

(Pinnacle treatment planning system screen shot by the researcher)

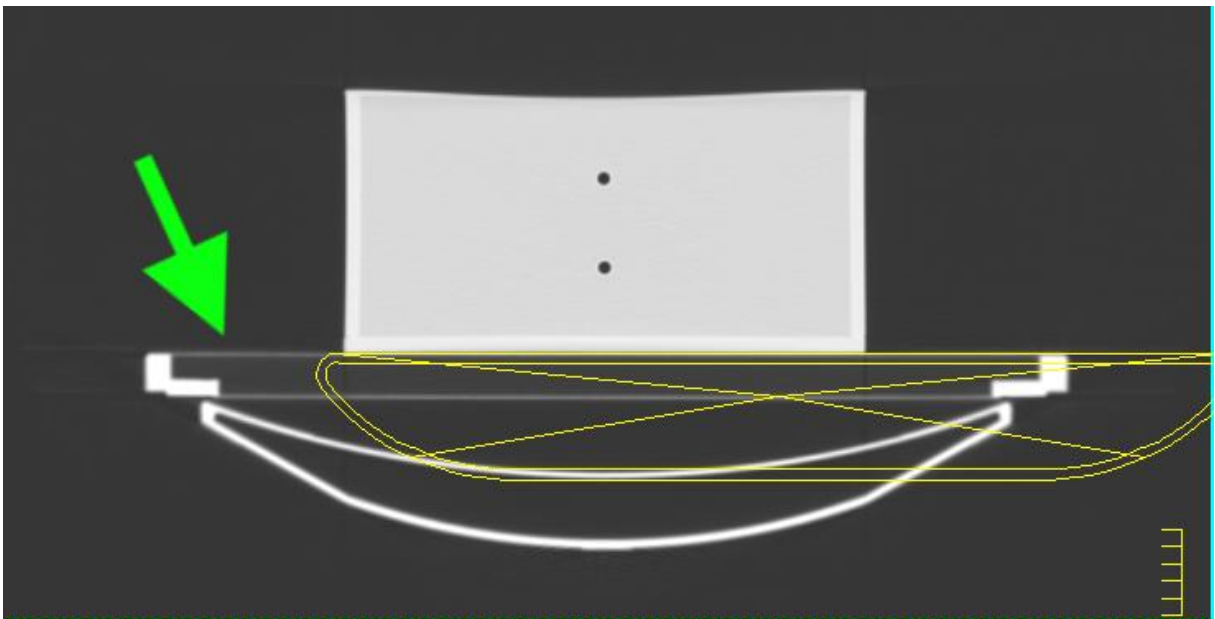


Figure 3.21: Showing how the CT scanner couch is not covered by the treatment couch structure

(In this case due to a lateral offset of the treatment couch)

(Pinnacle treatment planning system screen shot by the researcher)

3.9.4.2 Couch structures

Three main couch structures are created when the script is run. The first of these is the couch space. This is created on every CT slice in the scan set for the patient and this is used to simulate the removal of the CT Scanner couch. It has a density of zero and it overrides all the densities of the CT image pixels over which it is positioned. The couch space is just a

rectangular shape. The length of this structure spans the full length of the CT scan set (in the Z-direction) and the width spans the full width of the field of view (FOV) in the X-direction and its thickness is 7.5 cm in the Y-direction. The couch space structure is shown in Figure 3.22, but by default the display of the couch space structure is turned off for the 2D and 3D windows in the Pinnacle treatment planning system. The idea of using a couch space structure was described in a script done by Bjørne Riis (Riis, 2007).

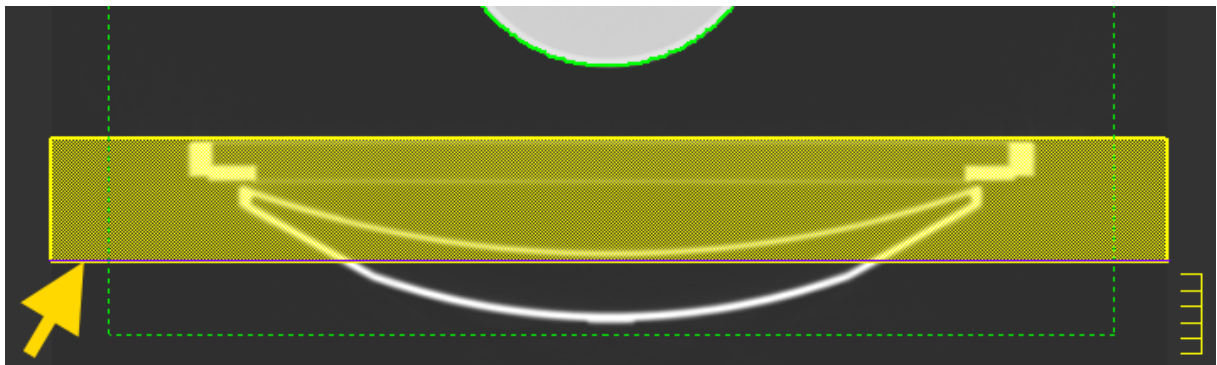


Figure 3.22: The couch space structure shown as a colourwash
The arrow indicates the new position of the couch removal plane.
(Pinnacle treatment planning system screen shot by the researcher)

The second main couch structure is the external couch (Figure 3.23). This represents the external surface of the actual treatment couch. This is created and its anterior is placed at the original level of the couch removal plane so that it is at the same position anteriorly as the CT Scanner couch (as well as the couch space structure). The density for the external couch structure was determined by looking at the dose calculated by the Pinnacle treatment planning system and modifying the density until the dose calculated matched the dose measured. This density then overrides the density of that part of the couch space on which it is positioned.

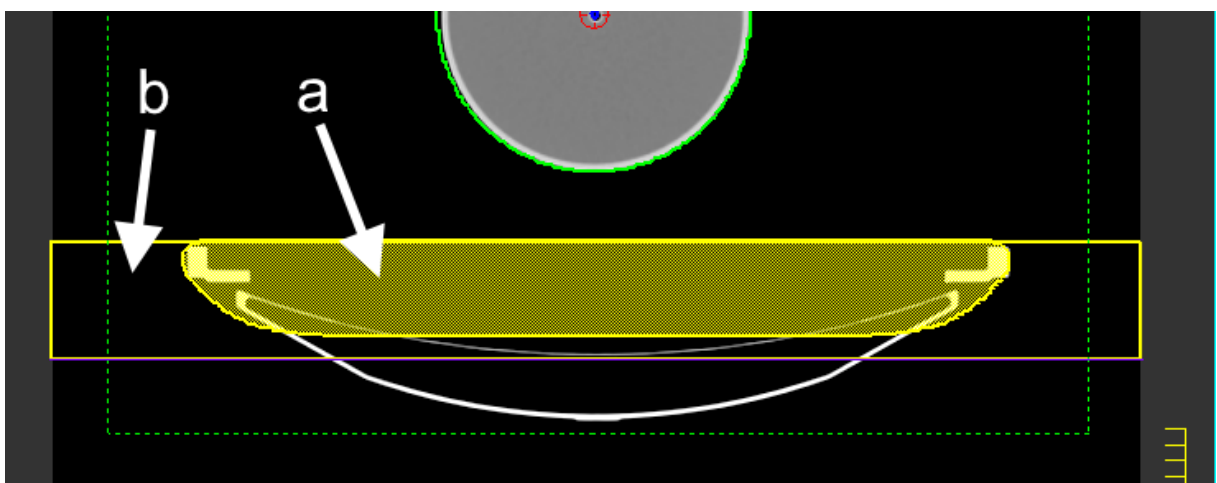


Figure 3.23: The external couch structure (a) shown in relation to the couch space structure (b)
(Pinnacle treatment planning system screen shot by the researcher)

The last main couch structure created by the script is the internal couch (Figure 3.25). This is positioned inside the external couch and the space between the external and internal couch structures represents the skin of the IGRT couch, and the space within the internal couch structure represents the core of the IGRT couch. The density of the inner couch overrides the density of that section of the external couch on which it is positioned.

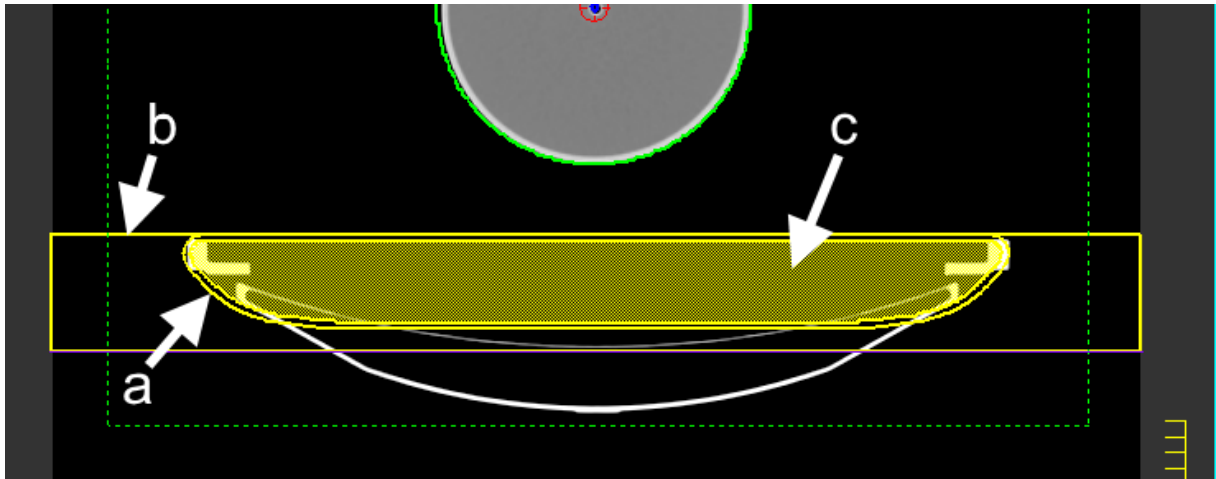


Figure 3.24: The internal couch structure (c) shown in relation to the external couch structure (a) and the couch space structure (b)

(Pinnacle treatment planning system screen shot by the researcher)

This section described the three main couch structures which needed to be created by the script algorithm, and the figures gave an idea of the shape of the contours for each structure. The next section describes how these structures were created.

3.9.4.3 Base coordinates

After analysing the shape and dimensions of the couch it was decided to create three base sets of coordinates. Each of these sets of coordinates represented accurately the cross-section of the couch for a particular position/section of the couch (Figure 3.25) in the XY-plane (the Z-plane in the Pinnacle treatment system is along the length of the couch in the superior-inferior direction). These base sets of coordinates were created so that they represent the cross-sections of the couch with the couch centred in the X-direction.

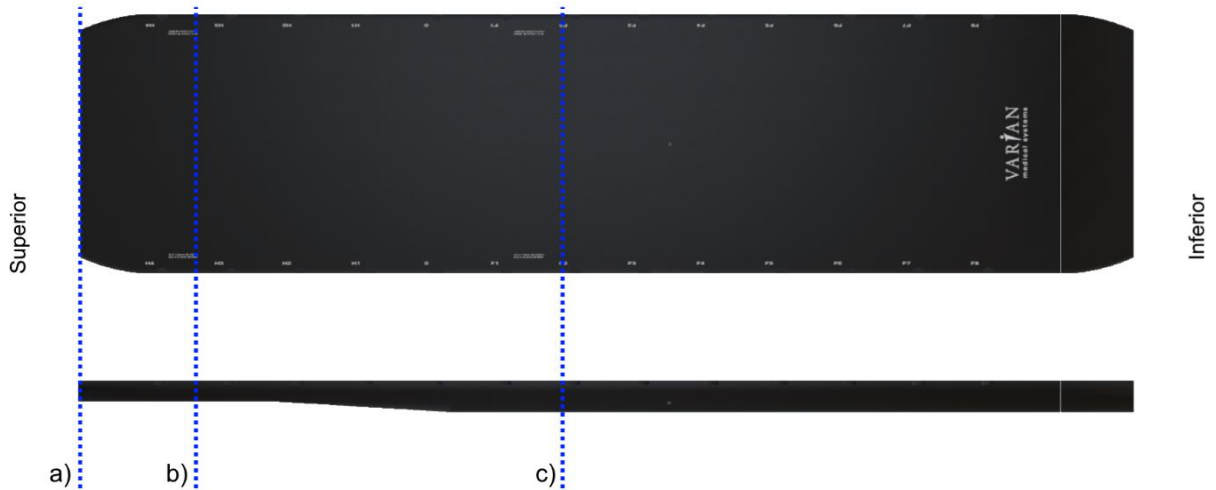


Figure 3.25: The cross-section levels of the couch for which the base contours were created

(a) The front (superior) end of the couch. (b) The thin section of the couch.

(c) The thick section of the couch.

(Radiotherapy Simulation software (Botha, 2019))

For illustration purposes these three sets of coordinates were plotted on a scatter chart to show the three base contours superimposed (Figure 3.26). Appendix H contains the complete three sets of coordinates for these base contours.

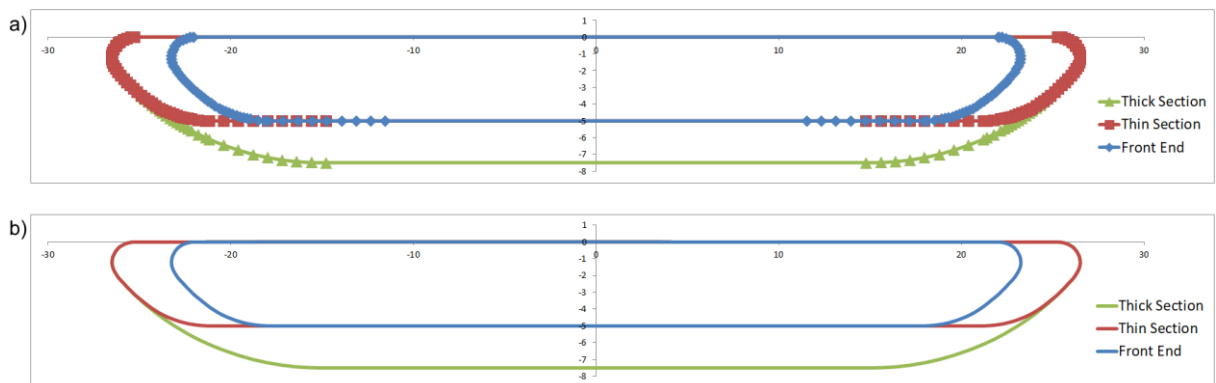


Figure 3.26: Superimposed scatter plots of the coordinates of the three sets of base contours of the couch

In (b) the point markers have been removed to see the contours clearer.

(Figures created by the researcher)

From these base contour sets the coordinates for each contour of the couch is calculated in the Python script by using translations and interpolations every time the script is run for a patient plan.

The script checks the Z-coordinates of all the slices of the CT scan set of the patient to determine which part of the treatment couch coincides with each slice of the CT scan set for that specific patient. Some slices might not be on that part of the couch at all if the patient was positioned with that in mind. For every slice which needs a couch structure, the script then creates contours for the cross-section of the couch for that particular slice Z-coordinate and writes the contour coordinates to the ROI files. At the end of the script the structure is then imported from the ROI file into the plan and each slice which requires it will have the couch structures as part of the plan (Figure 3.27). This just shows the outlines of the external couch and internal couch structures to make it easier to visualise.



Figure 3.27: The couch structure added on the CT slice after the ROI files imported
The couch structure includes contours for the external couch, the internal couch, as well as the couch space (not shown here).

(Pinnacle treatment planning system screen shot by the researcher)

3.9.4.4 Translations

The translations result in positioning the whole couch structure in the correct position relative to the patient on the plan. The script receives three translation values from the patient's plan and the user. These values are the X-value for the lateral offset, a Y-value for the anterior-posterior position where the user specified the couch removal plane, and a Z-value. The Z-value is determined by the couch notch that the user specified and the longitudinal offset relative to the notch for the longitudinal offset, as well as the reference slice position. In the script, the couch notches are each represented by a distance from the superior end of the couch. This distance, together with the longitudinal offset and the reference slice position is used to calculate the Z-value. Each coordinate for the couch model is then adjusted by X-value, Y-value, Z-value.

3.9.4.5 Interpolations

Three separate interpolations were required to create the couch structure from the three base sets of coordinates. These interpolations will be called Interpolation A, Interpolation B and Interpolation C. The first two interpolation processes (A and B) were required for the external shape of the couch. Interpolation A was used for the superior part of the couch and Interpolation B for the sloping section (Figure 3.28). Interpolation C created the internal couch structure.



Figure 3.28: The two regions of the couch where interpolations were required to create the external shape of the couch, the superior region (a) and the sloping section (b)

(Radiotherapy Simulation software (Botha, 2019))

Interpolation A

The superior part of the couch stretches from the superior edge of the couch to where the uniform thin section of the couch starts. The superior part of the couch and the thin section of the couch have the same vertical (anterior-posterior) dimensions. For the superior part of the couch (Figure 3.28 a) the interpolation of the coordinates only needed to be done for the X-coordinates, because the corresponding coordinates of the front end base contour and the thin section base contour were created such that they have exactly the same Y-coordinates and the shapes of the front end base contour and thin section base contour only changed in the X-direction (Figure 3.29).

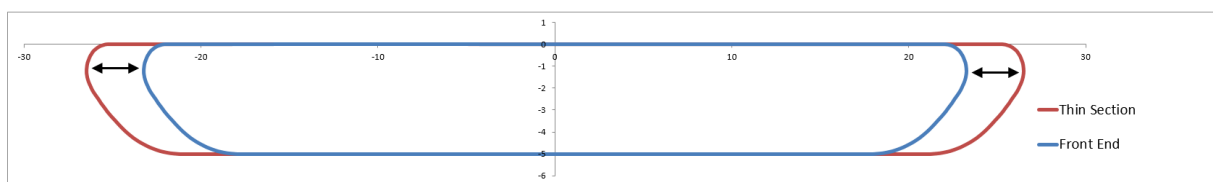


Figure 3.29: Showing how the base contours of the front end of the couch and the thin section of the couch only change in the X-direction

(Figure created by the researcher)

The starting point for Interpolation A was to determine the centre and radius of a circle whose arc would describe the shape of the maximum curve at the superior part of the couch as viewed from above (anteriorly). This is demonstrated in Figure 3.30. Each of the two curves at the front end (left and right curve) required its own circle.

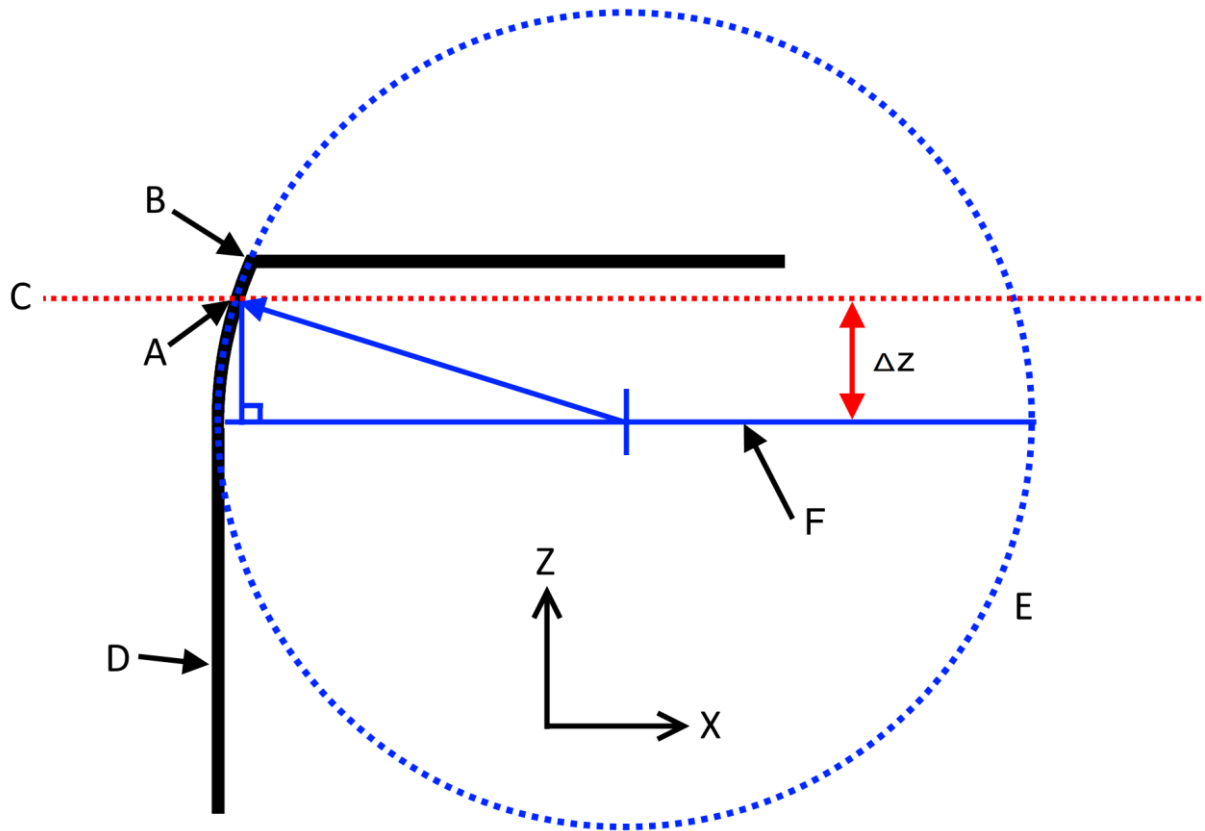


Figure 3.30: The logic behind Interpolation A for the superior part of the couch

A is the point at the maximum width on the curve at the level in the Z-plane where the interpolation is to be performed. Point B is the point at the maximum width of the couch at the superior edge of the couch. C is the level in the Z-plane where the current interpolation is performed. D is the couch outline. E is the circle whose arc describe the maximum curve of the superior end of the couch. F is the level in the Z-plane on which the centre of the circle falls.
 (Figure created by the researcher)

For each Z-level where the interpolation was required the algorithm calculated the distance (Δz) between the required Z-level (C in Figure 3.30) and the Z-coordinate of the centre of the circle (F in Figure 3.30).

$$\Delta z = F - C$$

This was then used to calculate the maximum width of the couch in the x-direction at level C (the level in the Z-plane where the interpolation is to be performed).

For the left curve:

$$\begin{aligned} \text{minX} = & \text{point_centre_leftcurve}[0] - \text{sqrt}(\text{pow}(\text{radius_curve}, 2) \\ & - \text{pow}((\text{point_centre_leftcurve}[1] - \text{zcoord}), 2)) \end{aligned}$$

For the right curve:

$$\begin{aligned} \text{maxX} = & \text{point_centre_rightcurve}[0] + \text{sqrt}(\text{pow}(\text{radius_curve}, 2) \\ & - \text{pow}((\text{point_centre_rightcurve}[1] - \text{zcoord}), 2)) \end{aligned}$$

The maximum width (in X-direction) at level C:

$$\text{max_curve_width_currentZ} = \text{abs}(\text{minX}) + \text{abs}(\text{maxX})$$

The difference in the X-value () at C:

$$\text{difference} = \text{abs}((\text{max_curve_width_currentZ} - \text{max_curve_width_frontend}) / 2)$$

The average difference could be used since the left and right sides of the couch are mirror images of each other.

This X-value difference was then used to interpolate the X-coordinate of all the points on the contour at C.

Interpolation B

Interpolation B was required for the sloping section of the couch (Figure 3.28 b). The sloping section starts at the end of the thin section and ends at the beginning of the thick section of the couch. The thin section and thick section have the same dimensions in the X-direction. The base contours for the thin and thick sections were created so that the corresponding coordinates have the same X-coordinates. Therefore, the interpolation for the sloping section only involved the Y-coordinates (Figure 3.31).

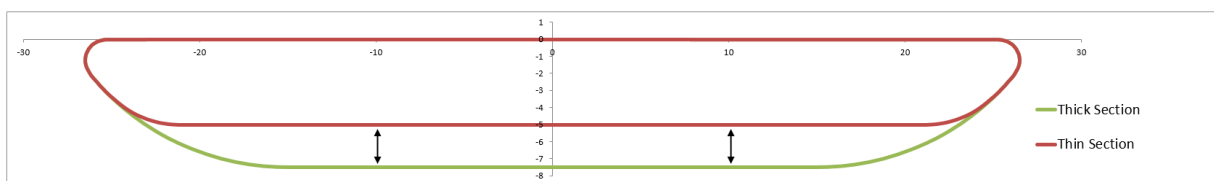


Figure 3.31: Showing how the base contours of the thin section of the couch and the thick section of the couch only change in the Y-direction
(Figure created by the researcher)

The sloping section is a linear section and the interpolation was a linear interpolation (Figure 3.32).

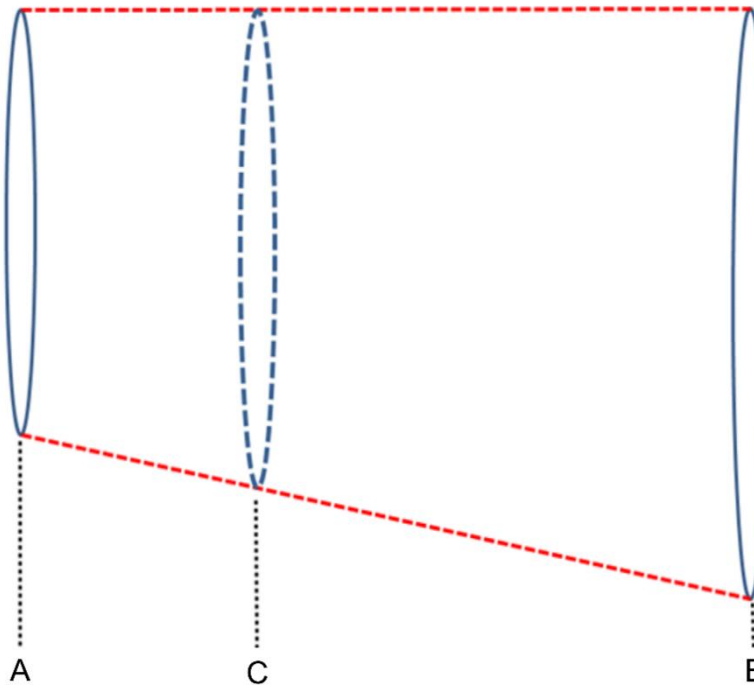


Figure 3.32: Linear interpolation for the sloping section

A is the top of the sloping section (at the intersection with the thin section). B is the bottom of the thick section (at the intersection of the thick section).

C is the level in the Z-plane where the current interpolation is performed.

(Figure created by the researcher)

Interpolation C

This interpolation was used to create the skin of the couch structure by creating another contour, the internal couch structure, within the external couch structure.

For each CT slice which requires a couch structure interpolation C uses the set of coordinates of the external couch contour for that particular CT slice. Interpolation C uses vector algebra. The following series of figures demonstrates how the problem was approached as a vector problem.

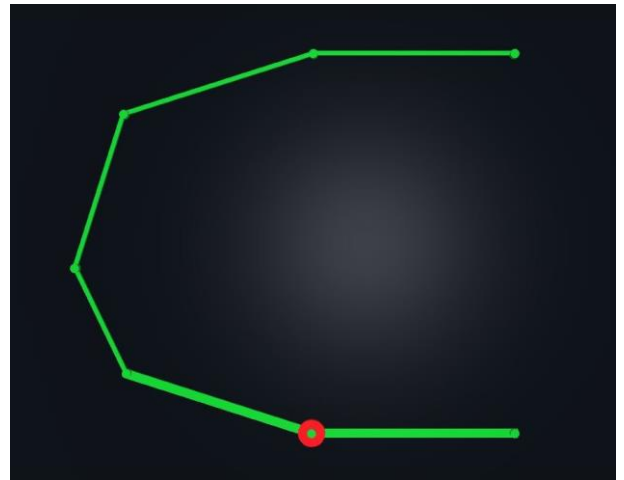
Each coordinate of the internal couch contour is calculated from a corresponding coordinate on the external couch contour (Figure 3.33 a). Each calculated internal couch coordinate is given the same Z-coordinate as its “parent” external couch contour coordinate, because they are on the same slice. For each coordinate on the external couch contour the two line segments on either side of it are treated as two unit vectors (Figure 3.33 b and c).

These two unit vectors are then bisected to get an interpolation direction vector pointing towards the inside of the couch (Figure 3.33 d). Once the direction of the 'bisection vector' is determined, the length/magnitude of the vector is set as equal to the couch skin thickness (Figure 3.33 e). This is used to determine the coordinate of the interpolated internal couch

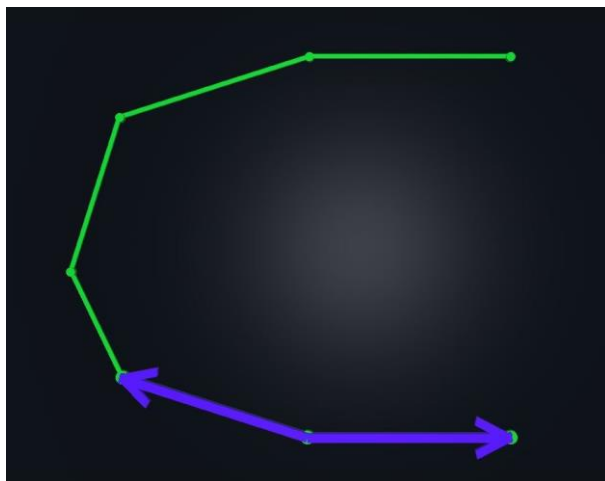
coordinate (Figure 3.33 f). After this is done for all the coordinates on the external couch contour an internal couch contour is created with the required distance from the external contour (Figure 3.33 g).



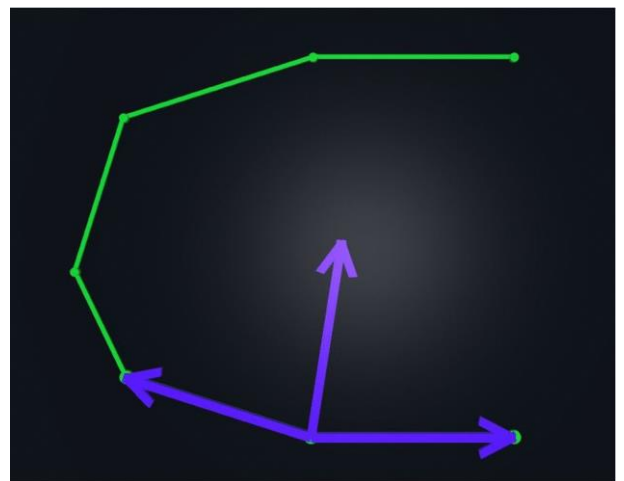
a)



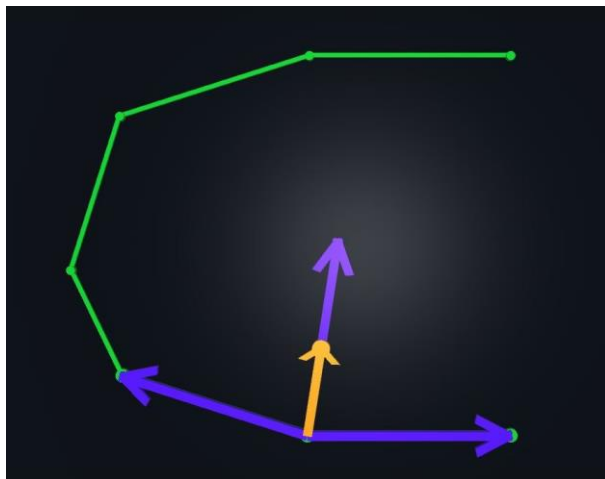
b)



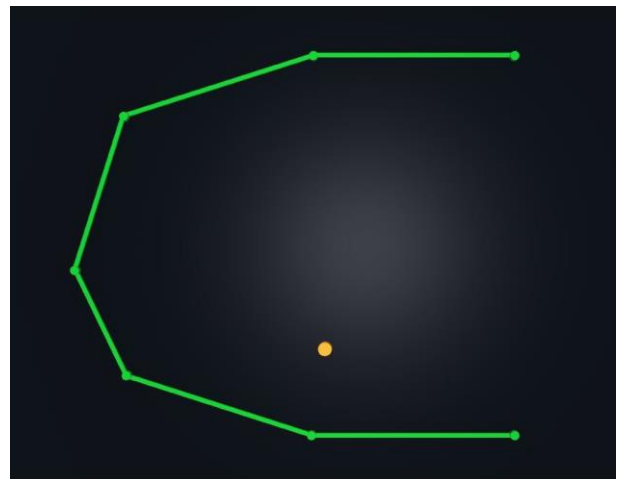
c)



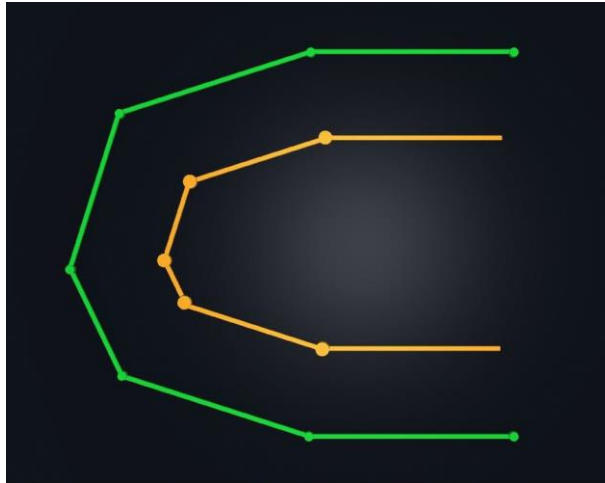
d)



e)



f)



g)

Figure 3.33: The logic for Interpolation C for creating the coordinates for the internal couch contours

(Figures created by the researcher)

3.9.4.6 Densities and skin thickness of the couch model

After the initial script was completed and it managed to create the couch structure accurately in terms of the external dimensions and shape, the next step was to investigate the radiological properties of the couch structure. Arbitrary values were selected for the densities of the couch outer skin and the couch inner core, as well as for the thickness of the skin. The plans on the Pinnacle treatment planning system (as mentioned in section 3.9.3) were then used to determine the predicted effect of this couch model on the radiation dose. It was soon discovered that having only the three single variables (couch skin density, couch core density, and uniform skin thickness) did not provide enough flexibility in order to create a couch model which would mimic the radiological properties of the real couch closely for all the sections of the couch, as well as for both the 6 MV and 18 MV radiation energies. It was also not an option to have multiple scripts to create different parts of the couch depending on which section of the couch the patient was positioned. One of the objectives of this study was to have a single algorithm which would create the full couch model. It was also important that the couch model be suitable for both beam energies, 6 MV and 18 MV. This meant that the final couch model needed to be a compromise between the 6 MV and 18 MV attenuation effects. Having separate couch models for the two beam energies would not have been an option, because there might be occasions where a single patient treatment plan requires beams of both energies. The decision was then made to add more flexibility into the couch model in terms of setting densities and skin thicknesses.

The initial problem was that only one density can be assigned to a structure and this meant that there could only be a single density for the skin thickness for all the sections (thin, sloping, thick) of the couch (Figure 3.34).



Figure 3.34: The initial couch skin (indicated here by the arrow) could only have a single density

(Pinnacle treatment planning system screen shot by the researcher)

The script was adjusted to be able to create the external part of the couch as two substructures, an anterior-posterior substructure (Figure 3.35) and a lateral substructure (Figure 3.36). Combined, these two substructures made up the full external shape of the couch (Figure 3.37). Thus, each of these substructures could be assigned a different density which provided more flexibility. The inner couch is then positioned as before (Figure 3.38) and the density of the inner couch overrides the densities of those parts of both external couch substructures on which it is positioned.

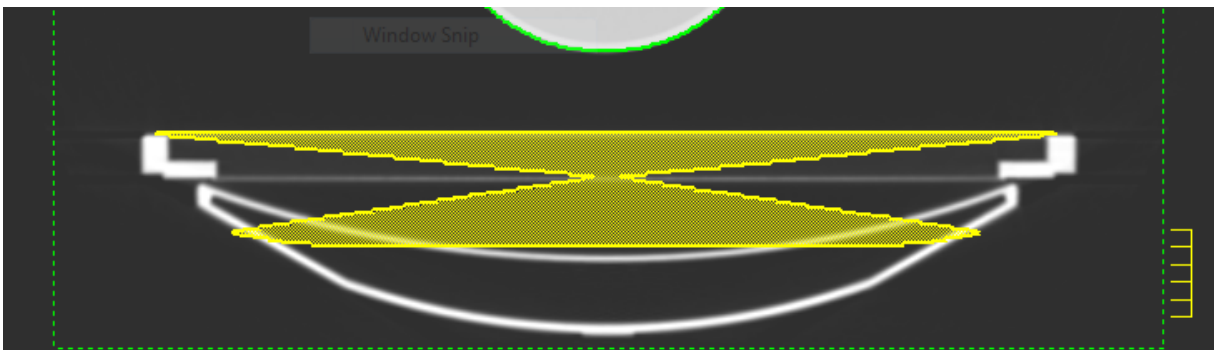


Figure 3.35: The new anterior-posterior contour for the external couch structure

(Pinnacle treatment planning system screen shot by the researcher)

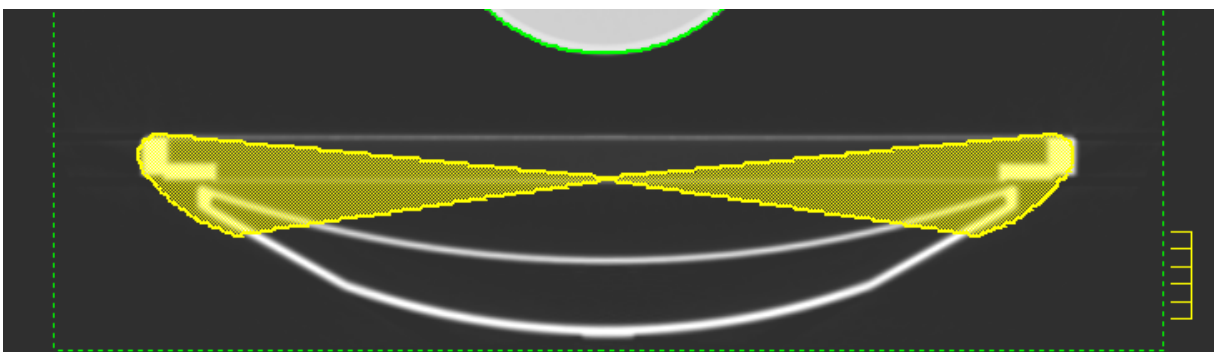


Figure 3.36: The new lateral contour for the external couch structure

(Pinnacle treatment planning system screen shot by the researcher)

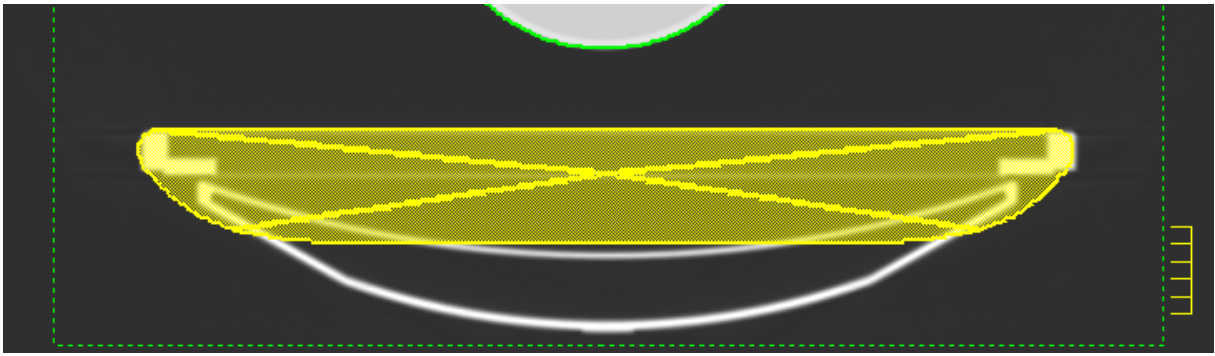


Figure 3.37: The new anterior-posterior contour and lateral contours combined for the external couch structure

(Pinnacle treatment planning system screen shot by the researcher)

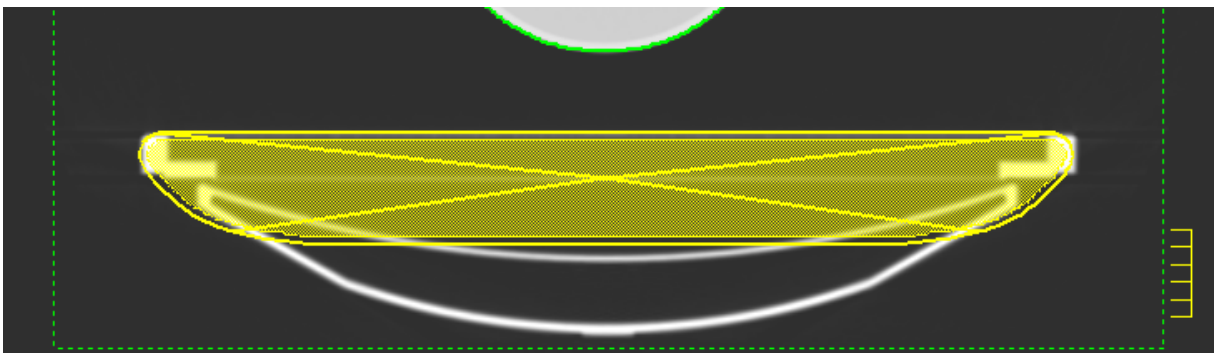


Figure 3.38: The inner couch structure overlying the new external couch structures

(Pinnacle treatment planning system screen shot by the researcher)

A further step in making the couch script provide more flexibility in the creation of the couch model was to add the ability to have a non-uniform skin thickness. This allowed the skin thickness to be adjusted in order to provide a couch model which would accurately mimic the radiological properties of the real Varian IGRT couch. This was accomplished by using a list of values in the script which was used for the individual interpolation of each coordinate which makes up the contour of the inner couch structure. This meant that a specific value for skin thickness could be assigned to each coordinate which makes up the couch contour. See Appendix I for the list of these individual skin thicknesses.

It is worth repeating that the aim was not necessarily to have the skin thicknesses of the couch model to be exactly the same as the skin thickness of the real couch. The same was true for the densities of the couch model and the real couch. The couch properties were therefore empirically modelled by having physical parameters that did not match the actual couch construction faithfully, nevertheless correctly modelling its radiological properties in order to correctly account for it in the treatment planning.

3.9.5 Script process

The main logic behind the script is for the script to loop through all the slices of the CT scan set of the patient and compare the Z-coordinate of each slice with the position of the real couch to determine on which section of the couch that particular slice is located (Figure 3.39). The position of the slices relative to the couch is determined by using the laser reference level when the patient was scanned relative to the indexing notches of the couch. It will then create a set of coordinates for the couch structure contours (the outer couch and the inner couch contours) for that particular slice and write the coordinates to the ROI files. For example, if the slice falls on (a) in Figure 3.39 the couch will be ignored and no contours created. If the slice falls on (b) or (d) in Figure 3.39 the couch contours will be created for that particular slice by using interpolation (Interpolation A and Interpolation B respectively). For (c) in Figure 3.39 the contours will be created by using translation in the Z-direction of the thin section base contour coordinates and for (e) in (Figure 3.39). In Figure 3.39 the contours will be created by using translation in the Z-direction of the thick section base contour coordinates.

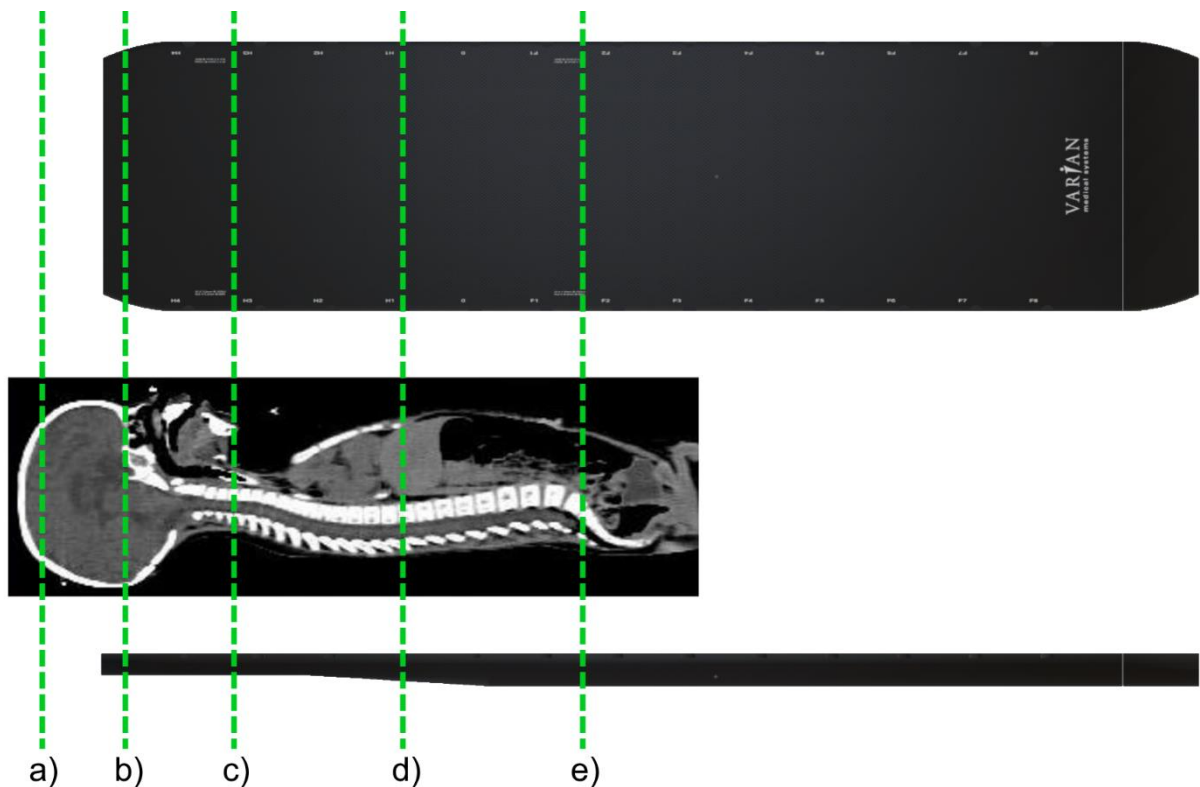


Figure 3.39: Showing how the CT Scan images are compared with the position of the couch to see which CT slices fall outside the couch

(a), on the superior part of the couch (b), on the thin section of the couch (c), on the sloping section of the couch (d), or on the thick section of the couch (e).

(Radiotherapy Simulation software (Botha, 2019))

The multiple substructures and the non-uniform skin thickness allowed the flexibility such that the final densities and individual skin thickness values were determined for the couch model.

The densities and skin thicknesses of the couch model were iteratively determined by setting them to arbitrary values and then running the scripts. Once the couch structures were created on the plan in Pinnacle, the plan doses were calculated, and the calculated/predicted attenuations of the couch model were compared with the measured attenuations of the real couch. Initially, the standard field size (10 x 10 cm²) for both energies for the thin section of the couch was used; then once these looked ‘tuned in’, the calculations were expanded to the plans for all the other field sizes and other sections of the couch.

A target dose value was determined for each attenuated beam used for the initial measurements. These doses represented what the Pinnacle calculated doses for those attenuated beams should be if they matched the measured doses. The calculated doses for the three open beams (0°, 90°, 270°) on the Pinnacle were used to determine this target calculated dose for each beam angle through the couch. This was done by using the mean of the three open beams for each plan (from Pinnacle) and multiplying it with the attenuation factor from the measured value for the corresponding combination of parameters (beam energy, field size, gantry angle, section of the couch). This result gave a value for what the attenuated dose for that combination of parameters should be on Pinnacle. These target doses were called the “Required Doses”. The calculation was as follows:

$$\text{Required dose} = \frac{\text{Measured Attenuated dose} * \text{Pinnacle Open dose}}{\text{Measured Open dose}}$$

The calculated dose by Pinnacle was then compared with these “Required dose” values by calculating percentage differences. The densities and skin thicknesses of the couch model were then adjusted in order to get the percentage differences within a target range. In this case for the creation of the model, the target range for the percentage differences was ±1%. The couch model was created specifically using the initial attenuation measurements and these measurements were used to ‘fine-tune’ the couch model parameters. Therefore, it was expected that the Pinnacle treatment planning system predicted doses and the measured doses for these beam configurations and geometries would correlate well. Ahnesjo and Aspradakis (1999) determined that a 1% accuracy is in line with an ultimate accuracy goal for dose calculations and for that reason 1% was chosen as the initial aim for the script development. The final densities used for the couch model are given in Table 3.1.

Table 3.1: The densities used for the various couch structures

| Description | Variable name in script | Density (in g/cm ³) |
|---|------------------------------|---------------------------------|
| Density of Couch space structure | CouchSpaceDensity | 0.000 |
| Density of Inner core structure (Inner couch) | CouchCoreDensity | 0.005 |
| Density for the anterior-posterior substructure for the thin section of the couch | CouchSkinDensity_Thin_AP | 0.600 |
| Density for the lateral substructure for the thin section of the couch | CouchSkinDensity_Thin_Sides | 0.600 |
| Density for the anterior-posterior substructure for the medium section of the couch | CouchSkinDensity_Med_AP | 0.610 |
| Density for the lateral substructure for the medium section of the couch | CouchSkinDensity_Med_Sides | 0.610 |
| Density for the anterior-posterior substructure for the thick section of the couch | CouchSkinDensity_Thick_AP | 0.620 |
| Density for the lateral substructure for the thick section of the couch | CouchSkinDensity_Thick_Sides | 0.600 |

With the final couch model loaded into the plan on Pinnacle the plans were calculated and then the calculated Pinnacle attenuated doses compared with the required doses to determine if the couch model has improved the predicted dose by Pinnacle for the attenuated beams. This comparison was calculated as a dose difference as follows:

$$\text{Dose difference} = \frac{\text{Pinnacle Attenuated dose} - \text{Required dose}}{\text{Required dose}} \times 100$$

3.9.6 Using the script

One of the research study objectives was that the algorithm be user-friendly, fast and reliable. The end-user would then need to apply specific parameters in order to run the script. One parameter required is the vertical height of the anterior part of the couch relative to the CT images on the plan. Before the script is run, this height is determined by selecting where the couch removal plane needs to be positioned, as described in the section 3.9.4.1 on “Removal of the CT Scanner couch” and shown in Figure 3.20. When the script is run, an input window appears (Figure 3.40) on which the user can enter the rest of the information. The algorithm then uses the information to position the couch model at the correct coordinates relative to the patient. The user also needs to specify at which level of the treatment couch the reference level of the particular patient will be. This information is entered in the form of the indexing

notch number (e.g. H1), as well as the longitudinal offset relative to this notch. Appendix K lists all the indexing notches of the Varian IGRT couch. The lateral offset of the patient on the couch can also be entered, if required. The reference CT image slice is displayed on the input window, but it can be changed by the user if a different slice needs to be the reference level.

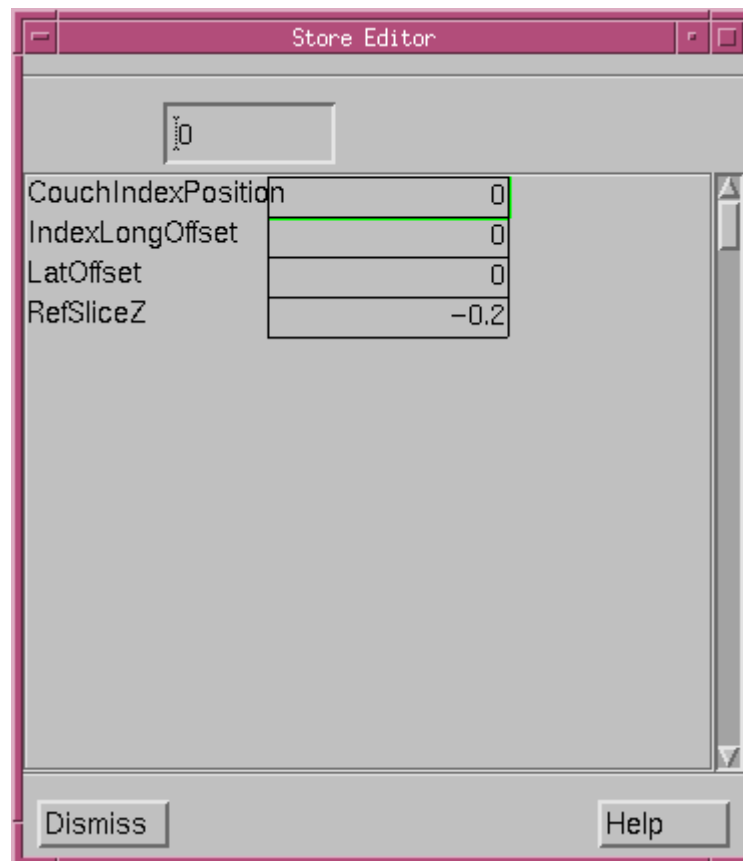


Figure 3.40: The information that the end-user can specify for the relative position of the couch inside the Pinnacle treatment plan

(Pinnacle treatment planning system screen shot by the researcher)

After the information has been entered and the script starts the algorithm does everything else. The .roi files are created and automatically imported into the current plan and displayed on the plan.

3.9.7 Limitations of the couch modelling method used

Creating the couch model by using contours has a limitation. The Pinnacle treatment planning system displays only contours which are within the field of view of the CT scanner. The contours falling outside the field of view are clipped. Any structures outside the field of view are also not included in the calculation of the dose. The couch width is 53 cm and in any CT scanner where the field of view is smaller than this, the model will not show the full width on

the Pinnacle treatment planning system. This was also found by Mihaylov et al. (2008). Additionally, if there is a lateral offset of the couch the edge of the couch furthest away from the midline might also fall outside the field of view and be clipped even if the CT scanner is a wide-bore scanner.

3.10 Generalisability of the couch model on the Pinnacle TPS

After the couch model was created on Pinnacle and the density and skin thickness values determined, the couch model enabled Pinnacle to predict the doses accurately for the sets of parameters which were used for the original measurements. In order to test if the couch model would be valid for more general scenarios as well, it was necessary to create some test plans containing more complex, non-standard, geometries than were initially used when the couch model was created.

For this phase of the project it was decided to use a different phantom in order to add extra variation to the dose measurements. The 30 x 30 cm² perspex square phantom was used. This phantom is 15 cm high and it has two cavities for a detector. The first cavity is at a depth of 5 cm from the top surface (10 cm from the bottom surface) and the second cavity at a depth of 10 cm from the top surface (5 cm from the bottom surface) (Figure 3.41 and Figure 3.42).

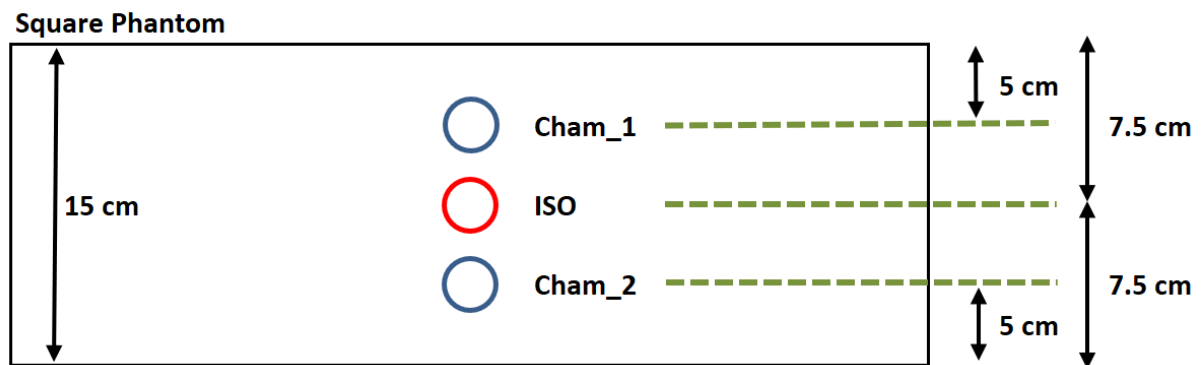


Figure 3.41: Schematic representation of the front view of the square phantom
 Cham_1 and Cham_2 represent the cavities which house the detector during measurements. ISO represents the level which was chosen as the isocentre for these measurements.

(Diagram created by the researcher)

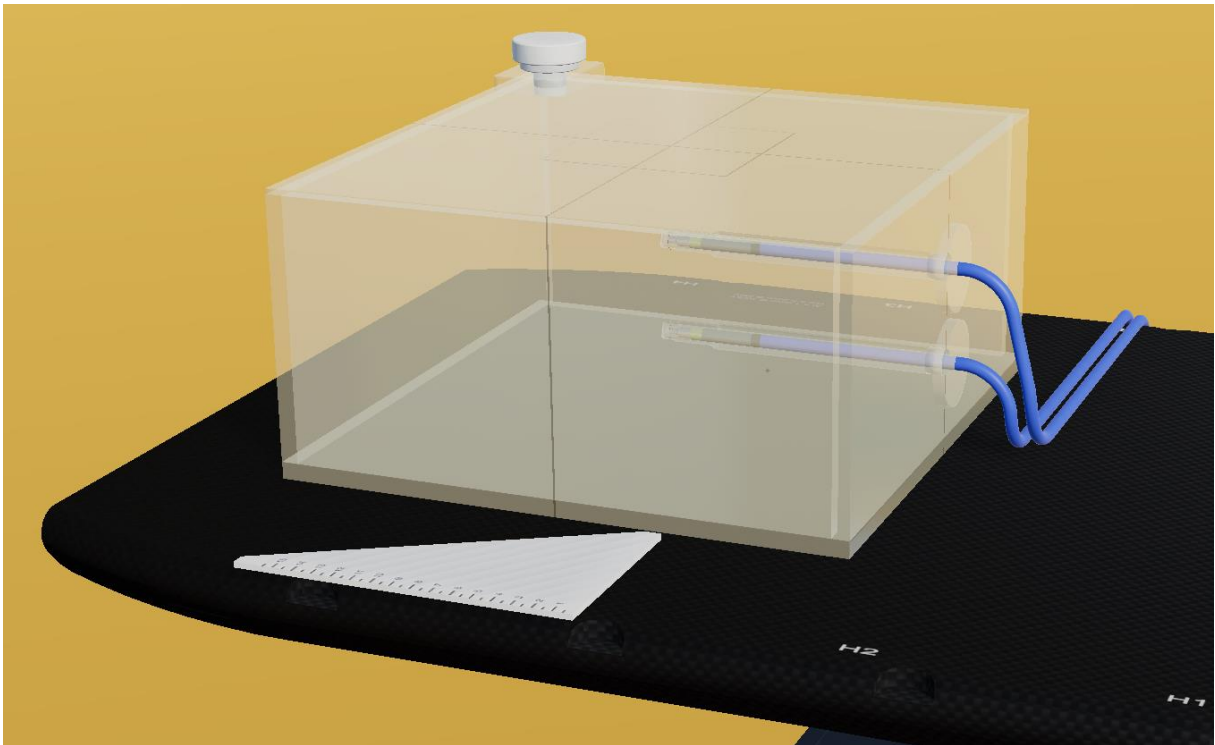


Figure 3.42: The square phantom showing the positions of the detector
(Radiotherapy Simulation software (Botha, 2019))

The first step was to scan the square phantom on the CT Scanner. The full length of the phantom was scanned in 2 mm slices. The phantom scan set was then imported into the Pinnacle treatment planning system. Six separate plans were then created to test the generalisability of the couch model. Each plan consisted of 6 MV and 18 MV beams and each 6 MV beam had an exact 18 MV beam duplicate in terms of the beam parameters.

Each plan included open beams at 0° , 90° and 270° gantry angles, and 10×10 field size for 6 MV and 18 MV. The beams at 0° were used as the reference beams, and the 90° and 270° beams were used to help check the lateral setup of the phantom. Then each plan also had an attenuated beam (beam traversing the treatment couch) for both 6 MV and 18 MV energies. The field parameters for the attenuated beam for both energies in a particular plan were exactly the same, except for the energies.

These six plans included four different positions along the length of the treatment couch, different field sizes (including rectangular fields and an asymmetric field), two dynamic wedges (EDW 30 and EDW 45) and a MLC field for both 6 MV and 18 MV energies (Table 3.2). For each plan the specific longitudinal position of the couch top relative to the phantom was set by specifying the relevant couch notch and longitudinal offset from that notch when the couch script was run.

The four longitudinal couch positions were as follows:

1. On the thin section of the couch: In line with the centre of the H3 notch (0 cm longitudinal offset);
2. In the middle of the sloping section of the couch: In line with the centre of the H1 notch (0 cm longitudinal offset);
3. In the sloping section of the couch towards the thin section: 3 cm superior to the centre of the H1 notch;
4. On the thick section of the couch: In line with the centre of the F1 notch (0 cm longitudinal offset).

Table 3.2: Summary of the attenuated beams in the six plans used for checking the generalisability of the couch model

| Beam parameters of the attenuated beams in each plan | | | | | | | | | | | Couch position | | | |
|--|--------|--------------|------------|-----|-----|-----|-----|--------|------|------------|----------------|-------------|------------------------|-----------------|
| | Energy | Gantry angle | Field Size | X1 | X2 | Y1 | Y2 | Wedge | MLC | Target POI | Couch Section | Index level | Offset | Thickness |
| | | | | | | | | | | | | | (from centre of notch) | of couch on C/A |
| Plan_1 | 6 MV | 147° | 10 x 10 | 5 | 5 | 5 | 5 | None | None | ISO | Thin | H3 | 0.0 | 5.0 |
| | 18 MV | 147° | 10 x 10 | 5 | 5 | 5 | 5 | None | None | ISO | Thin | H3 | 0.0 | 5.0 |
| Plan_2 | 6 MV | 160° | 12.6 x 7 | 3.5 | 3.5 | 6.3 | 6.3 | None | None | ISO | Thick | F1 | 0.0 | 7.5 |
| | 18 MV | 160° | 12.6 x 7 | 3.5 | 3.5 | 6.3 | 6.3 | None | None | ISO | Thick | F1 | 0.0 | 7.5 |
| Plan_3 | 6 MV | 220° | 15 x 15 | 7.5 | 7.5 | 7.5 | 7.5 | EDW 30 | None | ISO | Medium | H1 | 0.0 | 6.3 |
| | 18 MV | 220° | 15 x 15 | 7.5 | 7.5 | 7.5 | 7.5 | EDW 30 | None | ISO | Medium | H1 | 0.0 | 6.3 |
| Plan_4 | 6 MV | 200° | 7 x 7 | 3.5 | 3.5 | 3.5 | 3.5 | None | Yes | ISO | Thick | F1 | 0.0 | 7.5 |
| | 18 MV | 200° | 7 x 7 | 3.5 | 3.5 | 3.5 | 3.5 | None | Yes | ISO | Thick | F1 | 0.0 | 7.5 |
| Plan_5 | 6 MV | 210° | 8 x 17 | 8.5 | 8.5 | 4 | 4 | EDW 45 | None | ISO | Thin | H3 | 0.0 | 5.0 |
| | 18 MV | 210° | 8 x 17 | 8.5 | 8.5 | 4 | 4 | EDW 45 | None | ISO | Thin | H3 | 0.0 | 5.0 |
| Plan_6 | 6 MV | 225° | 9 x 9 | 3 | 6 | 4.5 | 4.5 | None | None | ISO | Medium | H1 | 3.0 | 6.1 |
| | 18 MV | 225° | 9 x 9 | 2 | 7 | 4.5 | 4.5 | None | None | ISO | Medium | H1 | 3.0 | 6.1 |

For each plan on Pinnacle the doses were calculated at both chamber positions within the phantom. This was done by positioning dose calculation points at these chamber positions and then recording the calculated doses at these points for each beam.

These plans were then set up on the treatment unit and the doses measured at both chamber positions in the phantom. For these measurements the PTW Farmer 0.6 cm³ detector (Type 30013) was used together with the PTW Unidos dosimeter to measure the doses.

For each plan, the phantom was positioned at the relevant longitudinal level on the couch using the couch notches as reference positions and the height of the isocentre above the couch was 7.5 cm. Each plan was measured in one session, i.e. all the beams for a particular plan were done together so that all the beams were measured under similar atmospheric conditions. This

was important because these were all relative measurements. Only one chamber was used for the measurements, so each plan was run twice in order to get measurements with the chamber in the top cavity, and then with the chamber in the bottom cavity.

Subsequently, each plan was set up and measured twice more for each of the two chamber positions, in order to provide three measurement sets for each plan at each chamber position.

The analyses of these doses were done using combinations of the dose values at both of these chamber positions.

First, looking at the doses at chamber position 1 (the most anterior position). For this analysis only dose values at the chamber position 1 were used, both for the attenuated beams and for the reference beams (Figure 3.43). The same dose position was used for the measurements at the treatment unit and within Pinnacle. The measured doses for 6 MV and 18 MV on the treatment unit were normalised to their respective reference beam doses at the chamber position 1. The same was done for the calculated doses from Pinnacle (also at chamber position 1). The percentage difference between the normalised calculated doses from Pinnacle and the normalised measured doses were then calculated:

$$\text{Dose difference} = \frac{\text{Pinnacle Normalised dose} - \text{Measured Normalised dose}}{\text{Measured Normalised dose}} \times 100$$

Square Phantom

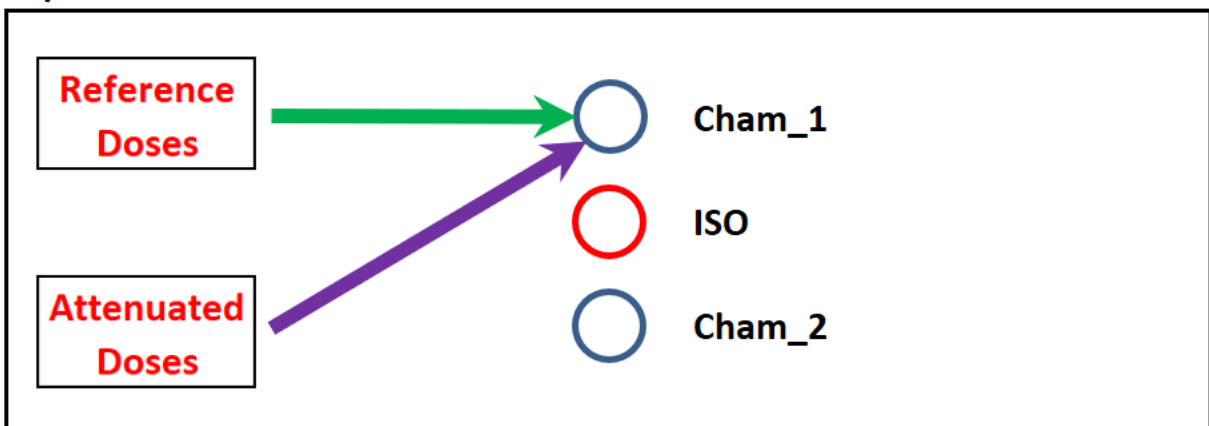


Figure 3.43: Schematic representation of the square phantom showing the dose reading position for the reference doses and the attenuated dose

(Diagram done by the researcher)

The measurements were also done with the chamber in the chamber position 2 (the posterior position) in the phantom. These measurements were then analysed using the doses for the 10 x 10 cm field and 0° gantry angles at the chamber position 2 as the reference doses (Figure

3.44). Here again the measured doses for 6 MV and 18 MV on the treatment unit were normalised to their respective reference beam doses (at the chamber position 2). The same was done for the calculated doses from Pinnacle (also at chamber position 2). The percentage difference between the normalised calculated doses from Pinnacle and the normalised measured doses were then calculated as above.

Square Phantom

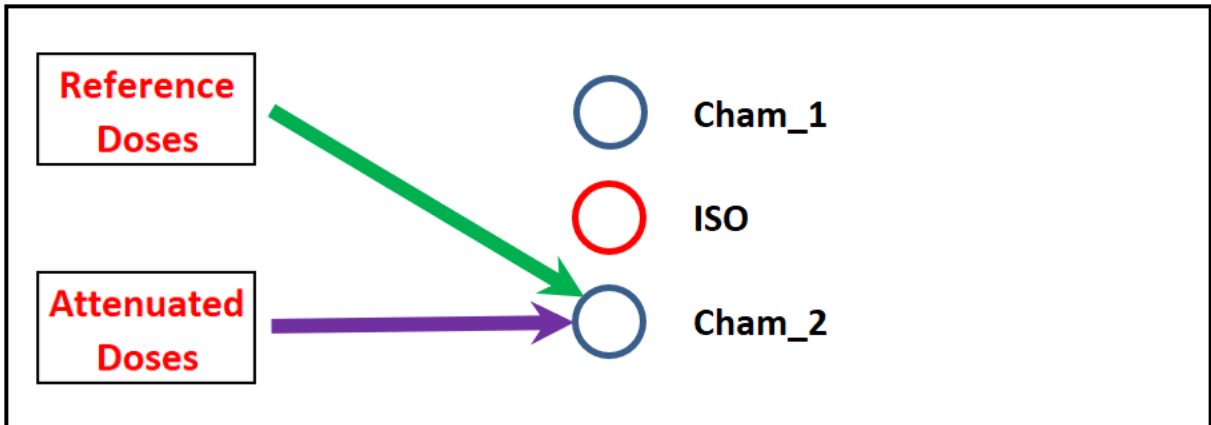


Figure 3.44: Schematic representation of the square phantom showing the dose reading position for the reference doses and the attenuated dose

(Diagram done by the researcher)

Lastly, for the verification plans, the data were also analysed using the attenuated dose readings at the chamber position 2 and the reference beam readings at the chamber position 1 (Figure 3.45).

Square Phantom

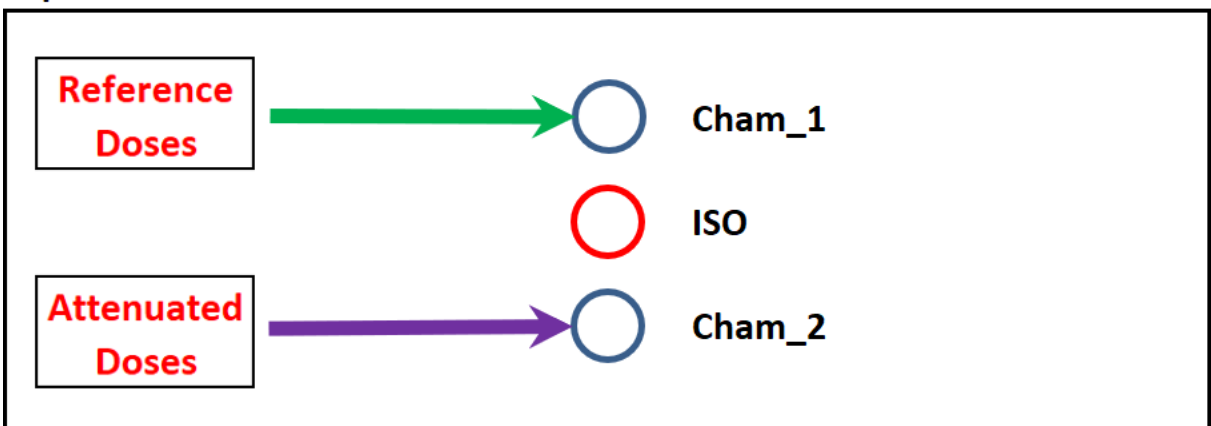


Figure 3.45: Schematic representation of the square phantom showing the dose reading positions for the reference doses of the attenuated dose

(Diagram done by the researcher)

The dose measurements for the attenuated fields at each chamber position were then compared with the predicted/calculated doses in the Pinnacle treatment planning system at the same chamber positions in order to evaluate the accuracy and generalisability of the couch model. All the results are analysed and reported in the Results chapter.

3.11 Surface dose

The literature review (Chapter 2) has shown that the treatment couch affects the surface doses to the patient for beams traversing the couch, but that the surface dose predictions by the treatment planning systems were unpredictable with or without a couch structure present. It was necessary, therefore, to investigate the accuracy of dose prediction, with, as well as without, the couch structure. Hypothesis 4 of the research question states that “The use of an algorithm that incorporates the dimensions and properties of the treatment couch will improve the accuracy of the predicted skin dose in the presence of a treatment couch”.

After a literature search to evaluate different methods and dosimeters for measuring surface doses, it was decided to use optically stimulated luminescence (OSL) technology to measure the surface dose effects of the Varian IGRT treatment couch on the phantom. A company in the United States of America, Landauer®, agreed to supply seventy (70) nanoDot™ dosimeters for use in this study (Figure 3.46). After exposure, the nanoDot dosimeters were sent back to Landauer to be read and they then supplied a report of the readings. Landauer also supplied six nanoDot dosimeters, labelled “Control” which were not to be used for the surface dose measurements. These were used to subtract any accumulated background radiation during shipping and storage from the nanoDot dosimeters used for the surface dose measurements.

The nanoDot dosimeters have a wide energy range of use, from 5 keV to 20 MeV. They also require no post-measurement correction factors (Appendix E3: nanoDot Dosimeters). The nanoDots used were screened nanoDots and they have a measurement accuracy of $\pm 5.5\%$. Landauer specifies that these accuracy claims are based on a Cs-137 exposure under laboratory conditions.

a)



b)



Figure 3.46: Examples of the nanoDot™ dosimeters in their plastic pouch

- (a) A Control nanoDot for subtraction of background radiation
- (b) A nanoDot used for the measurement of the surface doses

(Photos taken by the researcher)

Each measurement had to be done three times (to reduce random errors) and this meant with only seventy nanoDot dosimeters available, there was a limited number of variations in terms of beam parameters that could be tested. The plan was to test the following: the effect of the couch on the surface dose; the effect of field size on the surface dose, the effect of beam energy; and the effect of the incident angle.

The 30 x 30 cm² perspex square phantom was also used for the surface dose investigation. It was decided to have six plans in total, three each for the respective beam energies of 6 MV, and 18MV for the three sections of the couch. For each plan there were two open beams at 0° gantry angle, a 10 x 10 cm and a 20 x 20 cm. Each plan also included four beams traversing the treatment couch, a 10 x 10 cm and 20 x 20 cm field at 180° (90° incident angle to the couch), and a 10 x 10 cm and 20 x 20 cm field at 230° (50° incident angle). Table 3.3 shows the beam parameters for each setup. In Figure 3.47 the beams used for the surface dose measurements are demonstrated. On the treatment unit 100 monitor units were delivered for each beam.

Table 3.3: The three surface dose plans for each energy

| Plan | Field Name | Energy | Gantry angle | Field Size | Couch Information | | | |
|-------------|----------------|--------|--------------|------------|---------------------------|-------------|-------------------------------|---------------------------|
| | | | | | Couch Section | Index level | Offset (from centre of notch) | Thickness of couch on C/A |
| Plan_6X_THN | G_0_6X_S_REF | 6 MV | 0° | 10 x 10 | Beam not traversing couch | | | |
| | G_0_6X_L_REF | | 0° | 20 x 20 | Beam not traversing couch | | | |
| | G_180_6X_S_THN | | 180° | 10 x 10 | Thin | H3 | 0.00 | 5.00 |
| | G_180_6X_L_THN | | 180° | 20 x 20 | | | | |
| | G_230_6X_S_THN | | 230° | 10 x 10 | | | | |
| | G_230_6X_L_THN | | 230° | 20 x 20 | | | | |
| Plan_6X_MED | G_0_6X_S_REF | 6 MV | 0° | 10 x 10 | Beam not traversing couch | | | |
| | G_0_6X_L_REF | | 0° | 20 x 20 | Beam not traversing couch | | | |
| | G_180_6X_S_MED | | 180° | 10 x 10 | Medium | H1 | 0.00 | 6.30 |
| | G_180_6X_L_MED | | 180° | 20 x 20 | | | | |
| | G_230_6X_S_MED | | 230° | 10 x 10 | | | | |
| | G_230_6X_L_MED | | 230° | 20 x 20 | | | | |
| Plan_6X_THK | G_0_6X_S_REF | 6 MV | 0° | 10 x 10 | Beam not traversing couch | | | |
| | G_0_6X_L_REF | | 0° | 20 x 20 | Beam not traversing couch | | | |
| | G_180_6X_S_THK | | 180° | 10 x 10 | Thick | F1 | 0.00 | 7.50 |
| | G_180_6X_L_THK | | 180° | 20 x 20 | | | | |
| | G_230_6X_S_THK | | 230° | 10 x 10 | | | | |
| | G_230_6X_L_THK | | 230° | 20 x 20 | | | | |

| Plan | Field Name | Energy | Gantry angle | Field Size | Couch Information | | | |
|--------------|-----------------|--------|--------------|------------|---------------------------|-------------|-------------------------------|---------------------------|
| | | | | | Couch Section | Index level | Offset (from centre of notch) | Thickness of couch on C/A |
| Plan_18X_THN | G_0_18X_S_REF | 18 MV | 0° | 10 x 10 | Beam not traversing couch | | | |
| | G_0_18X_L_REF | | 0° | 20 x 20 | Beam not traversing couch | | | |
| | G_180_18X_S_THN | | 180° | 10 x 10 | Thin | H3 | 0.00 | 5.00 |
| | G_180_18X_L_THN | | 180° | 20 x 20 | | | | |
| | G_230_18X_S_THN | | 230° | 10 x 10 | | | | |
| | G_230_18X_L_THN | | 230° | 20 x 20 | | | | |
| Plan_18X_MED | G_0_18X_S_REF | 18 MV | 0° | 10 x 10 | Beam not traversing couch | | | |
| | G_0_18X_L_REF | | 0° | 20 x 20 | Beam not traversing couch | | | |
| | G_180_18X_S_MED | | 180° | 10 x 10 | Medium | H1 | 0.00 | 6.30 |
| | G_180_18X_L_MED | | 180° | 20 x 20 | | | | |
| | G_230_18X_S_MED | | 230° | 10 x 10 | | | | |
| | G_230_18X_L_MED | | 230° | 20 x 20 | | | | |
| Plan_18X_THK | G_0_18X_S_REF | 18 MV | 0° | 10 x 10 | Beam not traversing couch | | | |
| | G_0_18X_L_REF | | 0° | 20 x 20 | Beam not traversing couch | | | |
| | G_180_18X_S_THK | | 180° | 10 x 10 | Thick | F1 | 0.00 | 7.50 |
| | G_180_18X_L_THK | | 180° | 20 x 20 | | | | |
| | G_230_18X_S_THK | | 230° | 10 x 10 | | | | |
| | G_230_18X_L_THK | | 230° | 20 x 20 | | | | |

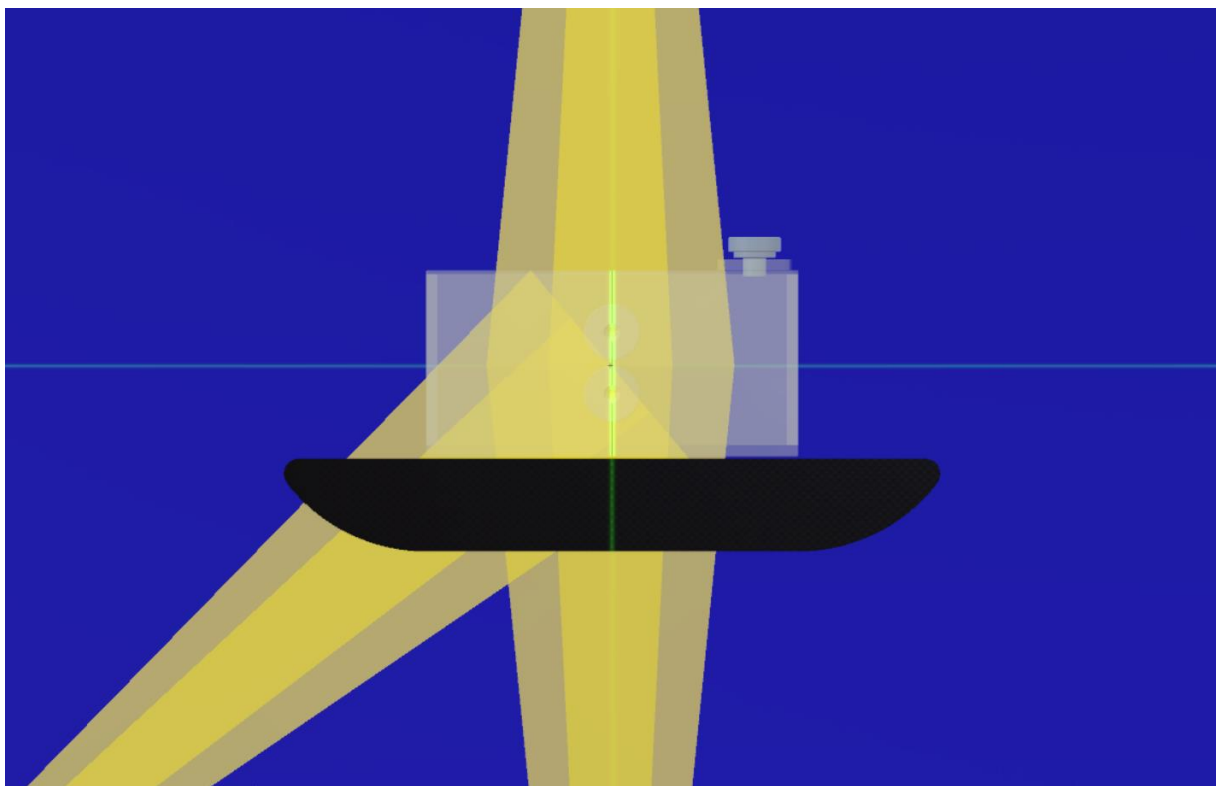


Figure 3.47: The beam arrangements used for the surface dose measurements (the 10 x 10 and 20 x 20 beams are shown superimposed)

(Radiotherapy Simulation software (Botha, 2019))

In order to use the number of nanoDot dosimeters as efficiently as possible, all three plans for an energy were measured in one session so that the reference doses at 0° needed to be measured once only for that session and could be shared by all three plans. Furthermore, measurements for the 230° 20 x 20 cm fields had to be omitted as well, due to a limited number of nanoDot dosimeters.

Table 3.4 shows the fields which were measured with the nanoDots. This meant that for each set of three plans for an energy, eleven nanoDot dosimeters were needed. In total for both energies and for three sets of measurements sixty-six nanoDot dosimeters were needed. That left four dosimeters spare for incidental occurrences.

Table 3.4: The fields for 6 MV that were actually measured using the nanoDots. The same field arrangements were also measured for 18 MV

| Plan | Field Name | Energy | Gantry angle | Field Size | Couch Information | | | |
|-------------|----------------|--------|--------------|------------|---------------------------|-------------|-------------------------------|---------------------------|
| | | | | | Couch Section | Index level | Offset (from centre of notch) | Thickness of couch on C/A |
| Plan_6X | G_0_6X_S_REF | 6 MV | 0° | 10 x 10 | Beam not traversing couch | | | |
| | G_0_6X_L_REF | | 0° | 20 x 20 | Beam not traversing couch | | | |
| Plan_6X_THN | G_180_6X_S_THN | 6 MV | 180° | 10 x 10 | Thin | H3 | 0.00 | 5.00 |
| | G_180_6X_L_THN | | 180° | 20 x 20 | | | | |
| | G_230_6X_S_THN | | 230° | 10 x 10 | | | | |
| Plan_6X_MED | G_180_6X_S_MED | 6 MV | 180° | 10 x 10 | Medium | H1 | 0.00 | 6.30 |
| | G_180_6X_L_MED | | 180° | 20 x 20 | | | | |
| | G_230_6X_S_MED | | 230° | 10 x 10 | | | | |
| Plan_6X_THK | G_180_6X_S_THK | 6 MV | 180° | 10 x 10 | Thick | F1 | 0.00 | 7.50 |
| | G_180_6X_L_THK | | 180° | 20 x 20 | | | | |
| | G_230_6X_S_THK | | 230° | 10 x 10 | | | | |

The aim was that the above-mentioned plans and fields would provide the following information.

- For the open fields (gantry at 0°) the readings for 10 x 10 cm and 20 x 20 cm were done to show the effect of field size on the surface dose of the phantom.
- For the attenuated fields (gantry at 180°) the readings for 10 x 10 cm and 20 x 20 cm were also done to show the effect of field size on the surface dose, as well as the effect of the treatment couch on the surface dose.
- Comparing the 0° and 180° 10 x 10 cm fields should give a direct indication of the effect of the treatment couch on the surface dose, and similarly for the 20 x 20 cm field size.

- Comparing the 180° and 230° 10 x 10 cm readings should give a direct indication of the effect of incident angle on the surface dose.
- Comparing all the attenuated fields for the different sections of the couch should indicate how different sections of the couch, and thus the distance that the beam traverses the couch, affects the surface doses.
- Lastly, comparing all the readings for two energies should demonstrate the effect of beam energy on the surface doses.

For each plan the central axis of the phantom was set up at the relevant couch index (notch) level. Laterally the couch was centred to the zero position. In summary, the three couch positions were as follows:

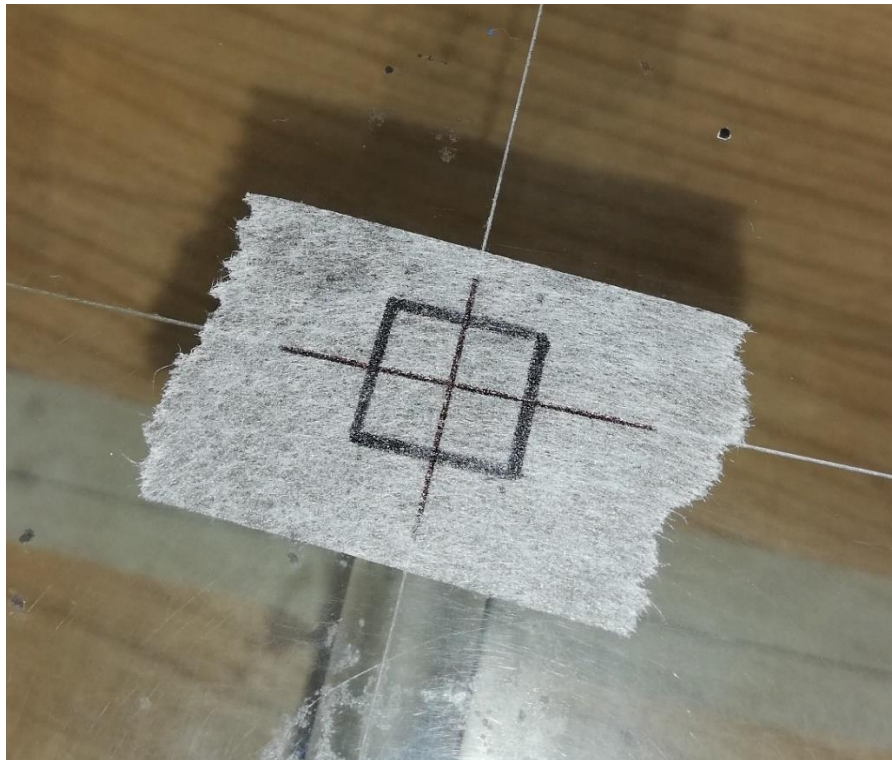
- On the thin section of the couch: through the centre of the H3 notch;
- In the sloping section of the couch: through the centre of the H1 notch;
- On the thick section of the couch: through the centre of the F1 notch.

For the 0° fields, the phantom isocentre was set at 7.5 cm above the treatment couch, i.e. in the middle of the phantom. The nanoDot dosimeters together with the plastic pouch had a thickness of 2 mm. The nanoDot dosimeters were used sealed in the plastic pouch in which they were received. The serial number on the pouch was used to identify the dosimeter and relate it to a particular measurement. Spacers of 2 mm were used to position the phantom for the readings through the couch to ensure that the phantom was still level with the nanoDot dosimeter positioned between the couch and the phantom. The spacers were positioned outside the field. The spacers resulted in the isocentre of the phantom being raised by 2 mm. It was decided, that because the spacers also created a small air gap between the couch and the phantom, to compromise and only lower the couch 1 mm for these fields traversing the couch.

As already mentioned, there were sixty-six measurements in total for the surface doses. For each field traversing the couch the phantom had to be moved in order to remove the nanoDot dosimeter and position the next one. Thus, each field was considered a new set-up for statistical purposes. There were three beam entry points on the phantom: 0°; 180°; and 230°. These entry point positions were measured from the plan and marked on the phantom. It was decided to draw a cross where the nanoDot dosimeters were to be positioned and to draw a square just larger than the size of a nanoDot dosimeter (Figure 3.48). This made it much easier and faster to position the nanoDot dosimeters consistently at the correct positions (Figure 3.49).

These measurements were done blindly as there was no immediate feedback from the readings to assess if there were any setup errors, for example a setup at the incorrect couch position. This was a concern due to the limited number of nanoDot dosimeters available and thus the incorrect exposure of the dosimeters had to be avoided. To try and get some visual cues as to the setup correctness, extra measurements were taken using the PTW Farmer 0.6 cm³ detector (Type 30013) together with the PTW Unidos dosimeter to measure the doses in the top chamber position in the phantom (Figure 3.50).

a)



b)

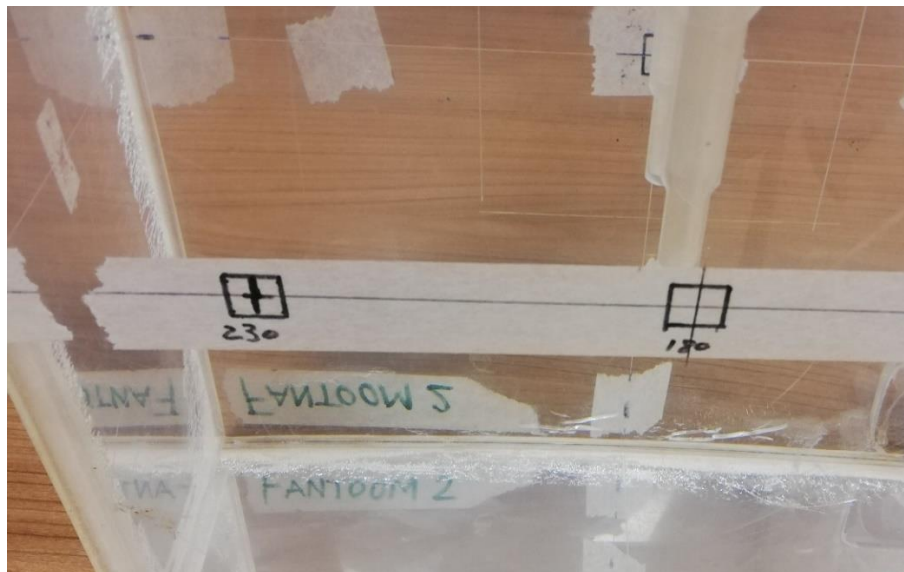


Figure 3.48: Beam entry points marked on phantom to facilitate nanoDot positioning
(a) shows the entry point at 0°. (b) shows the entry points at 180° and 230°

(Photos taken by the researcher)



Figure 3.49: The square enabled quick positioning of the nanoDot dosimeters
(Photo taken by the researcher)

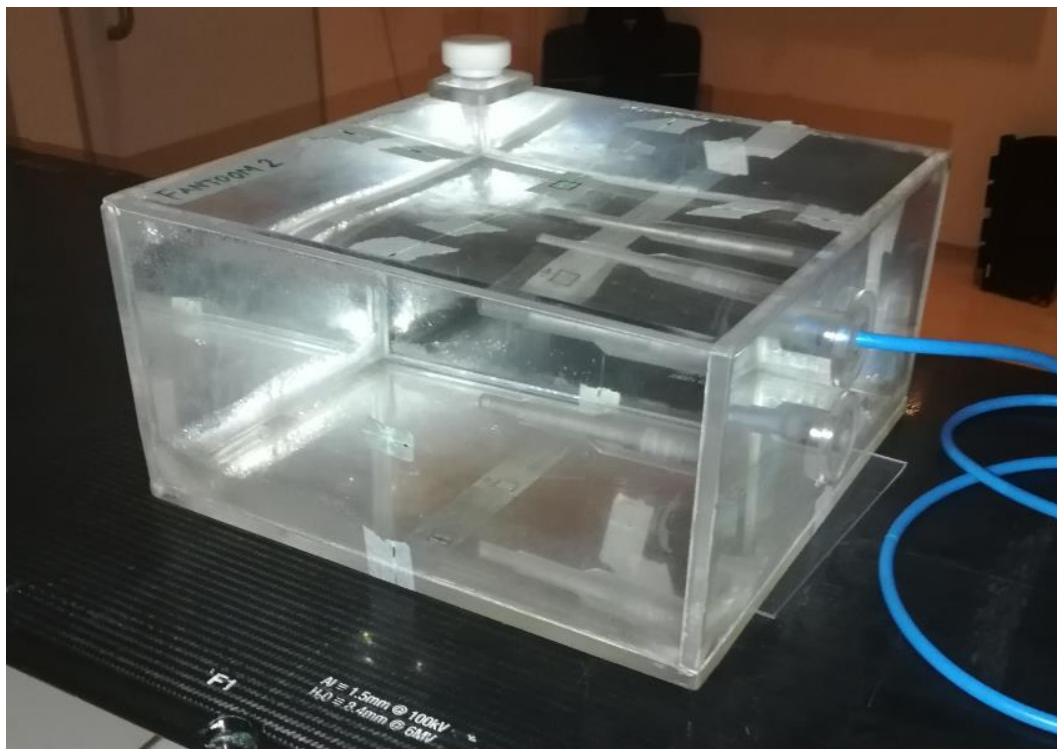


Figure 3.50: The extra measurements were taken with the chamber in the top chamber position
(Photo taken by the researcher)

Only attenuation data were used in the development of the couch model and the surface dose data were not taken into account during the process, but it was still important to look at the effect of the created couch model on the prediction of the surface doses by the Pinnacle treatment planning system.

On the Pinnacle treatment planning system, the plans used for the measurements were created. The same scan set for the 30 x 30 cm² perspex square phantom was used as for the generalisability check plans.

The Pinnacle plans were created with identical beam configurations and geometries as when the surface doses were measured at the treatment unit. Separate plans were created for each couch section. For each of the different couch section plans the script was run to add the couch model at the correct position for that plan.

A grid size of 0.2 x 0.2 x 0.2 cm was used on Pinnacle. As the first dose point on this grid is at a depth of 0.2 cm, this depth was used as a surrogate for surface dose on Pinnacle. The 0.2 cm difference in distance from the surface is considered small enough, and no inverse square law correction factors were required. The nanoDot dosimeters were positioned on the surface of the phantom for the measurements and compared to the surrogate dose points. Calculation points were positioned at the 0.2 cm depth for each of the three beam entry positions on the phantom to represent the surface doses at those points.

A further set of calculations dose points were also positioned at the D_{max} depth for each of the beams for 6 MV and 18 MV. These D_{max} depths were determined from the PDD charts for the 10 x 10 cm and 20 x 20 cm for the two beam energies. Figure 3.51 and Figure 3.52 represent the percentage depth dose data which is used by Pinnacle at the study site for 6 MV and 18 MV, respectively. The D_{max} depths used were 1.6 cm for 6 MV and 3.3 cm for 18 MV. The position of the calculation dose points are indicated in Figure 3.53 and Figure 3.54 for 6 MV and 18 MV, respectively. For each beam 100 monitor units were entered on Pinnacle, the plans calculated and the doses at the various dose calculations points recorded. The surface doses were then expressed as a percentage of the beam doses at D_{max} . The stability of the treatment unit was then checked against all the daily check diode readings and found to be stable. The researcher then made the assumption that the doses at D_{max} for each beam would be similar to those calculated by Pinnacle and these doses at D_{max} from Pinnacle were then used to express the measured surface nanoDot doses at the treatment unit as a percentage of these doses at D_{max} for each beam. The mean results from the nanoDots for the three measurement sets were then compared with the surface dose estimates from Pinnacle for the corresponding beams. This comparison represented an over- or under-estimation of the calculated surface

doses by Pinnacle. This was used to determine if the couch model had managed to improve the surface dose predictions by Pinnacle.

The Pinnacle over- or under-estimation were calculated as follows from the measured surface dose percentages and the calculated surface dose percentages:

$$\text{OverUnderEstimation} = \frac{\text{Pinnacle surface dose \%} - \text{Measured surface dose \%}}{\text{Measured surface dose \%}} \times 100$$

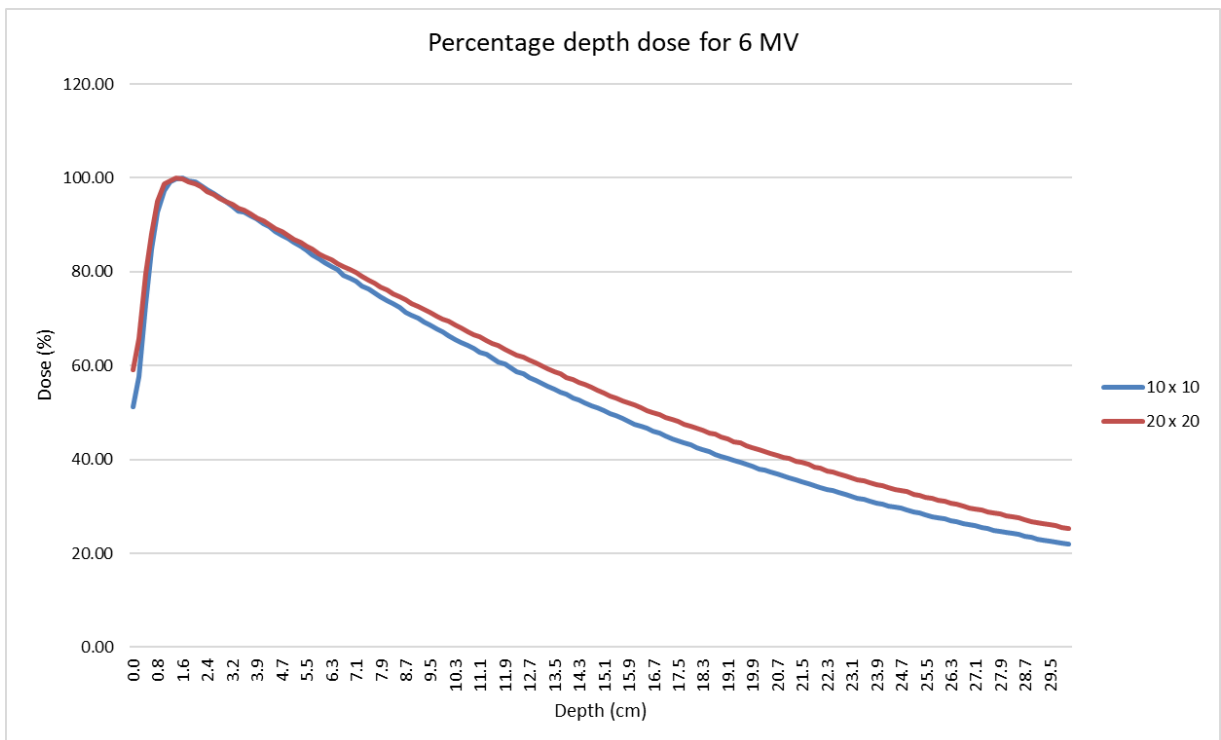


Figure 3.51: Percentage depth dose data on Pinnacle for 6 MV for 10 x 10 and 20 x 20
(Figure created by the researcher)

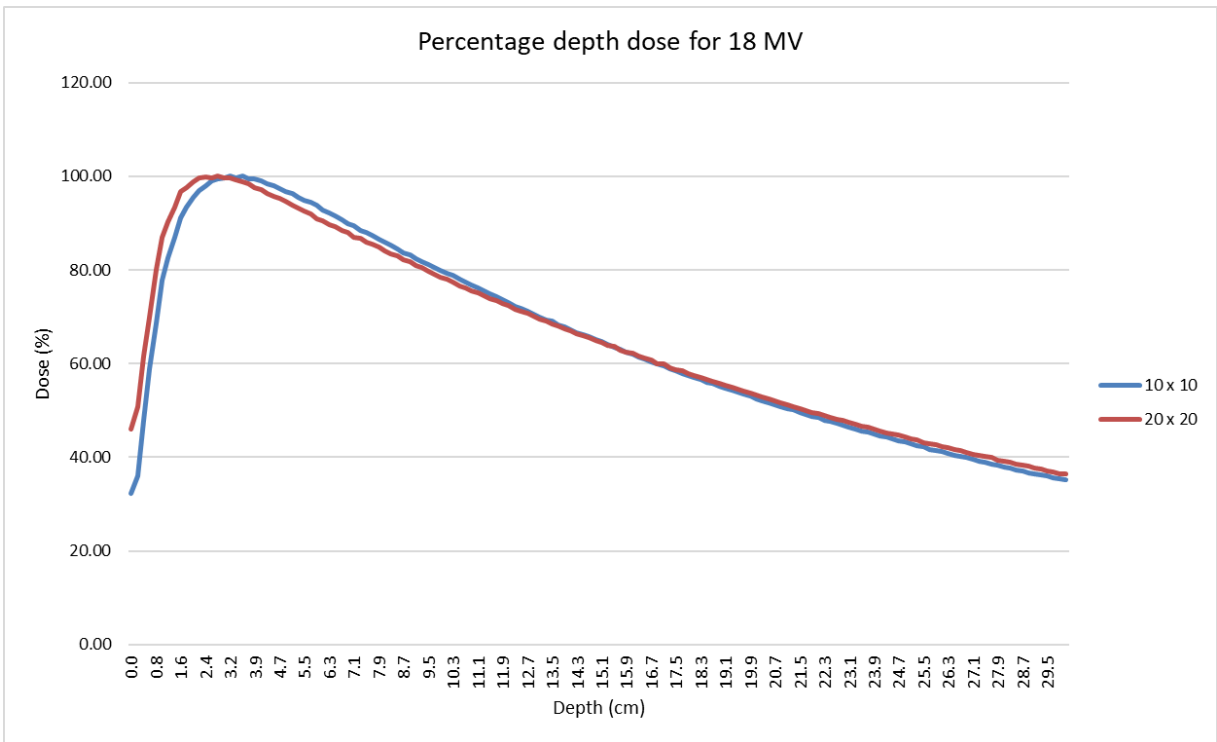


Figure 3.52: Percentage depth dose data on Pinnacle for 18 MV for 10 x 10 and 20 x 20
(Figure created by the researcher)

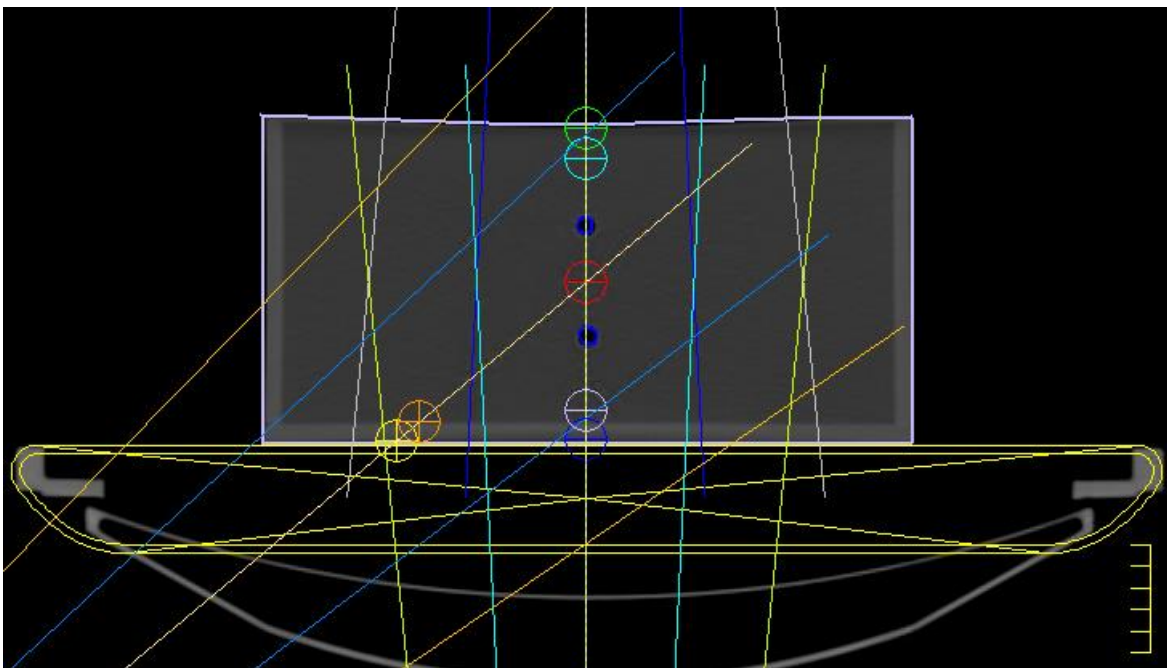


Figure 3.53: The calculation dose points used for the 6 MV beams
(Pinnacle treatment planning system screen shot by the researcher)

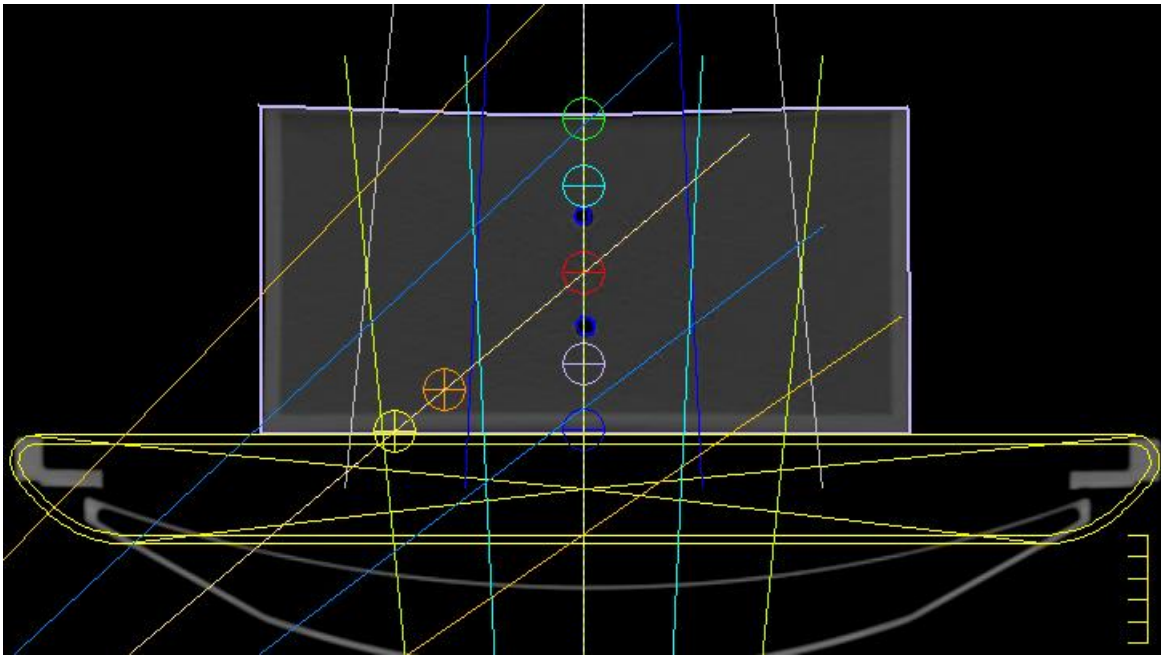


Figure 3.54: The calculation dose points used for the 18 MV beams
(Pinnacle treatment planning system screen shot by the researcher)

In addition to this it was also important to look at the surface doses which have been measured on the treatment unit with the actual Varian IGRT couch and compare them with the surface doses that the Pinnacle treatment planning system calculated if it does not take the treatment couch into account. This was to determine if the Pinnacle treatment planning system overestimates or underestimates the surface doses for beams which would traverse the treatment couch, and if so, by how much. Identical beam arrangements and geometries were created on Pinnacle as were used for the surface dose measurements at the treatment unit, except that on Pinnacle the couch model was omitted and the 180° and 230° beams did not traverse the couch. The calculated surface doses from Pinnacle were compared with the measured surface doses from the treatment unit. All the surface doses were again expressed as percentages of the beam doses at D_{max} .

The Pinnacle over- or under-estimation were again calculated using the same formula:

$$\text{OverUnderEstimation} = \frac{\text{Pinnacle surface dose \%} - \text{Measured surface dose \%}}{\text{Measured surface dose \%}} \times 100$$

An over-estimation by Pinnacle would be represented by positive results and an under-estimation by negative results.

These results are described and analysed in the Results chapter.

3.12 Conclusion

The couch model was created and all the required measurements completed.

CHAPTER FOUR: RESEARCH RESULTS

4.1 Introduction

In this chapter we look at the results of the different measurements and see what effect the treatment couch has on the radiation beam. We also look at what impact, if any, the couch model has on the accuracy of the predicted doses by the Pinnacle treatment planning system.

In this chapter the term “medium” couch section is used frequently. For this research study the medium section was used to refer to the middle of the sloping section where the couch thickness (anterior-posteriorly) is 6.25 cm. It was mentioned in section 3.8.2.1 that the setup for the measurements of the attenuation at the sloping section of the couch were done at the superior edge of notch H1, which is 3 mm superior to the middle of the sloping section. This was done to facilitate the reproducibility of the setup, and at this level the couch thickness is 6.23 cm. The term “medium” couch section was used for this position as well. For the initial plans on Pinnacle to create the couch model the same level of the couch was used as for the measurements.

For all the attenuation analysis the measurements at the 120° and 240° gantry angles have been excluded from the analysis. These angles were also excluded for the development and creation of the couch model script. In section 4.2.2 we shall look at these two gantry angles and the measurements thereof.

4.2 Actual treatment couch

4.2.1 Attenuation effect of the couch

The linear accelerator and PTW PinPoint chamber (Type 31016, 0.016 cm³) were stable (linear accelerator warmed up properly and the chamber was pre-irradiated and its temperature stabilised) for all the initial measurements over the three measurement sets. To demonstrate this, the highest relative standard deviation which was found for 18 MV was 1.1% of the reading. This was for the 15 x 15 cm field size and the 140° gantry angle on the medium section of the couch. The highest relative standard deviation for 6 MV was 1.2% of the reading. This was for 10 x 10 cm at the 220° gantry angle on the medium section.

The measurements showed that the gantry angle, and thus the incident angle to the treatment couch, has an effect on the amount of beam attenuation due to the couch. This is demonstrated in Figure 4.1 and Figure 4.2 for 6 MV and 18 MV, respectively. Apart from the gantry angle, Figure 4.1 and Figure 4.2 also show that the different sections of the couch result in different

amounts of attenuation. The attenuation effect of the different sections of the couch for a 10 x 10 cm field size is summarised in Table 4.1.

For the tables the attenuation percentage was calculated using:

$$\text{Attenuation} = \frac{\text{Open beam measurement} - \text{Closed beam measurement}}{\text{Open beam measurement}} \times 100$$

Table 4.1: Summary of attenuation by the treatment couch for the gantry angles (Figure 3.15) and the different sections of the couch

| Attenuation angles | 6 MV 10x10 | | | 18 MV 10x10 | | |
|--------------------|------------|--------|-------|-------------|--------|-------|
| | Thin | Medium | Thick | Thin | Medium | Thick |
| 130° | 3.2% | 3.1% | 3.9% | 1.8% | 1.6% | 2.1% |
| 140° | 2.9% | 3.4% | 4.0% | 1.5% | 1.8% | 2.2% |
| 160° | 2.3% | 2.7% | 3.5% | 1.2% | 1.5% | 1.9% |
| 180° | 2.3% | 2.6% | 3.3% | 1.1% | 1.3% | 1.8% |
| 200° | 2.5% | 2.8% | 3.7% | 1.3% | 1.5% | 2.0% |
| 220° | 3.2% | 3.6% | 4.2% | 1.7% | 2.0% | 2.4% |
| 230° | 3.5% | 3.4% | 4.0% | 2.0% | 1.9% | 2.2% |

The results indicate that for both energies the attenuation at 130° and 230° decreased for the medium and thick sections of the couch, compared to the attenuation at 140° and 220°. This was in contrast to the thin section of the couch where the attenuation at 130° and 230° increased, compared to the attenuations at 140° and 220°. This was true for all the attenuation measurements at these angles, and this observation pattern can be seen in all the figures showing the attenuation charts included below. As an example of this observation for 6 MV at the medium couch section the **reduction** in the attenuation as gantry moved from 140° to 130° ranged from 0.30% to 0.33%, and the **reduction** as gantry moved from 220° to 230° ranged from 0.16% to 0.37%. As mentioned, this was in contrast to what was seen for the thin couch section, for example, for 6 MV at the thin couch section the **increase** in the attenuation as gantry moved from 140° to 130° ranged from 0.24% to 0.37% and the **increase** as gantry moved from 220° to 230° ranged from 0.23% to 0.39%.

It is also noted that the amount of attenuation due to the couch for the medium couch section at 130° and 230° gantry angles seemed lower than that for the thin couch section at these angles (Figure 4.3).

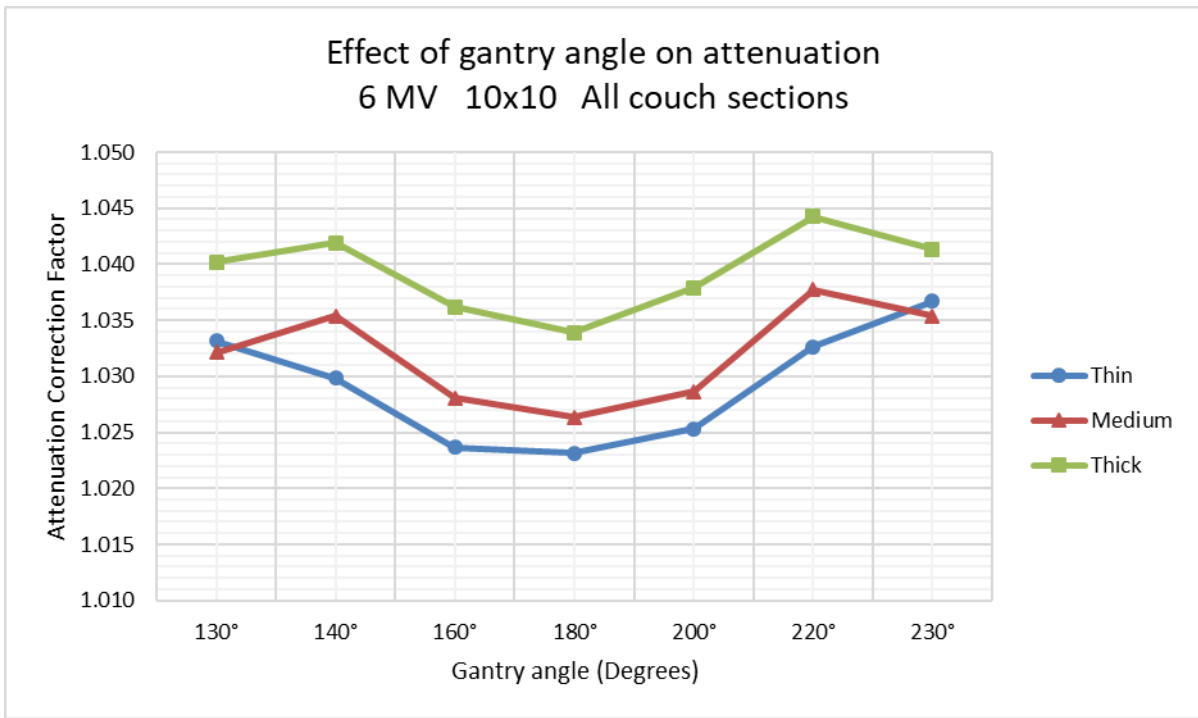


Figure 4.1: The effect of the gantry angle on the attenuation by the treatment couch for the 6 MV energy and all three sections of the treatment couch

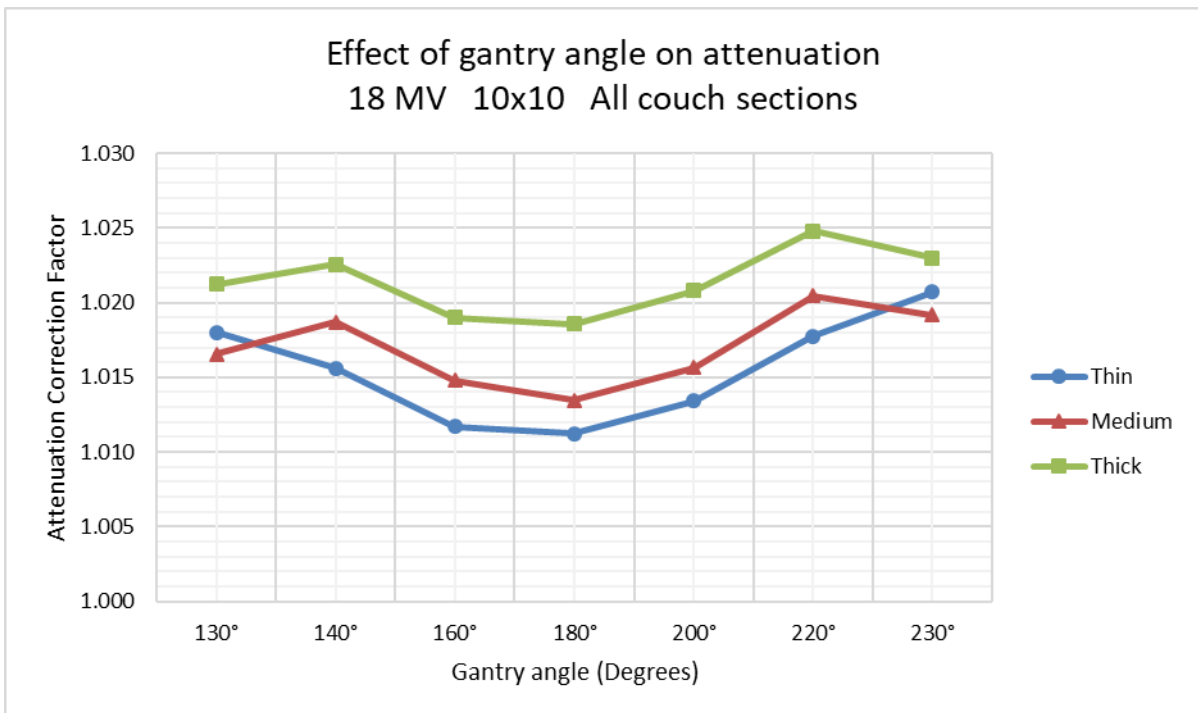


Figure 4.2: The effect of the gantry angle on the attenuation by the treatment couch for 18 MV energy and all three sections of the treatment couch

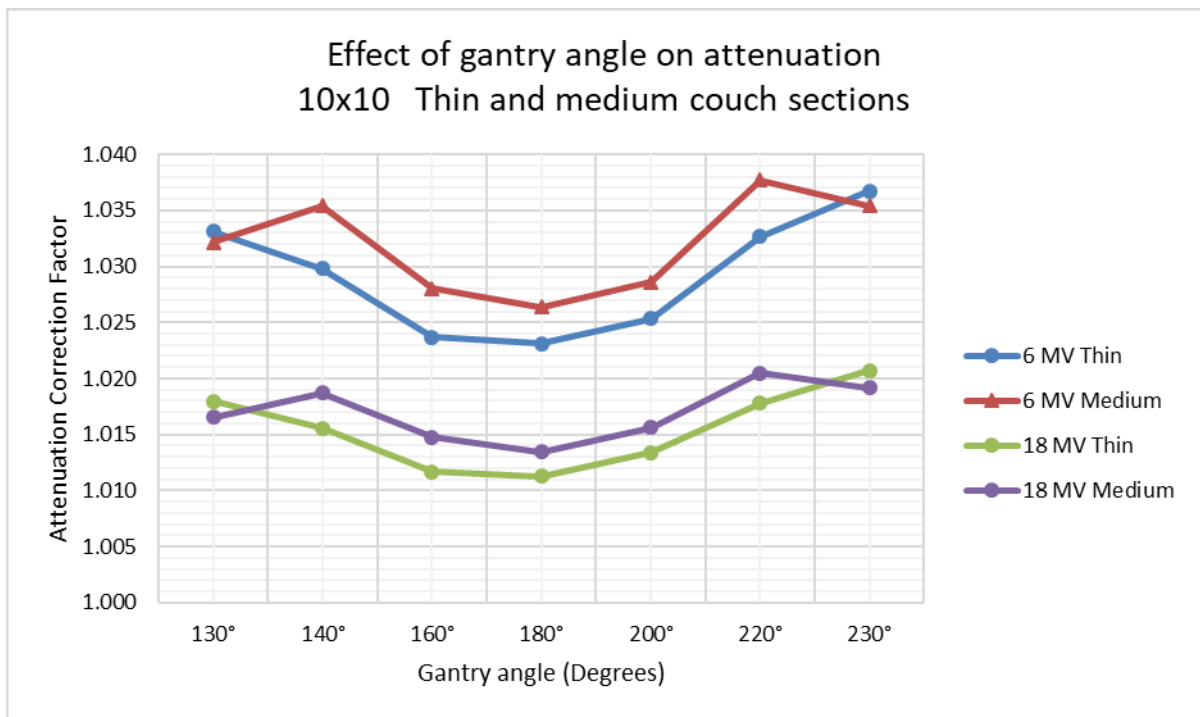


Figure 4.3: Demonstrating the reduced attenuation of the medium couch section at 130° and 230°, as compared to the thin couch section, for the 10 x 10 cm

The effect of field size and energy on attenuation is shown on the next pages in Figures 4.4 – 4.9 and Tables 4.2 and 4.3. For a particular energy, gantry angle, and couch section a decrease in attenuation is observed with increase in field size. The change in attenuation with field size is more pronounced for 6 MV as compared to 18 MV, with the largest variation observed for 6 MV field sizes larger than 10 x 10 cm. The decrease in attenuation as field size increases held for all the gantry angles measured, except again at the angles of 130° and 230° where the attenuation for the 10 x 10 cm field size seemed more for the 5 x 5 cm field size than for some of the measurements for 6 MV (Figure 4.4, Figure 4.5 and Figure 4.6).

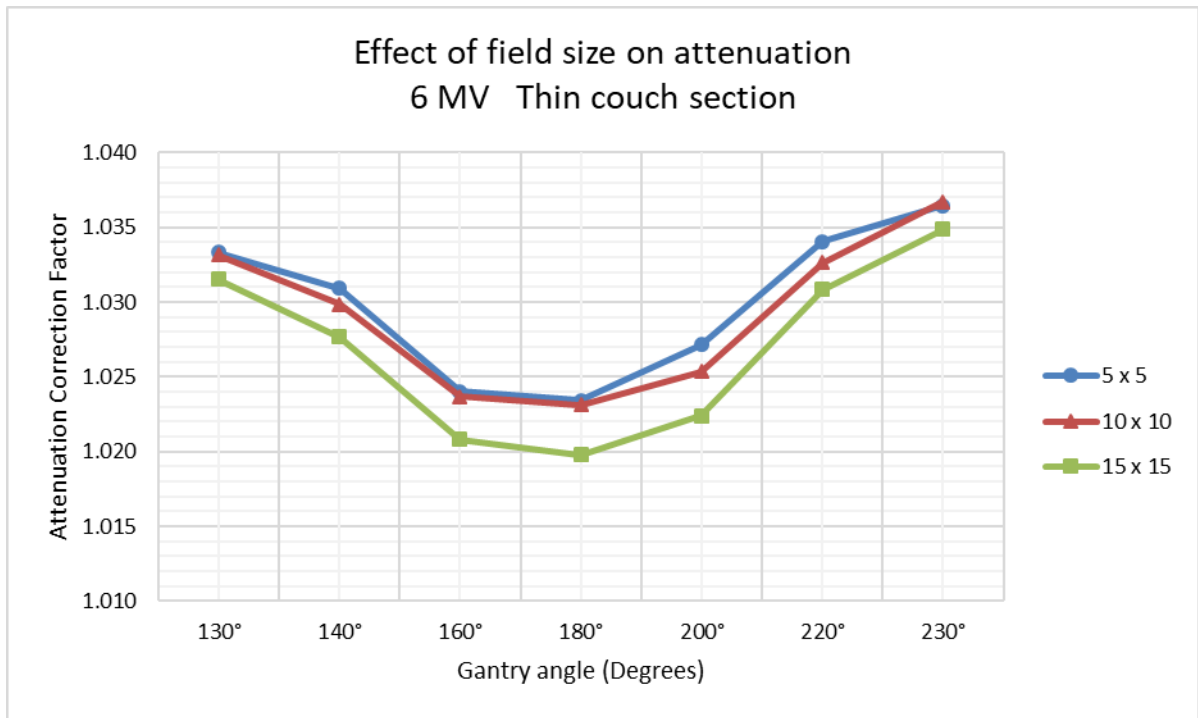


Figure 4.4: The effect of the field size on the attenuation by the treatment couch of 6 MV energy and the thin section of the treatment couch

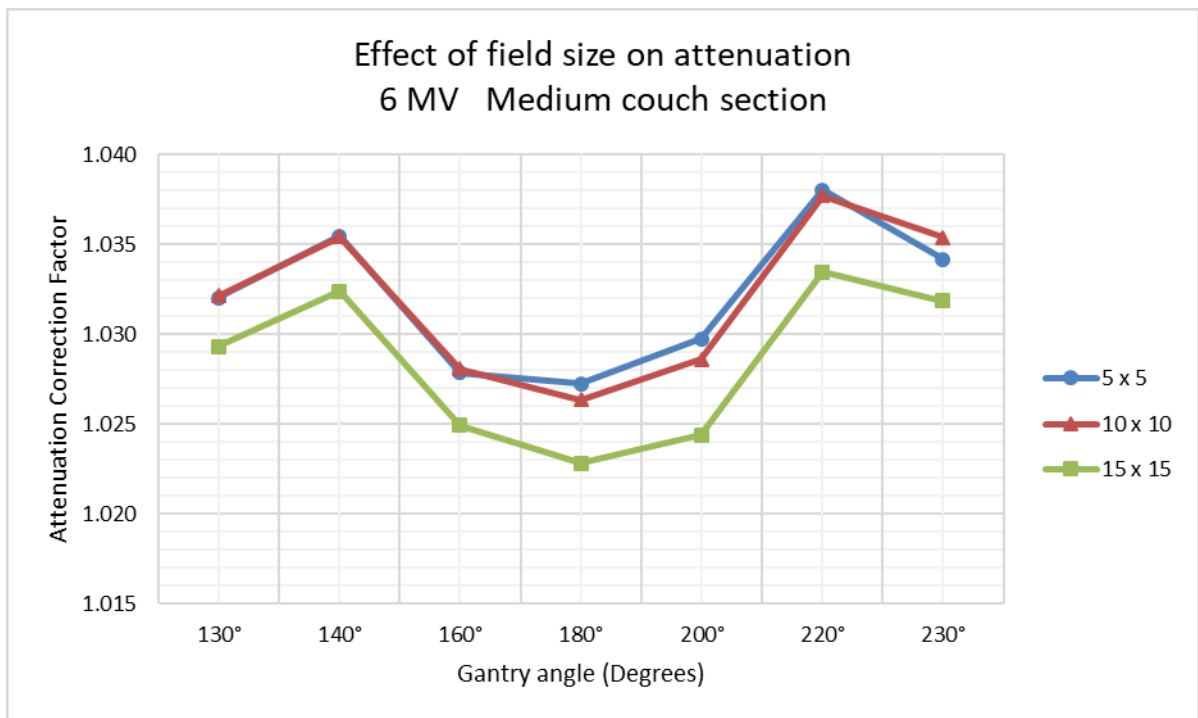


Figure 4.5: The effect of the field size on the attenuation by the treatment couch for 6 MV energy and the medium section of the treatment couch

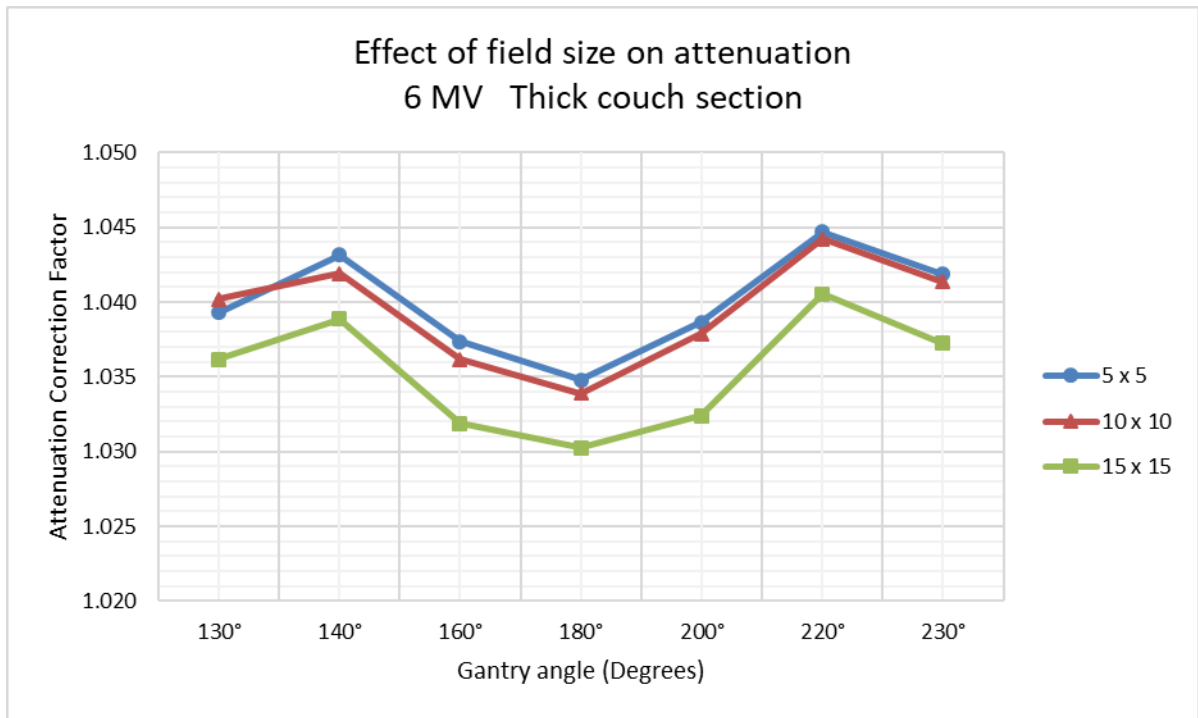


Figure 4.6: The effect of the field size on the attenuation by the treatment couch for 6 MV energy and the thick section of the treatment couch

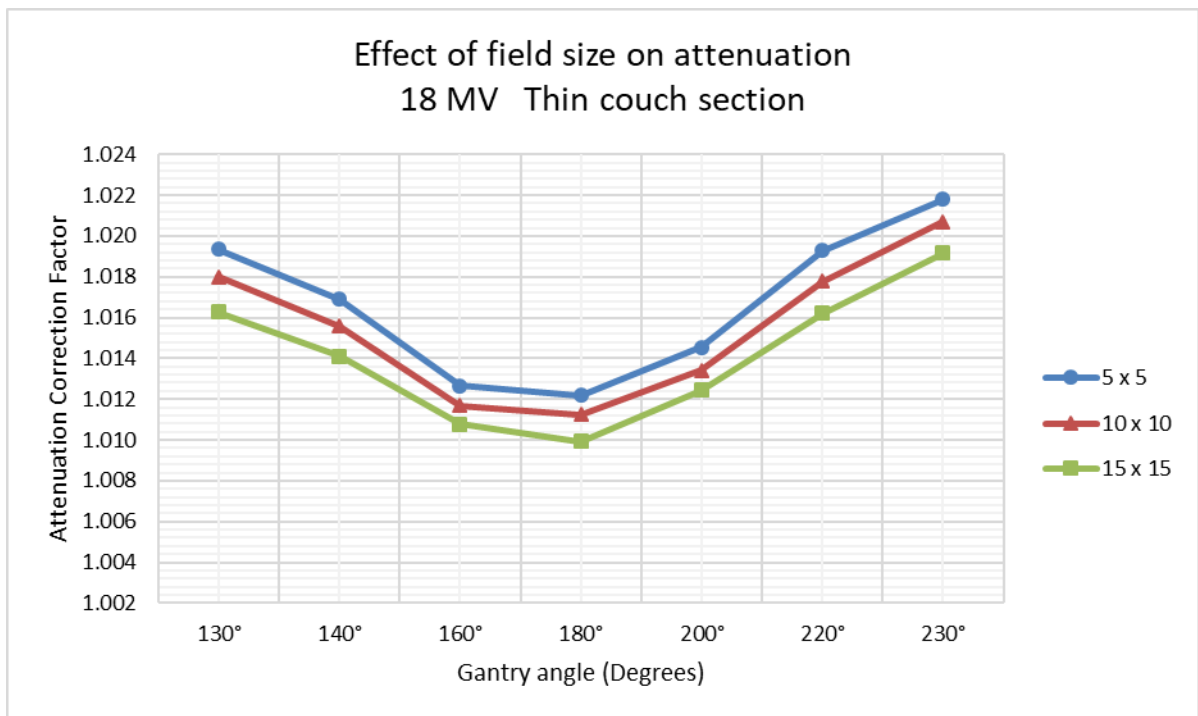


Figure 4.7: The effect of the field size on the attenuation by the treatment couch for 18 MV energy and the thin section of the treatment couch

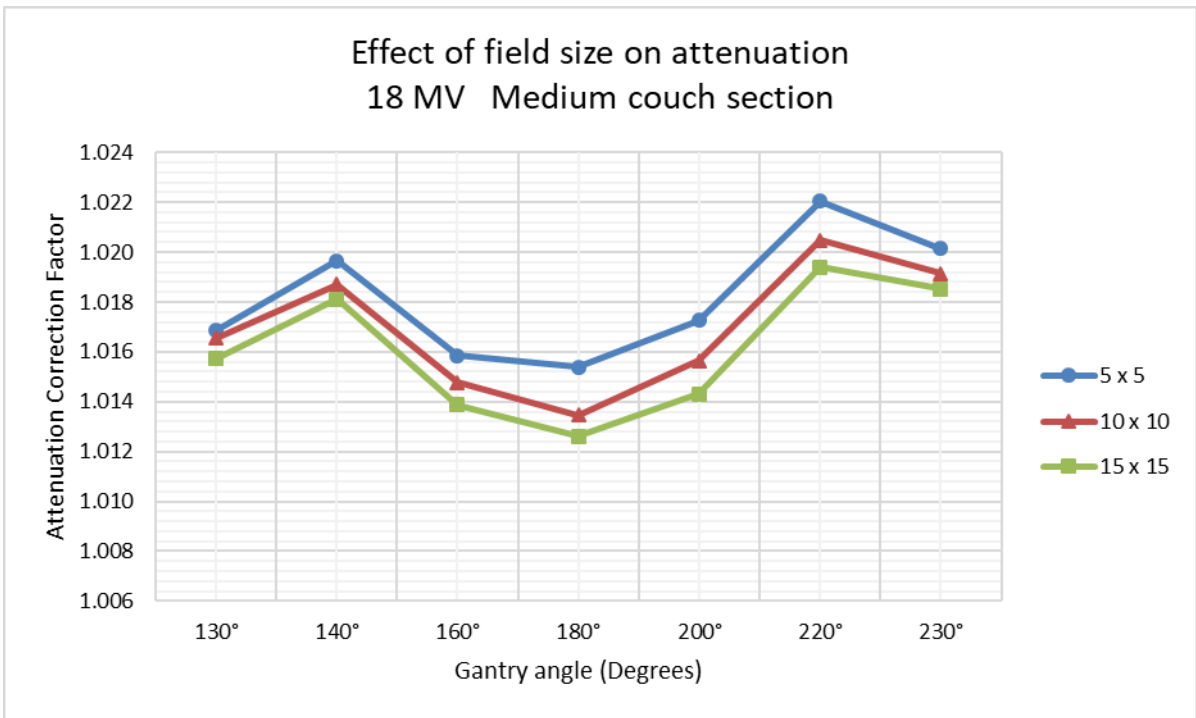


Figure 4.8: The effect of the field size on the attenuation by the treatment couch for 18 MV energy and the medium section of the treatment couch

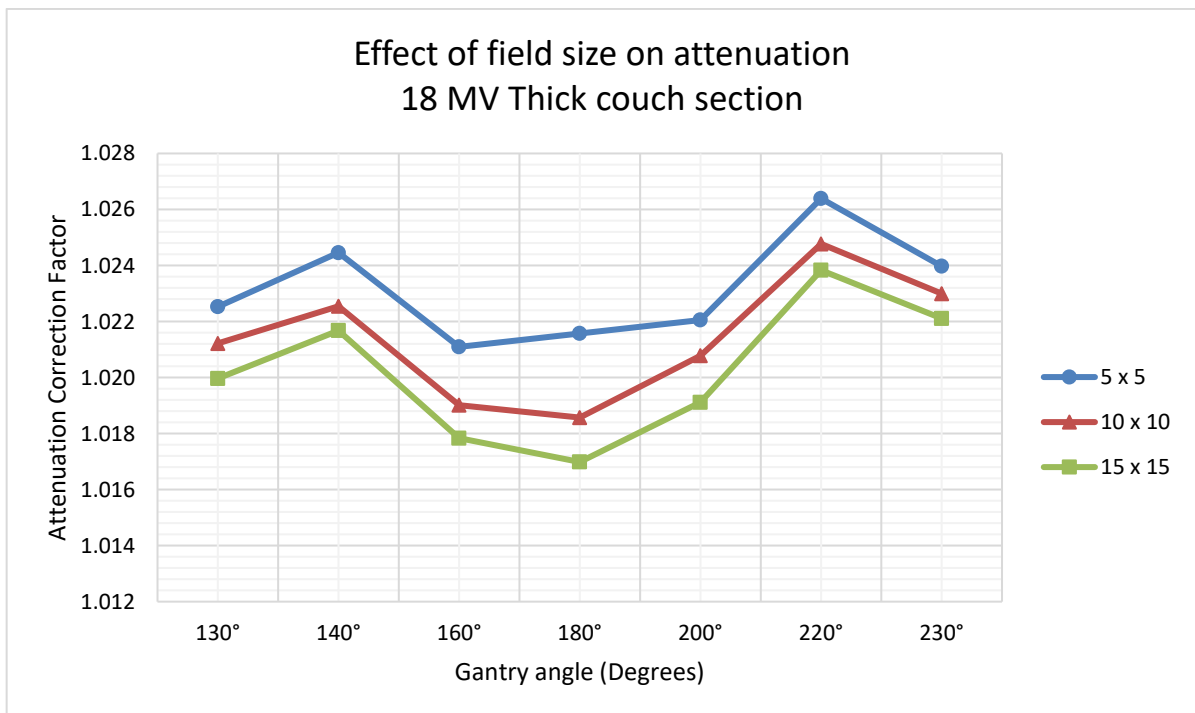


Figure 4.9: The effect of the field size on the attenuation by the treatment couch for 18 MV energy and the thick section of the treatment couch

Table 4.2: Summary of the influence of field size on the attenuation by the treatment couch for 6 MV

| Attenuation angles | 6 MV Thin | | | 6 MV Medium | | | 6 MV Thick | | |
|--------------------|-----------|---------|----------|-------------|---------|----------|------------|---------|----------|
| | 5 x 5 | 10 x 10 | 15 x 15% | 5 x 5 | 10 x 10 | 15 x 15% | 5 x 5 | 10 x 10 | 15 x 15% |
| 130° | 3.2% | 3.2% | 3.1% | 3.1% | 3.1% | 2.8% | 3.8% | 3.9% | 3.5% |
| 140° | 3.0% | 2.9% | 2.7% | 3.4% | 3.4% | 3.1% | 4.1% | 4.0% | 3.7% |
| 160° | 2.3% | 2.3% | 2.0% | 2.7% | 2.7% | 2.4% | 3.6% | 3.5% | 3.1% |
| 180° | 2.3% | 2.3% | 1.9% | 2.7% | 2.6% | 2.2% | 3.4% | 3.3% | 2.9% |
| 200° | 2.6% | 2.5% | 2.2% | 2.9% | 2.8% | 2.4% | 3.7% | 3.7% | 3.1% |
| 220° | 3.3% | 3.2% | 3.0% | 3.7% | 3.6% | 3.2% | 4.3% | 4.2% | 3.9% |
| 230° | 3.5% | 3.5% | 3.4% | 3.3% | 3.4% | 3.1% | 4.0% | 4.0% | 3.6% |

Table 4.3: Summary of the influence of field size on the attenuation by the treatment couch for 18 MV

| Attenuation angles | 18 MV Thin | | | 18 MV Medium | | | 18 MV Thick | | |
|--------------------|------------|---------|----------|--------------|---------|----------|-------------|---------|----------|
| | 5 x 5 | 10 x 10 | 15 x 15% | 5 x 5 | 10 x 10 | 15 x 15% | 5 x 5 | 10 x 10 | 15 x 15% |
| 130° | 1.9% | 1.8% | 1.6% | 1.7% | 1.6% | 1.5% | 2.2% | 2.1% | 2.0% |
| 140° | 1.7% | 1.5% | 1.4% | 1.9% | 1.8% | 1.8% | 2.4% | 2.2% | 2.1% |
| 160° | 1.3% | 1.2% | 1.1% | 1.6% | 1.5% | 1.4% | 2.1% | 1.9% | 1.8% |
| 180° | 1.2% | 1.1% | 1.0% | 1.5% | 1.3% | 1.2% | 2.1% | 1.8% | 1.7% |
| 200° | 1.4% | 1.3% | 1.2% | 1.7% | 1.5% | 1.4% | 2.2% | 2.0% | 1.9% |
| 220° | 1.9% | 1.7% | 1.6% | 2.2% | 2.0% | 1.9% | 2.6% | 2.4% | 2.3% |
| 230° | 2.1% | 2.0% | 1.9% | 2.0% | 1.9% | 1.8% | 2.3% | 2.2% | 2.2% |

The results also indicated that the beam energy played a role in the amount of attenuation of the treatment couch. For a particular field size, gantry angle, and couch section a decrease in attenuation is observed with increase in beam energy. For all the measurements, the attenuation due to the treatment couch was higher for the 6 MV energy compared to that of the 18 MV. For the thin couch section the amount of attenuation for the 6 MV ranged from 1.9% to 3.5%, and from 1.0% to 2.1% for 18 MV. For the medium couch section it ranged from 2.2% to 3.7% for 6 MV, and from 1.2% to 2.2% for 18 MV. For the thick couch section the ranges were from 2.9% to 4.3% and from 1.7% to 2.6% for 6 MV and 18 MV, respectively. This is demonstrated for the 10 x 10 cm field size for all three sections of the treatment couch in Figure 4.10, Figure 4.11 and Figure 4.12, with a summary of all the couch sections in Table 4.4.

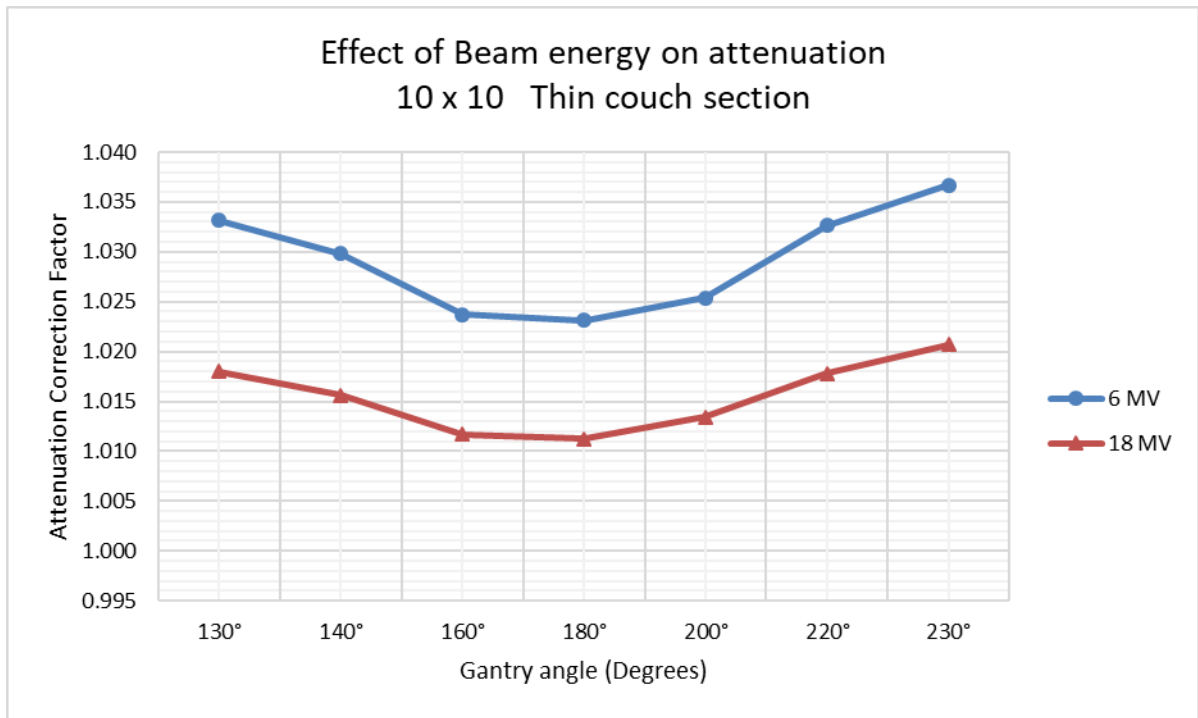


Figure 4.10: The effect of the beam energy on the attenuation by the treatment couch for 10 x 10 cm field size and the thin section of the treatment couch

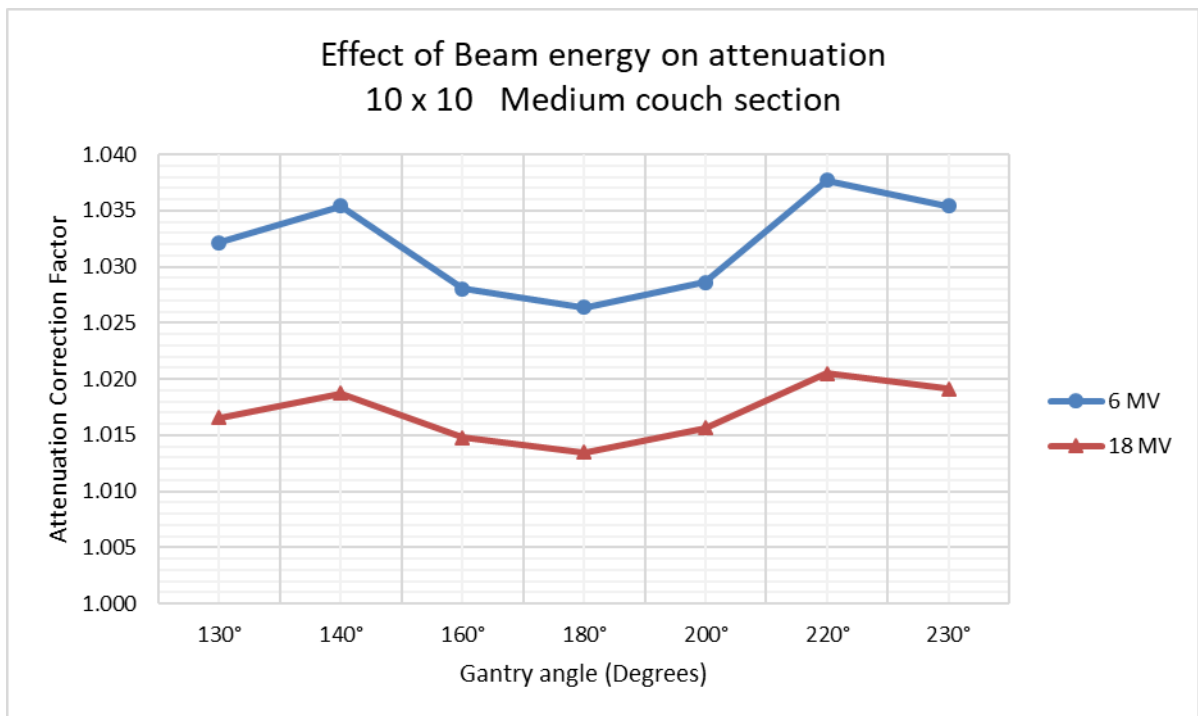


Figure 4.11: The effect of the beam energy on the attenuation by the treatment couch for 10 x 10 cm field size and the medium section of the treatment couch

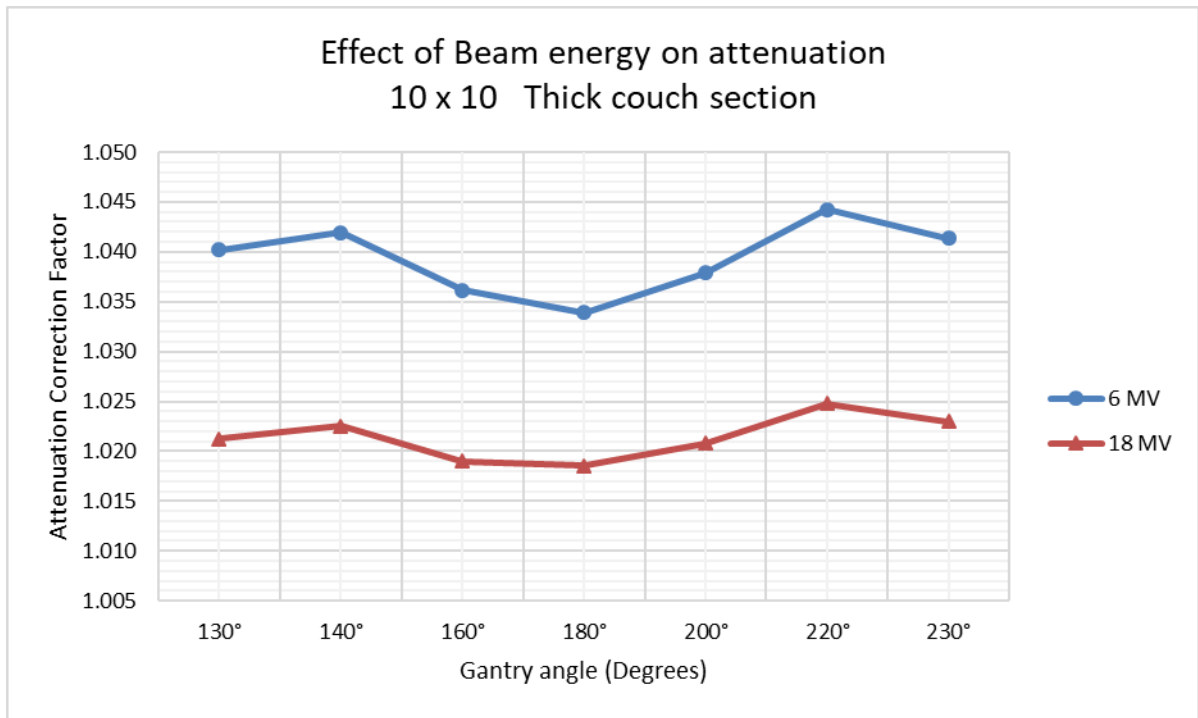


Figure 4.12: The effect of the beam energy on the attenuation by the treatment couch for 10 x 10 cm field size and the thick section of the treatment couch

Table 4.4: Summary of the influence of beam energy on the attenuation by the treatment couch

| Attenuation angles | 6 MV | 18 MV | 6 MV | 18 MV | 6 MV | 18 MV |
|--------------------|-------|-------|---------|---------|---------|---------|
| | 5 x 5 | 5 x 5 | 10 x 10 | 10 x 10 | 15 x 15 | 15 x 15 |
| | THIN | THIN | THIN | THIN | THIN | THIN |
| 130° | 3.2% | 1.9% | 3.2% | 1.8% | 3.1% | 1.6% |
| 140° | 3.0% | 1.7% | 2.9% | 1.5% | 2.7% | 1.4% |
| 160° | 2.3% | 1.3% | 2.3% | 1.2% | 2.0% | 1.1% |
| 180° | 2.3% | 1.2% | 2.3% | 1.1% | 1.9% | 1.0% |
| 200° | 2.6% | 1.4% | 2.5% | 1.3% | 2.2% | 1.2% |
| 220° | 3.3% | 1.9% | 3.2% | 1.7% | 3.0% | 1.6% |
| 230° | 3.5% | 2.1% | 3.5% | 2.0% | 3.4% | 1.9% |

| Attenuation angles | 6 MV | 18 MV | 6 MV | 18 MV | 6 MV | 18 MV |
|--------------------|-------|-------|---------|---------|---------|---------|
| | 5 x 5 | 5 x 5 | 10 x 10 | 10 x 10 | 15 x 15 | 15 x 15 |
| | MED | MED | MED | MED | MED | MED |
| 130° | 3.1% | 1.7% | 3.1% | 1.6% | 2.8% | 1.5% |
| 140° | 3.4% | 1.9% | 3.4% | 1.8% | 3.1% | 1.8% |
| 160° | 2.7% | 1.6% | 2.7% | 1.5% | 2.4% | 1.4% |
| 180° | 2.7% | 1.5% | 2.6% | 1.3% | 2.2% | 1.2% |
| 200° | 2.9% | 1.7% | 2.8% | 1.5% | 2.4% | 1.4% |
| 220° | 3.7% | 2.2% | 3.6% | 2.0% | 3.2% | 1.9% |
| 230° | 3.3% | 2.0% | 3.4% | 1.9% | 3.1% | 1.8% |

| Attenuation angles | 6 MV | 18 MV | 6 MV | 18 MV | 6 MV | 18 MV |
|--------------------|-------|-------|---------|---------|---------|---------|
| | 5 x 5 | 5 x 5 | 10 x 10 | 10 x 10 | 15 x 15 | 15 x 15 |
| | THICK | THICK | THICK | THICK | THICK | THICK |
| 130° | 3.8% | 2.2% | 3.9% | 2.1% | 3.5% | 2.0% |
| 140° | 4.1% | 2.4% | 4.0% | 2.2% | 3.7% | 2.1% |
| 160° | 3.6% | 2.1% | 3.5% | 1.9% | 3.1% | 1.8% |
| 180° | 3.4% | 2.1% | 3.3% | 1.8% | 2.9% | 1.7% |
| 200° | 3.7% | 2.2% | 3.7% | 2.0% | 3.1% | 1.9% |
| 220° | 4.3% | 2.6% | 4.2% | 2.4% | 3.9% | 2.3% |
| 230° | 4.0% | 2.3% | 4.0% | 2.2% | 3.6% | 2.2% |

Table 4.5 gives a summary of the extent of the attenuation at the research study site for the Varian IGRT treatment couch for the 6 MV energy, and Table 4.6 for the 18 MV energy.

Table 4.5: Summary of the attenuation produced by the IGRT treatment couch for 6 MV (the highest values are highlighted)

| Couch section | Energy | Field Size | Mean attenuation | Standard Deviation | Range | Maximum attenuation | Maximum attenuation angle | Attenuation @ 180° |
|---------------|--------|------------|------------------|--------------------|-------|---------------------|---------------------------|--------------------|
| Thin | 6MV | 5 x 5 | 2.9% | 0.5% | 1.2% | 3.5% | 230° | 2.3% |
| Thin | 6MV | 10 x 10 | 2.8% | 0.5% | 1.3% | 3.5% | 230° | 2.3% |
| Thin | 6MV | 15 x 15 | 2.6% | 0.6% | 1.4% | 3.4% | 230° | 1.9% |
| Medium | 6MV | 5 x 5 | 3.1% | 0.4% | 1.0% | 3.7% | 220° | 2.7% |
| Medium | 6MV | 10 x 10 | 3.1% | 0.4% | 1.1% | 3.6% | 220° | 2.6% |
| Medium | 6MV | 15 x 15 | 2.8% | 0.4% | 1.0% | 3.2% | 220° | 2.2% |
| Thick | 6MV | 5 x 5 | 3.8% | 0.3% | 0.9% | 4.3% | 220° | 3.4% |
| Thick | 6MV | 10 x 10 | 3.8% | 0.3% | 1.0% | 4.2% | 220° | 3.3% |
| Thick | 6MV | 15 x 15 | 3.4% | 0.4% | 1.0% | 3.9% | 220° | 2.9% |

Table 4.6: Summary of the attenuation produced by the IGRT treatment couch for 18 MV (the highest values are highlighted)

| Couch section | Energy | Field Size | Mean attenuation | Standard Deviation | Range | Maximum attenuation | Maximum attenuation angle | Attenuation @ 180° |
|---------------|--------|------------|------------------|--------------------|-------|---------------------|---------------------------|--------------------|
| Thin | 18MV | 5 x 5 | 1.6% | 0.4% | 0.9% | 2.1% | 230° | 1.2% |
| Thin | 18MV | 10 x 10 | 1.5% | 0.3% | 0.9% | 2.0% | 230° | 1.1% |
| Thin | 18MV | 15 x 15 | 1.4% | 0.3% | 0.9% | 1.9% | 230° | 1.0% |
| Medium | 18MV | 5 x 5 | 1.8% | 0.2% | 0.6% | 2.2% | 220° | 1.5% |
| Medium | 18MV | 10 x 10 | 1.7% | 0.2% | 0.7% | 2.0% | 220° | 1.3% |
| Medium | 18MV | 15 x 15 | 1.6% | 0.3% | 0.7% | 1.9% | 220° | 1.2% |
| Thick | 18MV | 5 x 5 | 2.3% | 0.2% | 0.5% | 2.6% | 220° | 2.1% |
| Thick | 18MV | 10 x 10 | 2.1% | 0.2% | 0.6% | 2.4% | 220° | 1.8% |
| Thick | 18MV | 15 x 15 | 2.0% | 0.2% | 0.7% | 2.3% | 220° | 1.7% |

4.2.2 Mirror angle differences

A mirrored beam geometry was used for all measurements to ensure that the phantom was placed in the centre of the couch (laterally). The pairs of mirror angles used were the following:

- 160° and 200° (20° incident angles)
- 140° and 220° (40° incident angles)
- 130° and 230° (50° incident angles)
- 120° and 240° (60° incident angles).

Due to a partial hit on the couch edge at 120° and 240°, these two angles proved to be very sensitive to positioning errors compared to other mirror angle pairs (Figure 4.13, Figure 4.14, Figure 4.15 and Figure 4.16). As this was a geometric concern and not relating to the study, the angles were not included in the final results.

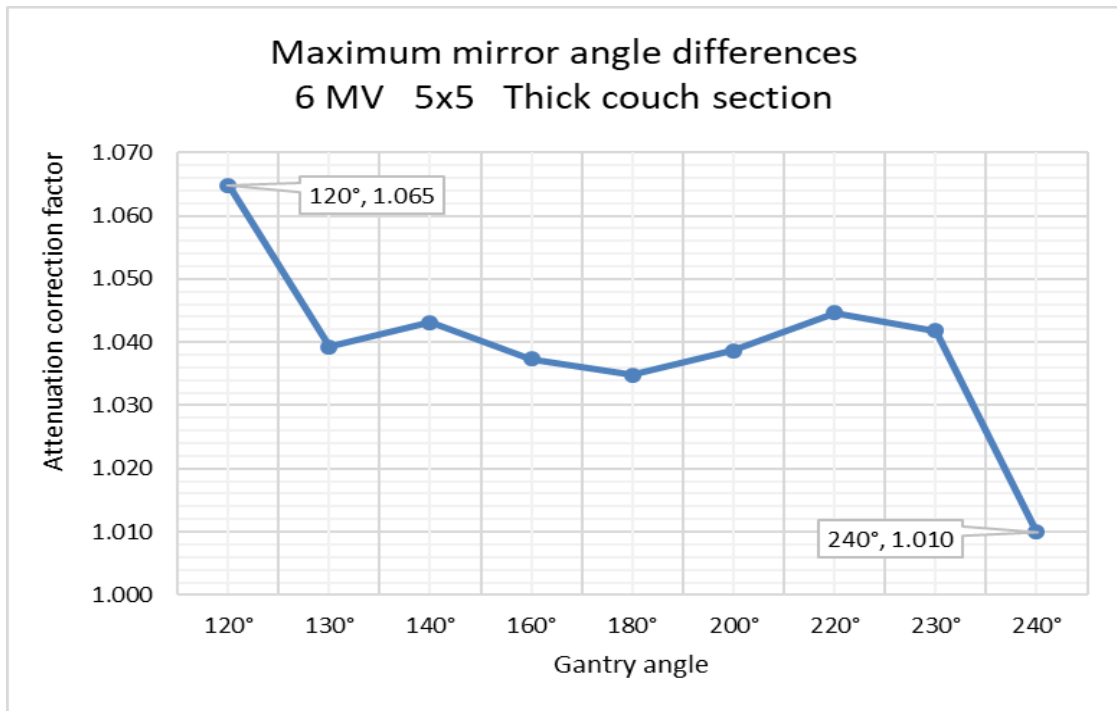


Figure 4.13: Chart showing maximum differences in measurements between 120° and 240° angle

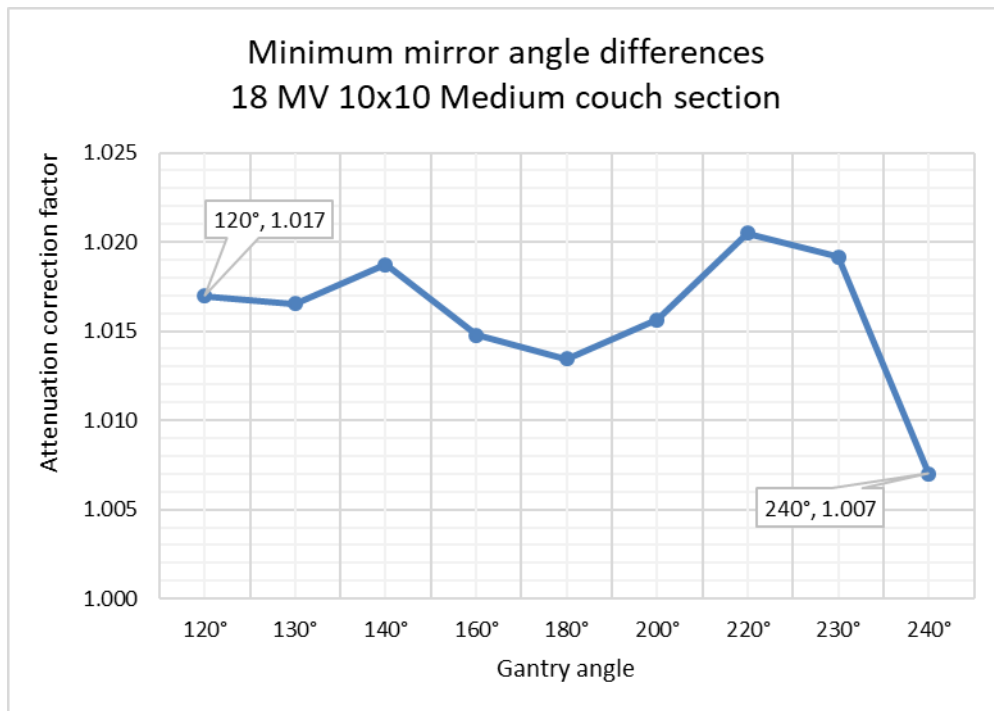


Figure 4.14: Chart showing minimum differences in measurements between 120° and 240° angle

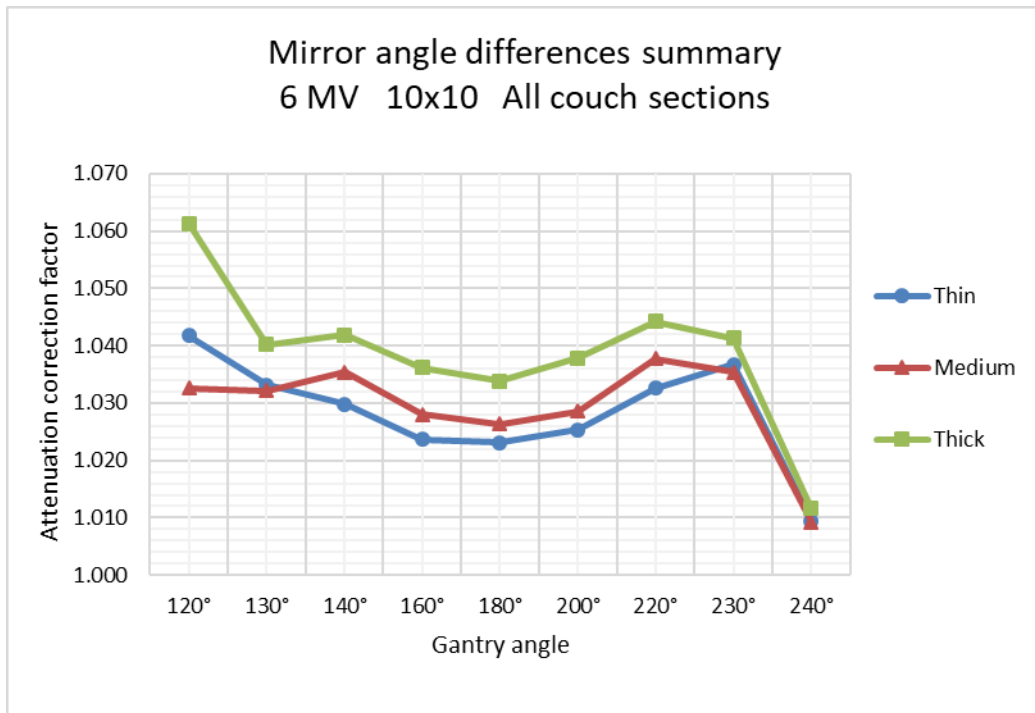


Figure 4.15: Chart showing that the 120° and 240° differences are consistent for all three sections of the couch for 6 MV, 10 x 10 cm field size

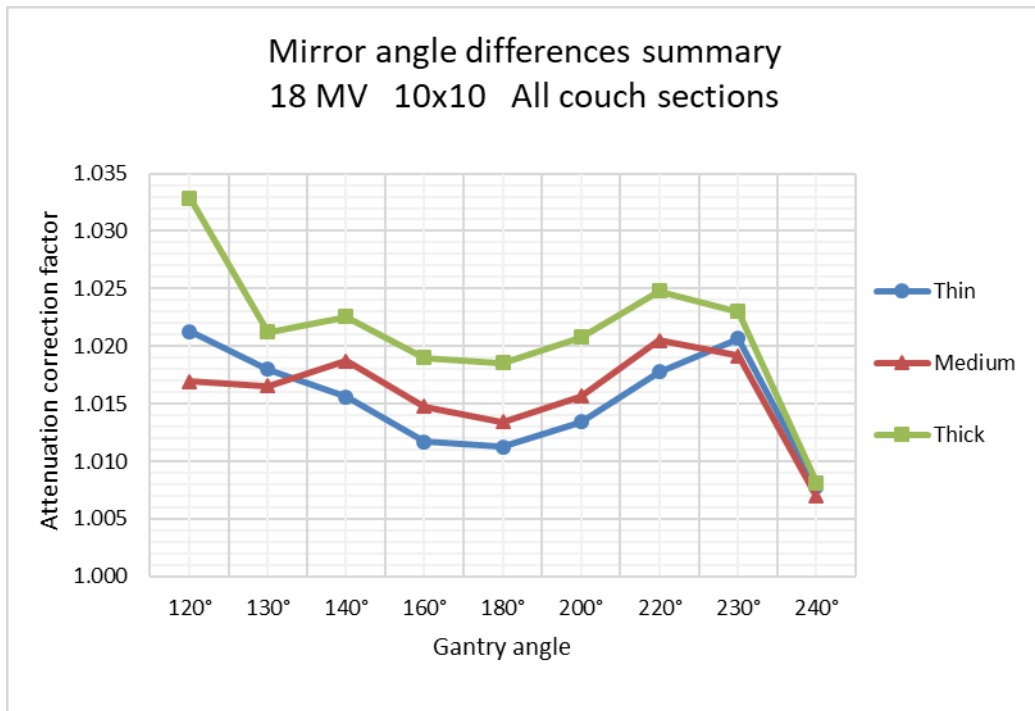


Figure 4.16: Chart showing that the 120° and 240° differences are consistent for all three sections of the couch for 18 MV, 10 x 10 cm field size

4.2.3 Surface dose effects of the couch

All surface doses are reported as a percentage of the dose at D_{max} for that particular beam. The D_{max} depths used in this research study were 1.6 cm for 6 MV and 3.3 cm for 18 MV. These D_{max} depths were determined from the percentage depth dose data used by Pinnacle at the study site.

For 6 MV the nanoDot measured surface doses as a percentage of the beam D_{max} doses for the open beams were 36.19% and 47.07% for the 10 x 10 cm and 20 x 20 cm field sizes, respectively; and, for 18 MV for the open beams the surface doses were 23.33% and 36.64% for 10 x 10 cm and 20 x 20 cm, respectively (Figure 4.17).

There was an uncertainty in the accuracy of the nanoDot readings due to the limited number of nanoDot dosimeters available for the study. For 6 MV the maximum relative standard deviation was 3.51% (+/- 0.039 Gy SD). This was for the thin section of the couch at gantry 180° and the 20 x 20 cm field size where the mean measurement was 1.119 Gy \pm 3.51% (1.119 \pm 0.039 Gy). For 18 MV the maximum relative standard deviation was also for the thin section of the couch at gantry 180°, but for the 10 x 10 cm field size where the mean measurement was 0.703 Gy \pm 3.32% (0.703 \pm 0.023 Gy).

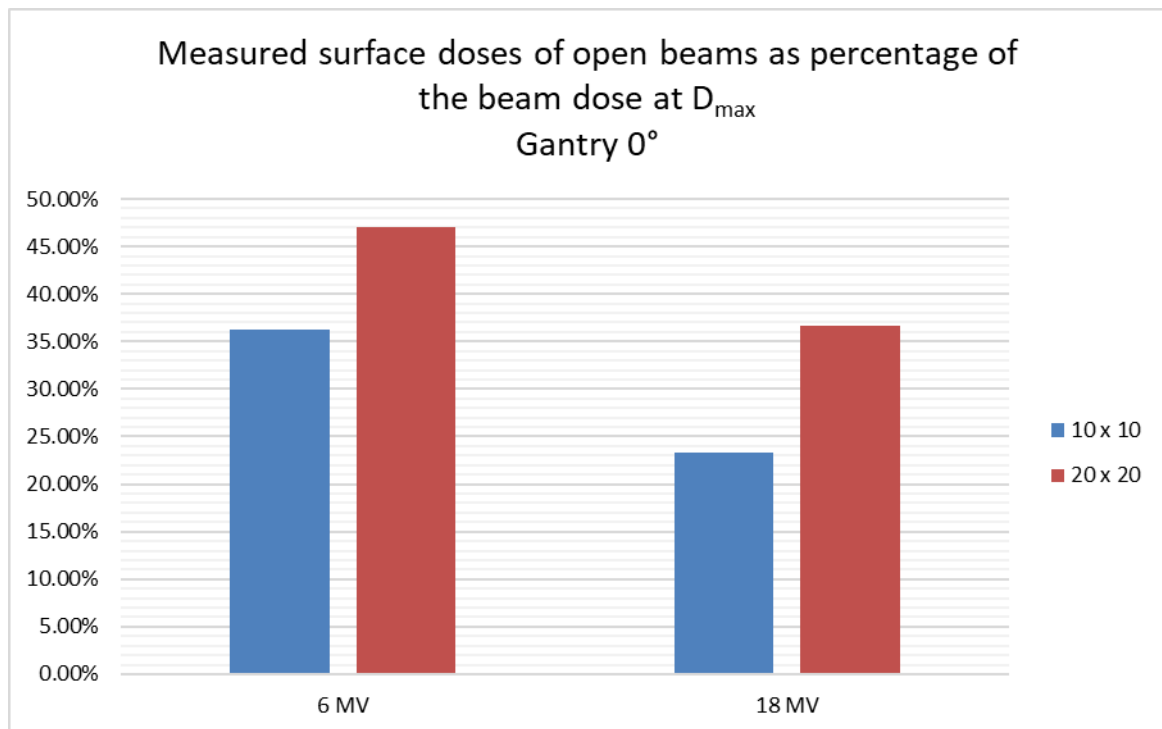


Figure 4.17: Comparing the influence of field size on the measured surface doses for the 6 MV and 18 MV

For the 180° gantry angles through the couch, the measured surface doses for the 6 MV 10 x 10 cm field size were 86.45%, 88.83% and 92.44% for the thin, medium and thick couch sections, respectively, and 93.40%, 93.69% and 98.39% for 20 x 20 cm for the thin, medium and thick couch sections, respectively (Figure 4.18).

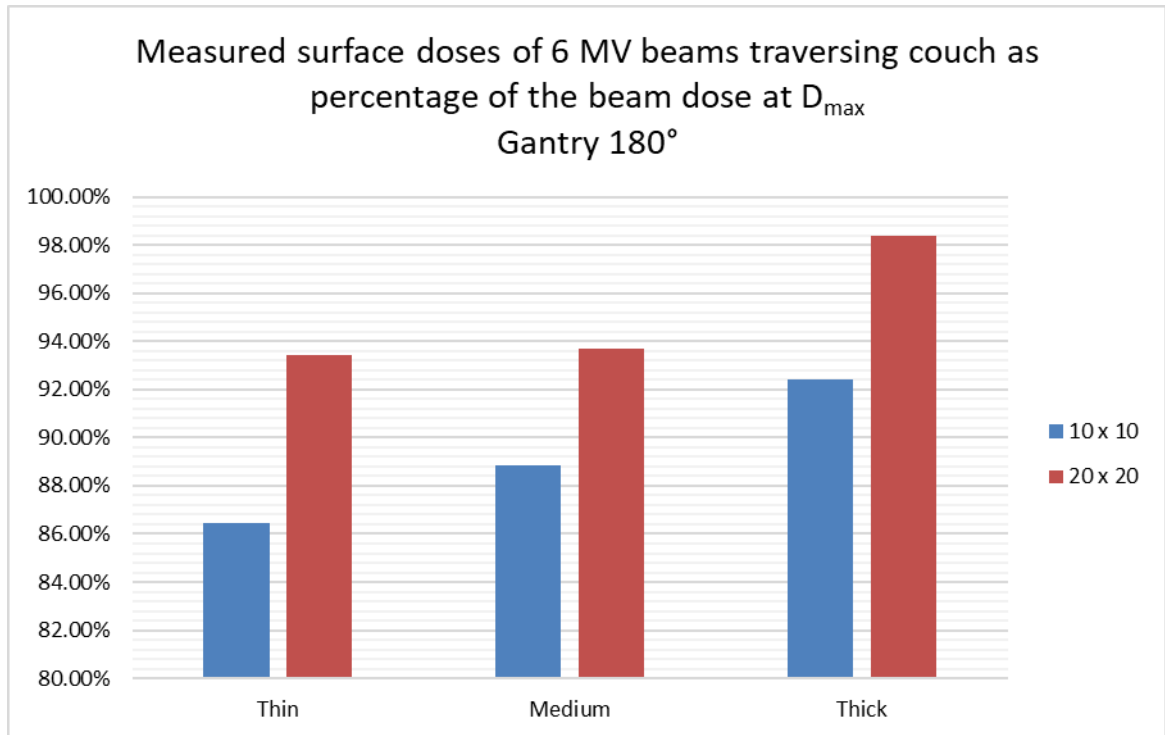


Figure 4.18: Comparing the influence of field size and the treatment couch on the measured surface doses for 6 MV

For 18 MV the measured surface doses for thin, medium and thick couch sections at 180° and 10 x 10 cm were 60.53%, 64.34% and 67.38%, and for 20 x 20 cm they were 75.18%, 76.74% and 83.45% (Figure 4.19).

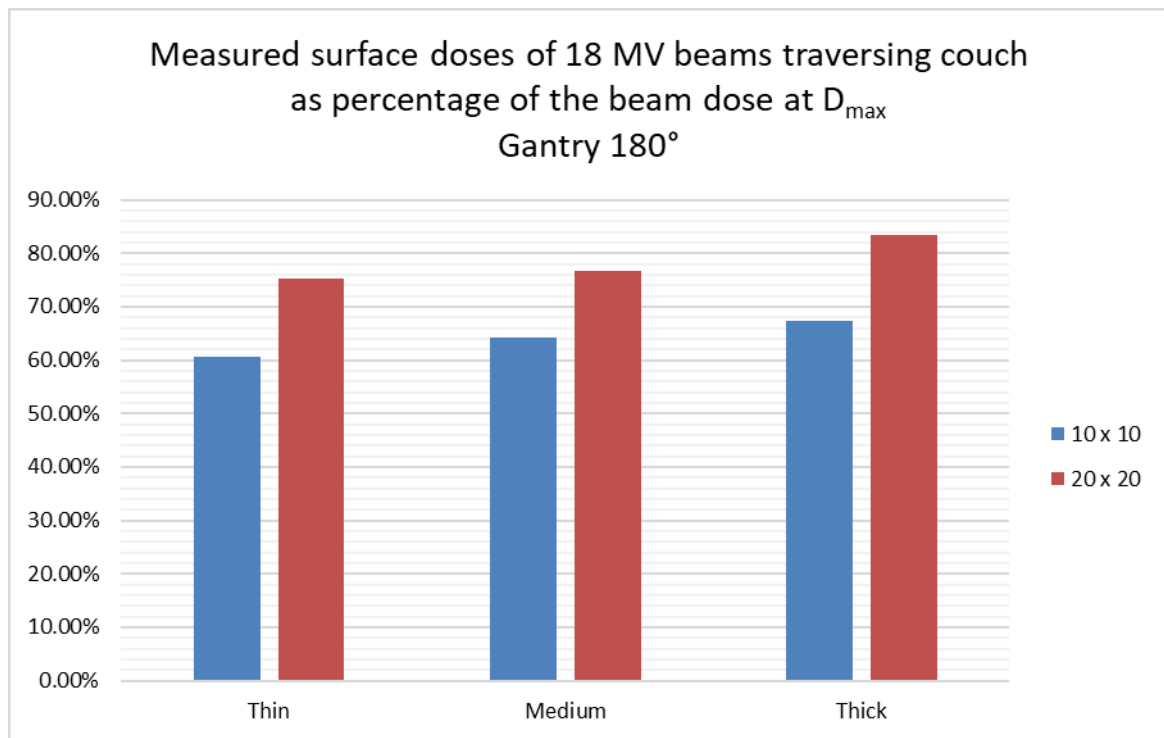


Figure 4.19: Comparing the influence of field size and the treatment couch on the measured surface doses for 18 MV

There were also measurements done for 10 x 10 cm field size and an oblique angle through the three sections of the couch at gantry 230° for both energies. The surface doses at 230° for 6 MV for thin, medium and thick were 96.66%, 94.19% and 96.90%, respectively, and 74.30%, 75.91% and 82.35% for 18 MV. This is shown for 6 MV in Figure 4.20 and for 18 MV in Figure 4.21.

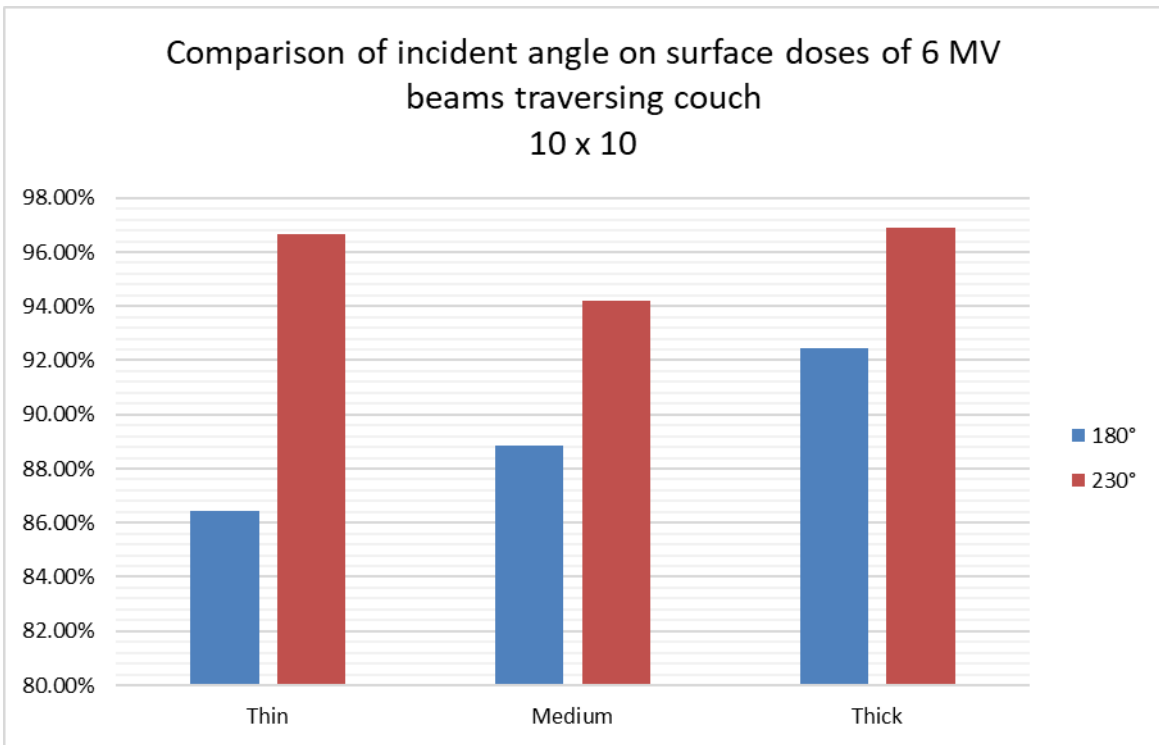


Figure 4.20: Comparing the influence of incident angle on the measured surface doses for 6 MV for the three couch sections

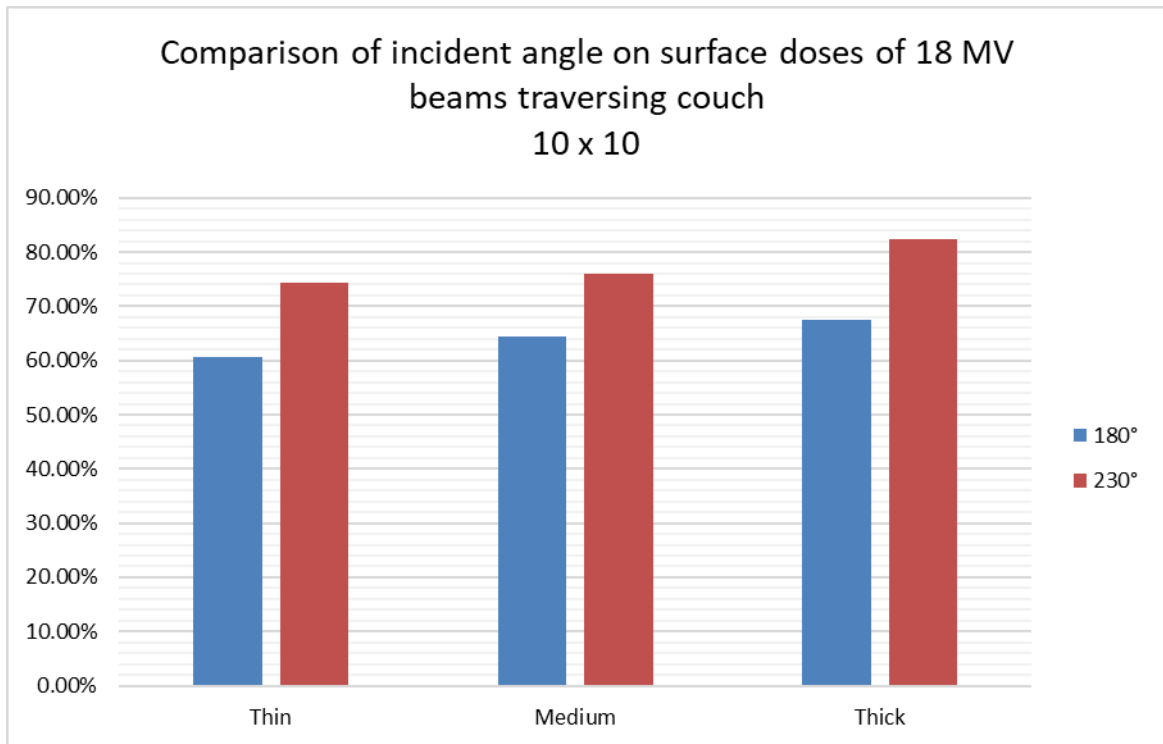


Figure 4.21: Comparing the influence of incident angle on the measured surface doses for 18 MV for the three couch sections

When looking at the surface doses for the open beams which did not traverse the couch (gantry 0°) it was found that for both 10 x 10 cm and 20 x 20 cm the predicted surface doses from Pinnacle were consistently higher than the measured surface doses for both energies. The surface doses were again analysed as a percentage of the beam doses at D_{max} .

For 6 MV and 10 x 10 cm the surface dose as percentage of beam dose at D_{max} was 55.62% for Pinnacle, compared to 36.19% for the measured nanoDot surface dose, and for 20 x 20 cm it was 57.26% and 47.07% for Pinnacle and the measured surface doses, respectively (Figure 4.22). For 18 MV it was 35.50% and 23.33% for 10 x 10 cm, and 52.35% and 36.64% for 20 x 20 cm (Figure 4.23). When calculating the percentage differences between the open beam surface doses as calculated by Pinnacle and the nanoDot surface doses, it was noted that the percentage difference is more than 50% for the 10 x 10 cm field size for both energies, and for 20 x 20 cm the percentage differences were 21.66% for 6 MV and 42.87% for 18 MV (Figure 4.24). In contrast, the differences between the Pinnacle surface doses and the measured surface doses for the beams traversing the couch were much smaller. For these beams and with the couch model being used on Pinnacle, this over- or under-estimation by Pinnacle ranged from -10.13% to 2.73% for 6 MV, and from -6.49% to 8.04% for 18 MV. The surface doses calculated by Pinnacle were similar to the doses found on the Pinnacle percentage depth dose data for the depth range 0.0 to 0.2 cm (Table 4.7).

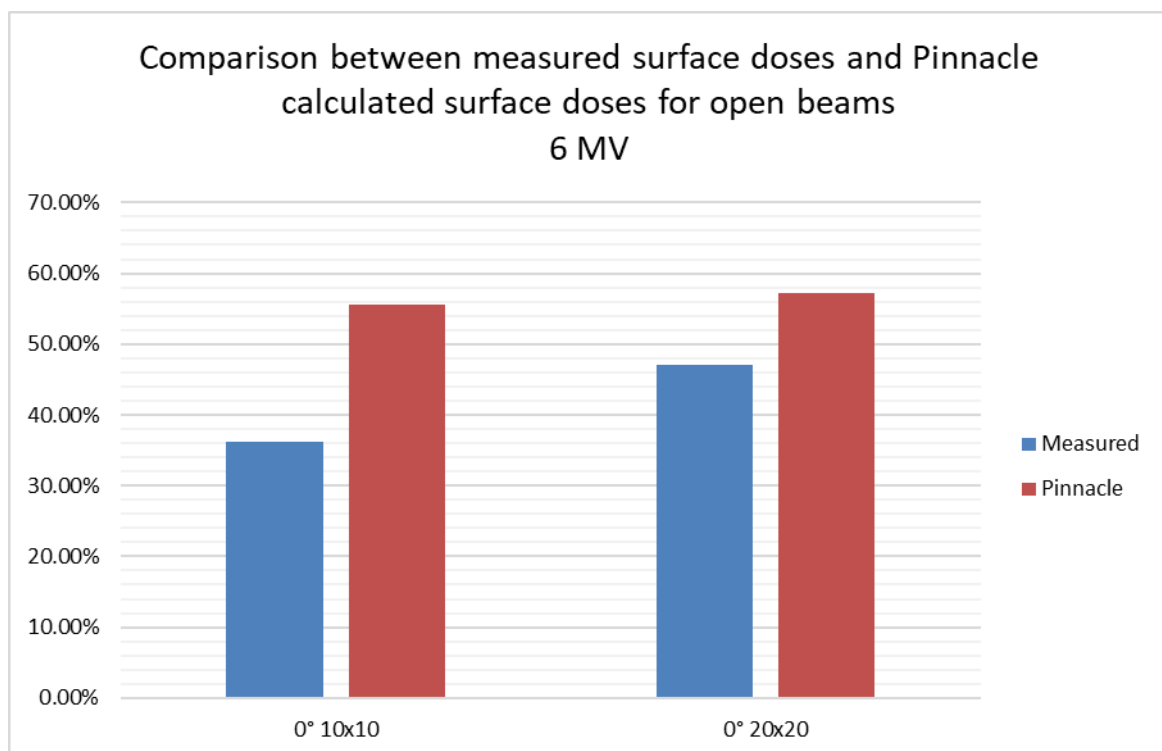


Figure 4.22: Demonstrating the open beam surface dose differences between the measured doses and the doses calculated by Pinnacle for 6 MV

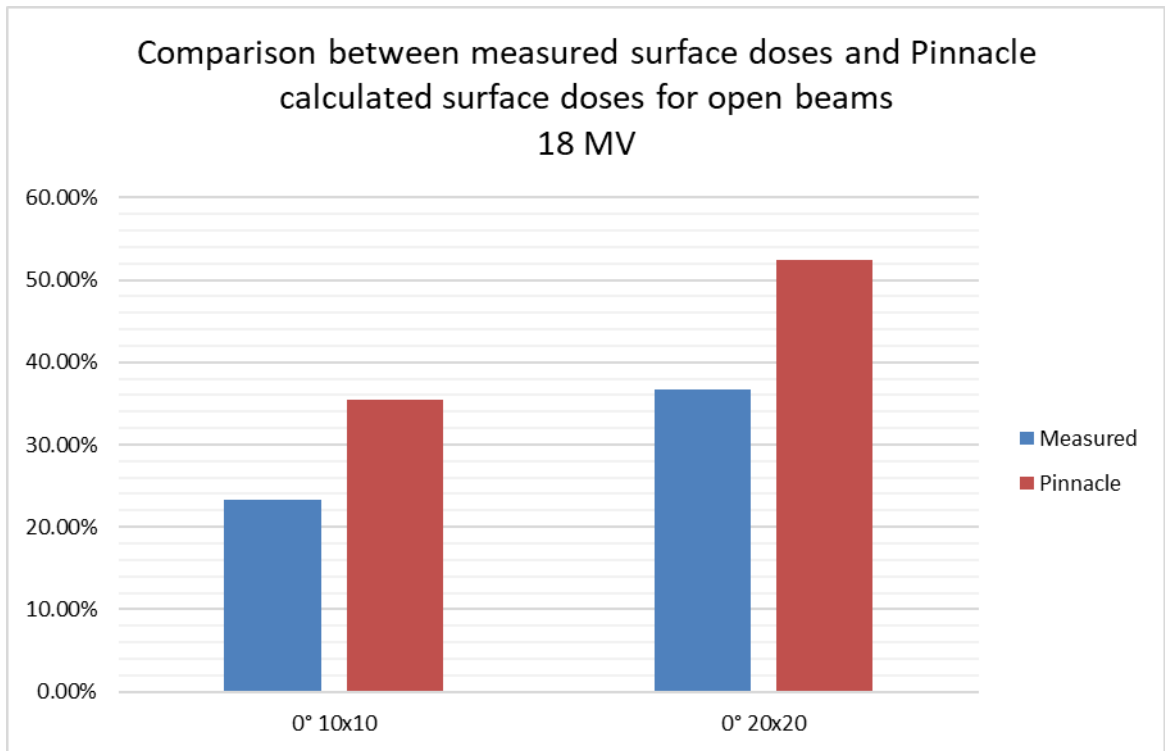


Figure 4.23: Demonstrating the open beam surface dose differences between the measured doses and the doses calculated by Pinnacle for 18 MV

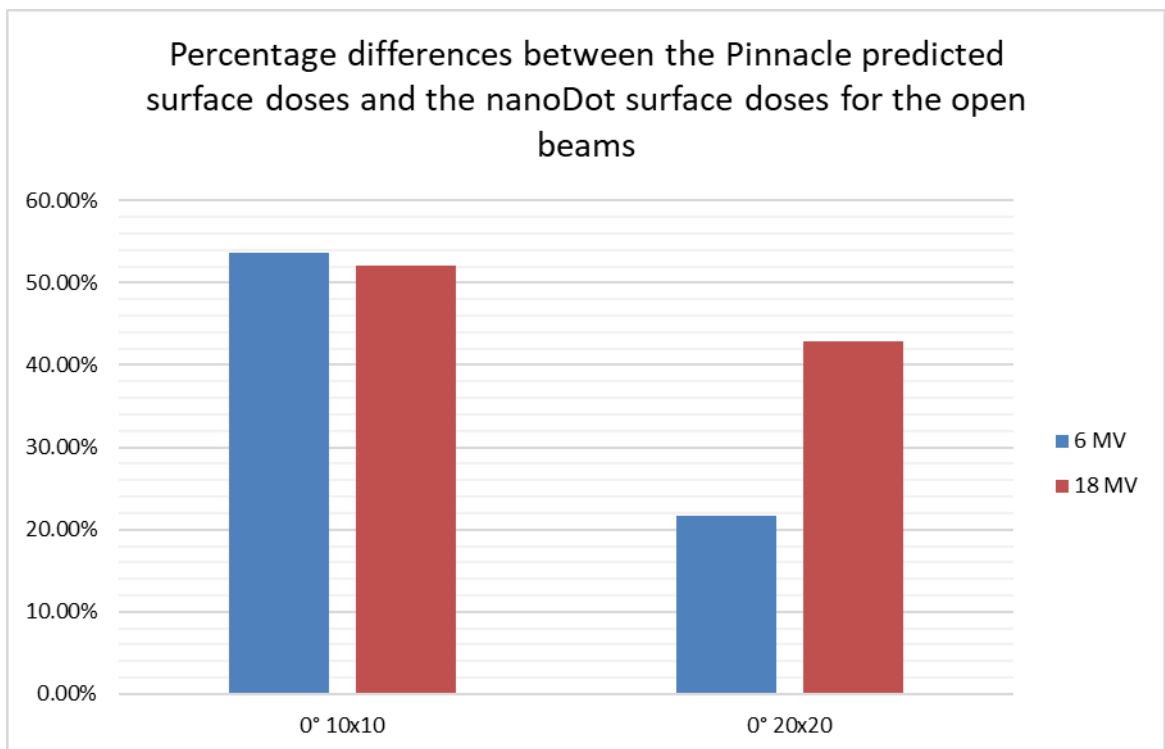


Figure 4.24: Demonstrating the percentage differences between the Pinnacle predicted surface doses and the nanoDot surface doses for the open beams

Table 4.7: The Pinnacle percentage depth dose data for the surface region

| 6X 10x10 | | 6X 20x20 | | 18X 10x10 | | 18X 20x20 | |
|----------|-------|----------|-------|-----------|-------|-----------|-------|
| Depth | PDD | Depth | PDD | Depth | PDD | Depth | PDD |
| 0.0 | 51.15 | 0.0 | 59.08 | 0.0 | 32.24 | 0.0 | 45.97 |
| 0.2 | 57.65 | 0.2 | 65.66 | 0.2 | 36.10 | 0.2 | 50.83 |
| 0.4 | 73.15 | 0.4 | 79.70 | 0.4 | 47.95 | 0.4 | 61.53 |

The results found in this research study with regard to the 6 MV, 10 x 10 cm, PDD data are similar to those found by Apipunyasopon et al. (2013). Their study used various methods for measuring surface doses, including CC13 ionisation chamber and TLD chips on the Varian Clinac 23EX linear accelerator, which is a similar model to the linear accelerator used in this research study. Apipunyasopon et al. (2013) results for the surface doses were in the region of 55% for the CC13 chamber, and in the region of 42% for the TLD chips (Figure 4.25). These results were in line with the 55.62% and 36.19% found in this research study for the Pinnacle and nanoDot, respectively, for 6 MV and 10 x 10.

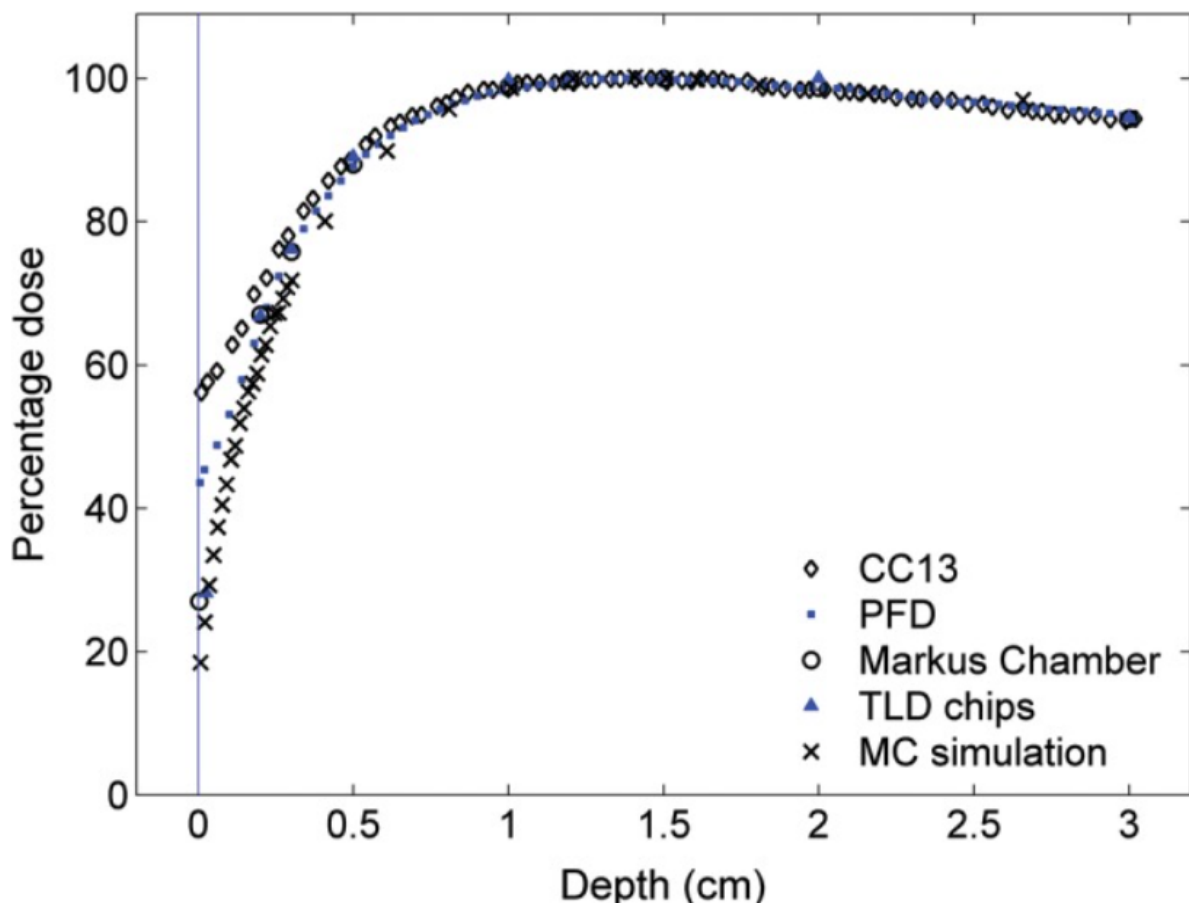


Figure 4.25: The percentage depth dose curves obtained using the CC13 chamber, PFD dosimeter, Markus chamber, TLD chips and the Monte Carlo simulation, for the 6 MV photon beam with a 10 x 10 cm field

(Apipunyasopon et al., 2013:378)

4.3 Pinnacle predicted doses without a couch structure

4.3.1 Calculated attenuation effect without couch

In this section the doses which have been measured on the treatment unit with the actual Varian IGRT couch were compared with the doses that the Pinnacle treatment planning system calculated if it does not take the treatment couch into account. This was to see if the Pinnacle treatment planning system overestimates or underestimates the doses for beams which traverse the treatment couch, and if so, by how much. These doses were all measured at depth in the middle of the cylindrical phantom at the isocentre.

It was found that, when Pinnacle ignored the attenuation effect of the treatment couch, the calculated Pinnacle doses were higher than the measured doses for all the beams traversing the treatment couch. The overestimations of these doses by Pinnacle were expressed as percentage differences between the Pinnacle calculated doses and the measured doses.

For 6 MV the lowest overestimation by Pinnacle was 1.85% for the thin section of the couch and 15 x 15 cm field size. The highest overestimation was 4.14% for the thick couch section and 10 x 10 cm field size. Table 4.8 shows all the overestimations for 6 MV with the lowest and highest values highlighted. The lowest value is highlighted in red and the highest value in blue. For 18 MV the lowest overestimation was 0.93% also for the thin section of the couch and 15 x 15 cm field size. The highest overestimation was 2.43% for the thick couch section and 5 x 5 cm field size. Table 4.9 shows all the overestimations for 18 MV with the lowest and highest values highlighted here also. Figure 4.26 and Figure 4.27 demonstrate the amounts of overestimation for the three couch sections for a 10 x 10 cm field size for the 6 MV and 18 MV energies, respectively.

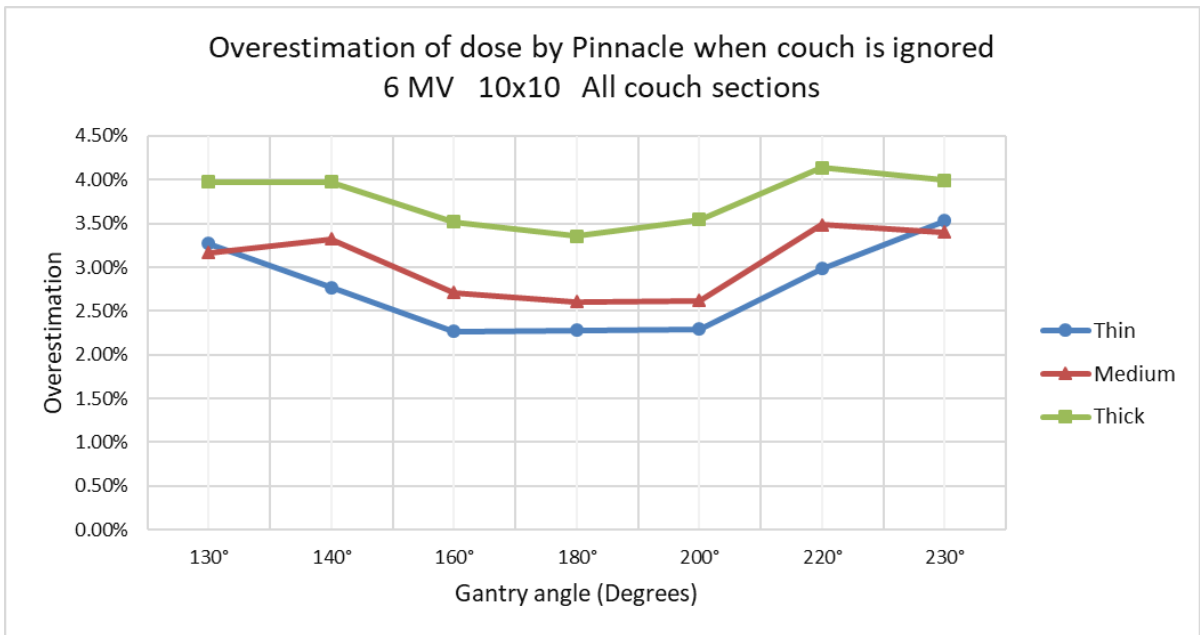


Figure 4.26: Overestimation by the Pinnacle treatment planning system for 6 MV, 10 x 10 cm for the three couch sections

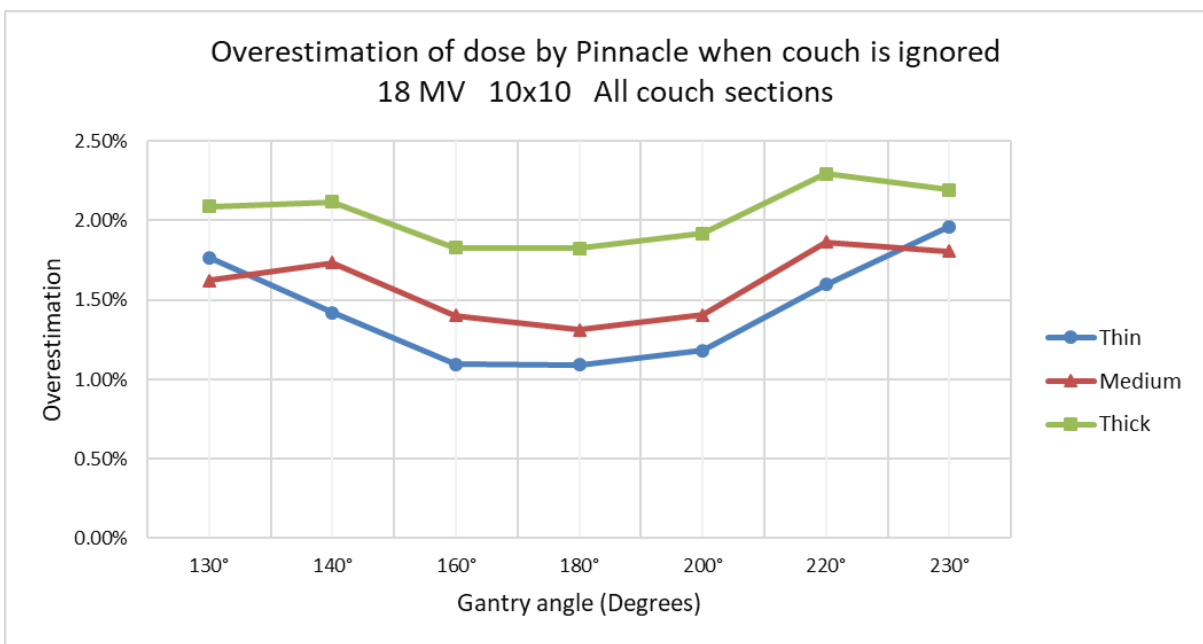


Figure 4.27: Overestimation by the Pinnacle treatment planning system for 18 MV, 10 x 10 cm for the three couch sections

Table 4.8: Summary of the overestimation of the dose by Pinnacle if treatment couch is ignored for the 6 MV energy
 (The maximum overestimation is highlighted in blue and the minimum overestimation in red)

| Couch section | Energy | Field Size | Gantry Angle | | | | | | |
|---------------|--------|------------|--------------|-------|-------|-------|-------|-------|-------|
| | | | 130° | 140° | 160° | 180° | 200° | 220° | 230° |
| Thin | 6MV | 5 x 5 | 3.19% | 2.88% | 2.19% | 2.17% | 2.37% | 3.06% | 3.30% |
| Thin | 6MV | 10 x 10 | 3.27% | 2.77% | 2.27% | 2.28% | 2.29% | 2.98% | 3.53% |
| Thin | 6MV | 15 x 15 | 3.20% | 2.70% | 2.06% | 1.85% | 2.09% | 2.90% | 3.39% |
| Medium | 6MV | 5 x 5 | 3.06% | 3.33% | 2.58% | 2.56% | 2.63% | 3.46% | 3.07% |
| Medium | 6MV | 10 x 10 | 3.17% | 3.32% | 2.71% | 2.60% | 2.62% | 3.49% | 3.40% |
| Medium | 6MV | 15 x 15 | 2.98% | 3.18% | 2.47% | 2.16% | 2.29% | 3.16% | 3.09% |
| Thick | 6MV | 5 x 5 | 3.79% | 4.10% | 3.52% | 3.31% | 3.52% | 4.12% | 3.84% |
| Thick | 6MV | 10 x 10 | 3.97% | 3.97% | 3.52% | 3.35% | 3.55% | 4.14% | 3.99% |
| Thick | 6MV | 15 x 15 | 3.67% | 3.83% | 3.16% | 2.90% | 3.09% | 3.86% | 3.63% |

Table 4.9: Summary of the overestimation of the dose by Pinnacle if treatment couch is ignored for the 18 MV energy
 (The maximum overestimation is highlighted in blue and the minimum overestimation in red)

| Couch section | Energy | Field Size | Gantry Angle | | | | | | |
|---------------|--------|------------|--------------|-------|-------|-------|-------|-------|-------|
| | | | 130° | 140° | 160° | 180° | 200° | 220° | 230° |
| Thin | 18MV | 5 x 5 | 1.85% | 1.58% | 1.14% | 1.12% | 1.25% | 1.72% | 1.97% |
| Thin | 18MV | 10 x 10 | 1.77% | 1.42% | 1.09% | 1.09% | 1.18% | 1.60% | 1.96% |
| Thin | 18MV | 15 x 15 | 1.64% | 1.35% | 1.05% | 0.93% | 1.13% | 1.49% | 1.84% |
| Medium | 18MV | 5 x 5 | 1.60% | 1.85% | 1.46% | 1.43% | 1.52% | 2.00% | 1.80% |
| Medium | 18MV | 10 x 10 | 1.62% | 1.73% | 1.40% | 1.31% | 1.40% | 1.87% | 1.81% |
| Medium | 18MV | 15 x 15 | 1.58% | 1.75% | 1.36% | 1.20% | 1.32% | 1.80% | 1.77% |
| Thick | 18MV | 5 x 5 | 2.17% | 2.33% | 1.98% | 2.05% | 2.00% | 2.43% | 2.19% |
| Thick | 18MV | 10 x 10 | 2.09% | 2.12% | 1.83% | 1.83% | 1.92% | 2.29% | 2.19% |
| Thick | 18MV | 15 x 15 | 2.01% | 2.11% | 1.75% | 1.64% | 1.80% | 2.25% | 2.13% |

4.3.2 Calculated surface doses without couch

A comparison was done between the nanoDot measured results and the Pinnacle predicted dose without a scripted couch structure. All the surface doses were reported as a percentage of the dose at D_{max} for the particular beam. The overestimation or underestimation of these doses by Pinnacle were expressed as percentage differences between the Pinnacle predicted doses and the nanoDot measured doses.

Results show that Pinnacle underestimated the surface doses for both energies and for all the beams traversing the couch. For 6 MV the underestimation ranged from 36.96% to 45.27% with the highest underestimation for the gantry 180°, 20 x 20 cm field at the thick section of the

couch. For 18 MV the underestimation ranged from 32.26% to 52.97% with the highest underestimation for the gantry 230°, 10 x 10 cm field at the thick section of the couch.

Figure 4.28 and Figure 4.29 demonstrate the underestimation for the three couch sections for the beams traversing the couch which were investigated for the 6 MV and 18 MV energies, respectively.

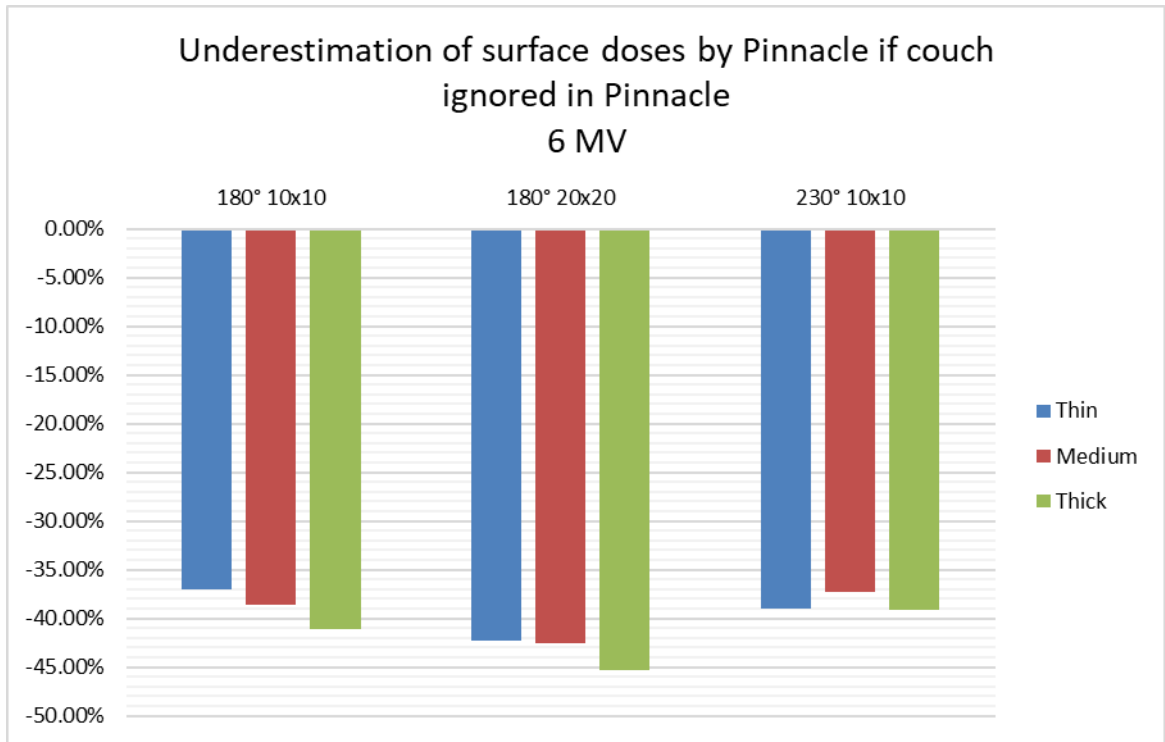


Figure 4.28: Demonstrating the degree of underestimation of the surface dose by Pinnacle treatment planning system for 6 MV if the treatment couch is ignored

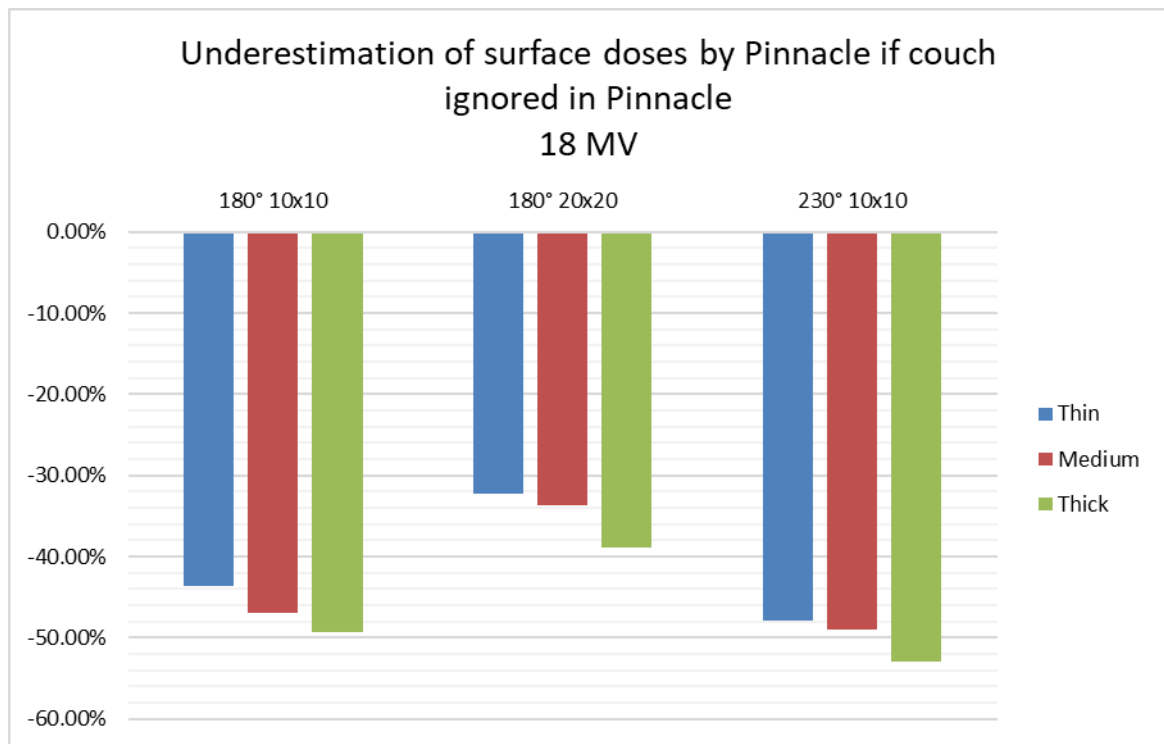


Figure 4.29: Demonstrating the degree of underestimation of the surface dose by Pinnacle treatment planning system for 18 MV if the treatment couch is ignored

4.4 Couch model

4.4.1 Ease of use

In order to run the script the user needs only four parameters. The script is run by clicking on the script in the list of scripts, and then the script calculates and creates the couch model and incorporates the model in the correct position within the plan relative to the patient images.

The speed and reproducibility of the script was tested by running it on a number of difference plans and CT scan sets, including on a CT scan set containing over 400 slices. The majority of the scan sets used for patients have fewer slices, so this was a good test of the speed at which a couch model is calculated, created and incorporated into the plan of the patient. The script process consistently needed less than five seconds to complete.

Every time the script was run with a particular set of values for the required parameters (vertical position of the couch, couch notch, longitudinal offset, and lateral offset), the couch model was positioned in exactly the same position relative to the patient images. Furthermore, the calculated doses within Pinnacle were always exactly the same for the couch model in a particular position within the plan.

4.4.2 Dimensions and shape

Objective 1 (a) for this study was to create a couch model which would be accurate in terms of the external shape and dimensions. Figure 4.30 shows a side-by-side comparison of the shape at the superior/front end of the real Varian IGRT couch and the couch model in the Pinnacle treatment planning system.

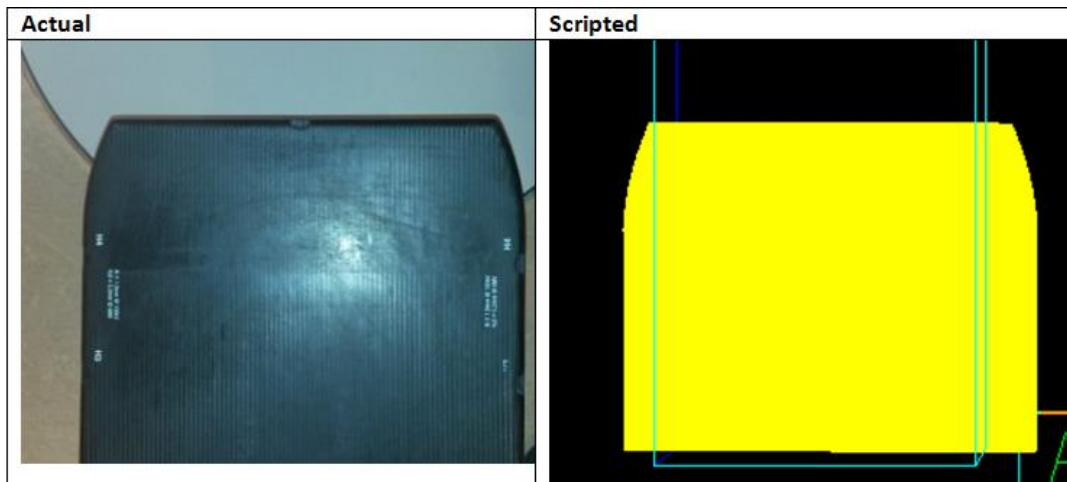


Figure 4.30: Comparing the shapes of the superior sections of the real Varian IGRT couch (on the left) and the scripted couch model in the Pinnacle treatment planning system (on the right)
(Photo and Pinnacle treatment planning system screen shot by the researcher)

A more informative test for shape and dimensions was to run the script on a CT scan of the Varian IGRT couch and see how closely it matches the outline and shape of the couch on the CT images. A scan set of the couch was acquired and imported into Pinnacle. When the Varian IGRT couch was scanned it was not perfectly level or straight along the longitudinal axis, but it did provide a good test of the couch model accuracy in terms of shape and dimensions. The real Varian IGRT couch has two round grooves underneath the couch on either side, along its length, but it was decided not to model these grooves. The couch notches were also not modelled. The Pinnacle screen shots below demonstrate how the couch model follows the outline of the couch images on the CT scan (Figure 4.31 – Figure 4.39).

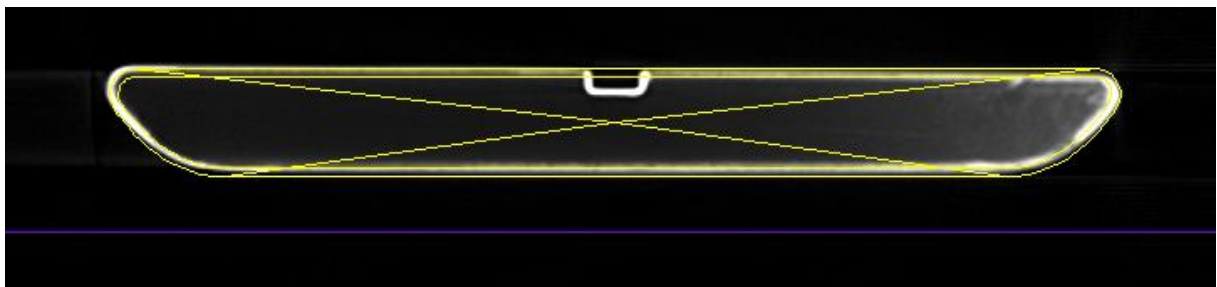


Figure 4.31: The couch model structures on the CT scan of the Varian IGRT couch at a level superior to H4 notch on superior end of couch
(Pinnacle treatment planning system screen shot by the researcher)

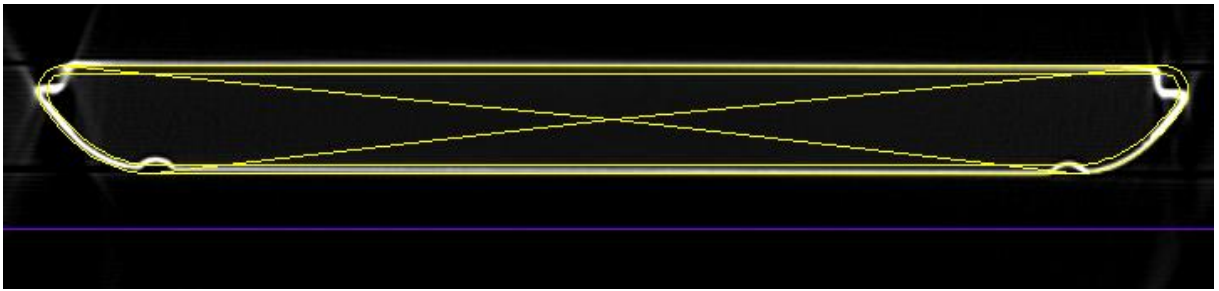


Figure 4.32: The couch model structures on the CT scan of the Varian IGRT couch on the level of the H4 notch

(Pinnacle treatment planning system screen shot by the researcher)

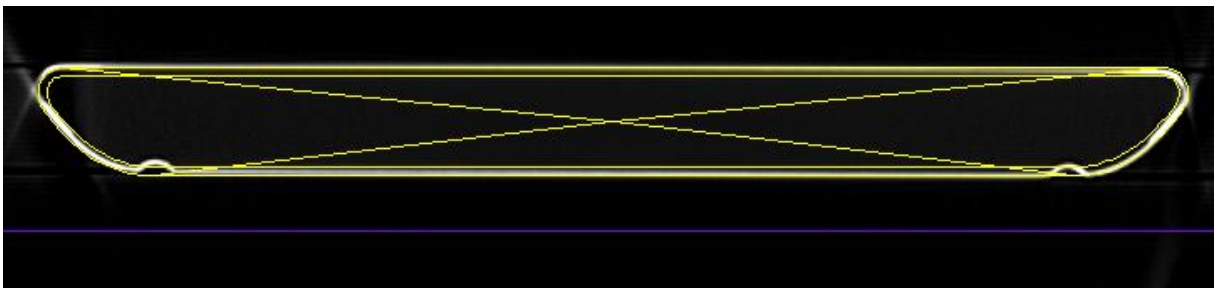


Figure 4.33: The couch model structures on the CT scan of the Varian IGRT couch at a level between the H3 and H4 notches

(Pinnacle treatment planning system screen shot by the researcher)

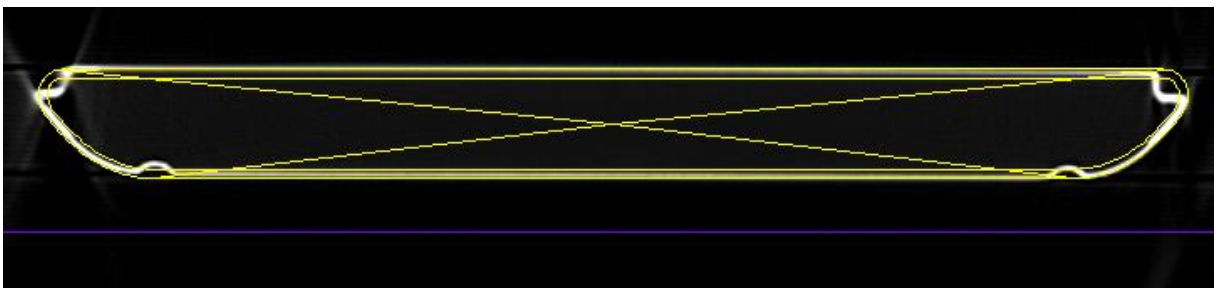


Figure 4.34: The couch model structures on the CT scan of the Varian IGRT couch on the level of the H3 notch

(Pinnacle treatment planning system screen shot by the researcher)

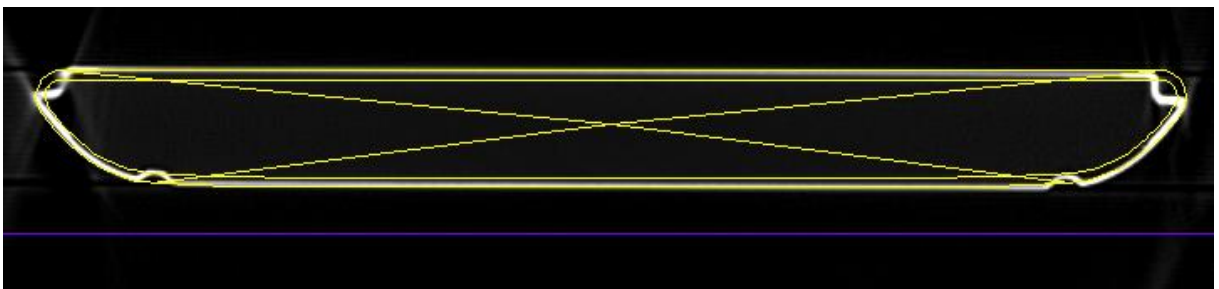


Figure 4.35: The couch model structures on the CT scan of the Varian IGRT couch on the level of the H2 notch

(Pinnacle treatment planning system screen shot by the researcher)

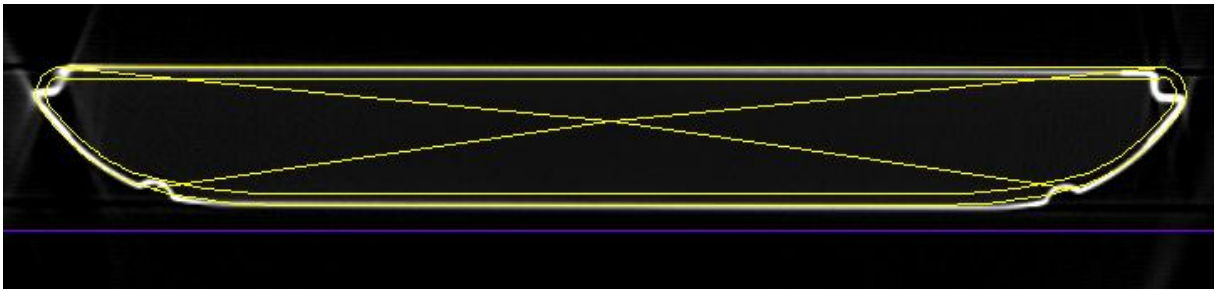


Figure 4.36: The couch model structures on the CT scan of the Varian IGRT couch on the level of the H1 notch

(Pinnacle treatment planning system screen shot by the researcher)

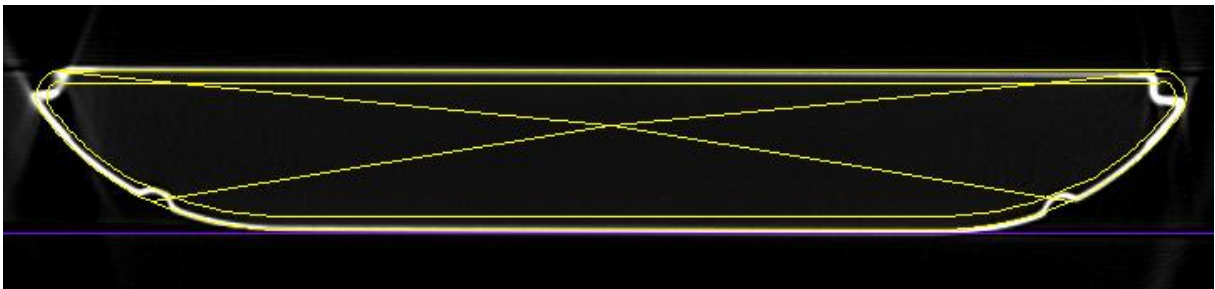


Figure 4.37: The couch model structures on the CT scan of the Varian IGRT couch on the level of the 0 notch

(Pinnacle treatment planning system screen shot by the researcher)

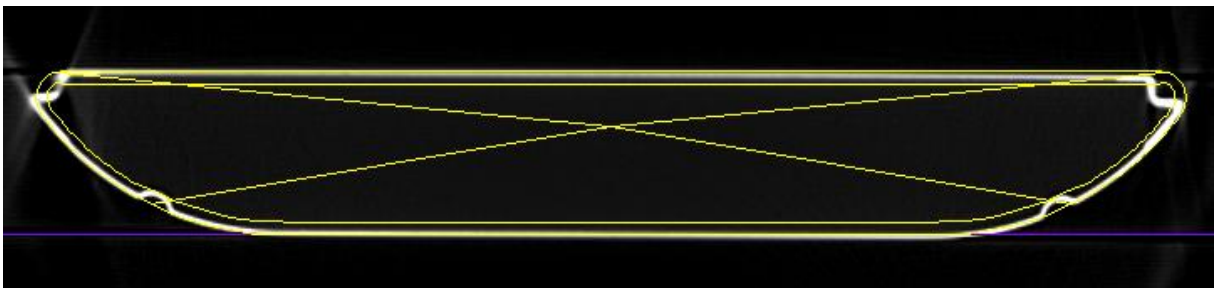


Figure 4.38: The couch model structures on the CT scan of the Varian IGRT couch on the level of the F1 notch

(Pinnacle treatment planning system screen shot by the researcher)

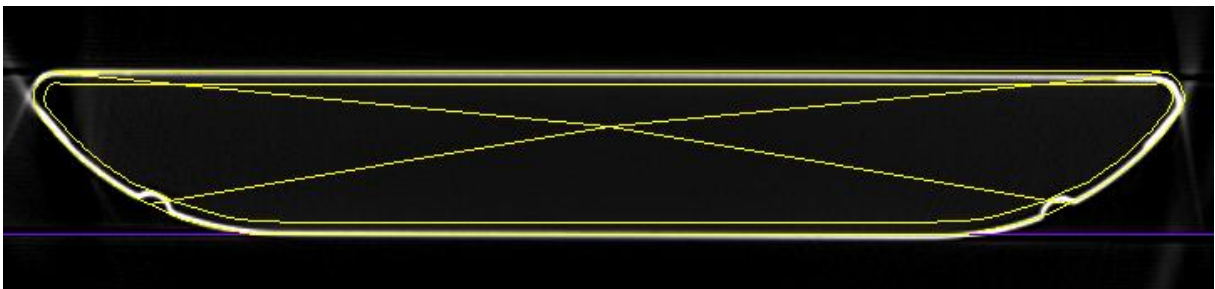


Figure 4.39: The couch model structures on the CT scan of the Varian IGRT couch between the F1 and F2 notches

(Pinnacle treatment planning system screen shot by the researcher)

4.4.3 Attenuation effects of the couch model

The initial attenuation measurements at depth were used to determine expected doses for Pinnacle. These expected doses were the doses that Pinnacle should calculate if the couch was correctly taken into consideration. The researcher named these expected doses the "Required doses". After the couch model was created and incorporated in Pinnacle, a comparison was done between the Pinnacle calculated attenuated doses and the measured attenuated doses.

The percentage differences between the Pinnacle doses and required doses for 6 MV ranged from -0.56% to 0.31%. All the dose comparisons for 6 MV are shown in Table 4.10. For 18 MV the percentage differences ranged from -0.61% to 0.01%. All the dose comparisons for 18 MV are shown in Table 4.11. In both tables the lowest and highest percentage differences have been highlighted. A comparison between the measured doses at depth and the predicted doses by Pinnacle (both with the couch, and if the couch was ignored) for a 10 x 10 cm field size at the thick section of the couch are demonstrated in Figure 4.40 and Figure 4.41 for 6 MV and 18 MV, respectively.

Table 4.10: The percentage difference between the Pinnacle calculated doses and required doses for 6 MV
 (The red highlight represents the bottom of the range and the blue highlight the upper value in the range)

| Couch section | Energy | Field Size | 130° | 140° | 160° | 180° | 200° | 220° | 230° |
|---------------|--------|------------|--------|--------|--------|--------|--------|--------|--------|
| Thin | 6MV | 5 x 5 | -0.37% | -0.40% | -0.45% | -0.29% | -0.28% | -0.23% | -0.28% |
| Thin | 6MV | 10 x 10 | -0.22% | -0.40% | -0.29% | -0.12% | -0.27% | -0.13% | 0.02% |
| Thin | 6MV | 15 x 15 | -0.18% | -0.27% | -0.26% | -0.56% | -0.28% | -0.04% | 0.01% |
| Medium | 6MV | 5 x 5 | -0.50% | -0.44% | -0.30% | -0.04% | -0.25% | -0.13% | -0.47% |
| Medium | 6MV | 10 x 10 | -0.36% | -0.40% | -0.06% | 0.20% | -0.15% | 0.03% | -0.12% |
| Medium | 6MV | 15 x 15 | -0.40% | -0.32% | -0.01% | -0.23% | -0.23% | -0.11% | -0.25% |
| Thick | 6MV | 5 x 5 | -0.48% | -0.33% | -0.20% | -0.09% | -0.21% | -0.14% | -0.38% |
| Thick | 6MV | 10 x 10 | -0.18% | -0.30% | 0.00% | 0.31% | 0.01% | 0.04% | -0.18% |
| Thick | 6MV | 15 x 15 | -0.28% | -0.18% | -0.09% | 0.00% | -0.21% | 0.05% | -0.27% |

Table 4.11: The percentage difference between the Pinnacle calculated doses and required doses for 18 MV
 (The red highlight represents the bottom of the range and the blue highlight the upper value in the range)

| Couch section | Energy | Field Size | 130° | 140° | 160° | 180° | 200° | 220° | 230° |
|---------------|--------|------------|--------|--------|--------|--------|--------|--------|--------|
| Thin | 18MV | 5 x 5 | -0.33% | -0.45% | -0.49% | -0.41% | -0.40% | -0.31% | -0.23% |
| Thin | 18MV | 10 x 10 | -0.37% | -0.49% | -0.45% | -0.37% | -0.37% | -0.29% | -0.18% |
| Thin | 18MV | 15 x 15 | -0.39% | -0.44% | -0.37% | -0.53% | -0.30% | -0.28% | -0.19% |
| Medium | 18MV | 5 x 5 | -0.61% | -0.45% | -0.35% | -0.20% | -0.30% | -0.23% | -0.39% |
| Medium | 18MV | 10 x 10 | -0.54% | -0.49% | -0.29% | -0.17% | -0.29% | -0.25% | -0.34% |
| Medium | 18MV | 15 x 15 | -0.44% | -0.34% | -0.17% | -0.25% | -0.24% | -0.20% | -0.24% |
| Thick | 18MV | 5 x 5 | -0.46% | -0.37% | -0.31% | -0.03% | -0.30% | -0.23% | -0.44% |
| Thick | 18MV | 10 x 10 | -0.45% | -0.45% | -0.29% | 0.01% | -0.21% | -0.21% | -0.37% |
| Thick | 18MV | 15 x 15 | -0.37% | -0.28% | -0.23% | -0.07% | -0.21% | -0.09% | -0.24% |

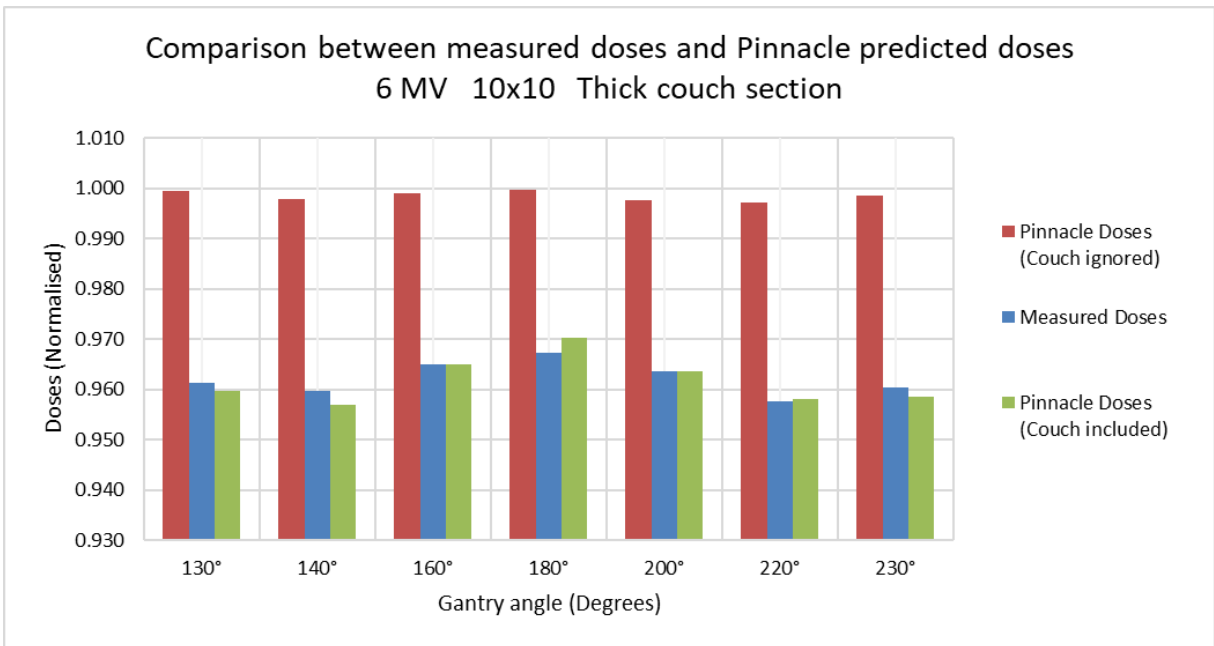


Figure 4.40: Comparison of the measured attenuated doses, and the Pinnacle predicted doses (with and without the couch) for 6 MV beams traversing the couch

This graph represents the 10 x 10 cm field size at the thick section of the couch.

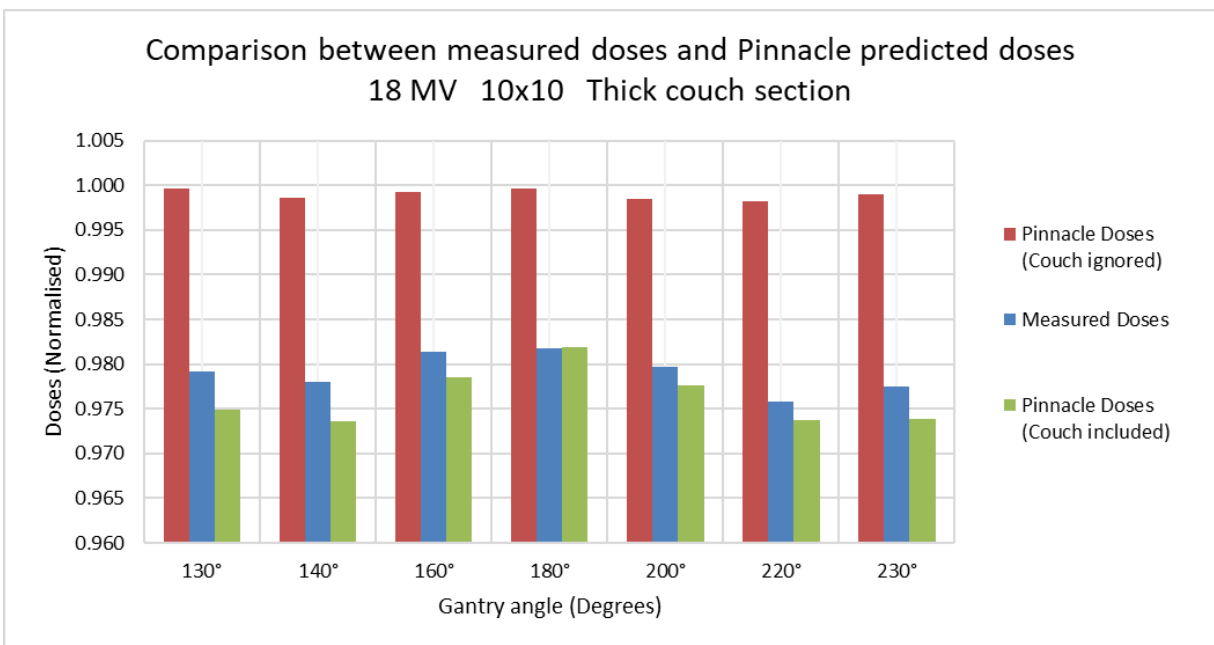


Figure 4.41: Comparison of the measured attenuated doses, and the Pinnacle predicted doses (with and without the couch) for 18 MV beams traversing the couch when the couch model incorporated

This graph represents the 10 x 10 cm field size at the thick section of the couch.

4.5 Generalisability of the couch model

In addition to the standard geometry measurements described in the previous section, additional complex geometry measurements were done to confirm generalisability of the couch

model. Doses in the complex geometry setup were calculated using either the chamber 1 or 2 as reference as detailed below.

The attenuated doses were normalised to the reference doses for the 10 x 10 cm field at gantry 0°. All these doses were measured at depth. The normalised, attenuated doses were used and the comparison was done as percentage differences between the Pinnacle doses and the measured doses.

First, looking at the doses at chamber position 1 (the most anterior position). For this analysis only dose values at the chamber position 1 were used, both for the attenuated beams and for the reference beams (Figure 4.42).

Square Phantom

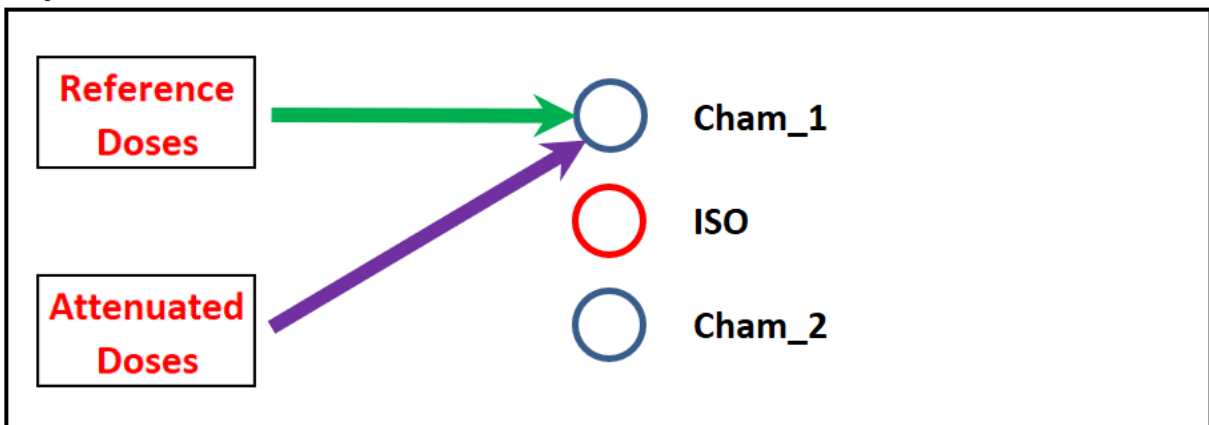


Figure 4.42: Schematic representation of the square phantom showing the dose reading position for the reference doses and the attenuated doses

(Diagram created by the researcher)

Analysing the percentage differences between the Pinnacle calculated doses and the measured doses for these verification plans it was found that for 6 MV the percentage differences ranged from -1.20% to 1.39% (Table 4.12). The percentage differences for the 18 MV beams ranged from 0.13% to 1.39% (Table 4.13).

Table 4.12: Percentage differences between Pinnacle calculated doses and measured dose for the verification plans for the 6 MV beams (measured at chamber position 1, and using reference doses at chamber position 1)
 (The red highlight indicates the bottom limit of the range and the blue highlight the top limit)

| Attenuated Beams | | | | |
|------------------|-----------------|----------------------------------|----------------------------------|-----------------------------|
| Plan | Attenuated beam | Pinnacle Attenuated dose (Norm.) | Measured Attenuated dose (Norm.) | Perc Diff. Attenuated beams |
| Plan_1_ISO | G_147_6X | 0.69 | 0.68 | 1.39% |
| Plan_2_ISO | G_160_6X | 0.71 | 0.70 | 1.17% |
| Plan_3_ISO | G_220_6X | 0.53 | 0.54 | -1.20% |
| Plan_4_ISO | G_200_6X | 0.67 | 0.66 | 0.58% |
| Plan_5_ISO | G_210_6X | 0.54 | 0.54 | 0.95% |
| Plan_6_ISO | G_225_6X | 0.62 | 0.62 | 0.55% |

Table 4.13: Percentage differences between Pinnacle calculated doses and measured dose for the verification plans for the 18 MV beams (measured at chamber position 1, and using reference doses at chamber position 1)
 (The red highlight indicates the bottom limit of the range and the blue highlight the top limit)

| Attenuated Beams | | | | |
|------------------|-----------------|----------------------------------|----------------------------------|-----------------------------|
| Plan | Attenuated beam | Pinnacle Attenuated dose (Norm.) | Measured Attenuated dose (Norm.) | Perc Diff. Attenuated beams |
| Plan_1_ISO | G_147_18X | 0.78 | 0.77 | 1.39% |
| Plan_2_ISO | G_160_18X | 0.79 | 0.78 | 0.82% |
| Plan_3_ISO | G_220_18X | 0.66 | 0.65 | 0.89% |
| Plan_4_ISO | G_200_18X | 0.76 | 0.75 | 0.42% |
| Plan_5_ISO | G_210_18X | 0.65 | 0.64 | 1.15% |
| Plan_6_ISO | G_225_18X | 0.73 | 0.73 | 0.13% |

The measurements were also done with the chamber in the chamber position 2 (the posterior position) in the phantom. These measurements were then first analysed using both the attenuated and reference doses at the chamber position 2 (Figure 4.43) and then repeated with the standard geometry readings from chamber 1 as reference (Figure 4.44).

Square Phantom

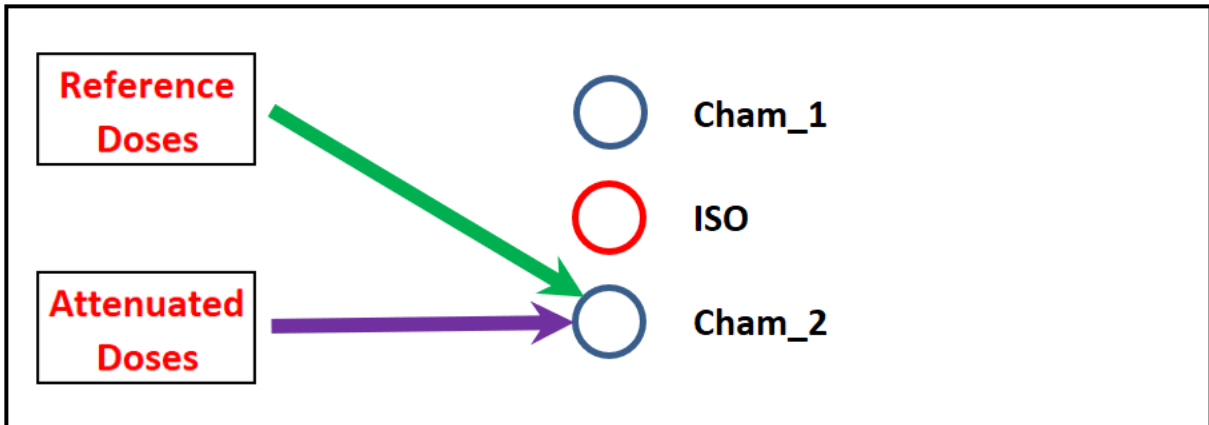


Figure 4.43: Schematic representation of the square phantom showing the dose reading position for the reference doses and the attenuated doses

(Diagram created by the researcher)

For the chamber 2 readings referenced against the chamber 2 standard geometry readings, the percentage differences between the Pinnacle calculated doses and the measured doses for these verification plans ranged from -1.25% to 1.22% for 6 MV (Table 4.14) and from -0.59% to 1.33% for 18 MV (Table 4.15).

Table 4.14: Percentage differences between Pinnacle calculated doses and measured dose for the verification plans for the 6 MV beams (measured at chamber position 2, and using reference doses at chamber position 2)

(The red highlight indicates the bottom limit of the range and the blue highlight the top limit)

| Plan | Attenuated Beams | | | |
|------------|------------------|----------------------------------|----------------------------------|-----------------------------|
| | Attenuated beam | Pinnacle Attenuated dose (Norm.) | Measured Attenuated dose (Norm.) | Perc Diff. Attenuated beams |
| Plan_1_ISO | G_147_6X | 1.23 | 1.22 | 0.47% |
| Plan_2_ISO | G_160_6X | 1.23 | 1.23 | 0.06% |
| Plan_3_ISO | G_220_6X | 0.93 | 0.95 | -1.25% |
| Plan_4_ISO | G_200_6X | 1.18 | 1.17 | 0.41% |
| Plan_5_ISO | G_210_6X | 1.08 | 1.08 | 0.17% |
| Plan_6_ISO | G_225_6X | 1.11 | 1.10 | 1.22% |

Table 4.15: Percentage differences between Pinnacle calculated doses and measured dose for the verification plans for the 18 MV beams (measured at chamber position 2, and using reference doses at chamber position 2)
 (The red highlight indicates the bottom limit of the range and the blue highlight the top limit)

| Plan | Attenuated Beams | | | |
|------------|------------------|----------------------------------|----------------------------------|-----------------------------|
| | Attenuated beam | Pinnacle Attenuated dose (Norm.) | Measured Attenuated dose (Norm.) | Perc Diff. Attenuated beams |
| Plan_1_ISO | G_147_18X | 1.18 | 1.18 | 0.05% |
| Plan_2_ISO | G_160_18X | 1.18 | 1.19 | -0.59% |
| Plan_3_ISO | G_220_18X | 0.99 | 0.98 | 0.72% |
| Plan_4_ISO | G_200_18X | 1.13 | 1.13 | 0.10% |
| Plan_5_ISO | G_210_18X | 1.07 | 1.06 | 0.82% |
| Plan_6_ISO | G_225_18X | 1.08 | 1.07 | 1.33% |

For the chamber 2 readings referenced against the chamber 1 standard geometry readings, the percentage differences between the Pinnacle calculated doses and the measured doses ranged from -2.03% to 0.50% for 6 MV (Table 4.16), and from -0.76% to 1.18% for 18 MV (Table 4.17).

Square Phantom

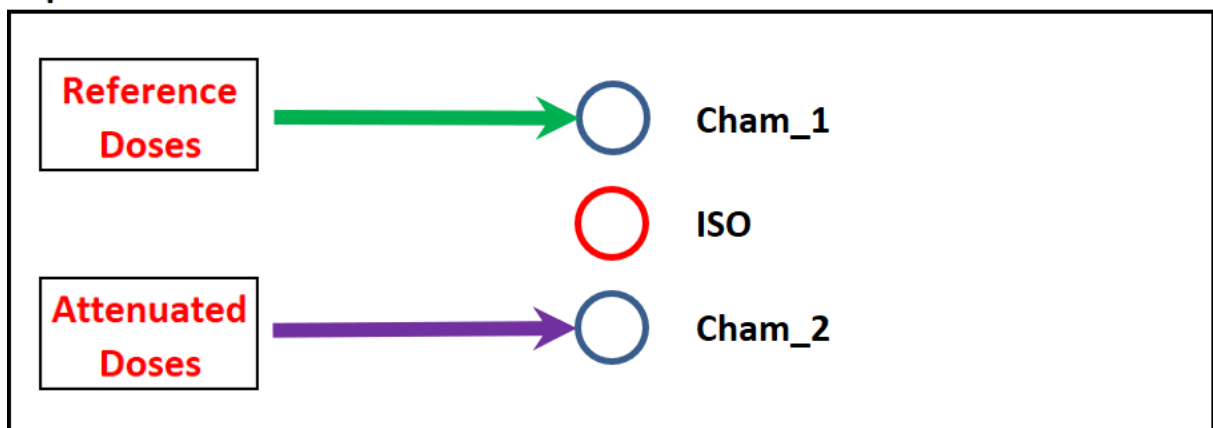


Figure 4.44: Schematic representation of the square phantom showing the dose reading position for the reference doses and the attenuated doses

(Diagram created by the researcher)

Table 4.16: Percentage differences between Pinnacle calculated doses and measured dose for the verification plans for the 6 MV beams (attenuation dose readings at chamber position 2, reference doses readings at chamber position 1)
 (The red highlight indicates the bottom limit of the range and the blue highlight the top limit)

| Plan | Attenuated Beams | | | |
|------------|------------------|----------------------------------|----------------------------------|-----------------------------|
| | Attenuated beam | Pinnacle Attenuated dose (Norm.) | Measured Attenuated dose (Norm.) | Perc Diff. Attenuated beams |
| Plan_1_ISO | G_147_6X | 0.94 | 0.94 | -0.22% |
| Plan_2_ISO | G_160_6X | 0.94 | 0.95 | -0.63% |
| Plan_3_ISO | G_220_6X | 0.71 | 0.73 | -2.03% |
| Plan_4_ISO | G_200_6X | 0.90 | 0.90 | -0.31% |
| Plan_5_ISO | G_210_6X | 0.83 | 0.83 | -0.45% |
| Plan_6_ISO | G_225_6X | 0.85 | 0.85 | 0.50% |

Table 4.17: Percentage differences between Pinnacle calculated doses and measured dose for the verification plans for the 18 MV beams (attenuation dose readings at chamber position 2, reference doses readings at chamber position 1)
 (The red highlight indicates the bottom limit of the range and the blue highlight the top limit)

| Plan | Attenuated Beams | | | |
|------------|------------------|----------------------------------|----------------------------------|-----------------------------|
| | Attenuated beam | Pinnacle Attenuated dose (Norm.) | Measured Attenuated dose (Norm.) | Perc Diff. Attenuated beams |
| Plan_1_ISO | G_147_18X | 0.97 | 0.97 | -0.15% |
| Plan_2_ISO | G_160_18X | 0.97 | 0.98 | -0.76% |
| Plan_3_ISO | G_220_18X | 0.81 | 0.81 | 0.55% |
| Plan_4_ISO | G_200_18X | 0.93 | 0.93 | 0.00% |
| Plan_5_ISO | G_210_18X | 0.88 | 0.88 | 0.63% |
| Plan_6_ISO | G_225_18X | 0.89 | 0.88 | 1.18% |

A summary of the percentage differences between the Pinnacle calculated doses and the measured doses for the generalisability/verification plans are shown in Figure 4.45 and Figure 4.46 for 6 MV and 18 MV, respectively.

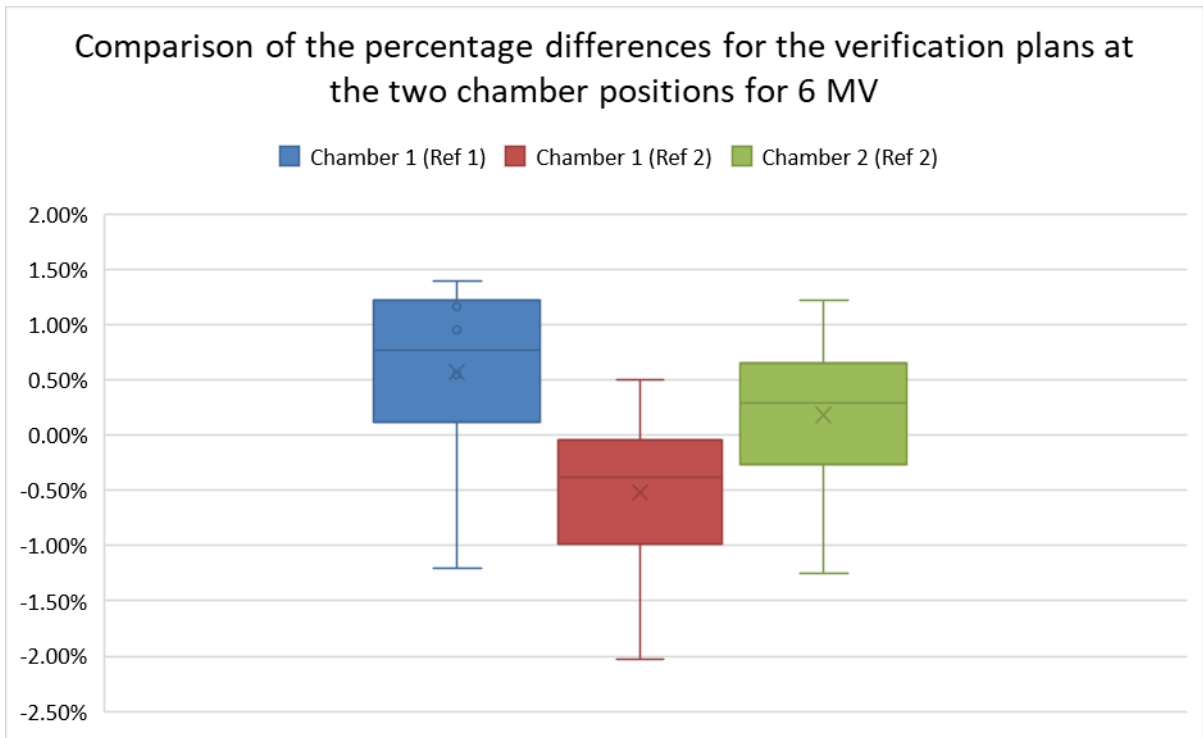


Figure 4.45: Comparison of the percentage differences between the Pinnacle calculated doses and measured doses for the 6 MV verification plans for the different chamber position analyses

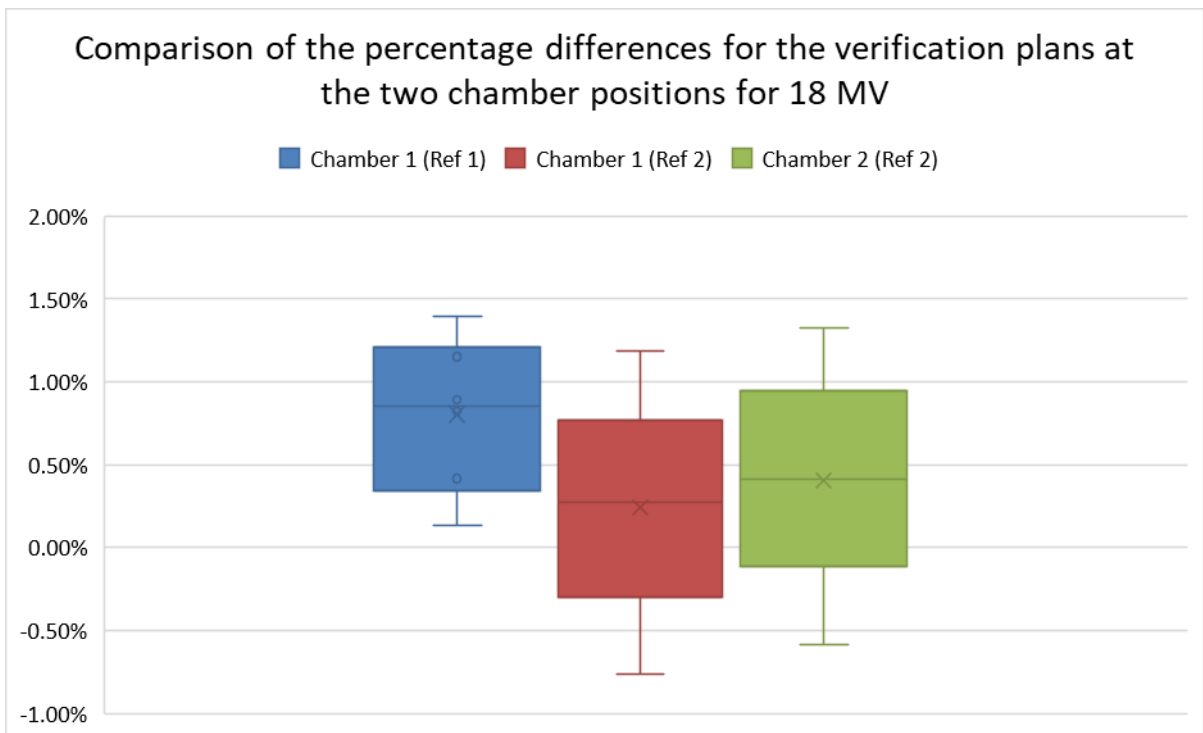


Figure 4.46: Comparison of the percentage differences between the Pinnacle calculated doses and measured doses for the 18 MV verification plans for the different chamber position analyses

4.6 Surface doses of the couch model

Only attenuation data were used in the development of the couch model and the surface dose data were not taken into account during the process, but it was still important to look at the effect of the created couch model on the prediction of the surface doses by the Pinnacle treatment planning system. The Pinnacle surface doses calculated for the beams traversing the couch were then compared with the measured nanoDot surface dose. As with the other surface dose analyses used in this research study, the beam surface doses were also expressed as percentages of the dose at D_{\max} for the particular beam.

The results for the surface dose measurements are shown in Table 4.18 and Table 4.19 for 6 MV and 18 MV, respectively.

The percentage differences were also calculated between the Pinnacle predicted surface doses and the nanoDot measured surface doses, both for if Pinnacle uses the couch model and if the couch model was ignored. The comparisons between the percentage differences with and without the couch model are illustrated in Figure 4.47, Figure 4.48 and Figure 4.49 for 6 MV for the different couch sections and in Figure 4.50, Figure 4.51 and Figure 4.52 for 18 MV.

Table 4.18: Summary of the measured surface doses and the Pinnacle predicted surface doses for the beams traversing the treatment couch for 6 MV

(The last column represents the surface doses predicted by Pinnacle if the couch is ignored)

| Energy | Couch section | Gantry | Field size | Measured Surface dose as % of beam dose @ D_{max} | Pinnacle Surface dose as % of beam dose @ D_{max} | Pinnacle Surface dose as % of beam dose @ D_{max} |
|--------|---------------|--------|------------|---|---|---|
| | | | | With Couch | With Couch | Couch Ignored |
| 6 MV | Thin | 180° | 10 x 10 | 86.45% | 82.35% | 54.50% |
| | | 180° | 20 x 20 | 93.40% | 83.94% | 53.85% |
| | | 230° | 10 x 10 | 96.66% | 92.75% | 59.02% |
| Energy | Couch section | Gantry | Field size | Measured Surface dose as % of beam dose @ D_{max} | Pinnacle Surface dose as % of beam dose @ D_{max} | Pinnacle Surface dose as % of beam dose @ D_{max} |
| | | | | With Couch | With Couch | Couch Ignored |
| 6 MV | Medium | 180° | 10 x 10 | 88.83% | 89.88% | 54.50% |
| | | 180° | 20 x 20 | 93.69% | 94.03% | 53.85% |
| | | 230° | 10 x 10 | 94.19% | 96.77% | 59.02% |
| Energy | Couch section | Gantry | Field size | Measured Surface dose as % of beam dose @ D_{max} | Pinnacle Surface dose as % of beam dose @ D_{max} | Pinnacle Surface dose as % of beam dose @ D_{max} |
| | | | | With Couch | With Couch | Couch Ignored |
| 6 MV | Thick | 180° | 10 x 10 | 92.44% | 90.19% | 54.50% |
| | | 180° | 20 x 20 | 98.39% | 90.67% | 53.85% |
| | | 230° | 10 x 10 | 96.90% | 97.32% | 59.02% |

Table 4.19: Summary of the measured surface doses and the Pinnacle predicted surface doses for the beams traversing the treatment couch for 18 MV

(The last column represents the surface doses predicted by Pinnacle if the couch is ignored)

| Energy | Couch section | Gantry | Field size | Measured Surface dose as % of beam dose @ D _{max} | Pinnacle Surface dose as % of beam dose @ D _{max} | Pinnacle Surface dose as % of beam dose @ D _{max} |
|--------|---------------|--------|------------|--|--|--|
| | | | | With Couch | With Couch | Couch Ignored |
| 18 MV | Thin | 180° | 20 x 20 | 60.53% | 60.08% | 34.14% |
| | | 180° | 10 x 10 | 75.18% | 73.67% | 50.92% |
| | | 230° | 0.00% | 74.30% | 74.92% | 38.73% |
| Energy | Couch section | Gantry | Field size | Measured Surface dose as % of beam dose @ D _{max} | Pinnacle Surface dose as % of beam dose @ D _{max} | Pinnacle Surface dose as % of beam dose @ D _{max} |
| | | | | With Couch | With Couch | Couch Ignored |
| 18 MV | Medium | 180° | 10 x 10 | 64.34% | 67.32% | 34.14% |
| | | 180° | 20 x 20 | 76.74% | 82.92% | 50.92% |
| | | 230° | 10 x 10 | 75.91% | 81.10% | 38.73% |
| Energy | Couch section | Gantry | Field size | Measured Surface dose as % of beam dose @ D _{max} | Pinnacle Surface dose as % of beam dose @ D _{max} | Pinnacle Surface dose as % of beam dose @ D _{max} |
| | | | | With Couch | With Couch | Couch Ignored |
| 18 MV | Thick | 180° | 10 x 10 | 67.38% | 66.94% | 34.14% |
| | | 180° | 20 x 20 | 83.45% | 78.03% | 50.92% |
| | | 230° | 10 x 10 | 82.35% | 81.82% | 38.73% |

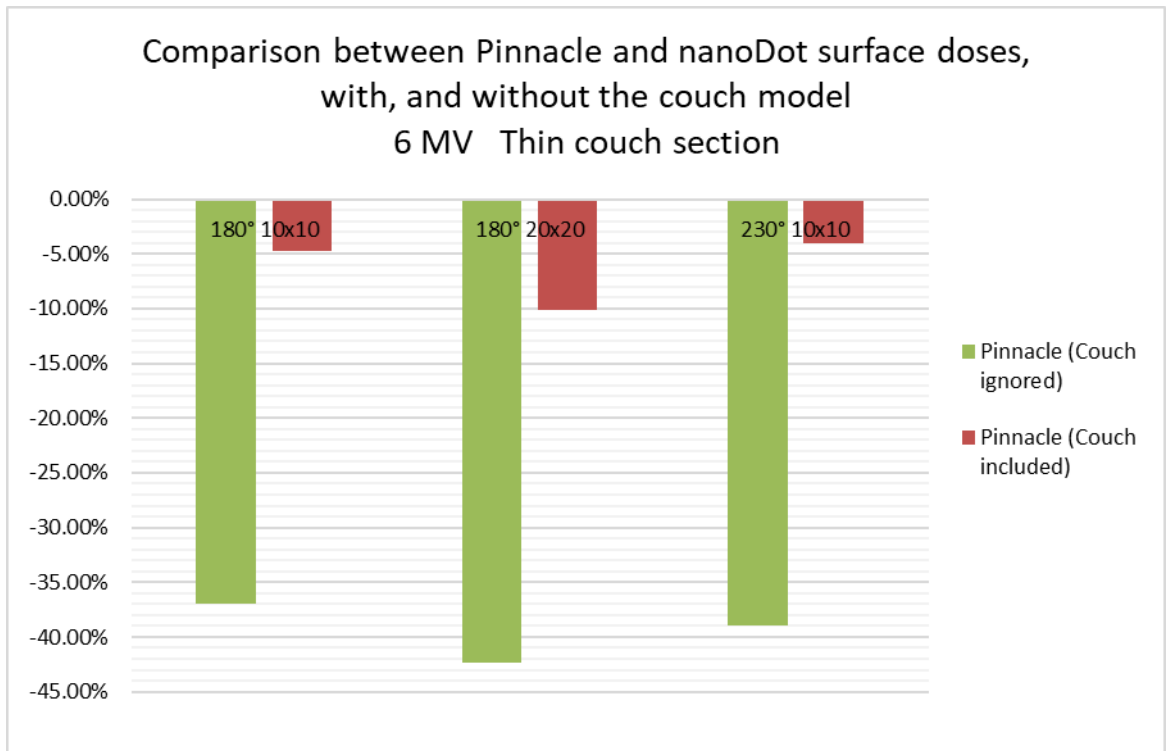


Figure 4.47: Comparing the percentage differences between the Pinnacle predicted surface doses and the nanoDot surface doses, with, and without the couch model for 6 MV through the thin section of the couch

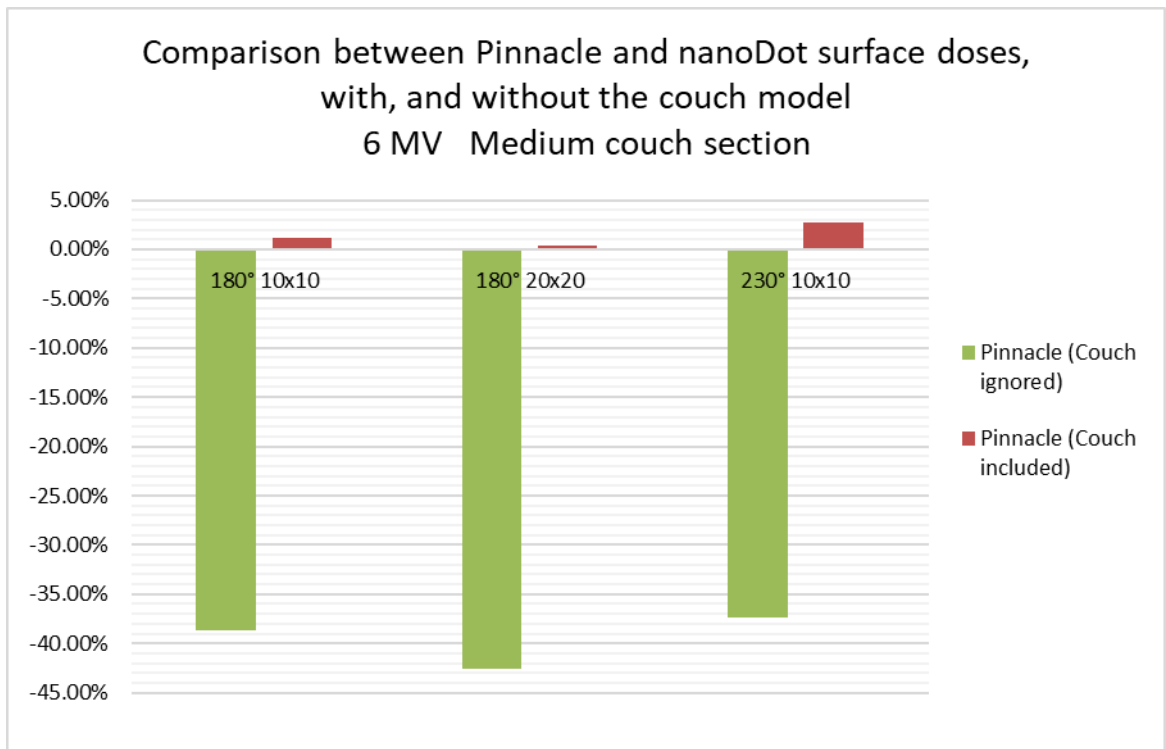


Figure 4.48: Comparing the percentage differences between the Pinnacle predicted surface doses and the nanoDot surface doses, with, and without the couch model for 6 MV through the medium section of the couch

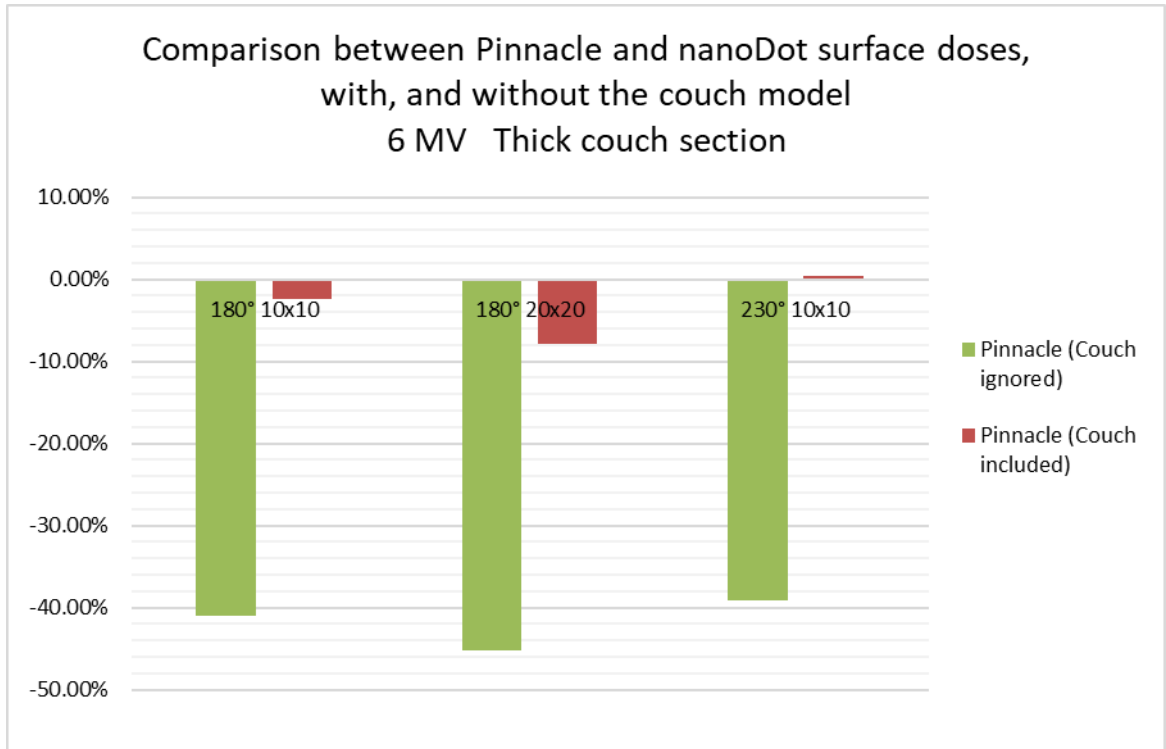


Figure 4.49: Comparing the percentage differences between the Pinnacle predicted surface doses and the nanoDot surface doses, with, and without the couch model for 6 MV through the thick section of the couch

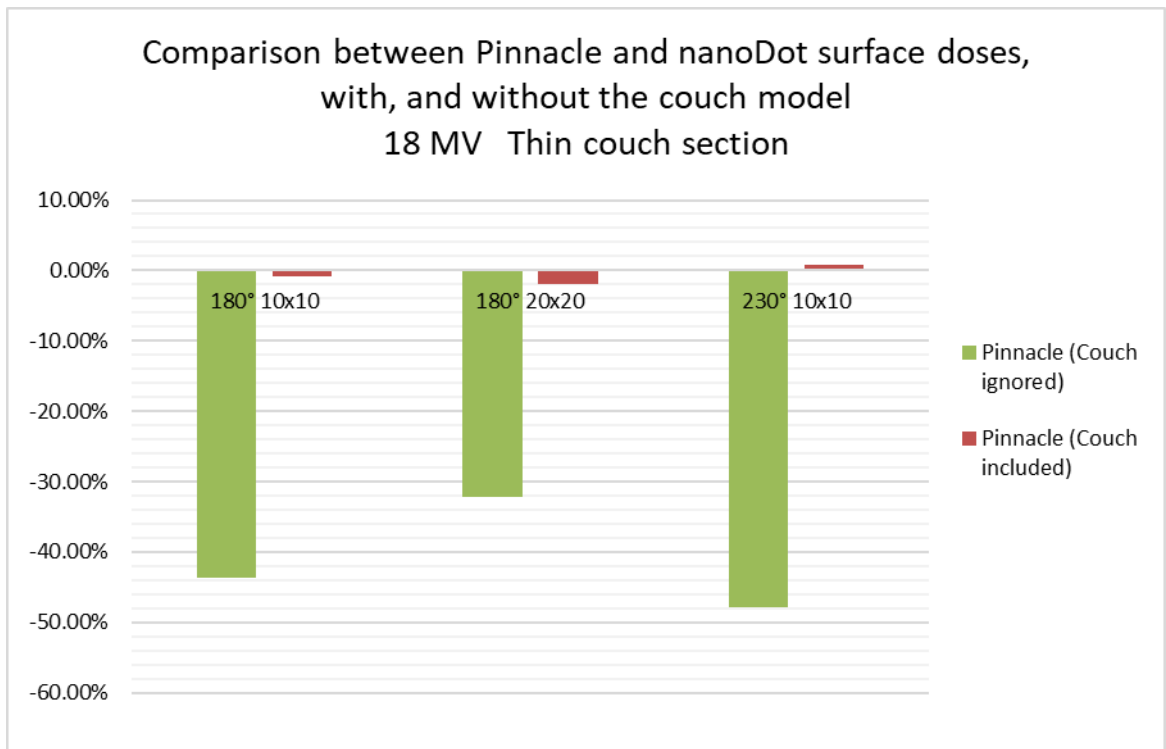


Figure 4.50: Comparing the percentage differences between the Pinnacle predicted surface doses and the nanoDot surface doses, with, and without the couch model for 18 MV through the thin section of the couch

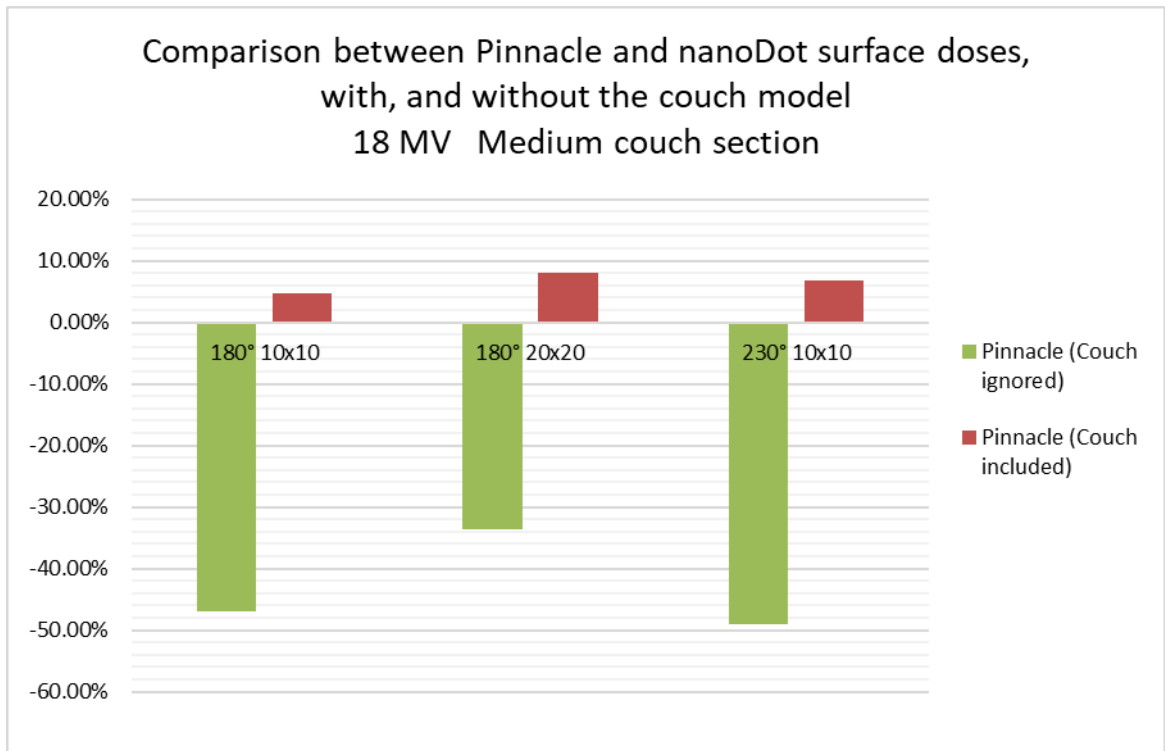


Figure 4.51: Comparing the percentage differences between the Pinnacle predicted surface doses and the nanoDot surface doses, with, and without the couch model for 18 MV through the medium section of the couch

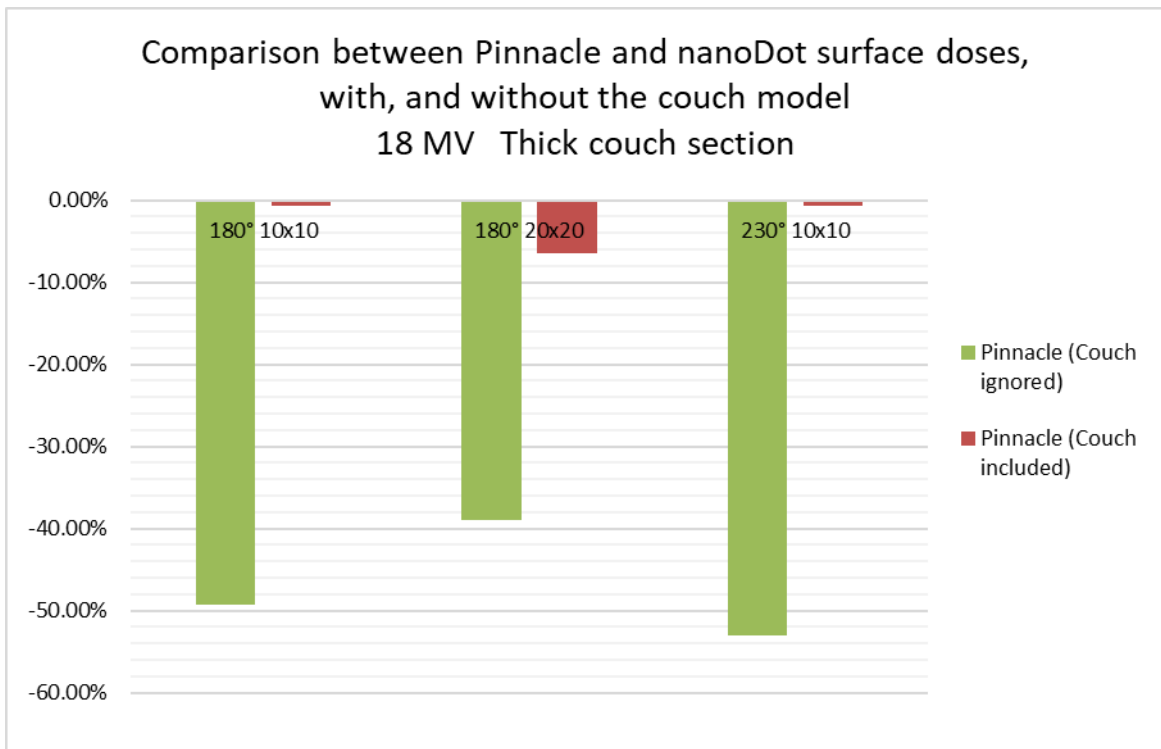


Figure 4.52: Comparing the percentage differences between the Pinnacle predicted surface doses and the nanoDot surface doses, with, and without the couch model for 18 MV through the thick section of the couch

4.7 Conclusion

This chapter reported the relevant data from the research study. The next chapter will discuss these results and findings in answer to the research question and sub-questions (hypotheses) posed by the researcher.

CHAPTER FIVE: DISCUSSION AND CONCLUSION

5.1 Introduction

This chapter summarises and review the findings of the research study. For ease of reference the research question and hypotheses are stated here again.

Can the accuracy of the dose calculation on the Pinnacle treatment planning system be improved for beams that are directed through the treatment couch by introducing an algorithm that models the effect of the couch?

Hypothesis 1: The use of an algorithm that incorporates the dimensions and properties of the treatment couch will improve the accuracy of dose determination at depth, compared to no couch structure included during the planning process.

Hypothesis 2: The angle of beam delivery through the couch affects the dose correction required at depth.

Hypothesis 3: The energy of the beam affects the dose correction required at depth.

Hypothesis 4: The use of an algorithm that incorporates the dimensions and properties of the treatment couch will improve the accuracy of the predicted skin dose in the presence of a treatment couch.

5.2 Actual treatment couch

5.2.1 Attenuation effect of the couch

In order to determine the accuracy of prediction of dose at depth, the impact of the couch on attenuation was investigated for various scenarios.

The pattern of attenuation observed in this study was similar to that found in literature. The beam energy, field size, gantry angle, and couch section all had an impact on the extent of the attenuation of the beam by the couch. Thus:

- For a particular energy, field size, and couch section combination the extent of the attenuation generally increased slightly with increasing incident angle. This was also seen in studies done by McCormack et al. (2005), Poppe et al. (2007). However, a change in this pattern is observed at 130° and 230° degrees where a slight decrease

in attenuation is observed. This is discussed in more detail in the following paragraph below.

- For a particular energy, gantry angle and couch section the extent of the attenuation decreased with increasing field size. This is similar to what was seen by Myint et al. (2006).
- For a particular gantry angle, field size, and couch section the extent of the attenuation decreased with increasing beam energy. This was also described by Myint et al. (2006), and Poppe et al. (2007).
- For a particular energy, gantry angle and field size the extent of the attenuation increased as the thickness of the couch section increased.

The maximum attenuation produced by the treatment couch was 4.3%. This was for the 6 MV energy for 5 x 5 cm field size through the thick section of the couch at gantry angle 220°. Overall, the attenuation for 6 MV due to the treatment couch ranged from 1.9% to 4.3%. The maximum attenuation as a result of the treatment couch for 18 MV was 2.6%. This was also found for the 5 x 5 cm field size at the thick section of the couch and gantry angle of 220°. The attenuation for 18 MV ranged from 1.0% to 2.6%. It can also be seen that for all the plans the maximum amount of attenuation was at the steeper gantry angles, at 230° for the thin section of the couch and at 220° for the rest of the couch. The lowest degree of attenuation was measured for the 0° incident angles to the couch with gantry angle 180°. The maximum attenuation at 180° was 3.4%. This was found for the 6 MV energy for 5 x 5 cm field size through the thick section of the couch

As mentioned above, an anomaly was observed in terms of the change in attenuation relating to change in gantry angle for the medium and thick sections of the couch. It was noted in the measurements that the attenuation decreased slightly at the gantry angles 130° and 230° compared to 140° and 220°, respectively. This may be as a result of the change in geometry in the couch at these angles, both in terms of the couch inner as well as the couch shell (Figure 5.1). This may impact on the pathlength and effective pathlength. As the change is not significant (< 0.5%) it was not investigated further.

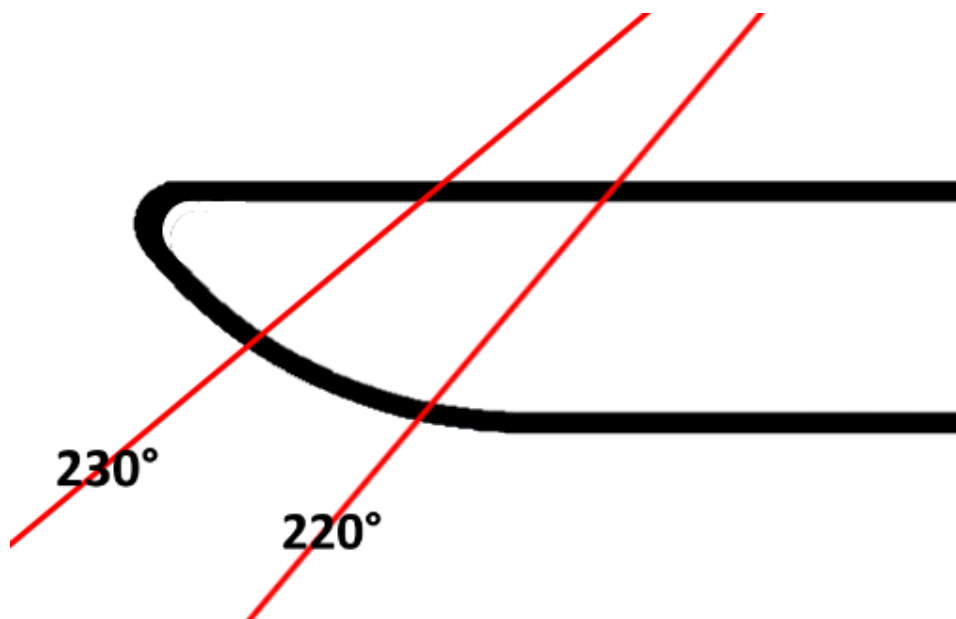


Figure 5.1: Cross-section of thick section of treatment couch showing the paths the centres of the beams at 220° and 230° will travel through skin of couch

(Figure created by the researcher)

5.2.2 Mirror angle differences

As discussed in section 4.2.2 the measurements at the mirror angles of 120° and 240° showed a larger difference in the results compared to other mirror angles. Analysis of the beam geometry showed that this was as a result of the field only partially including the couch edge at these angles, with a very small lateral change in setup resulting in a large change in the attenuation (Figure 5.2). As these specific angles were not critical to the study they were excluded from the analysis.

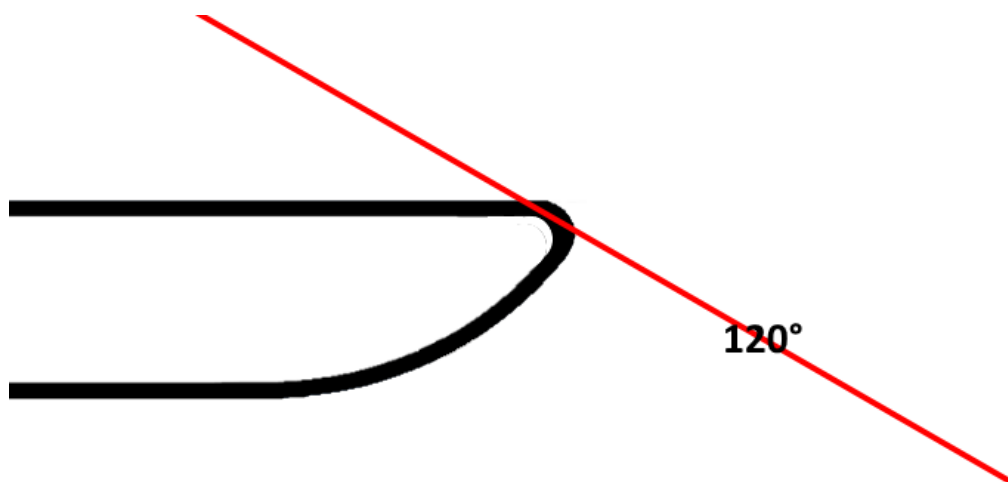


Figure 5.2: Cross-section of thick section of treatment couch showing the paths the centres of the beams at 120° might travel through skin of the couch

(Figure created by the researcher)

5.2.3 Surface dose effect of the couch

The nanoDot dosimeters were found to be user friendly, with the only drawback being the delay in obtaining results. The immediate readout on electrometer and ionisation chamber readouts allows for direct response to setup errors or other concerns. However, with nanoDots the results were delayed due to shipping and remote readout.

All the surface doses were analysed as a percentage of the dose at D_{max} for that particular beam. The results that were obtained are listed below.

- Surface doses decrease with an increase in energy (6MV vs. 18 MV).
- For a given gantry angle and couch section combination, the surface dose increases with an increase in field size (10 x 10 cm to 20 x 20 cm).
- For a given energy and couch section combination, the surface dose increases from gantry 180° (90° incident angle to the couch) to gantry 230° (50° incident angle).
- For a given field size, gantry angle and energy combination, surface dose increases systematically from the thin to the medium and thick sections of the couch. An anomaly was noted for 6 MV (10 x 10 cm field size) at 230° where a lower surface dose was noted for the medium couch section (Figure 4.20). As all the available nanoDots were used during the research study, this measurement could not be repeated and should be investigated further in future.

All these findings were similar to those found by other researchers in their studies with regard to the general factors affecting the surface dose.

Furthermore, it was seen that for the open beams (gantry 0°) there was a large difference in the predicted surface doses for Pinnacle compared to the measured surface doses. The predicted surface doses as a percentage of the beam doses at D_{max} for the gantry 0° beams seemed to be what can be expected from Pinnacle on the surface when looking at the PDD data used by Pinnacle. The surface doses as percentage of D_{max} doses for 6 MV were 55.62% and 57.26% for 10 x 10 and 20 x 20, respectively, and for 18 MV they were 35.50% and 52.35% for 10 x 10 and 20 x 20, respectively. The depth of the calculation points for the surface dose measurements in Pinnacle were at 2 mm to allow for Pinnacle to have a meaningful calculation depth. Assessing the surface dose results from Pinnacle they were found to be similar to what might be expected from Pinnacle for the depth range 0.0 to 0.2 cm when one considers the Pinnacle PDD data for those depths (Table 4.7).

Considering the differences between the measured surface doses and Pinnacle surface doses for the open beams the assumption is made that the nanoDot readings are probably correct, and that Pinnacle overestimates the surface doses in the surface and build-up region. This

overestimation in Pinnacle can be due primarily to the difficulty of measuring the build-up region doses. When doing the dose measurements to create the PDD data, the closer to the surface of the water the ionisation chamber is positioned, the more the chamber will be outside the water, with a resultant loss of accuracy.

It was mentioned in the previous chapter that the results found in this research study with regard to 6 MV, 10 x 10 cm, the PDD data are similar to that found by Apipunyasopon et al. (2013). The results found in that study were in line with the 55.62% and 36.19% found in this study for the Pinnacle and nanoDot, respectively, for 6 MV and 10 x 10 (Figure 4.25).

The Pinnacle seems more accurate in determining the surface doses for the beams traversing the couch, because for these beams once penetrating the couch structure the dose calculation starts; and the beam is already in a calculation data area when it reaches the dose point for the surface dose.

5.3 Pinnacle predicted doses without a couch structure

5.3.1 Calculated attenuation effect without couch

When comparing the attenuation measurements of the actual Varian IGRT treatment couch with the doses that the Pinnacle treatment planning system calculates where it does not consider the effect of the treatment couch, it was shown that Pinnacle TPS overestimates the doses in the absence of the couch structure.

These overestimations were greater for 6 MV than for 18 MV. It was also seen that for each energy the overestimation increased as the thickness of the couch increased. The maximum overestimation, due to the fact that the couch structure was not taken into account, was 4.14%. As this is higher than the 3% dosimetric accuracy level required on the treatment planning system (as specified and described in the aims for the research study), it confirms the need for a couch structure to be incorporated into the Pinnacle TPS.

5.3.2 Calculated surface doses without couch

These analyses were done to determine if the Pinnacle treatment planning system over- or under-estimates the surface doses when the effect of the treatment couch is ignored. The surface doses were all reported as a percentage of the beam dose at D_{max} .

The results have pointed out that Pinnacle does underestimate the surface doses for both beam energies, and for all the beam configurations and geometries which were measured for beams traversing the couch. For 6 MV the highest underestimation was 45.27% (here the

Pinnacle predicted surface dose was 53.85% and measured surface dose 98.39%). For 18 MV the highest underestimation was 52.97% where the Pinnacle predicted surface dose was 38.73% and measured surface dose 82.35%. This means that for some situations the surface dose to the patient potentially could be double the surface dose that Pinnacle predicts if the surface dose effect of the treatment couch is ignored. If clinical decisions rely on the calculated surface doses from Pinnacle, then careful consideration is required before deciding to ignore the surface dose effect of the treatment couch.

5.4 Couch model

5.4.1 Ease of use

The script was designed to be easy and quick to use. The user requires only a few parameters, as mentioned in section 3.9.6 where how to use the script was described. At the study site the CT Scanner couch has markings with the same labels and at the same levels as the couch notches on the Varian IGRT couch. When the patient is scanned the reference laser level of the patient can then easily be noted down, and when the script is run this couch level and the longitudinal and the lateral offsets can be entered into the Pinnacle script information screen. It was also seen that the script is fast and efficient, for example for a patient with more than 400 CT slices it required less than five seconds to complete the process and display the couch in the correct position relative to the patient. If a mistake is made with some of the input parameters, the script can be run again with the correct parameters.

5.4.2 Dimensions and shape

The important objective of the study was to create a couch model which would have the same dimensions and shape as the real Varian IGRT couch. This is important because often accurate measurements are required from the treatment plans, for example SSD measurements. The couch structure on the plan is also sometimes used as a visual cue to see if there might be risk of collisions between the gantry and couch, and this is especially important for non-coplanar treatments. If the couch model is not accurate in terms of shape and dimensions, then the measurements and visual cues cannot be relied upon.

It was shown that the couch model created by the script in this study is accurate, both in shape and dimensions. This was demonstrated, both with a side-by-side view (Figure 4.30), as well as superimposing the couch model on a CT scan of the Varian IGRT couch by running the script on that CT scan set.

5.4.3 Attenuation effects of the couch model

In the absence of a couch structure deviations of up to 4.1% were noted between the predicted and the actual doses at depth. For 6 MV the percentage differences ranged from 1.85% to 4.14%. For 18 MV the percentage differences ranged from 0.93% to 2.43%. Pinnacle over-estimated the doses for all the attenuated beams for both energies, as is shown in Table 4.8 and Table 4.9 for 6 MV and 18 MV, respectively.

After the couch model was implemented, it improved the predicted doses on simple geometries on the Pinnacle treatment planning system for all the attenuated beams for both energies. With the couch model algorithm applied, the percentage differences ranged from -0.56% to 0.31% for 6 MV, and from -0.61% to 0.01% for 18 MV.

It was noted that there is an asymmetry in the results between the two edges of the couch model. This could be as a result of the method in which the couch model was created by calculating the contour in one direction only. Future studies can investigate modelling the couch in both a clockwise and counter-clockwise direction and then using the average.

5.5 Generalisability of the couch model

An analysis of the impact of the couch script on more complex geometries was investigated. Six plans were created for the 6 MV and 18 MV energies, respectively, and these plans incorporated the various parameters which are often seen in patient plans, including different dynamic wedges, and an MLC-shaped field. These verification plans also covered the different couch sections. The doses were measured at both dosimeter positions in the phantom, and the analyses of the dose values were done using different combinations of these dosimeter positions, as mentioned in section 4.5.

The purpose of these plans was to look at the generalisability of the couch model; in other words, to assess whether its usefulness extends beyond the beam arrangements and parameters which were used for the initial attenuation measurements. When examining the results for the percentage differences between Pinnacle predicted doses and the measured doses, it was found that the maximum percentage difference was 2.03%, which is below the required accuracy level of 3%, as specified in the aims for the research study.

5.6 Surface doses of the couch model

Although surface dose data were not included in the parameters used for the creation of the initial couch structure, the impact of the final couch structure on these doses was investigated.

The results have shown that, for all beams traversing the couch, the couch model improved the Pinnacle treatment planning system predicted surface doses compared to scenarios where no couch structure is considered. When the treatment couch is ignored in Pinnacle, the Pinnacle surface doses ranged from -45.27% to -36.96% for 6 MV, and for 18 MV from -52.97% to -32.26%. When the couch model is used, this ranged from -10.13% to 2.73% for 6 MV, and from -6.49% to 8.04% for 18 MV. As a reminder, the negative values represent an underestimation of the surface dose by Pinnacle and the positive values an overestimation. This means that the couch model improved the predicted surface doses to within $\pm 10\%$ of the surface dose to the patient, compared to an underestimation of almost 50% for 6 MV, and an underestimation of more than 50% for 18 MV when the couch is not considered by the treatment planning system.

There was an uncertainty in the possible accuracy of the nanoDot readings due to the limited number of nanoDot dosimeters available and for future studies the nanoDot measurements should be repeated with more nanoDot dosimeters per sampling point in order to decrease this uncertainty in the accuracy.

5.7 Conclusion

This research study investigated the creation and evaluation of a couch model of the Varian IGRT treatment couch top for the Pinnacle treatment planning system.

The initial steps were to evaluate the actual Varian IGRT couch to determine its impact on the attenuation of the radiation dose at depth, as well as its impact on the surface dose. It has been shown that the couch has an effect on the attenuation of the radiation dose at depth. The maximum attenuation of the dose was 4.3% for 6 MV, and 2.6% for 18 MV. It was also shown that various factors affect the amount of attenuation produced by the couch. The extent of the attenuation generally increased with increasing incident angle, decreased with increasing field size, decreased with increasing beam energy, and increased as the thickness of the couch section increased. The couch also had an impact on the surface dose. All surface doses were reported as a percentage of the dose at D_{\max} for that particular beam. The surface dose results have shown that the extent of the surface dose as a result of the treatment couch generally decreased as the beam energy increased, increased as field size increased, and increased as incident angle increased. These findings were all in agreement with what were found in literature.

The couch model was created, and it has the functionality to be incorporated and positioned accurately for each patient plan in the Pinnacle treatment planning system via a script. A single

script was created, and it creates the full Varian IGRT treatment couch top with all three couch sections. The dimensions and shape of the resultant couch model are accurate and were confirmed against a CT scan of the actual couch. The radiological properties of the couch model were also verified using verification plans to confirm the generalisability of the couch model. It was found that the couch model improved the accuracy of the Pinnacle predicted doses at depth to within 2.03% of the measured doses. The aim of the research study was to improve the accuracy of the Pinnacle predicted doses to within 3%.

The couch model can be used by any department using the Pinnacle treatment planning system, with the only caveat that every department needs to verify the couch model against their own measurements before using the couch model for clinical applications.

Overall, all the required criteria of this research study were met in terms of the research question, aims and objectives.

This aim of this study was to develop an algorithm which would accurately incorporate a couch model of the Varian IGRT couch in the Pinnacle treatment planning system in order for the predicted doses calculated by the treatment planning system to reflect the real-life doses when the treatment is ultimately delivered. The couch model was evaluated by using static beam therapy and measuring the doses in phantoms. Future research can be done to determine the effectiveness of the couch model for more dynamic techniques, for example IMRT and Arc therapies. Studies can also be done to determine the effect of the Varian IGRT couch on the actual plan quality by using real patients, as suggested by Pulliam et al. (2011). In addition, the effectiveness and generalisability of the couch model created in this study can then be tested using real patient plans.

REFERENCES

- Abshire, D. & Lang, M. K. 2018. The Evolution of Radiation Therapy in Treating Cancer. *Semin Oncol Nurs*, 34: 151-157.
- Ahnesjo, A. & Aspradakis, M. M. 1999. Dose calculations for external photon beams in radiotherapy. *Phys Med Biol*, 44: R99-155.
- Akbas, U., Kesen, N. D., Koksall, C. A. & Bilge, H. 2016. Surface and Buildup Region Dose Measurements with Markus Parallel-Plate Ionization Chamber, GafChromic EBT3 Film, and MOSFET Detector for High-Energy Photon Beams. *Advances in High Energy Physics*, 2016.
- American Cancer Society 2016. The Science Behind Radiation Therapy. American Cancer Society.
- Apipunyasopon, L., Srisatit, S. & Phaisangittisakul, N. 2013. An investigation of the depth dose in the build-up region, and surface dose for a 6-MV therapeutic photon beam: Monte Carlo simulation and measurements. *J Radiat Res*, 54: 374-82.
- Aslam, A., Kakakhel, M. B., Shahid, S. A., Younas, L. & Zareen, S. 2016. Soft tissue and water substitutes for megavoltage photon beams: An EGSnrc-based evaluation. *J Appl Clin Med Phys*, 17: 408-415.
- Bandi, P., Zsoter, N., Seres, L., Toth, Z. & Papp, L. 2011. Automated patient couch removal algorithm on CT images. *Conf Proc IEEE Eng Med Biol Soc*, 2011: 7783-6.
- Barrett, A., Dobbs, J., Morris, S. & Roques, T. 2009. *Practical Radiotherapy Planning*, London, Hodder Arnold.
- Bedford, J. L., Childs, P. J., Nordmark Hansen, V., Mosleh-Shirazi, M. A., Verhaegen, F. & Warrington, A. P. 2003. Commissioning and quality assurance of the Pinnacle(3) radiotherapy treatment planning system for external beam photons. *Br J Radiol*, 76: 163-76.
- Bolderston, A., Lloyd, N. S., Wong, R. K., Holden, L., Robb-Blenderman, L. & Supportive Care Guidelines Group of Cancer Care Ontario Program in Evidence-Based, C. 2006. The prevention and management of acute skin reactions related to radiation therapy: a systematic review and practice guideline. *Support Care Cancer*, 14: 802-17.
- Botha, J. J. 2019. Radiotherapy Simulation.
- Bray, F., Ferlay, J., Soerjomataram, I., Siegel, R. L., Torre, L. A. & Jemal, A. 2018. Global cancer statistics 2018: GLOBOCAN estimates of incidence and mortality worldwide for 36 cancers in 185 countries. *CA Cancer J Clin*, 68: 394-424.
- Butson, M. J., Cheung, T. & Yu, P. K. 2007. Megavoltage x-ray skin dose variation with an angle using grid carbon fibre couch tops. *Phys Med Biol*, 52: N485-92.
- Butson, M. J., Cheung, T., Yu, P. K. & Webb, B. 2002. Variations in skin dose associated with linac bed material at 6 MV x-ray energy. *Phys Med Biol*, 47: N25-30.
- Butson, M. J., Yu, P. K. & Metcalfe, P. E. 1998. Measurement of off-axis and peripheral skin dose using radiochromic film. *Phys Med Biol*, 43: 2647-50.
- Buzdar, S. A., Afzal, M., Nazir, A. & Gadhi, M. A. 2013. Accuracy requirements in radiotherapy treatment planning. *J Coll Physicians Surg Pak*, 23: 418-23.

- Carl, J. & Vestergaard, A. 2000. Skin damage probabilities using fixation materials in high-energy photon beams. *Radiother Oncol*, 55: 191-8.
- Chan, M. F., Chiu-Tsao, S. T., Li, J., Schupak, K., Parhar, P. & Burman, C. 2012. Confirmation of skin doses resulting from bolus effect of intervening alpha-cradle and carbon fiber couch in radiotherapy. *Technol Cancer Res Treat*, 11: 571-81.
- Cherry, P. & Duxbury, A. 2009. *Practical Radiotherapy Physics and Equipment*, Blackwell Publishing Ltd.
- Childs, P. J. & Bidmead, M. 2012. 10 Principles and practice of radiation treatment planning. In: SYMONDS, P., DEEHAN, C., MEREDITH, C. & MILLS, J. (eds.) *Walter and Miller's Textbook of Radiotherapy*. Seventh ed.: Churchill Livingstone Elsevier.
- Chopra, K. L., Leo, P., Kabat, C., Rai, D. V., Avadhani, J. S., Kehwar, T. S. & Sethi, A. 2018. Evaluation of dose calculation accuracy of treatment planning systems in the presence of tissue heterogeneities. *Therapeutic Radiology and Oncology*, 2.
- Chung, H., Jin, H., Dempsey, J. F., Liu, C., Palta, J., Suh, T. S. & Kim, S. 2005. Evaluation of surface and build-up region dose for intensity-modulated radiation therapy in head and neck cancer. *Med Phys*, 32: 2682-9.
- Chyou, T. Y. & Lorenz, F. 2017. Couch modelling for volumetric modulated arc therapy (VMAT). *Australas Phys Eng Sci Med*, 40: 471-480.
- Collins, A. 2018. Assessment and management of radiotherapy-induced skin reactions. *Wounds UK*, 14: 64-70.
- Court, L., Urribarri, J. & Makrigiorgos, M. 2010. Letters to the Editor: Carbon fiber couches and skin sparing. *J Appl Clin Med Phys*, 11: 3241.
- De Mooy, L. 1991. The use of carbon fibres in radiotherapy. *Radiother Oncol*, 22: 140-142.
- De Ost, B., Vanregemorter, J., Schaeken, B. & Van Den Weyngaert, D. 1997. The effect of carbon fibre inserts on the build-up and attenuation of high energy photon beams. *Radiother Oncol*, 45: 275-7.
- Delaney, G., Jacob, S., Featherstone, C. & Barton, M. 2005. The role of radiotherapy in cancer treatment: estimating optimal utilization from a review of evidence-based clinical guidelines. *Cancer*, 104: 1129-37.
- Devic, S., Seuntjens, J., Abdel-Rahman, W., Evans, M., Olivares, M., Podgorsak, E. B., Vuong, T. & Soares, C. G. 2006. Accurate skin dose measurements using radiochromic film in clinical applications. *Med Phys*, 33: 1116-24.
- Evans, E. & Staffurth, J. 2017. Principles of cancer treatment by radiotherapy. *Surgery (Oxford)*, 36: 111-116.
- Eyadeh, M. M., Wierzbicki, M. & Diamond, K. R. 2017. Measurement of skin surface dose distributions in radiation therapy using poly(vinyl alcohol) cryogel dosimeters. *J Appl Clin Med Phys*, 18: 153-162.
- Fiandra, C., Ricardi, U., Ragona, R., Anglesio, S., Giglioli, F. R., Calamia, E. & Lucio, F. 2006. Clinical use of EBT model Gafchromic™ film in radiotherapy. *Med. Phys.*, 33: 4314-4319.

- Foo, J. & Stensmyr, R. 2013. Depth dose comparison of measured and calculated dose for the Eclipse virtual carbon couch top models with air gap variation. *Australas Phys Eng Sci Med*, 36: 457-63.
- Fraass, B., Doppke, K., Hunt, M., Kutcher, G., Starkschall, G., Stern, R. & Van Dyke, J. 1998. American Association of Physicists in Medicine Radiation Therapy Committee Task Group 53: quality assurance for clinical radiotherapy treatment planning. *Med Phys*, 25: 1773-829.
- Geoghegan, S. 2007. *Scripting on the Pinnacle³ Treatment Planning System*.
- Gerig, L. H., Niedbala, M. & Nyiri, B. J. 2010. Dose perturbations by two carbon fiber treatment couches and the ability of a commercial treatment planning system to predict these effects. *Med Phys*, 37: 322-8.
- Gianfaldoni, S., Gianfaldoni, R., Wollina, U., Lotti, J., Tchernev, G. & Lotti, T. 2017. An Overview on Radiotherapy: From Its History to Its Current Applications in Dermatology. *Open Access Maced J Med Sci*, 5: 521-525.
- Glover, D. & Harmer, V. 2014. Radiotherapy-induced skin reactions: assessment and management. *Br J Nurs*, 23: S28, S30-5.
- Gopan, O., Zeng, J., Novak, A., Nyflot, M. & Ford, E. 2016. The effectiveness of pretreatment physics plan review for detecting errors in radiation therapy. *Med Phys*, 43: 5181.
- Gursoy, G., Eser, E., Yigitoglu, I., Koç, H., Kahraman, F. C. & Yamcicier, S. 2018. Investigation of the effects of a carbon-fiber tabletop on the surface dose and attenuation dose for megavoltage photon beams. *International Journal of Radiation Research*, 16: 235-241.
- Harris, R., Probst, H., Beardmore, C., James, S., Dumbleton, C., Bolderston, A., Faithfull, S., Wells, M. & Southgate, E. 2012. Radiotherapy skin care: A survey of practice in the UK. *Radiography*, 18: 21-27.
- Hawley, L. 2013. Principles of radiotherapy. *Br J Hosp Med (Lond)*, 74: C166-9.
- Hayashi, N., Obata, Y., Uchiyama, Y., Mori, Y., Hashizume, C. & Kobayashi, T. 2009. Assessment of spatial uncertainties in the radiotherapy process with the Novalis system. *Int J Radiat Oncol Biol Phys*, 75: 549-57.
- Hayashi, N., Shibamoto, Y., Obata, Y., Kimura, T., Nakazawa, H., Hagiwara, M., Hashizume, C. I., Mori, Y. & Kobayashi, T. 2010. Megavoltage photon beam attenuation by carbon fiber couch tops and its prediction using correction factors. *J Radiat Res*, 51: 455-63.
- Hoppe, B. S., Laser, B., Kowalski, A. V., Fontenla, S. C., Pena-Greenberg, E., Yorke, E. D., Lovelock, D. M., Hunt, M. A. & Rosenzweig, K. E. 2008. Acute skin toxicity following stereotactic body radiation therapy for stage I non-small-cell lung cancer: who's at risk? *Int J Radiat Oncol Biol Phys*, 72: 1283-6.
- Hu, Z., Dai, J., Li, L., Cao, Y. & Fu, G. 2011. Evaluating and modeling of photon beam attenuation by a standard treatment couch. *J Appl Clin Med Phys*, 12: 3561.
- Hussain, A. & Muhammad, W. 2017. *An Introduction to Medical Physics, Biological and Medical Physics, Biomedical Engineering*, Springer International Publishing.

- Jafar, M. M., Reeves, J., Ruthven, M. A., Dean, C. J., Macdougall, N. D., Tucker, A. T. & Miquel, M. E. 2016. Assessment of a carbon fibre MRI flatbed insert for radiotherapy treatment planning. *Br J Radiol*, 89: 20160108.
- Khan, F. M. 2011. *Khan's Lectures Handbook of the Physics of Radiation Therapy*, Baltimore, Lippincott Williams & Wilkens.
- Kinhikar, R. A., Murthy, V., Goel, V., Tambe, C. M., Dhote, D. S. & Deshpande, D. D. 2009. Skin dose measurements using MOSFET and TLD for head and neck patients treated with tomotherapy *Applied Radiation and Isotopes*, 67: 1683-1685.
- Kirithi Koushik, A. S., Harish, K. & Avinash, H. U. 2013. Principles of radiation oncology: a beams eye view for a surgeon. *Indian J Surg Oncol*, 4: 255-62.
- Kunz, G., Hasenbalg, P. & Pемler, P. 2010. Absorption measurements for a carbon fiber couch top and its modelling in a treatment planning system. *Conference Paper*.
- Langmack, K. A. 2012. The use of an advanced composite material as an alternative to carbon fibre in radiotherapy. *Radiography*, 18: 74-77.
- Leventhal, J. & Young, M. R. 2017. Radiation Dermatitis: Recognition, Prevention, and Management. *Oncology (Williston Park)*, 31: 885-7, 894-9.
- Li, H., Lee, A. K., Johnson, J. L., Zhu, R. X. & Kudchadker, R. J. 2011. Characterization of dose impact on IMRT and VMAT from couch attenuation for two Varian couches. *J Appl Clin Med Phys*, 12: 3471.
- Malicki, J. 2012. The importance of accurate treatment planning, delivery, and dose verification. *Rep Pract Oncol Radiother*, 17: 63-5.
- Mani, K. R., Bhuiyan, M. A., Hossain, M. I., Rahman, M. S. & Islam, M. S. M. A. 2017. Determination of Beam Quality of High Energy Photons in Non-Standard Reference Condition Using Linear Fit Method. *Nuclear Science and Applications*, 26: 17-21.
- Mccormack, S., Diffey, J. & Morgan, A. 2005. The effect of gantry angle on megavoltage photon beam attenuation by a carbon fiber couch insert. *Med Phys*, 32: 483-7.
- Meara, S. J. & Langmack, K. A. 1998. An investigation into the use of carbon fibre for megavoltage radiotherapy applications. *Phys Med Biol*, 43: 1359-66.
- Mellenberg, D. E. 1995. Dose behind various immobilization and beam-modifying devices. *Int J Radiat Oncol Biol Phys*, 32: 1193-7.
- Meydanci, T. P. & Kemikler, G. 2008. Effect of a carbon fiber tabletop on the surface dose and attenuation for high-energy photon beams. *Radiat Med*, 26: 539-44.
- Meyer, J., Mills, J. A., Haas, O. C., Burnham, K. J. & Parvin, E. M. 2001. Accommodation of couch constraints for coplanar intensity modulated radiation therapy. *Radiother Oncol*, 61: 23-32.
- Mihaylov, I. B., Bzdusek, K. & Kaus, M. 2011. Carbon fiber couch effects on skin dose for volumetric modulated arcs. *Med Phys*, 38: 2419-23.
- Mihaylov, I. B., Corry, P., Yan, Y., Ratanatharathorn, V. & Moros, E. G. 2008. Modeling of carbon fiber couch attenuation properties with a commercial treatment planning system. *Med Phys*, 35: 4982-8.

- Mihaylov, I. B., Penagaricano, J. & Moros, E. G. 2009. Quantification of the skin sparing effect achievable with high-energy photon beams when carbon fiber tables are used. *Radiother Oncol*, 93: 147-52.
- Mills, J. A. 2012. 10 Quality control. In: SYMONDS, P., DEEHAN, C., MEREDITH, C. & MILLS, J. (eds.) *Walter and Miller's Textbook of Radiotherapy*. Seventh ed.: Churchill Livingstone Elsevier.
- Morgan, K. 2014. Radiotherapy-induced skin reactions: prevention and cure. *Br J Nurs*, 23: S24, S26-32.
- Munjal, R. K., Negi, P. S., Babu, A. G., Sinha, S. N., Anand, A. K. & Kataria, T. 2006. Impact of 6MV photon beam attenuation by carbon fiber couch and immobilization devices in IMRT planning and dose delivery. *J Med Phys*, 31: 67-71.
- Myint, W. K., Niedbala, M., Wilkins, D. & Gerig, L. H. 2006. Investigating treatment dose error due to beam attenuation by a carbon fiber tabletop. *J Appl Clin Med Phys*, 7: 21-7.
- Njeh, C. F., Parker, J., Spurgin, J. & Rhoe, E. 2012. A validation of carbon fiber imaging couch top modeling in two radiation therapy treatment planning systems: Philips Pinnacle3 and BrainLAB iPlan RT Dose. *Radiat Oncol*, 7: 190.
- Njeh, C. F., Raines, T. W. & Saunders, M. W. 2009. Determination of the photon beam attenuation by the Brainlab imaging couch: angular and field size dependence. *J Appl Clin Med Phys*, 10: 2979.
- Nystrom, H. & Thwaites, D. I. 2008. Physics and high-technology advances in radiotherapy: are they still worth it? *Radiother Oncol*, 86: 1-3.
- Olch, A. J., Gerig, L., Li, H., Mihaylov, I. & Morgan, A. 2014. Dosimetric effects caused by couch tops and immobilization devices: report of AAPM Task Group 176. *Med Phys*, 41: 061501.
- Opoku, S., Hanson, J., Yarney, J. & Tagoe, S. 2012. Variations in Couch Transmission Factors' with Treatment Depths in Isocentric Technique at the National Radiotherapy Center, Korle-Bu Teaching Hospital, Accra. Ghana. *Science Journal of Medicine and Clinical Trials*, 2012.
- Owadally, W. & Staffurth, J. 2015. Principles of cancer treatment by radiotherapy. *Surgery (Oxford)*, 33: 127-130.
- Philips Medical Systems 2013a. Classic Pinnacle³ Planning: Instructions for use. Release 9.8 ed. United States of America: Philips Medical Systems.
- Philips Medical Systems 2013b. Pinnacle³ Physics Reference Guide. Release 9.8 ed. United States of America: Philips Medical Systems.
- Podgorsak, E. B. 2005. *Radiation Oncology Physics: A Handbook for Teachers and Students*, Vienna, International Atomic Energy Agency.
- Poppe, B., Chofer, N., Ruhmann, A., Kunth, W., Djouguela, A., Kollhoff, R. & Willborn, K. C. 2007. The effect of a carbon-fiber couch on the depth-dose curves and transmission properties for megavoltage photon beams. *Strahlenther Onkol*, 183: 43-8.
- Pulliam, K. B., Howell, R. M., Followill, D., Luo, D., White, R. A. & Kry, S. F. 2011. The clinical impact of the couch top and rails on IMRT and arc therapy. *Phys Med Biol*, 56: 7435-47.

- Riis, B. 2007. Tisch.Script.bj.
- Rijken, J., Kairn, T., Crowe, S., Munoz, L. & Trapp, J. 2018. A simple method to account for skin dose enhancement during treatment planning of VMAT treatments of patients in contact with immobilization equipment. *J Appl Clin Med Phys*, 19: 239-245.
- Savini, A., Bartolucci, F., Fidanza, C., Rosica, F. & Orlandi, G. 2016. Modeling of couch transmission in the RayStation treatment planning system. *Phys Med*, 32: 735-40.
- Sedaghatian, T., Momennezhad, M., Rasta, S. H., Makhdoomi, Y. & Abdollahian, S. 2017. An Update of Couch Effect on the Attenuation of Megavoltage Radiotherapy Beam and the Variation of Absorbed Dose in the Build-up Region. *J Biomed Phys Eng*, 7: 279-288.
- Seite, S., Bensadoun, R. J. & Mazer, J. M. 2017. Prevention and treatment of acute and chronic radiodermatitis. *Breast Cancer (Dove Med Press)*, 9: 551-557.
- Seppala, J. K. & Kulmala, J. A. 2011. Increased beam attenuation and surface dose by different couch inserts of treatment tables used in megavoltage radiotherapy. *J Appl Clin Med Phys*, 12: 3554.
- Sheykhoo, A., Abdollahi, S., Hadizadeh Yazdi, M. H., Ghorbani, M. & Mohammadi, M. 2017. Effects of Siemens TT-D carbon fiber table top on beam attenuation, and build up region of 6 MV photon beam. *Rep Pract Oncol Radiother*, 22: 19-28.
- Spezi, E., Angelini, A. L., Romani, F., Guido, A., Bunkheila, F., Ntreta, M. & Ferri, A. 2008. Evaluating the influence of the Siemens IGRT carbon fibre tabletop in head and neck IMRT. *Radiother Oncol*, 89: 114-22.
- Tamura, M., Monzen, H., Matsumoto, K., Okumura, M., Doi, H. & Nishimura, Y. 2018. Reduction of Potential Risk for Skin Toxicity in Megavoltage Radiotherapy Using a Novel Rigid Couch. *In Vivo*, 32: 531-536.
- The Royal College of Radiologists, Society and College of Radiographers, Institute of Physics and Engineering in Medicine, National Patient Safety Agency & British Institute of Radiology 2008. *Towards Safer Radiotherapy*, London, The Royal College of Radiologists.
- Tugrul, T. 2018. Absorption ratio of treatment couch and effect on surface and build-up region doses. *Rep Pract Oncol Radiother*, 23: 1-5.
- Van Prooijen, M., Kanesalingam, T., Islam, M. K. & Heaton, R. K. 2010. Assessment and management of radiotherapy beam intersections with the treatment couch. *J Appl Clin Med Phys*, 11: 3171.
- Vanetti, E., Nicolini, G., Clivio, A., Fogliata, A. & Cozzi, L. 2009. The impact of treatment couch modelling on RapidArc. *Phys Med Biol*, 54: N157-66.
- Venselaar, J., Welleweerd, H. & Mijnheer, B. 2001. Tolerances for the accuracy of photon beam dose calculations of treatment planning systems. *Radiother Oncol*, 60: 191-201.
- Vieira, S. C., Kaatee, R. S., Dirkx, M. L. & Heijmen, B. J. 2003. Two-dimensional measurement of photon beam attenuation by the treatment couch and immobilization devices using an electronic portal imaging device. *Med Phys*, 30: 2981-7.

- Wagner, D. & Vorwerk, H. 2011. Treatment Couch Modeling in the Treatment Planning System Eclipse. *Journal of Cancer Science & Therapy*, 3: 007-012.
- Wiernik, G. 1961. A new radiotherapy couch. *Br Med J*, 2: 824-5.
- World Health Organisation 2017. World health statistics 2017: monitoring health for the SDGs, Sustainable Development Goals.
- Yu, C. Y., Chou, W. T., Liao, Y. J., Lee, J. H., Liang, J. A. & Hsu, S. M. 2017. Impact of radiation attenuation by a carbon fiber couch on patient dose verification. *Sci Rep*, 7: 43336.
- Zeman, E. M., Schreiber, E. C. & Tepper, J. E. 2013. Basics of Radiation Therapy. *Abeloff's Clinical Oncology*.
- Zhang, R., Gao, Y. & Bai, W. 2017. Quantification and comparison the dosimetric impact of two treatment couch model in VMAT. *J Appl Clin Med Phys*: 1-7.

APPENDICES

APPENDIX A: SASQART LINEAR ACCELERATORS

Link to SASQART Medical Linear Accelerator document:

https://drive.google.com/file/d/0B5d_I5LIOhwTNE9QV0s0UHVyU28/view?ts=5bfad15

APPENDIX B: SASQART DOSIMETERS

Link to SASQART DOSIMETRY document:

https://drive.google.com/file/d/0B5d_I5LIOhwTRV8zeGF1RHNyaW8/view?ts=5fbfaf8c

APPENDIX C: SASQART TREATMENT PLANNING SYSTEMS

Link to SASQART Treatment Planning Systems document:

https://drive.google.com/file/d/0B5d_I5LIOhwTcGRnMzhSZ0xHN2c/view?ts=5fbfb111

APPENDIX D: VARIAN EXACT IGRT COUCH SPECIFICATIONS

[See Separate document]

APPENDIX E: DOSIMETERS

Appendix E1: PinPoint Chambers

[See Separate document]

Appendix E2: Farmer Chambers

[See Separate document]

Appendix E3: nanoDot Dosimeters

Link to Landauer nanoDot Dosimeter document:

<https://www.landauer.com/sites/default/files/product-specification-file/50749%20NanoDot%20FDA.pdf>

APPENDIX F: PINNACLE SCRIPT FILES

Appendix F1: Couch_Varian_IGRT_v_3_8.Script

[See Separate document]

Appendix F2: SliceCaptureZ.Script

[See Separate document]

APPENDIX G: PYTHON SCRIPT FILE

[See Separate document]

APPENDIX H: COUCH BASE COORDINATES

[See Separate document]

APPENDIX I: COUCH SKIN THICKNESSES

[See Separate document]

APPENDIX J: ETHICS APPROVALS

Appendix J1: Ethics Approval (Cape Peninsula University of Technology)



HEALTH AND WELLNESS SCIENCES RESEARCH ETHICS COMMITTEE (HWS-REC)
Registration Number NHREC: REC- 230408-014

P.O. Box 1906 • Bellville 7535 South Africa
Symphony Road Bellville 7535
Tel: +27 21 959 6917
Email: sethn@cput.ac.za

13 March 2020
REC Approval Reference No:
CPUT/HW-REC 2018/H7 (renewal)

Faculty of Health and Wellness Sciences – Medical Imaging and Therapeutic Sciences

Dear Mr Jacobus Johannes Botha,

Re: APPLICATION TO THE HWS-REC FOR ETHICS RENEWAL

Approval was granted by the Health and Wellness Sciences-REC to Mr Botha for ethical clearance on 29 March 2018. This approval is for research activities related to student research in the Department of Medical Imaging and Therapeutic Sciences at this institution.

TITLE: The evaluation of an algorithmic model, created for the image guided radiotherapy (IGRT) treatment couch for integration into the Pinnacle Treatment Planning System (TPS)

Supervisors: Ms BD Wyrley-Birch and Ms H Burger

Comment:

Approval will not extend beyond 7 May 2021. An extension should be applied for 6 weeks before this expiry date should data collection and use/analysis of data, information and/or samples for this study continue beyond this date.

The investigator(s) should understand the ethical conditions under which they are authorized to carry out this study and they should be compliant to these conditions. It is required that the investigator(s) complete an **annual progress report** that should be submitted to the HWS-REC in December of that particular year, for the HWS-REC to be kept informed of the progress and of any problems you may have encountered.

Kind Regards,

A handwritten signature in black ink that reads "M. le Roes-Hill".

Dr Marilize Le Roes-Hill
Deputy Chairperson – Research Ethics Committee
Faculty of Health and Wellness Sciences

HEALTH AND WELLNESS SCIENCES RESEARCH ETHICS COMMITTEE (HW-REC)
Registration Number NHREC: REC- 230408-014

P.O. Box 1906 • Bellville 7535 South Africa
Symphony Road Bellville 7535
Tel: +27 21 959 6917
Email: sethn@cput.ac.za

6 May 2019
REC Approval Reference No:
CPUT/HW-REC 2018/H7

Dear Mr Jacobus Johannes Botha

Re: APPLICATION TO THE HW-REC FOR ETHICS CLEARANCE

Approval was granted by the Health and Wellness Sciences-REC to Mr Botha for ethical clearance on 29 March 2018. This approval is for research activities related to student research in the Department of Medical Imaging and Therapeutic Sciences at this Institution.

TITLE: The evaluation of an algorithmic model, created for the image guided radiotherapy (IGRT) treatment couch for integration into the Pinnacle Treatment Planning System (TPS)

Supervisor: Ms B Wyrley-Bierch and Ms H Burger

Comment:

Approval will not extend beyond 7 May 2020. An extension should be applied for 6 weeks before this expiry date should data collection and use/analysis of data, information and/or samples for this study continue beyond this date.

The investigator(s) should understand the ethical conditions under which they are authorized to carry out this study and they should be compliant to these conditions. It is required that the investigator(s) complete an annual progress report that should be submitted to the HWS-REC in December of that particular year, for the HWS-REC to be kept informed of the progress and of any problems you may have encountered.

Kind Regards



Dr. Navindhra Naidoo
Chairperson – Research Ethics Committee
Faculty of Health and Wellness Sciences

HEALTH AND WELLNESS SCIENCES RESEARCH ETHICS COMMITTEE (HW-REC)
Registration Number NHREC: REC- 230408-014

P.O. Box 1906 • Bellville 7535 South Africa
Symphony Road Bellville 7535
Tel: +27 21 959 6917
Email: sethn@cput.ac.za

23 April 2018
REC Approval Reference No:
CPUT/HW-REC 2018/H7

Dear Mr Jacobus Johannes Botha

Re: APPLICATION TO THE HW-REC FOR ETHICS CLEARANCE

Approval was granted by the Health and Wellness Sciences-REC to Mr Botha for ethical clearance on 29 March 2018. This approval is for research activities related to student research in the Department of Medical Imaging and Therapeutic Sciences at this Institution.

TITLE: The evaluation of an algorithmic model, created for the image guided radiotherapy (IGRT) treatment couch for integration into the Pinnacle Treatment Planning System (TPS)

Supervisor: Ms B Wyrley-Bierch and Ms H Burger

Comment:

Approval will not extend beyond 24 April 2019. An extension should be applied for 6 weeks before this expiry date should data collection and use/analysis of data, information and/or samples for this study continue beyond this date.

The investigator(s) should understand the ethical conditions under which they are authorized to carry out this study and they should be compliant to these conditions. It is required that the investigator(s) complete an **annual progress report** that should be submitted to the HWS-REC in December of that particular year, for the HWS-REC to be kept informed of the progress and of any problems you may have encountered.

Kind Regards



Mr. Navindhra Naidoo
Chairperson – Research Ethics Committee
Faculty of Health and Wellness Sciences

Appendix J2: Ethics Approval (Research Committee, Groote Schuur Hospital)



Western Cape
Government

Health



GROOTE SCHUUR HOSPITAL

Enquiries: Dr Bernadette Eick

E-mail : Bernadette.Eick@westerncape.gov.za

Mr J.J. (Kobus) Botha
CPUT – HEALTH & WELLNESS SCIENCES

E-mail: Kobus.Botha@uct.ac.za

Dear Mr Botha,

RESEARCH PROJECT EXTENSION: The Evaluation Of An Algorithmic Created For The Image Guided Radiotherapy (IGRT) Treatment Couch For integration Into The Pinnacle Treatment Planning System (TPS)

Your recent communication to the hospital refers.

The extension of your research is approved in accordance with UCT Ethics clearance, until 7 May 2021.

As previously mentioned:

- a) Your research may not interfere with normal patient care.
- b) Hospital staff may not be asked to assist with the research.
- c) As previously mentioned, no additional costs to the Hospital should be incurred i.e. Lab, consumables or stationary. If access to TRACK Care/NHLS is required, kindly attach our letter of approval to the application form.
- d) No patient folders may be removed from the premises or be inaccessible.
- e) No patient folders may be removed from the premises or be inaccessible.
- f) Please provide the research assistant/field worker with a copy of this letter as verification of approval.
- g) Confidentiality must always be maintained.
- h) Once the research is complete, please submit a copy of the publication or report.

I would like to wish you every success with the project.

Yours sincerely

DR BERNADETTE EICK
CHIEF OPERATIONAL OFFICER
Date: 17 March 2020

C.C. Mr L. Naidoo

G46 Management Suite, Old Main Building,
Observatory 7925

Tel: +27 21 404 6288 fax: +27 21 404 6125

Private Bag X,
Observatory, 7935

www.westerncape.gov.za/health



Western Cape
Government

Health



GROOTE SCHUUR HOSPITAL

Enquiries: Dr Bernadette Eick

E-mail : Bernadette.Eick@westerncape.gov.za

Mr J. Botha
Cape Peninsula University of Technology

E-mail: Kobus.Botha@uct.ac.za

Dear Mr. Botha,

RESEARCH PROJECT EXTENSION: The Evaluation Of An Algorithmic Model, Created For The Image Guided Radiotherapy (IGRT) Treatment Couch For Integration Into The Pinnacle Treatment Planning System (TPS)

Your recent communication to the hospital refers.

The extension of your research is approved in accordance with UCT Ethics clearance, until **7 May 2020**.

As previously mentioned:

- a) Your research may not interfere with normal patient care.
- b) Hospital staff may not be asked to assist with the research.
- c) No hospital consumables and stationary may be used.
- d) **No patient folders may be removed from the premises or be inaccessible.**
- e) Please provide the research assistant/field worker with a copy of this letter as verification of approval.
- f) Confidentiality must be maintained at all times.
- g) Once the research is complete, please submit a copy of the publication or report.

I would like to wish you every success with the project.

Yours sincerely

DR BERNADETTE EICK
CHIEF OPERATIONAL OFFICER

Date: 17 May 2019

C.C. Mr L. Naidoo
Dr H. Aziz
Professor J. Parkes

G46 Management Suite, Old Main Building,
Observatory 7925

Tel: +27 21 404 6288 fax: +27 21 404 6125

Private Bag X,
Observatory, 7935

www.capegateway.gov.za



Western Cape
Government

Health



GROOTE SCHUUR HOSPITAL

Enquiries: Dr Bernadette Eick

E-mail : Bernadette.Eick@westerncape.gov.za

Mr J. J. Botha
Cape Peninsula University of Technology

E-mail: Kobus.Botha@uct.ac.za / Hester.Burger@uct.ac.za

Dear Mr Botha

RESEARCH PROJECT: The Evaluation Of An Algorithmic Model, Created For The Image Guided Radiotherapy (IGRT) Treatment Couch For Integration Into The Pinnacle Treatment Planning System (TPS)

Your recent letter to the hospital refers.

You are granted permission to proceed with your research, which is valid until 24 April 2019.

Please note the following:

- a) Your research may not interfere with normal patient care.
- b) Hospital staff may not be asked to assist with the research.
- c) No additional costs to the hospital should be incurred i.e. Lab, consumables or stationary.
- d) **No patient folders may be removed from the premises or be inaccessible.**
- e) Please provide the research assistant/field worker with a copy of this letter as verification of approval.
- f) Confidentiality must be maintained at all times.
- g) Should you at any time require photographs of your subjects, please obtain the necessary indemnity forms from our Public Relations Office (E45 OMB or ext. 2187/2188).
- h) Should you require additional research time beyond the stipulated expiry date, please apply for an extension.
- i) Please discuss the study with the HOD before commencing.
- j) Please introduce yourself to the person in charge of an area before commencing.
- k) On completion of your research, please forward any recommendations/findings that can be beneficial to use to take further action that may inform redevelopment of future policy / review guidelines.
- l) **Kindly submit a copy of the publication or report to this office on completion of the research.**

I would like to wish you every success with the project.

Yours sincerely

DR BERNADETTE EICK
CHIEF OPERATIONAL OFFICER

Date: 11 June 2018

C.C. Mr L. Naidoo
Dr H. Aziz
Dr Z. Mohamed

G46 Management Suite, Old Main Building,
Observatory 7925
Tel: +27 21 404 6288 fax: +27 21 404 6125

Private Bag X,
Observatory, 7935
www.capegateway.gov.za

Appendix J3: Data Collection Permission Approval (Radiation Oncology Department, Groote Schuur Hospital)



Western Cape
Government

Health

DIRECTORATE: HEALTH

Groote Schuur Hospital

Enquiries: DR Z MOHAMED

HEAD CLINICAL UNIT: Radiation Oncology Dept

E-mail : zainab.mohamed@uct.ac.za

[Tel 0214044268/4510](tel:0214044268/4510)

Ms Hester Burger and Mr Jacobus Johannes Botha
Division of Medical physics
GSH/UCT/CPUT
Date: 02 May 2018

Dear Ms Burger and Mr Jacobus Johannes Botha

Re research project: The evaluation of an algorithmic model created for the image guided radiotherapy (IGRT) treatment couch for integration into the Pinnacle Treatment Planning System (TPS). (Masters candidate: Mr Jacobus Johannes Botha)

Mr Kobus Botha has requested permission to perform the abovementioned research project in the Department of Radiation Oncology, Groote Schuur Hospital. The study involves access to the Pinnacle Radiotherapy Treatment Planning System. No patient data will be used for the study, and all measurements and evaluations will be performed on medical physics phantoms.

The Department of Radiation Oncology grants you permission to access the data on the Pinnacle system to perform the research project above provided you have CPUT Research Ethics and institutional approval.

Yours sincerely

Dr Zainab Mohamed
Head Clinical Unit: Department Radiation Oncology

G46 Management Suite, Old Main Building
Observatory 7925

Tel: +27 21 404 4263 fax: +27 21 404 5259




Private Bag X,
Observatory, 7935

www.capegateway.gov.za

APPENDIX K: NOTCHES ON COUCH

Positions of Varian Exact IGRT couch indexing notches

S ————— Superior end of couch



| | Varian IGRT Couch | | | CT Scanner Couch |
|----|-------------------|-----------------|--|------------------|
| | Top of notch | Middle of Notch | | Middle of Line |
| H4 | 157 | 170 | | 165 |
| H3 | 297 | 310 | | 305 |
| H2 | 437 | 450 | | 445 |
| H1 | 577 | 590 | | 585 |
| O | 717 | 730 | | 725 |
| F1 | 857 | 870 | | 865 |
| F2 | 997 | 1010 | | 1005 |
| F3 | 1137 | 1150 | | 1145 |
| F4 | 1277 | 1290 | | 1285 |
| F5 | 1417 | 1430 | | 1425 |
| F6 | 1557 | 1570 | | 1565 |
| F7 | 1697 | 1710 | | 1705 |
| F8 | 1837 | 1850 | | 1845 |

All measurement taken from **S**. All measurements are in millimetres (mm)

Notch size

